

Arbeitsbericht NAB 17-42

**Local topography and hillslope
processes in the Jura Ost siting
region (and surrounding area)**

March 2018

A. Ludwig

**National Cooperative
for the Disposal of
Radioactive Waste**

Hardstrasse 73
P.O. Box 280
5430 Wettingen
Switzerland
Tel. +41 56 437 11 11
www.nagra.ch

Arbeitsbericht NAB 17-42

**Local topography and hillslope
processes in the Jura Ost siting
region (and surrounding area)**

March 2018

A. Ludwig

KEYWORDS

Jura Ost, long-term landscape evolution, exposure scenario,
erosion, local topography, hillslope processes, landslides,
stream longitudinal profiles, GIS analysis

**National Cooperative
for the Disposal of
Radioactive Waste**

Hardstrasse 73
P.O. Box 280
5430 Wettingen
Switzerland
Tel. +41 56 437 11 11
www.nagra.ch

Nagra Arbeitsberichte ("Working Reports") present the results of work in progress that have not necessarily been subject to a comprehensive review. They are intended to provide rapid dissemination of current information.

"Copyright © 2018 by Nagra, Wettingen (Switzerland) / All rights reserved.

All parts of this work are protected by copyright. Any utilisation outwith the remit of the copyright law is unlawful and liable to prosecution. This applies in particular to translations, storage and processing in electronic systems and programs, microfilms, reproductions, etc."

Table of Content

Table of Content.....	I
List of Tables.....	II
List of Figures	II
List of Appendices	IV
1 Introduction	1
1.1 Motivation	1
1.2 Detailed objectives.....	1
1.3 Report structure	3
2 Study Area and Related Studies.....	5
3 Data and Methods.....	9
3.1 Input datasets	9
3.2 Manual mapping of landslides and (hillslope) process domains	11
3.2.1 Classification scheme and definitions.....	12
3.2.2 Mapping procedure and criteria.....	14
3.3 Quantitative synthesis of landslides and map of (hillslope) process domains.....	18
3.3.1 Areal proportion of process domains within lithostratigraphic units.....	18
3.3.2 Distribution of pixel-based slope orientation within the hillslope domain.....	19
3.3.3 Surface characteristics of individual landslides / landslide complexes	20
3.4 Intersecting former base levels of erosion with present topography	22
3.5 Stream longitudinal profiles	23
3.5.1 Selection of stream courses	23
3.5.2 Extraction of elevation values and presentation of profiles.....	24
3.5.3 Identification and interpretation of knickpoints / anomalies	25
3.6 Extracting topographic / geological profiles.....	28
3.7 Calculation of topographic parameters for map representations	29
4 Results and Discussion	31
4.1 Hillslope process domains: spatial distribution, topographic and geological control	31
4.1.1 Regional spatial pattern	31
4.1.2 "Landslide susceptibility" of lithostratigraphic units.....	32
4.1.3 Topographic / morphometric characteristics of landslides and hillslopes	33
4.2 Landslide types.....	36
4.2.1 Characteristics and types of large, deep-seated landsliding.....	36
4.2.2 Earthflows.....	40
4.2.3 Additional landslide types	44
4.3 Stream longitudinal profiles	45

4.3.1	"Rinikerfeld" catchment (LP-1, -12, -13, -14, -15).....	47
4.3.2	"Villnachern" catchment (LP-2, -3, -4)	48
4.3.3	"Sissle" catchment (LP-5, -6, -7, -8).....	49
4.3.4	"Ittenthal", "Sulzerbach", "Bürerbach" catchments (LP-9, -10, -11).....	50
4.3.5	Synthesis.....	51
5	Conclusions	55
6	Literaturverzeichnis	57

List of Tables

Tab. 1:	Characteristics of lithostratigraphic units of the study area.....	8
Tab. 2:	Subclasses of the hillslope domain in this study and analogy to the "Symbolbaukasten zur Kartierung der Phänomene" (BWG / BUWAL 1995).....	12
Tab. 3:	Classification system of landslide types by Hungr et al. (2014).....	14
Tab. 4:	"Landslide susceptibility" estimated as percentage of totally mapped landslide surface in relation to the total hillslope area of a given lithostratigraphic unit.....	32

List of Figures

Fig. 1:	Tectonic and geographical setting of the Jura Ost siting region (modified from Madritsch 2015).	6
Fig. 2:	Lithostratigraphic column of the Jura Ost siting region (modified from Nagra 2008).....	7
Fig. 3:	Input datasets (white boxes) directly or indirectly used for GIS-based tasks (grey boxes).	10
Fig. 4:	Exemplary comparison of landslide-related map elements of the digitised Swiss Geological Atlas 1:25'000 (GeoCover) and the interpreted landslide extent (this study) based on visual interpretation of the DTM-AV.	11
Fig. 5:	Classification scheme for mapping of process domains.	12
Fig. 6:	Local examples of landslide / (hillslope) process domain mapping using contextual criteria from different base maps.	16
Fig. 7:	Representation of slope orientation by local normal vectors on terrain surface (from McKean & Roering 2004).	20

Fig. 8:	Selected stream courses for analysis of stream longitudinal profiles (LP).....	24
Fig. 9:	Concepts used for the interpretation of anomalies in stream longitudinal profiles.....	26
Fig. 10:	Histogram and statistical measures of slope gradients within the hillslope domain of the study area, separated for individual lithostratigraphic units.....	35
Fig. 11:	Simplified geological cross section with interpreted "rock slope deformation" on opposite hillslopes of Frickberg.....	38
Fig. 12:	Surface morphology of hillslopes potentially affected by slow but continuous "rock slope deformation" (indicated by red arrows) on northwestern flank of Frickberg.	39
Fig. 13:	Simplified geological cross section with interpretation of large deep-seated landslide on south flank of Geissberg and more shallow slope deformation on opposite hillslope.	40
Fig. 14:	Geological cross section of Schinberg (Hartmann 1928, p. 58).	41
Fig. 15:	Present-day situation at Schinberg, as seen from the west.	42
Fig. 16:	Earthflow at Schinberg from February 1924 to 1926 (Hartmann 1928, p. 61).....	42
Fig. 17:	Earthflow at Schinberg in spring 1939 (Haefeli 1940, p. 182).....	43
Fig. 18:	Earthflow reaching the Aare near Böttstein in March 1876 (Baltzer 1876, p. 290).	43
Fig. 19:	Interpreted (tongue-shaped) earthflow south of Böttstein, attributed to the Passwang-Formation according to the Geological Atlas of Switzerland 1:25'000.	44
Fig. 20:	Head scarp of a medium-sized landslide (~ 0.07 km ²) within Wildeggen-Formation, potentially representing sliding along a (nearly) planar rupture surface corresponding to well-defined bedding planes.....	45
Fig. 21:	Stream longitudinal profiles of the study area, grouped according to different catchments.	46
Fig. 22:	View from southeastern hillslope of Geissberg (east of Remigen) towards Riniken.....	47
Fig. 23:	Large landslide on south flank of Geissberg, potentially "counteracting" fluvial incision along stream longitudinal profile LP-12 by lateral material input.	48
Fig. 24:	Knickpoint in LP-5 (northwest of Linn, 490 m a.s.l.), interpreted as lithologically controlled by higher substrate resistance within the Villigen-Formation (LP-5).....	50
Fig. 25:	"Perched low-relief landscape" in headwater region of LP-1 (Kirchbözberg).	53

List of Appendices

Appendix 1 Map Representations

- 1.A Geographical overview
- 1.B Geological overview (based on Nagra 2014a)
- 1.C Map of (hillslope) process domains (+ geological features)
- 1.D Map of (hillslope) process domains (+ base level HDS / TDS)
- 1.E Landslide map (+ slope gradient map)
- 1.F Landslide map (+ local relief map)
- 1.G Map of (hillslope) process domains (+ stream analysis)

Appendix 2 Quantitative Synthesis of Hillslope Processes

- 2.A Tertiary (Molasse)
- 2.B Villigen-Formation
- 2.C Wildegg-Formation
- 2.D Ifenthal-Formation
- 2.E Hauptrogenstein / Klingnau-Formation
- 2.F Passwang-Formation
- 2.G Opalinus Clay

Appendix 3 Stream Analysis "Jura Ost"

- 3.A Longitudinal profile LP-1 "Rinikerfeld" catchment
- 3.B Longitudinal profile LP-2 "Villnachern" catchment
- 3.C Longitudinal profile LP-3 "Villnachern" catchment
- 3.D Longitudinal profile LP-4 "Villnachern" catchment
- 3.E Longitudinal profile LP-5 "Sissle" catchment
- 3.F Longitudinal profile LP-6 "Sissle" catchment
- 3.G Longitudinal profile LP-7 "Sissle" catchment
- 3.H Longitudinal profile LP-8 "Sissle" catchment
- 3.J Longitudinal profile LP-9 "Ittenthal" catchment
- 3.K Longitudinal profile LP-10 "Sulzerbach" catchment
- 3.L Longitudinal profile LP-11 "Bürerbach" catchment
- 3.M Longitudinal profile LP-12 "Rinikerfeld" catchment
- 3.N Longitudinal profile LP-13 "Rinikerfeld" catchment
- 3.O Longitudinal profile LP-14 "Rinikerfeld" catchment
- 3.P Longitudinal profile LP-15 "Rinikerfeld" catchment

Appendix 4 Regional Topographic / Geological Profiles "Jura Ost"

- 4.A West – East directed
- 4.B North – South directed

Appendix 5 List of GIS Datasets

- 5.A Input datasets
- 5.B Output datasets (2 pages)

Appendix 6 Technical Documentation

- 6.A Quantitative synthesis of mapping results
- 6.B Intersecting former base levels of erosion with present topography
- 6.C Extracting stream longitudinal profiles
- 6.D Extracting topographic / geological profiles

1 Introduction

This work is a contribution to Nagra's investigations on the long-term landscape evolution of Northern Switzerland. It specifically focuses on (GIS-based) mapping and analysis of the spatial distribution, controls and effects of hillslope / landslide processes in the Jura Ost siting region, a section of the Jura Mountains that is closely linked to the Aare/Rhine drainage system by several tributary valleys. The analysis of stream longitudinal profiles along these valleys also represents an integral part of the study, to investigate potential dynamics along the fluvial network and their effects on (and coupling with) hillslope processes. Overall, the work should form a site-specific, qualitative – and partly quantitative – basis for future landscape evolution scenarios (on the hillslope scale).

It is acknowledged, that this is an "as-is state" investigation based on the present state of topography that might be transient as a result of the past geological history (see Schnellmann et al. 2014) and under prevalent interglacial climate conditions. Locally, anthropogenic perturbation might bias the analysis, but is generally regarded as negligible, or indicated elsewhere.

1.1 Motivation

Future research directions within Nagra's "Research Development and Demonstration plan" (Nagra 2016) identified the need for a better understanding of the evolution of local topography and associated processes in the Jura Ost siting region. Important topics related to this overall objective include:

- the role of hillslope / landslide processes (and their geological / topographic control) for **landscape evolution**
- better understanding of the **coupling between hillslopes and the fluvial network**, particularly hillslope response to base level drop and knickpoint migration
- consideration of landslides in Opalinus Clay and its covering lithostratigraphic units as one possible **exposure scenario** of the repository at its late stage

Ideally, a site-specific geomorphic transport law regarding the quantitative contribution of hillslope processes to erosion would be expected, which could then be transferred to a predictive landscape evolution model. Although this is not achieved by this study, a basis is provided by more qualitative considerations and partly supported by quantitative analyses.

1.2 Detailed objectives

As already indicated, it is the general aim of this study to extract information from the present-day landscape, that potentially help to address the topics from section 1.1. The methodological approach consists in GIS-based mapping and analysis of digital terrain models (DTM) as well as additional spatial data (e.g. geological maps). While some locations have additionally been visited and inspected in the field, a solid ground truthing (also concerning the depth of landslides) was not part of this study.

As a basis for the final discussion, the results are illustrated and synthesised by various maps, profiles and diagrams.

Specifically, the following objectives are pursued:

Creating a map of (hillslope) process domains ¹ across the different lithostratigraphic units of the Jura Ost siting region to...

- visualise the spatial pattern of landslide-affected hillslopes, where have landslides been active, where not (yet)?
- provide an area-covering terrain classification regarding the state of hillslope processes
- provide a base map for quantitative topographic analyses regarding hillslope processes (see below)

Quantitatively analysing the relationships of the mapping result with topographic and lithological variables to...

- indicate landslide susceptibility of different lithostratigraphic units
- describe the topographic characteristics of individual landslides (area, internal relief, slope gradient and aspect of landslide surface) and their dependence on lithology
- describe the distribution of hillslope orientations for the different lithostratigraphic units (summarised for both failed and unfailed hillslopes)

Interpreting and characterising different landslide types in the study area to indicate...

- the variety of processes
- their dependence on the geological and topographic setting (potential causes and control mechanisms)
- implications on affected areas, volumes and rates of movement (qualitative considerations only)
- possible scenarios relevant to landslide-caused exposure of a repository

Investigating the spatial distribution of hillslope processes with respect to stream longitudinal profiles and former base levels of erosion to...

- identify potential coupling and feedbacks between incision and hillslope processes along the fluvial network, particularly hillslope erosion in response to knickpoint migration (if existing)
- identify landscape sections with different history of fluvial incision
- infer rough age constraints of possible landslide initiation based on relative comparison of landslide elevation and the former base levels

¹ The map of process domains extends the mapping of landslides by classifying the rest of the terrain as either "unfailed hillslopes", "upland low-relief areas" and "Quaternary plains and terraces" (see further explanations in section 3.2).

1.3 Report structure

Following this introduction, Chapter 2 contains additional background on the geographic and geological setting as well as references to related investigations from the study area.

Section 3.1 gives an overview of the input datasets of this study and which GIS-based tasks they were used for. Sections 3.2 to 3.7 describe the individual tasks more extensively.

Section 4.1 discusses the results of mapping landslides and (hillslope) process domains. This is largely based on illustrations (map, diagrams, profiles) in Appendix 1, 2 and 4. The section also addresses the question of the topographic / geological controls on landslide / hillslope processes and geometry.

Specific landslide types of the study area are interpreted and characterised in section 4.2.

The third part of the discussion deals with the stream analysis (section 4.3). Here, similarities and differences of stream longitudinal profiles in the study region are discussed and analysed with respect to potential dynamics of fluvial incision in the present landscape. Also, possible relations to the observed pattern of hillslope / landslide processes are addressed.

Chapter 5 summarises the conclusions from this study. It relates to the initial motivation in section 1.1.

2 Study Area and Related Studies

The Jura Ost siting region represents one of three areas in Northern Switzerland, that are currently investigated by Nagra as potential locations for the deep geological disposal of radioactive waste (e.g. Nagra 2014a). As implied by the name, the area is located in the eastern part of the Jura Mountains, a mountain range in the Alpine foreland that is well explored by geological research (e.g. Becker 2000, Madritsch et al. 2008).

Within the Jura Mountains, the siting region is assigned to the tectonic regime of the "Deformed Tabular Jura", representing a transition zone between the "Tabular Jura" in the north and the "Folded Jura" in the south (Fig. 1; Madritsch 2015). The study area is characterised by few tectonic structures, the most prominent one being the "Mandach thrust fault" north of the siting region. Bedding planes within the Deformed Tabular Jura (and the Tabular Jura north of the Mandach thrust fault) are mostly flat or gently dipping southward (Nagra 2014a). The regional profiles in Appendix 4 indicate the subsurface orientation of thrust faults and lithostratigraphic boundaries.

As shown by the lithostratigraphic column in Fig. 2, the study area includes various (sedimentary) lithostratigraphic units², featuring different petrographic and geomechanical properties (Tab. 1). These variations suggest a controlling effect on terrain processes and morphology, which is of importance for the present study. As an example, Tab. 1 lists rock strength as a rough indicator for the resistance of each lithostratigraphic unit to erosion (e.g. Bursztyn et al. 2015).

With respect to landscape evolution, recent studies have extensively investigated the history of fluvial and glacial erosion and the reorganisation of drainage systems in Northern Switzerland over the last few million years (Ziegler & Fraefel 2009, Preusser et al. 2011, Yanites et al. 2013, Heuberger & Naef 2014, Heuberger et al. 2014). A regional elevation model of the bedrock surface, resulting from this complex geological history, was compiled by Pietsch & Jordan (2014). Results from these and other important studies related to the landscape evolution in Northern Switzerland are summarised in Schnellmann et al. (2014). While mostly looking at a larger regional (and temporal) scale, these previous studies build an important framework for studying the local topography in the Jura Ost siting region. Also, they have provided a basis to set up a numerical landscape evolution model for the eastern Jura Mountains (Yanites et al. 2017).

Present-day terrain elevation within the extended study area ranges from around 700 m a.s.l. at the highest hilltops of the Deformed Tabular Jura (Schinberg, Geissberg; Fig. 1) to 300 m a.s.l. at the outlet of the Sissle river into the Rhine. Given this local relief, hillslope processes play a relevant role in shaping the landscape of the Jura Ost siting region and its surrounding areas. For instance, historic landslides from the study area have been documented by Baltzer (1876), Hartmann (1928, 1950) and Haefeli (1940). These examples and other landslide-related features can be further identified in the Geological Atlas of Switzerland 1:25'000 (© swisstopo). To account for such processes, the numerical landscape evolution model by Yanites et al. (2017) uses a "hillslope erodibility" parameter to model hillslope erosion as a function of slope gradient and (optionally) rock type. In this case, hillslope erosion is treated as a diffusive process and erodibility is calibrated based on topographic metrics of the present-day landscape (e.g. distribution of hillslope gradients) at a spatial resolution of 250 m.

² If names of lithostratigraphic units include the term "formation", this report uses the German notation with a hyphen, e.g. "Villigen-Formation" instead of "Villigen Formation" (except in Fig. 2).

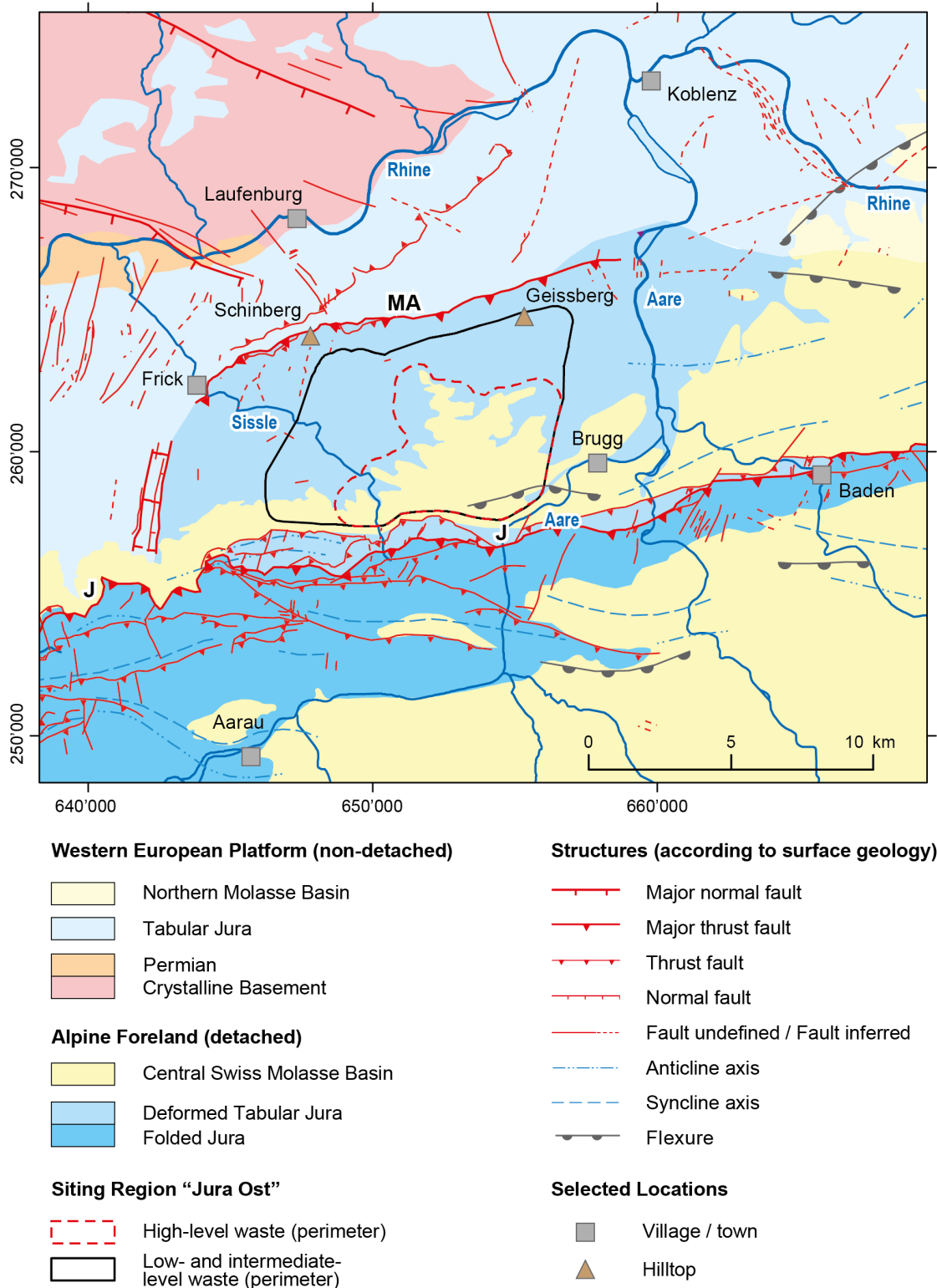


Fig. 1: Tectonic and geographical setting of the Jura Ost siting region (modified from Madritsch 2015).

The siting region is part of the Deformed Tabular Jura, which is confined by the "Mandach thrust fault" (MA) to the north and the "Jura main thrust" (J) to the south. Appendices 1.A, B and C contain additional maps with more detailed geographical and geological information.

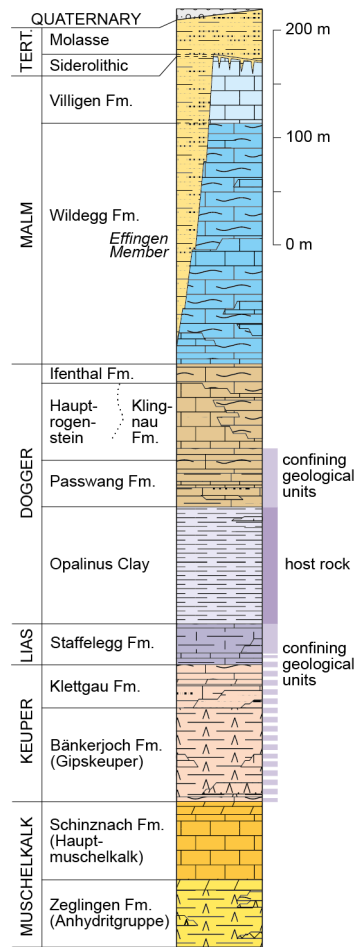


Fig. 2: Lithostratigraphic column of the Jura Ost siting region (modified from Nagra 2008).

Malm = Upper Jurassic; Dogger = Middle Jurassic; Lias = Lower Jurassic; Keuper and Muschelkalk = Triassic. See Nagra (2014a) for more detailed explanations on lithostratigraphic units.

Tab. 1: Characteristics of lithostratigraphic units of the study area.

Lithologic descriptions are based on Biaggi et al. (2014), Enclosure 8 ("Zugangsbauwerk (Schacht) repräsentativ für Schachtstandorte JO-3+, Geologisches Profil Jura Ost mit Datenbändern nach SIA 199"). Data on rock strength correspond to Appendix A4 from the same report, representing estimates of uniaxial compressive strength of intact rock. While lithologic descriptions and rock strength specifically refer to the Jura Ost siting region (Biaggi et al. 2014), the mean content of clay minerals is based on general observations for Nagra's siting regions in Northern Switzerland (Nagra 2014b). Numbers in brackets indicate typical ranges. The lithostratigraphic units Hauptrogenstein and Klingnau-Formation represent different facies types of comparable stratigraphic age (see Fig. 2), with the former dominating in the western and the latter dominating in the eastern part of the study area (see Nagra 2014a).

Name	Lithologic description	Mean content of clay minerals [%]	Rock strength [MPa]
Tertiary sediments (Molasse)	Marls, sandstones, conglomerates	not listed	not listed
Villigen-Formation	Hard limestones, few thin marly layers	not listed	100 (100 – 200)
Wildeggen-Formation	Calcareous marls [a], some limestone sequences [b]	27 (20 – 40) [a] 12 (0 – 20) [b]	30 (10 – 60)
Ifenthal-Formation	Limestones, sand marls	not listed	30 (1 – 105)
Hauptrogenstein	Oolitic limestones, with thin marly layers	not listed	30 (14 – 140)
Klingnau-Formation	Marls and argillaceous limestones	not listed	
Passwang-Formation	Cyclic sequence of claystones [c], sand marls [c] and limestones [d]	46 (20 – 65) [c] 11 (5 – 15) [d]	50 (40 – 120)
Opalinus Clay	Claystones	60 (40 – 75)	15 (4 – 30)

3 Data and Methods

The present GIS-based analysis involves the processing of many existing datasets, which will be introduced in section 3.1. The subsequent sections outline the methodological approach of the different tasks, as follows:

- Manual mapping of landslides and process domains (section 3.2)
- Quantitative synthesis of landslides and map of process domains (section 3.3)
- Intersecting former base levels of erosion with present topography (section 3.4)
- Extracting stream longitudinal profiles (section 3.5)
- Extracting topographic / geological profiles (section 3.6)
- Calculating topographic parameters for (additional) map representations (section 3.7)

These sections provide an overview of the methodological approach and outline the working steps. More detailed information concerning datasets and the technical procedure in ArcGIS are shown in Appendix 5 and Appendix 6, respectively.

3.1 Input datasets

Fig. 3 provides an overview of the various input datasets and indicates the GIS-based tasks they are used for.

All these datasets are either publicly available from swisstopo or based on previous investigations by Nagra. The names of the datasets listed in Fig. 3 are used as references throughout this report, which should improve the readability in contrast to using filenames. A detailed list with links to filenames, sources and supplementary information on the datasets can be found in Appendix 5.

Sections 3.2 to 3.7 include further information on the datasets, where relevant to the approach and to the final interpretation of the results (Chapter 4).

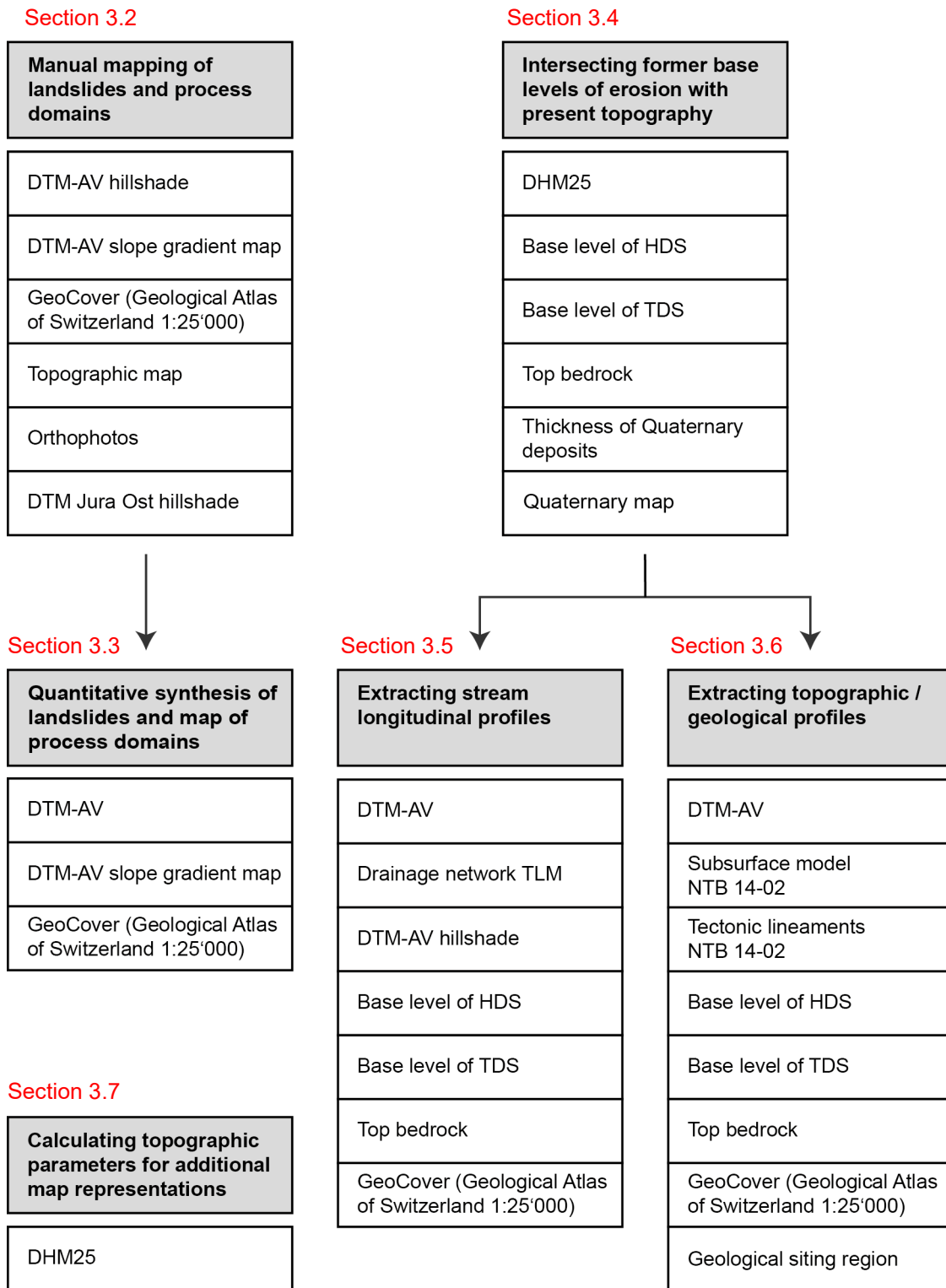


Fig. 3: Input datasets (white boxes) directly or indirectly used for GIS-based tasks (grey boxes).

These datasets are also partly used for map representations in Appendix 1.

3.2 Manual mapping of landslides and (hillslope) process domains

As outlined in section 1.2, an area-covering classification of the terrain with regard to landslides and (hillslope) process domains across the Jura Ost siting region is targeted. For this purpose, the time-consuming task of manual landslide mapping was necessary, due to the lack of an adequate dataset in this region (i.e. landslide inventory or natural hazard map³). Slope instabilities ("Rutschmasse", "Sackungsmasse") are partly indicated in the Geological Atlas of Switzerland 1:25'000 (© swisstopo). However, visual comparison of its digitised version 'GeoCover' with the DTM-AV hillshade (© swisstopo) reveals some problems for the present study (Fig. 4):

- Instead of landslides being mapped as contiguous polygons, they are typically represented by a combination of line objects (e.g. scarps, counterscarps) and smaller (isolated) polygon objects. Therefore, only parts of the landslide surface are mapped as such.
- The coarser scale of the Geological Atlas of Switzerland 1:25'000 sometimes produces deviations of mapped elements when compared to the 2 m-resolution DTM-AV, used for quantitative topographic analyses in this study.

For the present investigation, more complete mapping is therefore required.

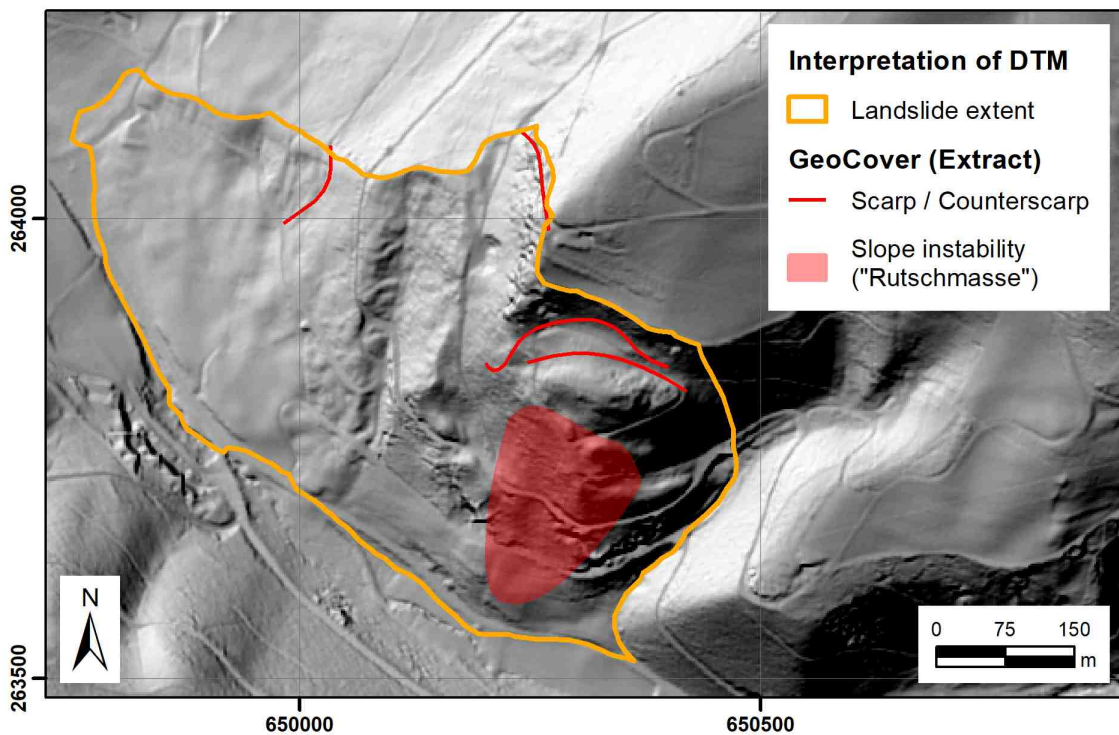


Fig. 4: Exemplary comparison of landslide-related map elements of the digitised Swiss Geological Atlas 1:25'000 (GeoCover) and the interpreted landslide extent (this study) based on visual interpretation of the DTM-AV.

³ Unlike other cantons, the Canton of Aargau has not published a natural hazard map ("Gefahrenkarte") concerning slope instabilities to this date.

3.2.1 Classification scheme and definitions

Fig. 5 shows the classification scheme representing the map of (hillslope) process domains. Apart from providing a visual impression of spatial patterns, the resulting map should allow for different area-based quantitative analyses.

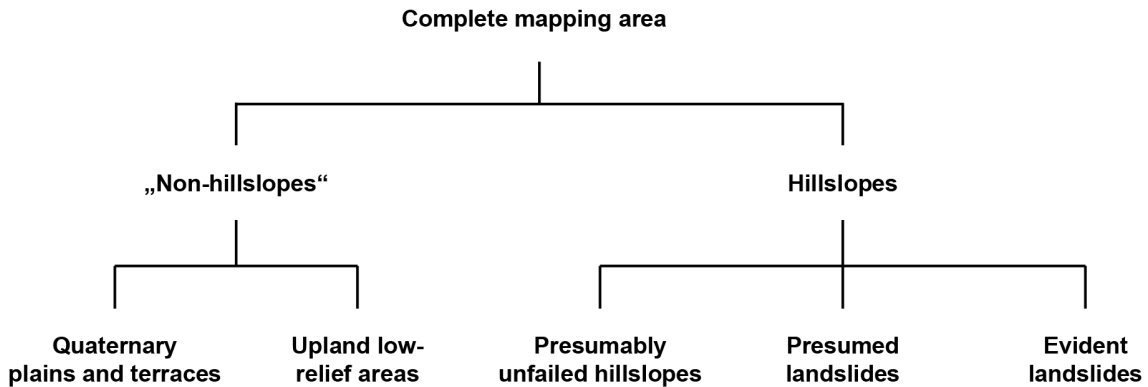


Fig. 5: Classification scheme for mapping of process domains.

The first splitting between "hillslopes" and "non-hillslopes", obviously separates segments potentially affected by hillslope / landslide processes from flatter areas, dominated by alternative geomorphologic processes (e.g. fluvial processes). The subsequent division within the "non-hillslopes" domain indicates, which areas rather correspond to accumulative domains below hillslopes ("Quaternary plains and terraces") vs. more bedrock-dominated and till-covered plateaus above hillslopes ("upland low-relief areas"), which may be eroded by future hillslope processes, once the latter approach these areas.

Within the "hillslopes" domain, the actual landslide mapping is executed. In analogy to recommendations by former agencies of the Swiss Federal Office for the Environment ("Symbolbaukasten zur Kartierung der Phänomene"; BWG / BUWAL 1995), the hillslope domain is subdivided into three classes (Tab. 2).

Tab. 2: Subclasses of the hillslope domain in this study and analogy to the "Symbolbaukasten zur Kartierung der Phänomene" (BWG / BUWAL 1995).

This study	"Symbolbaukasten zur Kartierung der Phänomene" (BWG / BUWAL 1995)
"Presumably unfailed hillslopes"	~ "potentieller Prozess" ⁴
"Presumed landslides"	~ "vermuteter Prozess" ⁵
"Evident landslides"	~ "erwiesener Prozess"

⁴ "Prozess, der an der betreffenden Stelle nicht gewirkt hat, der jedoch aufgrund der allgemeinen Konstellation (Topographie, Geologie, Hydrologie, Vegetation, Waldzustand, Bauten usw.) eintreten könnte" (BWG / BUWAL 1995, p. 18).

⁵ "Prozess, der an der betreffenden Stelle nicht mit Sicherheit erwiesenermassen gewirkt hat, der jedoch beispielsweise aufgrund schwer interpretierbarer Hinweise im Gelände, von vagen Aussagen, aufgrund von allgemeiner Erfahrung oder von Analogieschlüssen (Vergleich von vergleichbaren anderen Gefahrengebieten) gewirkt haben dürfte" (BWG / BUWAL 1995, p. 18).

The intermediate category of "presumed landslides" accounts for the uncertainty inherent to landslide mapping (e.g. Van den Eeckhaut et al. 2007). More details on the distinction of the different categories in the mapping procedure are given in section 3.2.2.

Landslides are here deliberately understood in a broad sense as hillslope processes which include gravity driven mass movements of semi-coherent masses. This basically involves the various landslide types according to Hungr et al. (2014), as listed in Tab. 3. However, some comments are required for clarification:

- The differentiation of landslide types is desired. However, this is not applicable in a systematic way for the (remote) mapping approach of the present study. To this end, more information for characterisation of individual landslides (e.g. knowledge from site-specific geological investigations, deformation measurements) would be needed than is provided by the available datasets (DTM derivatives, GeoCover, orthophotos). As pointed out in section 1.2, an attempt will however be made, to identify important landslide types in the study area and to describe them for suitable examples.
- The mapping is restricted to landslides of movement types "topple", "slide", "spread", "flow" and "slope deformation" according to Tab. 3. This implies that rock fall (type "fall") is not represented by the resulting map. The focus is put on the other movement types for the following reasons: i) they are usually identifiable as contiguous (extensive) landslides (instead of more discrete rock fall events, difficult to localise in the available datasets⁶); ii) in contrast to source areas of rock fall being usually located along the edge of plateaus, the other landslide types are often directly connected to the valley floor. Therefore, they are more of interest with respect to interpreting the coupling of hillslope processes and fluvial incision (while rock fall is more likely to have an indirect response, being interconnected with the fluvial system by other landslide processes at lower/intermediate hillslope sections). Still, rock fall is relevant to some lithostratigraphic units and will therefore be addressed again briefly in the discussion of section 4.2.

"Shallow" vs. "deep-seated" landslides

In agreement with BWG / BUWAL (1995) the term "deep-seated" ("tiefgründig") is here applied to landslides with a depth of movement > 10 m (up to several decameters). This is mostly assumed for large landslides, where high head scarps or large internal deformation features suggest a corresponding depth of (internal) deformation.

As opposed to this, "shallow landslides" here correspond to landslides with a depth of movement assumed to be less than 10 m ("flachgründig" or "mittelgründig" according to BWG / BUWAL 1995).

⁶ DTM hillshades and orthophotos showing mostly forested hillslopes.

Tab. 3: Classification system of landslide types by Hungr et al. (2014).

The words in italic are placeholders, indicating different material types that may be involved in the process.

Type of movement	Rock	Soil
Fall	1. <i>Rock/ice</i> fall	2. <i>Boulder/debris/silt</i> fall
Topple	3. Rock block topple 4. Rock flexural topple	5. <i>Gravel/sand/silt</i> topple
Slide	6. Rock rotational slide 7. Rock planar slide 8. Rock wedge slide 9. Rock compound slide 10. Rock irregular slide	11. <i>Clay/silt</i> rotational slide 12. <i>Clay/silt</i> planar slide 13. <i>Gravel/sand/debris</i> slide 14. <i>Clay/silt</i> compound slide
Spread	15. Rock slope spread	16. <i>Sand/silt</i> liquefaction spread 17. Sensitive clay spread
Flow	18. <i>Rock/ice</i> avalanche	19. <i>Sand/silt/debris</i> dry flow 20. <i>Sand/silt/debris</i> flowslide 21. Sensitive clay flowslide 22. Debris flow 23. Mud flow 24. Debris flood 25. Debris avalanche 26. Earthflow 27. Peat flow
Slope deformation	28. Mountain slope deformation 29. Rock slope deformation	30. Soil slope deformation 31. Soil creep 32. Solifluction

3.2.2 Mapping procedure and criteria

The extent of process domain mapping is roughly confined by the Mandach thrust fault in the north, the Sissle river in the southwest and the Aare river in the south and east (Fig. 1 and Appendix 1.A). Thus, the classification covers all major lithostratigraphic units of the Jura Ost siting region and includes the upper reaches of local tributaries to the Aare and Rhine rivers.

The mapping was executed manually in ArcGIS at a map scale of $\sim 1:2'000$, based on visual inspection of the following datasets (Appendix 5.A):

- DTM-AV hillshade⁷
- DTM Jura Ost hillshade
- DTM-AV slope gradient map
- GeoCover (Geological Atlas of Switzerland 1:25'000)
- Topographic map (1:25'000)
- Orthophotos

Individual terrain segments were manually mapped and labelled according to the classification scheme of Fig. 5.

"Hillslopes" and "non-hillslopes" were roughly differentiated based on the pixel-based slope gradient map of DTM-AV. As a rule of thumb, the mapped "non-hillslopes" are equivalent to larger terrain segments, where slope gradients are fairly homogenous and mostly $< 7^\circ$. This threshold is set rather low, in agreement with some known landslides in the surrounding area, that at least in some parts also show such low hillslope angles (Hartmann 1928). The distinction of "Quaternary plains and terraces" vs. "upland low-relief areas" was then made based on the relative position of the terrain segment with respect to hillslopes (below vs. above) and information from the GeoCover dataset (e.g. alluvial deposits).

Within the "hillslope domain", segments were differentiated according to the terms introduced in Fig 5. Fig. 6 contains examples to illustrate, how the different classes are assigned to the terrain, depending on the contextual information gathered from the different base maps.

It must be noted, that there is no completely objective set of rules available for the displayed segmentation and classification of hillslopes. Similarly, attempts of automated landslide mapping, e.g. using quantitative thresholds related to surface roughness or machine learning algorithms, are also subject to misclassifications (e.g. McKean & Roering 2004, Van den Eeckhaut et al. 2012), particularly if considering the variety of processes and lithological substrates of the study area.

⁷ Hillshades were calculated and used for the mapping at azimuth angle of the light source of 45° , 135° , 225° and 315° , respectively.

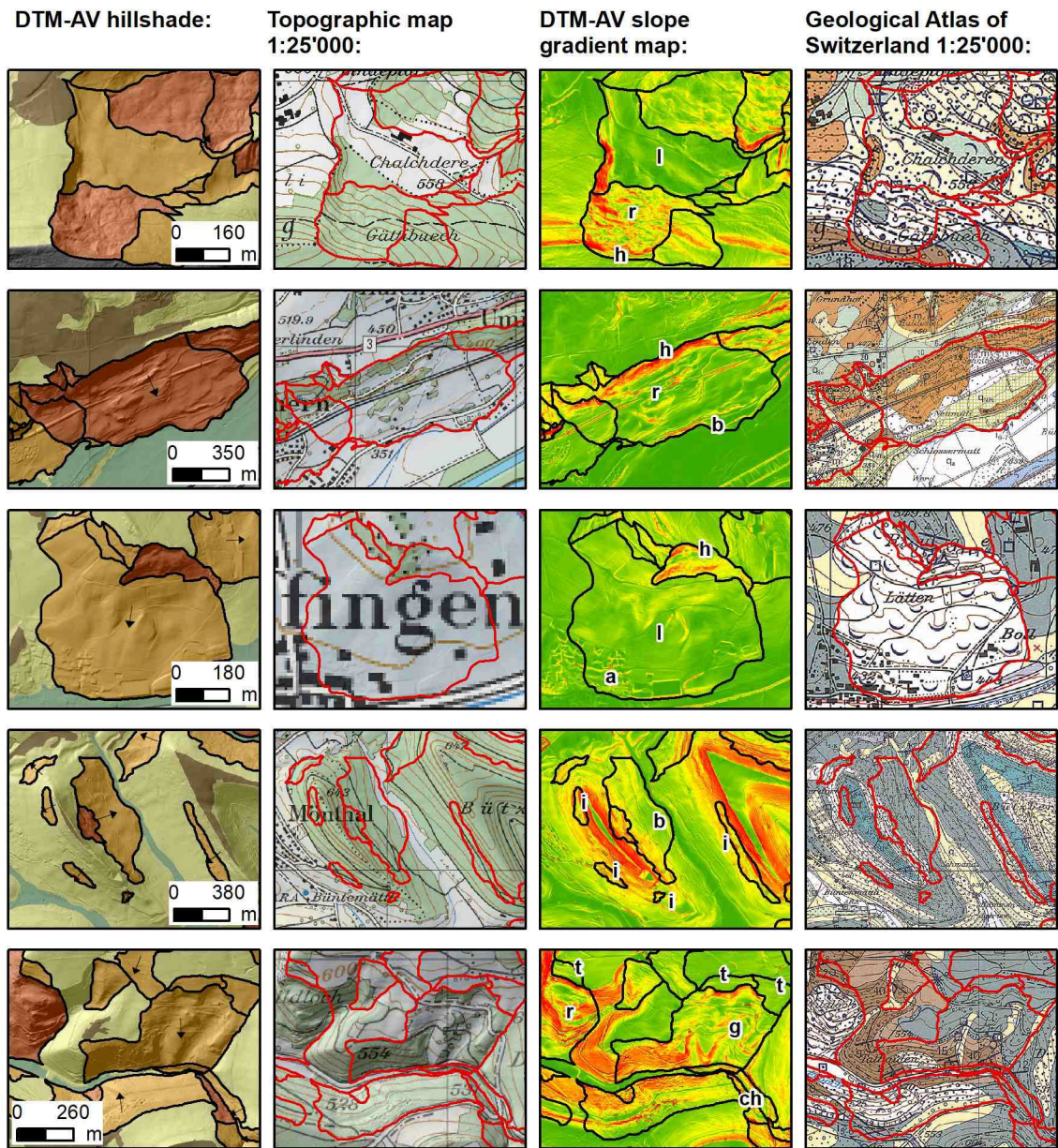


Fig. 6: Local examples of landslide / (hillslope) process domain mapping using contextual criteria from different base maps.

The column headers refer to the different base maps displayed in each column. Black or red outlines show segment boundaries from the mapping of landslide segments. Colours in the left-hand column indicate process domains as follows (see also Appendix 1.C for comparison): green = "Quaternary plains and terraces"; brown = "upland low-relief areas"; yellow = "presumably unfailed hillslopes"; orange = "presumed landslides"; red = "evident landslides". Black arrows in the left-hand column indicate mean slope aspect of landslide surfaces. Colours in the slope gradient map indicate steeper (red) vs. flatter (green) terrain sections. For explanation on the letters displayed in the slope gradient map ('h', 'r', 'l' etc.), see corresponding text sections of this report.

Some guidelines for the present mapping, however, are listed below and explained with reference to Fig. 6. Letters in brackets will refer to characteristic locations in Fig. 6:

- Key features used to identify landslides include distinctive head scarps ('h'), high surface roughness⁸ ('r') or "toe bulging" ('b'). Where such features are well expressed, landsliding is usually also indicated in the GeoCover dataset, except for relatively small landslides (< ~ 0.03 km²). Terrain sections will be mapped as "evident landslides", if two (typically 'h' and 'r') or all three criteria are well expressed and allow for a clear definition of the landslide's spatial extent.
- The class "presumed landslide" is chosen instead, where some of these features occur, but rather as isolated phenomena ('I'), less distinctly ('l') or modified by superimposing effects (anthropogenic effects 'a' or different geomorphological processes such as gully erosion 'g'). In contrast to segments of "evident landslides", the class "presumed landslide" is usually characterised by less discernible boundaries.
- The adjacency to streams can also increase the probability of landsliding by toe erosion. For this reason, small and steep segments of high surface roughness along stream channels are mapped as "evident landslides" ('ch'), even though other key features may not be recognisable due to their small size.
- Additionally, topological relations ('t') are accounted for. For instance, if a terrain segment immediately above a landslide segment indicates weak signals of slope movement (e.g. slightly increased surface roughness), this can be related to the main landslide activity on the downhill side. Therefore, such a segment is classified as "presumed landslide", while it might have been classified as "presumably unfailed hillslope" in another context (i.e. in the absence of an "adjacent landslide"). These "presumed landslide" sections are usually small relative to the main landslide segment.
- The "presumably unfailed hillslope" class is typically represented by smoother hillslopes, without distinct key features as described above. Surface roughness within this domain can locally be increased due to anthropogenic effects (e.g. road cuts or quarries) or features of fluvial erosion. Orthophotos and the topographic map have been used to prevent such features to be interpreted as landslide-related.

These considerations demonstrate that the mapping result will be affected by some subjectivity and potentially some misclassifications. The class "presumably unfailed hillslope" may contain landslide-affected sections, where these have not been recognised, e.g. in case of shallow and slow movement with little deformation or in case of old (inactive) landslides, "overprinted" by other surface processes. However, it can be assumed that many landslides and process domains are correctly identified.

⁸ Increased surface roughness is attributed to internal deformation of the landslide mass, often expressed by scarps, trenches, benches and counterscarps / reverse scarps (e.g. Hungr et al. 2014). Larger structures of these types are usually indicated in the GeoCover dataset (see also Fig. 4). Besides, such features (and increased surface roughness in general) are expressed in the hillshade view and slope gradient map by high heterogeneity of slope gradients.

3.3 Quantitative synthesis of landslides and map of (hillslope) process domains

The mapping results have been quantitatively analysed in different ways to support final discussions with respect to the objectives of Chapter 1. The resulting diagrams can be considered as a synthesis that complements the map representations. The analysis includes:

- Calculation of areal proportion of each process domain intersecting with a lithostratigraphic unit: This should indicate, whether certain lithostratigraphic units within the study area are rather dominated by the "hillslope" vs. "non-hillslope" domain and to what degree hillslopes tend to be landslide-affected (~ "landslide susceptibility" of lithostratigraphic units).
- Distribution of pixel-based slope orientation within hillslope domain, separated for different lithostratigraphic units: This should indicate the dependence of slope gradients on lithology and slope aspect. Additionally, it forms a reference frame for analysing slope orientations of landslide surfaces.
- Calculation of surface characteristics of individual landslides / landslide complexes: This includes topographic characteristics (area, mean slope orientation (gradient and aspect) and internal relief) and the lithostratigraphic composition, which should help to identify topographic and lithological controls on landslides.

The next sections will give an overview, how these tasks were executed. Detailed descriptions of the processing in ArcGIS are shown in Appendix 6 (section A).

3.3.1 Areal proportion of process domains within lithostratigraphic units

To calculate the areal proportion of different process domains within separate lithostratigraphic units, the "Zonal Histogram" tool in ArcGIS was used. As input for this, two raster datasets, representing both the process domains and lithostratigraphic domains, were required. The spatial resolution was defined at a grid size of 2 m. The "process domains (raster)" were simply created by converting the "process domains" resulting from section 3.2.

The raster representing the lithostratigraphic domains was created from a polyline dataset ("lithostratigraphic boundaries"), that in turn was manually extracted and partly interpolated from the Geological Atlas of Switzerland 1:25'000 and expert knowledge of the local geology (provided to Nagra by P. Jordan / Gruner Böhlinger AG, Oberwil). These "lithostratigraphic boundaries" are displayed in the map representation of Appendix 1.C and basically allow for separation of the lithostratigraphic units according to Tab. 1 (Chapter 2). The lithostratigraphic units Hauptrogenstein (west) and Klingnau-Formation (east) are aggregated in this dataset, as they represent different facies types of the same (or similar) stratigraphic age (Nagra 2014a), which are separated by a diffuse boundary along the geographical axis Gansingen – Schinznach (see Appendix 1.A for geographical locations).

While this represents the most reliable dataset available to this task, it remains an approximation of the true spatial extent of lithostratigraphic domains where bedrock outcrops are sparse. Moreover, it is important to note, that in areas covered by Quaternary deposits (see Appendix 1.B for spatial distribution), the lithostratigraphic boundaries are projected to the surface along the orientation of bedding planes at depth. This can produce horizontal offsets of surface boundaries with respect to top bedrock, as a function of the thickness of Quaternary deposits and the angle of projection. However, in most parts of the study area and particularly within the hillslope domain, Quaternary cover is shallow and therefore the dataset was used without further adjustment.

As an intermediate step of creating the "lithostratigraphic domains (raster)", the polylines had to be converted to polygons, which involved additional processing:

- Completion of polylines in two cases: i) the dataset "lithostratigraphic boundaries" (as displayed in Appendix 1.C) locally contains spatial gaps of a few meters between line elements marking the same lithostratigraphic boundary. These were connected linearly; ii) along the northern boundary of the mapping area, a more complex tectonic setting is observed, with lithostratigraphic boundaries being sometimes interrupted by intersection with tectonic lineaments (see Appendices 1.B and 1.C). Here, polylines representing boundaries of the same lithostratigraphic units were manually connected along these tectonic lineaments. The GeoCover dataset was used to verify, that different lithostratigraphic domains are correctly separated by the completed polylines.
- The resulting dataset "lithostratigraphic boundaries (completed)" was then intersected with a polygon that defines the "extent of process domain mapping".

The result is a polygon dataset which defines the different "lithostratigraphic domains". Since the dataset of "lithostratigraphic boundaries" in some cases did not allow a reliable separation of Lias (Lower Jurassic) and Triassic sediments in the most northern (tectonically more complex) region of the mapping area, these are partly summarised in an additional domain classified as "not differentiated". Analogously to the "process domains", the polygon dataset "lithostratigraphic domains" had to be converted to a raster dataset, "lithostratigraphic domains (raster)".

Once the two raster datasets of "process domains (raster)" and "lithostratigraphic domains (raster)" were created, the "Zonal Histogram" tool in ArcGIS allowed calculating a histogram, which shows the areal proportion of each process domain within each lithostratigraphic unit.

These areal proportions were finally illustrated in Adobe Illustrator (see Appendix 2 for graphical illustration).

3.3.2 Distribution of pixel-based slope orientation within the hillslope domain

The datasets of "process domains" and "lithostratigraphic domains" described in the previous section were also used to analyse the distribution of pixel-based slope orientation within the hillslope domain. Again, the calculations were made separately for the different lithostratigraphic domains.

The analysis was based on derivatives of DTM-AV at a grid size of 2 m. To represent slope orientation, three raster datasets were calculated which store the x-, y- and z-components of local normal vectors on terrain surface (Fig. 7), respectively. These were derived from pixel-wise calculations of slope gradient and slope aspect and transformation by trigonometric functions.

To reduce the vast number of data points resulting from the high resolution, a point feature class was created, to subsample only every tenth raster cell in both east – west and north – south direction. This point spacing of 20 m was deemed acceptable, given the spatial correlation of slope orientation observed for the terrain on short distances. The mask of sampling points was intersected with the polygons of the hillslope domain. The resulting "hillslope sampling points (20 m grid spacing)" were then used to extract the x- and -y components of local normal vectors on terrain surface together with the corresponding lithostratigraphic domain.

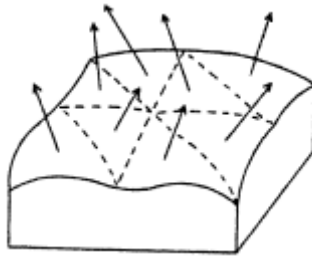


Fig. 7: Representation of slope orientation by local normal vectors on terrain surface (from McKean & Roering 2004).

Note that in the present study, the DTM-AV represents the surface as square cells instead of the depicted triangular elements.

Finally, based on their x- and y-components, data points were projected on a radial diagram, where slope gradients are indicated along the radial axis and slope aspect is represented by the azimuth direction. Filtering of the data points is possible by lithostratigraphic units (domains), which were previously assigned to the attribute table (see above).

For final illustration, points have been counted within subsections of the radial diagram (regularly divided by intervals of slope gradients (5°) and aspect (22.5°)). This allowed for displaying the frequencies of slope orientations for given lithostratigraphic units intersecting with the hillslope domain (see Appendix 2 for graphical results).

3.3.3 Surface characteristics of individual landslides / landslide complexes

Although the map of process domains indicates the spatial distribution of landslide-affected hillslopes, it does not necessarily delineate individual landslides. Instead, landslide-affected hillslopes in the study area often extend seamlessly over adjacent valley flanks with changing aspect. Also, individual landslides (complexes) are sometimes mapped by several segments that represent different degrees of evidence (see Fig. 6 and rest of section 3.2.2).

An attempt is therefore made, to separate individual landslides / landslide complexes within the map of process domains. The basic idea is to aggregate adjacent segments of the classes "evident landslides" and "presumed landslides", if their deformation likely occurs interdependently. This applies to:

- Adjacent segments with similar direction of movement (as inferred from slope orientation), unless they are separated by distinct topographical dissection (e.g. deeply incised gully) and are characterised by a different morphological expression.
- Adjacent segments with different direction of movement, if the deviating segment is very small in comparison to the rest of the landslide and likely to be related (e.g. based on the morphological expression).

Landslide segments are not aggregated if their slope orientation strongly deviates, e.g. in case of landslides on opposite hillslopes of a channel or in case of separation by a ridge.

These criteria are ambiguous in some cases. Thus, there is some subjectivity involved in this processing step, too. It is also acknowledged that by the aggregation procedure, superimposing processes may be summarised in one individual landslide / landslide complex (e.g. slow deep-seated processes with more rapid surficial processes; see more on this in section 4.2).

Once individual landslides have been merged (and converted into a raster dataset), their surface characteristics can be calculated from other raster datasets:

- DTM-AV
- Raster datasets representing the x-, y- and z-components of local normal vectors on terrain surface (see section 3.3.2)
- Raster dataset representing the lithostratigraphic domains (see section 3.3.1)

This is done with the "Zonal Statistics" and "Zonal Histogram" tools in ArcGIS in the following way:

- Calculating internal relief, i.e. maximum elevation difference across landslide surface, by "Zonal Statistics" (statistics type "RANGE" applied to DTM-AV)
- Calculating the normal vector representing the mean orientation of the landslide surface by "Zonal Statistics" (statistics type "MEAN" applied to raster datasets representing x-, y- and z-components of pixel-based normal vectors)
- Calculating the areal proportion of different lithostratigraphic units intersecting with the landslide surface, by "Zonal Histogram" (based on raster dataset of lithostratigraphic domains, section 3.3.1)
- Creating a point feature class, representing the centroids of the individual landslides / landslide complexes
- Adding the topographic and lithostratigraphic parameters calculated above to the attribute table of the landslide centroids
- Calculating mean slope gradient and mean slope aspect of landslide surface from the mean normal vector's components (by using trigonometric functions in the attribute table of the "landslide centroids" point feature class)

These attributes are finally illustrated by ArcGIS and Adobe Illustrator in the following ways (see Appendices 1.E, 1.F and 2 for graphical results):

- Arrows on landslide maps, indicating the mean aspect direction of the landslide surface, and being labelled with the mean slope gradient and internal relief
- Diagrams with pie chart representations of landslides intersecting with specific lithostratigraphic units, where: i) size of pie chart indicates landslide area; ii) segments of pie charts indicate areal proportion of different lithostratigraphic units intersecting with the landslide surface; iii) position of pie chart in diagrams represents topographic variables of landslide surface (slope gradient, slope aspect or internal relief; see Appendix 2 for illustration)

3.4 Intersecting former base levels of erosion with present topography

The aim of this processing step is to indicate a simplified minimum terrain elevation at the time of the former base levels "Höhere Deckenschotter" (HDS)⁹ and "Tiefere Deckenschotter" (TDS)¹⁰. This information can potentially be used:

- to interpret present stream longitudinal profiles (section 3.5)
- to identify younger vs. (possibly) older landscape segments
- to temporally constrain the initiation of mapped landslides

The two input datasets "base level of HDS" and "base level of TDS" (Heuberger & Naef 2014) represent regionally interpolated (nearly planar) surfaces. These interpolations are geometrically correct, but hypothetical in the physical sense. The base levels are best constrained by deposits of HDS and TDS near the Aare and Rhine river. However, they tend to get poorly constrained towards the upper reaches of tributary valleys, or in other words, towards the interior of the study area. Also, it must be considered, that in some locations the paleo-topography of the bedrock surface may already have been lower than these interpolated surfaces (in case of pre-existing local troughs or valley structures).

The regionally interpolated (base level) surfaces technically "undercut" the present topography, where the latter is higher. While this represents a real situation in regions presently covered by the corresponding Quaternary deposit (e.g. HDS), such "undercutting" surfaces are of course only theoretical in the absence of these deposits.

Therefore, new raster datasets have been created, where these "undercutting" surfaces are excluded in the absence of HDS or TDS deposits, respectively. This is done by intersecting the input raster datasets "base level of HDS" and "base level of TDS" with the digital terrain model DHM25 (© Swisstopo) and by taking into account the extent of HDS and TDS deposits from the "Quaternary map" (Heuberger et al. 2014). For illustration purposes, the resulting raster datasets are finally converted into polygon feature classes. On the map (Appendix 1.D), these polygon feature classes display the intersection of the projected base levels of HDS and TDS with present topography (DHM25). The details of the procedure in ArcGIS are explained in Appendix 6 (section B).

⁹ "Höhere Deckenschotter" (HDS): Early Pleistocene (predominantly glaciofluvial) deposits; approximately 2.5 to 1.8 million years old (Schnellmann et al. 2014).

¹⁰ "Tiefere Deckenschotter" (TDS): Early Pleistocene (predominantly glaciofluvial) deposits; approximately 1.2 to 0.8 million years old (Schnellmann et al. 2014).

3.5 Stream longitudinal profiles

In a steady-state landscape, where the fluvial system is considered to have fully adjusted to the history of tectonic uplift and erosion (and provided substrate resistance is homogeneous), stream longitudinal profiles are expected to follow the rule of the "graded river" concept (e.g. Kirby & Whipple 2012). According to this, streams show a graded (concave upwards) longitudinal profile, with the stream gradient gradually decreasing from the headwater towards the base level. This gradual decrease of stream gradient relates to the fact, that with increasing drainage area, the stream provides still enough discharge to remove the available bedload even at lower stream gradients.

Deviations from such graded stream longitudinal profiles may be observed as (convex) anomalies or knickpoints, potentially indicating transient signals of base level change / incision within a drainage system (as opposed to the steady state). The analysis of stream longitudinal profiles will therefore be of interest in the attempt to identify stream sections with different history of fluvial incision¹¹ and to study associated effects on hillslope processes (as inferred from the landslide mapping).

Stream longitudinal profiles have been extracted for 15 tributaries to the Aare and Rhine with headwaters in the Jura Ost siting region (Fig. 8 and Appendix 1.G). Apart from the present topography (DTM-AV), the resulting profiles (Appendix 3) display the following information:

- Base level of HDS (section 3.4)
- Base level of TDS (section 3.4)
- Top bedrock (where Quaternary deposits > 5 m)
- Lithostratigraphic units of bedrock surface

These illustrations aim at addressing the following questions:

- Are there any knickpoints / anomalies in the present topographic profile?
- If so, how can they be interpreted? For instance, a) are they associated with lithological variations along the stream, b) can they be related to former base levels of erosion?

The next sections (3.5.1 and 3.5.2) will outline the approach of profile extraction and editing. The detailed working steps in ArcGIS are again explained in Appendix 6 (section C). The final section (3.5.3) explains the approach and concepts of how knickpoints / anomalies have been interpreted in the context of the "graded river" concept introduced above.

3.5.1 Selection of stream courses

For extraction of stream longitudinal profiles, stream courses have been selected from the input dataset "drainage network TLM" (Fig. 8). These data are part of the Topographic Landscape Model 'TLM' by swisstopo, where streams are mapped as polylines according to their present course. These present stream courses may be anthropogenically altered locally. However, in contrast to drainage networks calculated from high-resolution DTMs, they are not subject to artefacts like artificial deflections of stream courses by road embankments and are therefore considered more appropriate for the present analysis.

¹¹ a) Incised sections below knickpoints; b) locations of present knickpoint migration; c) "Perched low-relief landscapes" above knickpoints.

In some cases, the polylines of the "drainage network TLM" had to be extended manually for the headwater regions (Fig. 8). This was done by visually following a drainage network that was calculated with the "Hydrology" toolbox in ArcGIS and Matlab from a resampled (3 m-grid) version of DTM-AV (hence referred to as "calculated drainage network"; provided to Nagra by M. Foster and R. Arrowsmith / Arizona State University). The DTM-AV hillshade was used to check, that the sections are not affected by major artefacts.

Each stream (longitudinal profile) has been assigned a number (LP-1 to LP-15) according to Fig. 8. These numbers are used as references throughout this report.

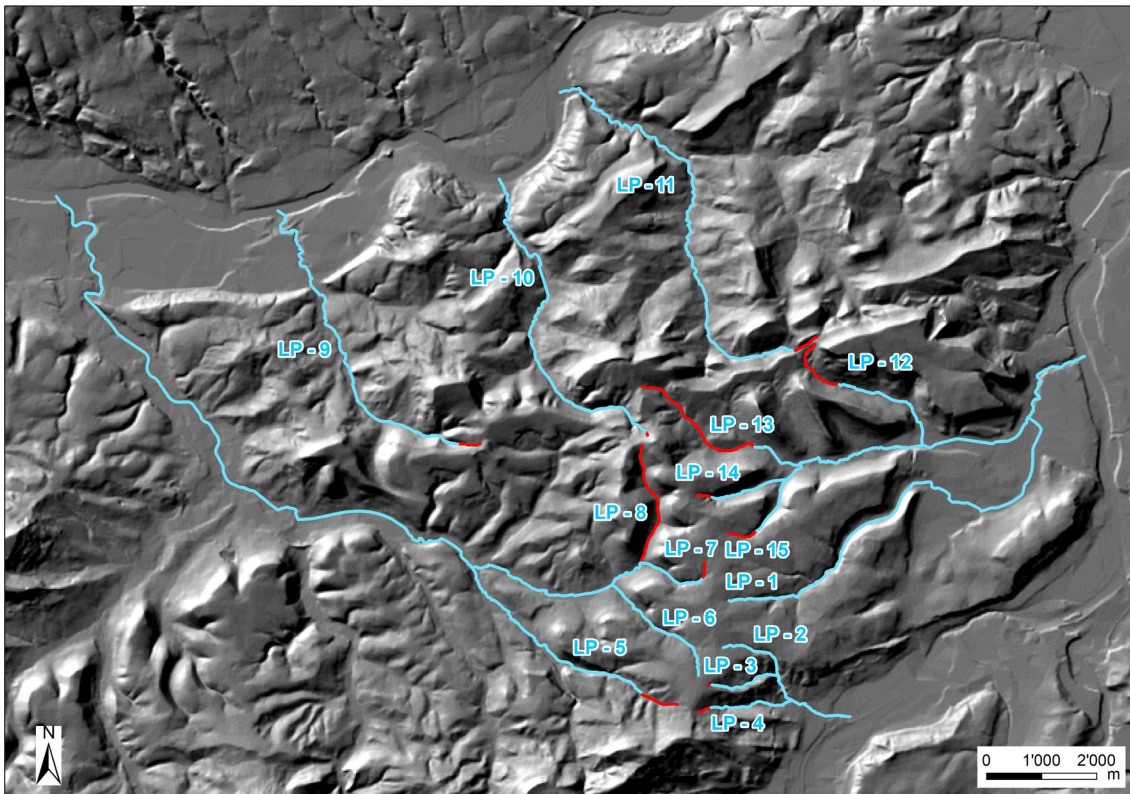


Fig. 8: Selected stream courses for analysis of stream longitudinal profiles (LP).

Blue sections correspond to the dataset "drainage network TLM", red sections have been extended manually based on the visual inspection of the "calculated drainage network" (provided to Nagra by M. Foster and R. Arrowsmith / Arizona State University) and "DTM-AV hillshade".

3.5.2 Extraction of elevation values and presentation of profiles

For each stream course, points have been generated along the polyline at horizontal distances of 10 m. Then, elevation values of the different surfaces (present topography (DTM-AV), base level of HDS and TDS (section 3.4), top bedrock) have been extracted at these point locations. The data points, representing the elevation of the different surfaces and the distance along the stream course, have then been used to construct the profiles. Elevation values have been scaled by factor 10, to accentuate changes in channel gradient in the illustrations. This task of profile construction was executed in ArcGIS (details in Appendix 6, section C).

Adobe Illustrator has been used for the final editing and illustration of the profiles. In this step, further context has been manually added to the profiles:

- Lithostratigraphic units of bedrock surface
- Data basis used for stream course extraction (according to Fig. 8)

The corresponding distances along the profiles have been determined by comparison with the 10 m spaced points (see above) located along the stream courses. The lithostratigraphic units are aligned according to the intersections of stream courses and the dataset "lithostratigraphic boundaries" (section 3.3.1). Since the latter dataset does not subdivide the Tertiary units, the GeoCover dataset (Geological Atlas of Switzerland 1:25'000) has been used as reference in case of LP-2, -3 and -4 (Appendix 3), to indicate potential discontinuities of substrate resistance along these profiles. However, this was only done in the presence of reliable constraints by mapped outcrops. Otherwise, the bedrock surface was classified as "not differentiated". Lower sections of tributaries to the Rhine (LP-5 to LP-11), which mainly intersect with Triassic sediments (Keuper, Muschelkalk; see Appendix 1.B), have not been differentiated either.





Finally, the presentation of stream longitudinal profiles in Adobe Illustrator also includes the interpretation of knickpoints / anomalies. Background is given in the subsequent section 3.5.3.

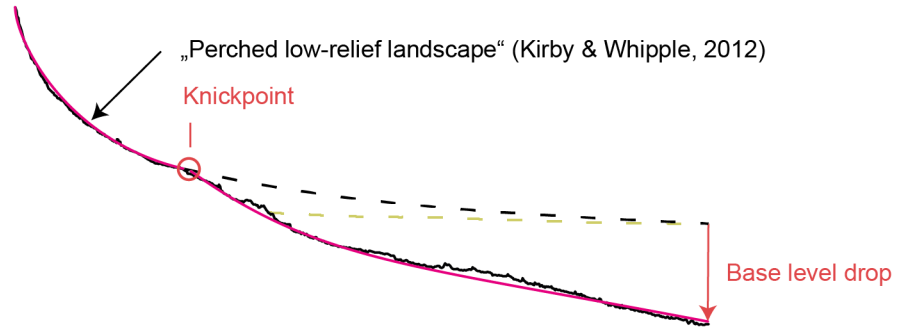
3.5.3 Identification and interpretation of knickpoints / anomalies

Based on the "graded river" concept, each stream longitudinal profile has been visually checked for anomalies. These may either be expressed as distinct knickpoints (with abruptly increasing stream gradient) or as less obvious "convex sections" along the profile. The visual / qualitative approach used here does not involve an objective / quantitative threshold for identification of knickpoints / anomalies. Therefore, the classification applies to features of various convexity and magnitude, as can be observed in the resulting profiles (Appendix 3 and Fig. 9). However, major transitions in the stream longitudinal profiles should be identified.

Convex sections described above can be expressed as irregular sections (see also Fig. 9C), with a series of multiple, sometimes small knickpoints. Although an effort is made to differentiate such individual knickpoints along a convex section, they may actually correspond to one single (higher-order) anomaly. This will be accounted for in the interpretation of results in section 4.3.

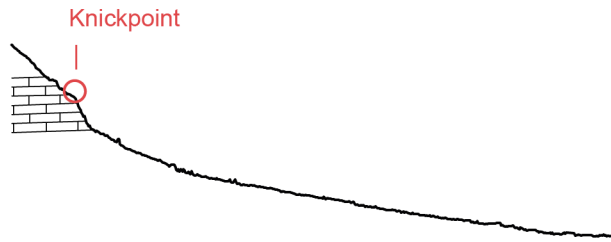
A) Base level drop:

-  Present topography
-  Idealized topography (transient state)
-  Base level of „Tiefere Deckenschotter“ (TDS), interpolated / projected
-  Projection of graded profile (hypothesized steady state at time of TDS)






B) Lithological control:

-  Present topography
-  Resistant bedrock



C) Landslides:

-  Present topography
-  Material input by lateral landslides
-  Idealized topography of a graded profile (steady state)

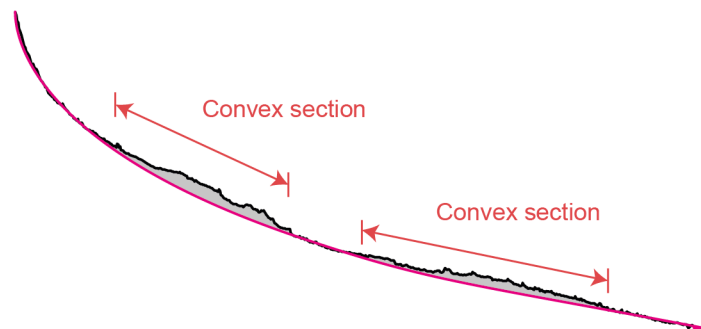


Fig. 9: Concepts used for the interpretation of anomalies in stream longitudinal profiles. Note that the effective (present) topography in the first and third sketch is identical.

Based on the distance along the profile, the locations of knickpoints / anomalies have been manually projected on the map in ArcGIS (output dataset "stream profile anomalies"). The context displayed in the stream longitudinal profile and map view is used to interpret their potential signals and dynamics. While the stream longitudinal profiles already include the information of former base levels of erosion and bedrock depth and substrate (section 3.5.2), the map view extends the context by:

- Landslide map (section 3.2)
- DTM-AV hillshade
- Topographic map
- Orthophotos

The latter three are used to identify anthropogenic effects, e.g. intersections with roads, or minor artefacts in the input datasets (e.g. local deviations of digitised stream courses in comparison with DTM-AV). Apart from such artificial causes, anomalies may be attributed to different natural causes. Fig. 9 is used to illustrate those that are thought to be most relevant for the study area:

- Signals of base level drop
- Signals of lithological control (heterogeneity of substrate resistance)
- Signals of landslides (material input to channel by lateral landsliding)

These will be explained in more detail in the following sections.

A) Signals of base level drop (Fig. 9A)

Differential rock uplift (Kirby & Whipple 2012), drainage reorganisation (Yanites et al. 2013) and other factors (e.g. climatic changes; Schumm 1993, Whipple & Tucker 1999, Blum & Törnqvist 2000) are potential causes of relative base level change in a drainage system. The erosional response is expected to propagate upstream, until the stream longitudinal profile reaches a new equilibrium. In the transient state, the profile shows a knickpoint, where the downstream section has already been adjusting to the new base level and the upstream section is (possibly) equilibrated to a former base level (e.g. base level of TDS). Kirby & Whipple (2012) also refer to such an upstream section as a "perched low-relief landscape".

Knickpoints associated with base level drop are expected to be mobile features that migrate upstream and may diffuse as they get to the headwater regions.

B) Signals of lithological control (Fig. 9B)

Given a specific drainage area, higher substrate resistance should result in a steeper channel gradient (e.g. Bursztyn et al. 2015). Thus, lithostratigraphic variations along the stream can produce convex anomalies and even distinct knickpoints, which usually are considered to represent fixed (non-migrating) features (Kirby & Whipple 2012). Nevertheless, migration might be possible or very slow, but is not inferable with the current analysis.

Also, cover effects from sediments along the channel bed have been found to modify stream gradients (Duvall et al. 2004), by affecting the substrate resistance. If bedload from resistant bedrock upstream is transported and deposited along downstream sections of weaker bedrock, this potentially increases the substrate resistance and stream gradient of the latter (downstream) section.

However, it is assumed here, that this "steepening" of the downstream section will rather reduce the concavity of the stream longitudinal profile, than turn into convex sections or knickpoints. Nevertheless, the effect will be considered, in the discussions of section 4.3.

C) Signals of landslides (Fig. 9C)

Similarly, material input by lateral landslides can cause convex sections or knickpoints in stream longitudinal profiles (e.g. Korup et al. 2010). These may represent fixed features (Kirby & Whipple 2012), or rather a transient state, where the upstream propagation of incision is decelerated until the additional sediment has been removed (e.g. Korup et al. 2010). In fact, landslides may often be the direct effect of knickpoint migration / fluvial incision in response to base level drop. In this case, however, the lateral material input to the channel is likely to modify the characteristic shape of knickpoints purely related to base level drop.

It is assumed here that the latter observation depends on the spatial and temporal characteristics of the landslide processes. One discrete event could form a distinct knickpoint, while a longer-term process, in which lateral material input by landsliding varies both spatially and temporarily along a certain stream section, could produce a more complex, convex shape (e.g. gradual "rock slope deformation" superimposed by smaller, occasional "debris slides" (see Hungr et al. 2014 for definitions).

Synthesis

In summary, it is important to note, that profile anomalies / knickpoints may be explainable by more than one of these signals, and in fact, they can also be the result of their interplay or superposition. This makes it potentially more difficult to assess, whether migrating knickpoints in response to base level drop are involved in the system.

As a rough guide, anomalies will be classified as (potentially) migrating knickpoints, where:

- a signal of base level drop can be inferred, and no lithological control is indicated
- a signal of lithological control is interpreted, however coinciding with the occurrence of lateral landslides

The latter may lead to some confusion with the more common notion, that lithologically controlled anomalies represent fixed features (e.g. Kirby & Whipple 2012). Nevertheless, it is assumed here, that lateral landslides can indicate a response to knickpoint migration, even where they spatially coincide with a change of substrate resistance along the stream profile.

3.6 Extracting topographic / geological profiles

Regional profiles across the study area were extracted in north – south and east – west direction as an additional way to illustrate the relation of mapped landslides (section 3.2) with the topographic and geological setting. The sampling lines of the topographic profiles have been defined manually, accounting for interesting locations across the study area (Appendix 1.A). The extraction of elevation values and the presentation of profiles followed the same procedure as for the stream longitudinal profiles (section 3.5.2). Again, sampling points have been generated along the profile lines at horizontal distances of 10 m. The detailed working steps in ArcGIS are described in Appendix 6 (section D).

In analogy to section 3.5, the following surfaces are displayed on the profiles in addition to the present topography: "base level of HDS", "base level of TDS", "top bedrock (where Quaternary deposits > 5 m)". Thus, the present landscape is again compared with former base levels of erosion.

Lithostratigraphic boundaries are shown on the profiles, to illustrate both their intersection with terrain or bedrock surface and their projection at depth. The latter also indicates the depth of the host rock (Opalinus Clay) within the siting region perimeter, relative to the present topography (and former base levels of erosion). Where defined, the lithostratigraphic boundaries at depth have been extracted from the input dataset "subsurface model NTB 14-02" (Nagra 2014a). This applies to: "Basis Tertiary", "Basis Malm (Basis Wildegg-Formation)", "Top Opalinus Clay", "Top Lias".

Within the "subsurface model NTB 14-02", the other lithostratigraphic boundaries are not defined for the study area. Therefore, they were manually aligned with the defined boundaries ("Basis Tertiary" etc., see above) and their intersection with terrain surface according to the "lithostratigraphic boundaries" as derived from the GeoCover dataset (Geological Atlas of Switzerland 1:25'000; see section 3.3.1).

Finally, landslides have been illustrated schematically, based on the map of process domains (section 3.2) or visual inspection of DTM-AV hillshade and GeoCover (Geological Atlas of Switzerland 1:25'000) for sections outside of the map extent.

Subsections of the regional topographic / geological profiles were also used for interpretation and illustration of landslide process types in the study area (see figures in section 4.2).

3.7 Calculation of topographic parameters for map representations

To compare the distribution of landslides with topographic parameters, additional map representations were created, where the landslide map from section 3.2 is displayed in combination with a) a slope gradient map (Appendix 1.E) and b) a local relief map (Appendix 1.F). Both were calculated based on the digital terrain model DHM25 (25 m grid size). The slope gradient was calculated with the standard algorithm implemented in ArcGIS. Local relief was calculated with the "Focal Statistics" toolbox (statistics type "RANGE", circular neighbourhood with radius = 500 m).

4 Results and Discussion

The results from the previously described mapping and analyses are here discussed and interpreted with reference to the motivation and objectives from Chapter 1. The presentation of results mostly takes place in the appendices:

- Map of process domains and landslide map, illustrated with different (additional) map content in Appendix 1; quantitative synthesis of the map of process domains in Appendix 2
- Surface characteristics of individual landslides: presentation of selected variables in Appendix 1, and synthesis diagrams in Appendix 2
- Stream longitudinal profiles in Appendix 3
- Regional topographic / geological profiles in Appendix 4

In sections 4.1 and 4.2, the spatial distribution and characteristics of (hillslope) process domains and landslides are analysed, highlighting different relations to topographic and geological variables.

In section 4.3, the present state and potential (future) dynamics of stream longitudinal profiles are interpreted.

4.1 Hillslope process domains: spatial distribution, topographic and geological control

The results of Appendices 1 and 2 are here used to discuss the spatial distribution of (hillslope) process domains and landslides as well as their topographic and geological controls. The diagrams of Appendix 2 contain a variety of information, with an attempt made here to extract some key observations. The terms "landslide" or "landslide-affected" subsequently summarise the process domains of both "evident landslides" and "presumed landslides".

4.1.1 Regional spatial pattern

Appendix 1.C shows that in general, the central part of the siting region appears rather "quiet" with respect to landsliding. A large proportion of this region consists of the "upland low-relief area" of the "Bözbergplateau" (see Appendix 1.A for location names) and "presumably unfailed hillslopes", associated with the lithostratigraphic domains of Tertiary sediments (Molasse), Villigen-Formation and Wildegg-Formation (Appendix 1.C). On the other hand, landslides within the mapping area appear particularly concentrated in the following regions:

- Within Tertiary sediments (Molasse) along the Aare river, i.e. southern margin of the Bözbergplateau (southeastern corner of siting region)
- Within various lithostratigraphic units along the Mandach thrust fault north of the siting region, from Frickberg in the west to Böttstein next to the Aare in the east

Not very surprisingly, Appendix 1.E and F indicate the correlation of this (regional-scale) pattern with slope gradient and local relief. Most mapped landslides of the study area spatially coincide with a local relief of > 100 m (calculated for a circular window of 1 km diameter), and corresponding values of $> \sim 200$ m are observed for most of the large landslides (threshold in Appendix 1.F arbitrarily set to ≥ 0.2 km²). This relation is further indicated in the regional topographic / geological profiles of Appendix 4.

4.1.2 "Landslide susceptibility" of lithostratigraphic units

The "landslide susceptibility" of the different lithostratigraphic units is here estimated from the map of process domains, as percentage of the totally mapped landslide surface in relation to the total hillslope area within a given lithostratigraphic unit (Tab. 4). The proportions are also indicated in Appendix 2.

Tab. 4: "Landslide susceptibility" estimated as percentage of totally mapped landslide surface in relation to the total hillslope area of a given lithostratigraphic unit.

Landslides surfaces include terrain segments of both "presumed landslides" and "evident landslides".

Lithostratigraphic unit	Total landslide surfaces [km ²]	Total hillslope area [km ²]	"Landslide susceptibility" [%]
Tertiary sediments (Molasse)	3.6	9.9	36.5
Villigen-Formation	0.6	5.2	12
Wildeggen-Formation	6.6	23.3	28
Ifenthal-Formation	1.25	2.6	48
Hauptrogenstein / Klingnau-Formation	1.6	4.6	34
Passwang-Formation	2.1	3.0	70
Opalinus Clay	3.8	4.7	81

It should be noted that these results must not be considered as absolute values, given the uncertainty generally involved in landslide mapping, the restriction to areal statistics (no volumes / rates) or the heterogeneous topographic conditions across the mapping area. Also, they are specific to the present study area and may differ in other regions. Nevertheless, the results indicate some trends that can partly be related to the lithologic descriptions and data on rock strength in Tab. 1 (Chapter 2). According to this, "landslide susceptibility" tends to increase from mostly calcareous (Villigen-Formation), to increasingly marly (e.g. Wildeggen-Formation) and finally clay-rich formations (Opalinus Clay), accompanied by a decrease in rock strength. It should be noted again, that these observations do not include and quantify rock fall processes (see explanations in section 3.2.1), which are nevertheless relevant to more brittle, calcareous lithostratigraphic units, particularly the Villigen-Formation and Hauptrogenstein.

As an important observation, the pie chart presentations of landslides in Appendix 2 as well as the lithostratigraphic boundaries in Appendix 1.C and Appendix 4 indicate, that many of the larger landslides involve more than one lithostratigraphic unit. This is particularly true for the northern boundary of the siting region, where different lithostratigraphic units crop out at the surface within short distance. This implies that the "landslide susceptibility" of a lithostratigraphic unit (as calculated above) can be influenced by its underlying unit. For instance, most of the larger landslides in the Passwang-Formation also involve Opalinus Clay (forming the lower hillslope sections of the landslides). Although at much a lower level (12 %), the "landslide susceptibility" of the Villigen-Formation also seems to be significantly controlled by destabilising effects of the Wildeggen-Formation at lower hillslope sections.

From the lithologic descriptions and rock strength data in Tab. 1, it can be inferred that within the study area, these multi-lithological landslides often correspond to a "hard-over-weak" setting, where the harder lithostratigraphic units at the top of hillslopes are rather "passively involved" in landsliding by destabilisation of their underlying (potentially weaker) lithostratigraphic units. This will be further discussed in the interpretation of landslide types in section 4.2.

4.1.3 Topographic / morphometric characteristics of landslides and hillslopes

This section particularly aims at interpreting the information on topographic / morphometric characteristics of landslides and hillslopes according to the diagrams of Appendix 2. Where helpful, again references to map representations from Appendix 1 will be made.

As indicated by the size of the pie charts, all lithostratigraphic units intersect with **landslides** of very different **size**, ranging from small landslides in the order of 0.001 km² to large and potentially deep-seated landslides in the order of a few 0.1 km² or even ~ 1 km². However, large landslides within the study area show some tendency of higher frequency in association with Opalinus Clay and within the Tertiary sediments (Molasse) towards the Aare (Appendix 1.C). This is attributed to: i) the spatial correlation with a higher **local relief** along the northern boundary of the mapping area and along the Aare (Appendix 1.F), combined with ii) the potential of Opalinus Clay and (possibly) marly layers within the Molasse sediments to facilitate deep-seated landslides.

While local relief thus seems to be a good predictor for the spatial distribution of **landslides**, a **relation with slope aspect** is less obvious in the study area. This is subsequently analysed in more detail:

- As pointed out in Chapter 2, bedding planes within the study area are mostly flat or gently dipping southward. A moderate southward directed steepening is observed near the Mandach thrust fault in the north and partly towards the Aare below the southern margin of the Bözbergplateau (Appendix 4.A).
- Assuming a strong structural control on landslides by the orientation of bedding planes, a concentration of landslide surfaces on south-facing slopes would therefore be plausible. At least for larger (and potentially deep-seated) landslides, this is observable for the Tertiary sediments (Molasse), while more vaguely indicated for the Villigen-Formation, the Wildeggen-Formation and Ifenthal-Formation (Appendix 2). In case of the Passwang-Formation and Opalinus Clay, this dependency is not indicated at all. The comparison with the pixel-based distribution of hillslope orientation (summarised for both unfailed and landslide-affected) within each lithostratigraphic unit (Appendix 2) suggests, that the distribution of landslide surface orientation is strongly controlled by the general distribution of hillslope exposition.
- These observations could indicate either that structural control (by orientation of bedding planes) plays a minor role for landsliding in certain lithostratigraphic units and/or that dip angles tend to be too flat in the study area to have a significant impact on landsliding.
- However, potential differences with respect to shallow vs. deep-seated landslides are not accounted for in this observation. Therefore, with respect to depth of landslides and erosion rates, slope aspect in relation to dip direction may still be a relevant factor, at least for some lithostratigraphic units. Also, the impact of slope aspect may vary in time, as dip angles and directions relative to topography can locally change during landscape incision (see subsurface projection of lithostratigraphic boundaries in Appendix 4).

Finally, Appendix 2 and map representations of Appendices 1.E and 1.F show the variability of **slope gradients of hillslopes and landslides** across different lithostratigraphic units. As an additional illustration, the pixel-based slope gradients of the hillslope domain displayed in the radial diagrams of Appendix 2, have been rearranged as histograms in Fig. 10. From these various illustrations, the following observations are made:

- Within the hillslope domain, typical hillslope angles between 5 and 25° degrees (pixel-based values, 2 m grid size) are observed in case of Tertiary sediments (Molasse), the Wildeg-Formation, Ifenthal-Formation and Opalinus Clay. These lithostratigraphic units, which include marls or claystones (Opalinus Clay), are characterised by a unimodal histogram of slope gradients in Fig. 10, with modal values around 10°.
- On the other hand, slope gradients > 30° are mostly associated with rock cliffs along plateaus formed by more competent calcareous rocks (Villigen-Formation, Hauptrogenstein). However, much lower values (< 15°) are observed within these lithostratigraphic units, too. This also reflects the fact, that the present analysis does not distinguish bedrock surfaces from hillslopes covered by Quaternary deposits / debris. In combination, the results are the bimodal histograms of the Villigen-Formation and Hauptrogenstein / Klingnau-Formation in Fig. 10.
- Although less pronounced, the bimodal character is also indicated in case of the Passwang-Formation. This can be explained by the fact, that this formation predominantly intersects with intermediate to higher hillslope sections beneath the Hauptrogenstein, where slope gradients typically are still higher than in lower hillslope sections (see also Appendix 1.E for comparison, however, in that case displayed for DHM25, with grid size of 25 m). Also, the internal stratification of the Passwang-Formation (Tab. 1, Chapter 2), including more competent limestone sequences aside from marls and claystones, may contribute to the distribution of slope gradients. In terms of hillslope gradients within the study area, the Passwang-Formation can thus be considered a "hybrid" of the two other groups described above.
- The median values of all lithostratigraphic units are higher than those calculated with a coarser spatial resolution of 250 m by Yanites et al. (2017), who found the following results for different rock types in the eastern Jura Mountains: shale = 7.4°, sandstone = 8.5°, limestone = 10.8°. This shows how finer-scale hillslope features with higher slope gradients are smoothed on the coarse analysis scale and are therefore not adequately represented in a larger-scale model. However, the relative increase of slope gradients from weak (shale) to more competent rock types (sandstones and limestone) is confirmed by both the coarse (Yanites et al. 2017) and the fine analysis scale (this study).
- With respect to landslide surfaces, Appendix 2 (and Appendices 1.E and 1.F) indicates a trend of decreasing mean slope angles with increasing area or internal relief. This observation is shared for all lithostratigraphic units. However, differences are again observed with respect to the range of slope angles. While the mean surface orientation of large landslides intersecting with Tertiary sediments (Molasse) or Opalinus Clay for instance shows typical slope gradients in the range of 10 to 15°, a shift to higher values (> 15°) is particularly observed for landslides intersecting with the Villigen-Formation (although dominated by the Wildeg-Formation). Also, some trend towards steeper landslide surfaces is observed for north-facing as opposed to south-facing landslides in several lithostratigraphic units. However, a differentiation of shallow vs. deep-seated landsliding is again not accounted for in this observation.

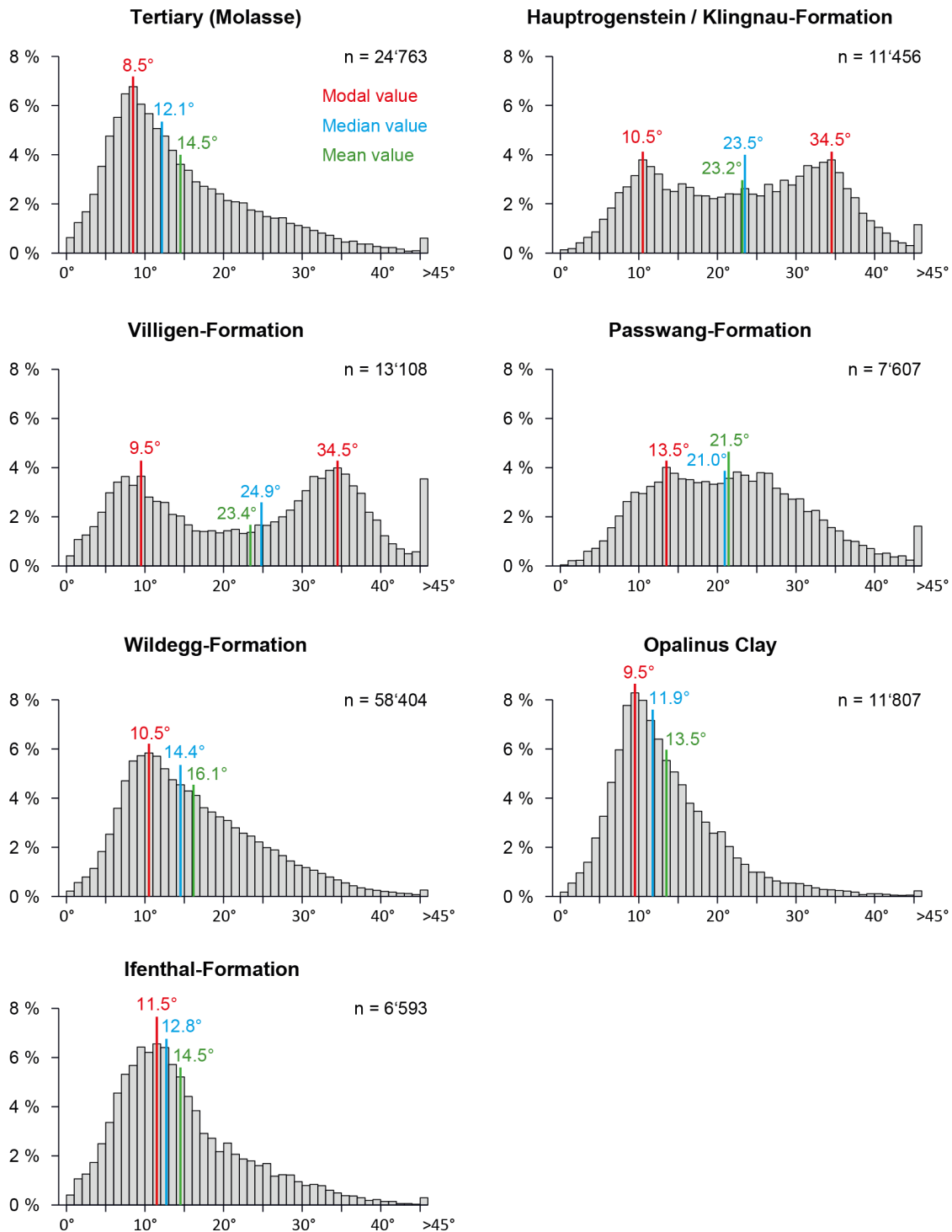


Fig. 10: Histogram and statistical measures of slope gradients within the hillslope domain of the study area, separated for individual lithostratigraphic units.

The hillslope domain summarises the classes "presumably unfailed hillslopes", "presumed landslides" and "evident landslides" according to the map of process domains (Appendix 1.C). Slope gradients correspond to a subsample of pixel-based values from DTM-AV (2 m grid size), with only every tenth raster cell in both East – West and North – South direction being represented (see section 3.3.2). Number 'n' indicates the resulting number of pixels for each lithostratigraphic unit. The same dataset is used in the radial diagrams of Appendix 2. Note that frequencies of values steeper than 45° are summarised in the histograms.

4.2 Landslide types

So far, landslide-affected hillslopes have been mostly considered without differentiating landslide types. As pointed out in section 3.2.1, this is also difficult and not systematically applicable in case of the general (remote) mapping approach of this study. Still, it has important implications, particularly with regard to spatiotemporal characteristics of hillslope erosion:

- Areal extent of landslide
- Depth of movement: i.e. deep-seated vs. shallow processes (according to section 3.2.1)
- Temporal behaviour: discrete vs. continuous / long-term processes; movement rate

Deformation measurements, which usually are a key to process description, have not been available for this study. An attempt in the context of this study to detect recent slope movement by subtraction of two temporally separated DTM records (DTM Jura Ost – DTM AV), did not reveal any signals either. The latter may indicate, that no significant landslides occurred over the considered time interval (2001 – 2015). On the other hand, deformation rates of continuous / long-term landslide processes in the order of mm to dm/year may also be too small to be identified by such change analysis (i.e. "digital elevation model of difference").

Important landslide types of the study area are therefore identified (or interpreted) by:

- Process description from historic records (available for few examples)
- Interpretation based on morphological and geological characteristics, therefore, analogies from other landslide descriptions are used (e.g. Hungr et al. 2014)

First, the focus is put on the kinematics of **large and potentially deep-seated landslides** / landslide complexes. "Large" means, that they typically affect an entire hillslope from a plateau / crest down to a valley floor or stream channel. The areal extent of such landslides in the study area ranges from a few 0.1 km² to approximately 1 km², while the internal relief ranges from ~ 100 m to a maximum of ~ 300 m. The term "deep-seated" is expected here to involve depths of movement in the order of > 10 m up to a few tens of meters (section 3.2.1). However, the latter is only inferred from analogies from literature (e.g. Reichelt 1967, Hungr et al. 2014) and from the construction of geological cross sections, where basal rupture surfaces are (speculatively) projected from the geometry of surface features (see below).

The second part presents **earthflows**, being a well-documented landslide type of the study area that potentially superimposes large deep-seated landslides (see below).

Finally, **other** (potentially) relevant landslide types such as shallow slides or rock fall are addressed.

4.2.1 Characteristics and types of large, deep-seated landsliding

Large, deep-seated landslides (according to definition above) seem to be relatively widespread in the study area. They are associated with correspondingly high local relief (> 100 m, see Appendix 1.F) along the northern boundary of the siting region and towards the Aare. As a result of their geographical distribution, they involve a variety of geological settings. This leads to different surface expressions and potentially different landslide kinematics.

As a key observation it is noted, that large parts of these landslide surfaces (and likely landslide rupture surfaces) intersect with potentially weak rock types of marly or clayey material. In accordance with Hungr et al. (2014), ductile deformation is therefore expected to play an important role for these landslides.

Mechanisms of brittle failure, on the other hand, are characteristic for more competent rock types. Within the study area, the latter are particularly represented by the calcareous rocks of the Villigen-Formation and Hauptrogenstein. Additionally, some competent layers can be expected within the Tertiary sediments (Molasse; not further differentiated here) or as more calcareous layers (alternating with marly layers) within the Wildeggen-Formation and Passwang-Formation.

Concerning brittle failure mechanisms, the following observations should be noted with respect to the study area:

- No large landslide types¹² have been observed, that would typically be associated with brittle failure (e.g. rapid rockslides ("Felssturz" / "Bergsturz") with long runout distance of fragmented rock material)
- The competent lithostratigraphic units of the Villigen-Formation and Hauptrogenstein typically occur as cap rocks, overlying weaker lithostratigraphic units of Wildeggen-Formation or Passwang-Formation / Opalinus Clay, respectively. In this setting, they are rather "passively involved" in large landslides, that have their basal rupture surface mainly located within the underlying (weaker) lithostratigraphic unit (see considerations in section 4.1 "Landslide susceptibility" of lithostratigraphic units).

The corresponding "hard-over-weak" setting is illustrated by simplified geological cross sections in Figs. 11 and 13 for two different geological settings of the study area. Since in these cases, the landslide is "favored" by the weaker lithostratigraphic unit in the lower section of the hillslope, large deep-seated landslides may also occur without the displayed cap rock of more competent material (i.e. Villigen-Formation or Hauptrogenstein). Such examples are for instance found in the domain of Tertiary sediments (Molasse) in the southeastern corner of the mapping area or in the most northern region of the study area, where the Hauptrogenstein has been completely eroded.

While the large deep-seated landslides of the study area seem to involve some degree of ductile deformation as a common feature, the specific landslide types (kinematics) may still vary. The lithostratigraphic units involved and the relative orientation of discontinuities with respect to hill-slope orientation are important factors in this process-related context. With respect to kinematics, a distinction is made between "slides" along a well-defined (discrete) rupture surface and the landslide type "rock slope deformation", where the deformation rate shows a more continuous transition with depth. Keeping this distinction in mind, the following landslide types (according to Hungr et al. 2014; Tab. 3, section 3.2.1 this study) have been attributed to different lithostratigraphic units of the study area and observed morphologies:

- **"Rock slope deformation"**: This involves potentially long-term but very slowly acting (~ mm to cm year¹³), ductile deformation, without a fully defined basal rupture surface (see above). This is typical for weak claystones and marls and is therefore suggested for landslides intersecting with Opalinus Clay (Fig. 11), but also possible for marly layers of the Tertiary sediments (Molasse), Wildeggen-Formation, Ifenthal-Formation, Klingnau-Formation and Passwang-Formation. It is assumed and supported by observation (e.g. deformation of opposite hillslopes in Figs. 11 and 12) that "rock slope deformation" is favored by dip slopes, however, also commonly observed where slope aspect is opposed or oblique to the orientation of bedding planes / discontinuities. This is explained here by the assumption that, similar to soil, a deformation zone may evolve more independently from structural controls within such geomechanically weak material.

¹² For smaller (rock fall) processes, see end of this section.

¹³ Periodical acceleration with higher rates can occur.

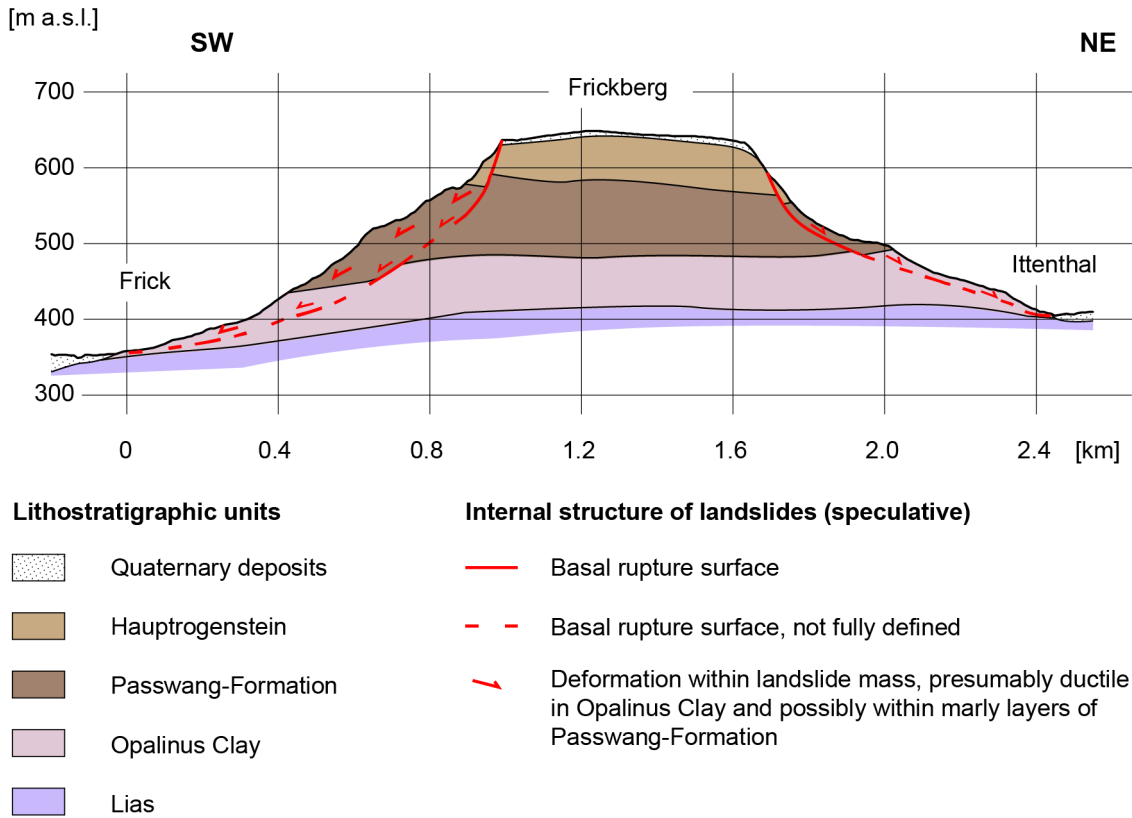


Fig. 11: Simplified geological cross section with interpreted "rock slope deformation" on opposite hillslopes of Frickberg.

Note that vertical axis is scaled by factor 2. See Appendices 1.A and 4.B for geographical location. For parts of the southwestern hillslope of Frickberg, an event or period of increased activity is documented for the year 1843, according to the Geological Atlas of Switzerland 1:25'000.



Fig. 12: Surface morphology of hillslopes potentially affected by slow but continuous "rock slope deformation" (indicated by red arrows) on northwestern flank of Frickberg.

This hillslope is opposed to the dip slope. For location of Frickberg, see Appendix 1.A.

As mentioned above, "slides" involve movement along a fully developed basal rupture surface. Depending on the geometry of this rupture surface, Hungr et al. (2014) distinguish different landslide types, with implications for the internal and surficial deformation of the surface mass and landslide velocity. It is assumed that many of the slides of the study area correspond to the type **"rock compound slide"**, where the rupture surface is defined by "several planes, or a surface of uneven curvature" (Hungr et al. 2014, p. 175). In contrast to a purely planar or cylindrical rupture surface, this geometry requires significant internal deformation of the landslide mass. For many landslides of the study area, such deformation is supported by corresponding roughness features at the surface, as seen for instance in the DTM derivatives of Fig. 6 (section 3.2.2).

An interpreted example of a rock compound slide is illustrated in the cross section of Fig. 13. In contrast to the "rock slope deformation" of Fig. 11, this illustration should indicate a stronger structural control, where lithostratigraphic units are internally characterised by a sequence of less competent (e.g. marly) vs. more competent (e.g. calcareous) layers, with deformation favored along the weaker bedding planes¹⁴. While the example is shown for the Wildegge-Formation, the characterisation of lithostratigraphic units in Tab. 1 (Chapter 2) suggests, that such behavior may also apply to the Tertiary sediments (Molasse), the Ifenthal-Formation, Klingnau-Formation and Passwang-Formation.

According to Hungr et al. (2014) rock compound slides may be slow or rapid. The temporal behavior is certainly modified by detailed properties of the rupture surface, i.e. i) lithological properties, e.g. rather ductile / slower deformation in case of marly and clayey rupture surfaces, ii) higher velocities in case of steeper and more planar surfaces, iii) influence of water on rupture surfaces.

Some of the large deep-seated landslides of the study area may also represent a transition between slide types and "rock slope deformation". Hungr et al. (2014, p. 189) observe, that rock slope deformation "may facilitate the development of compound rock slides by pre-shearing weak horizons". In any case, a final classification will remain difficult in the absence of deformation measurements and knowledge of the landslide structure at depth.

¹⁴ Although referring to a smaller landslide (< 0.1 km²), Fig. 20 suggests how sliding occurs along such well-defined (and at least locally planar) bedding planes within the Wildegge-Formation.

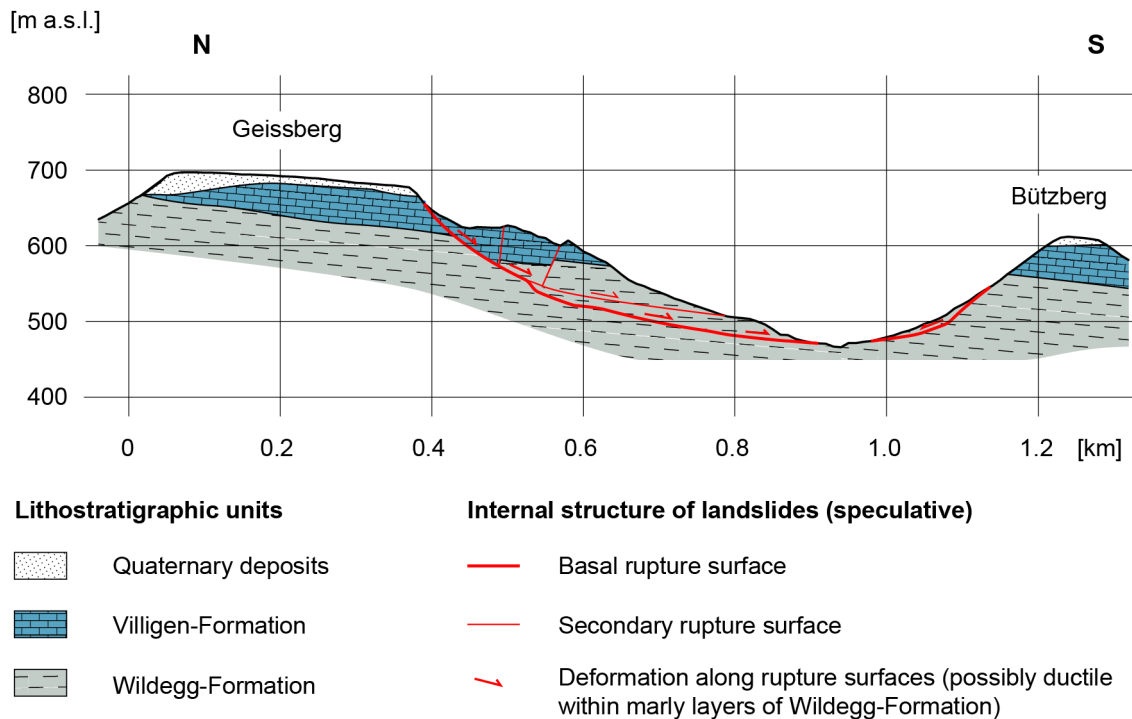


Fig. 13: Simplified geological cross section with interpretation of large deep-seated landslide on south flank of Geissberg and more shallow slope deformation on opposite hill-slope.

Signatures within lithostratigraphic units indicate approximate orientation of bedding planes (according to Geological Atlas of Switzerland 1:25'000). A photograph of the south flank of Geissberg is shown in Fig. 23 for comparison. For location, see Appendices 1.A and 4.A.

4.2.2 Earthflows

As a special feature of the study area, several earthflow-like landslides have been documented and are partly still expressed in the landscape as earthflow "tongues". Based on their number and depth of deformation, earthflows may be less important for the overall contribution to regional hillslope erosion or to an exposure of the repository than the deep-seated landslides described above. However, with potential velocities in the order of m/day or m/hour they represent a hazardous phenomenon, which explains some of the attention they have received, and which is documented in historic records (Baltzer 1876, Hartmann 1928 and 1950, Haefeli 1940). According to Hungr et al. (2014, p. 187), earthflows are defined as:

- "Rapid or slower, intermittent flow-like movement of plastic, clayey soil, facilitated by a combination of sliding along multiple discrete shear surfaces, and internal shear strains. Long periods of relative dormancy alternate with rapid 'surges'".

Within the study area, examples are found for the area of Schinberg (Figs. 14 to 17) and towards the Aare near Böttstein (Figs. 18 and 19). Except for the example in Fig. 19 (Passwang-Formation), the earthflows presented here are associated with Opalinus Clay. Earthflows can superimpose deep-seated landslide complexes (for instance earthflow on south flank of Nassberg, Fig. 19).

Initiation or surges of earthflows may be explained by changes in pore water pressure. Accordingly, Hartmann (1928) and Haefeli (1940) identify springs, snowmelt and periods of increased rainfall as potential factors for triggering or acceleration of earthflows. In some cases, land-use change (e.g. forest to farming, with potential impacts on hillslope hydrology and root cohesion) might historically have influenced the occurrence of earthflows.

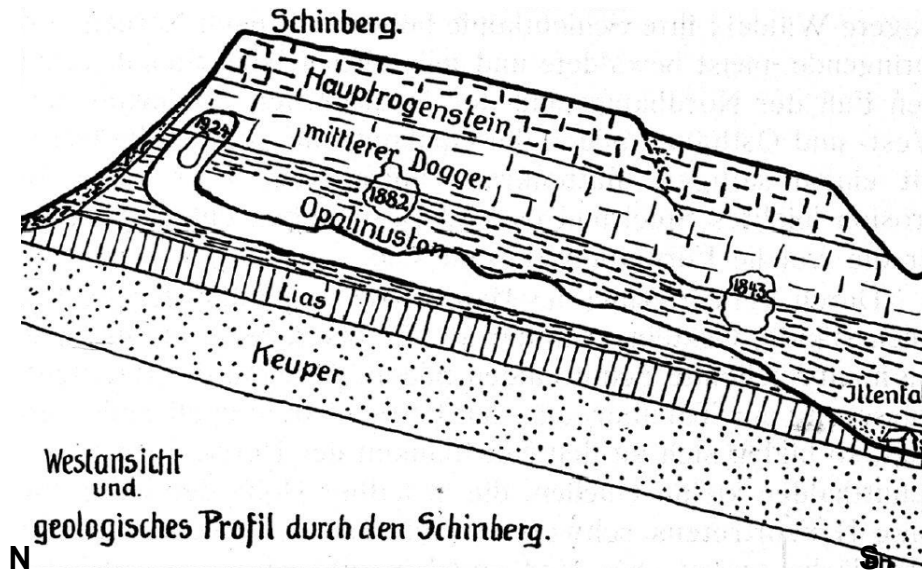


Fig. 14: Geological cross section of Schinberg (Hartmann 1928, p. 58).

In analogy to Fig. 11, weak lithologies are overlain by more competent Hauptrogenstein. Landslides (mostly interpreted as earthflow-like landslides) have been recorded in 1843, 1882, 1926 and 1939 (Haefeli 1940). While the general dip direction points southward, these landslides occurred on the southwestern, western and northern slopes, which indicates that the occurrence of these landslides seems to be rather topographically/lithologically than structurally controlled. For location of Schinberg, see Appendix I.A.

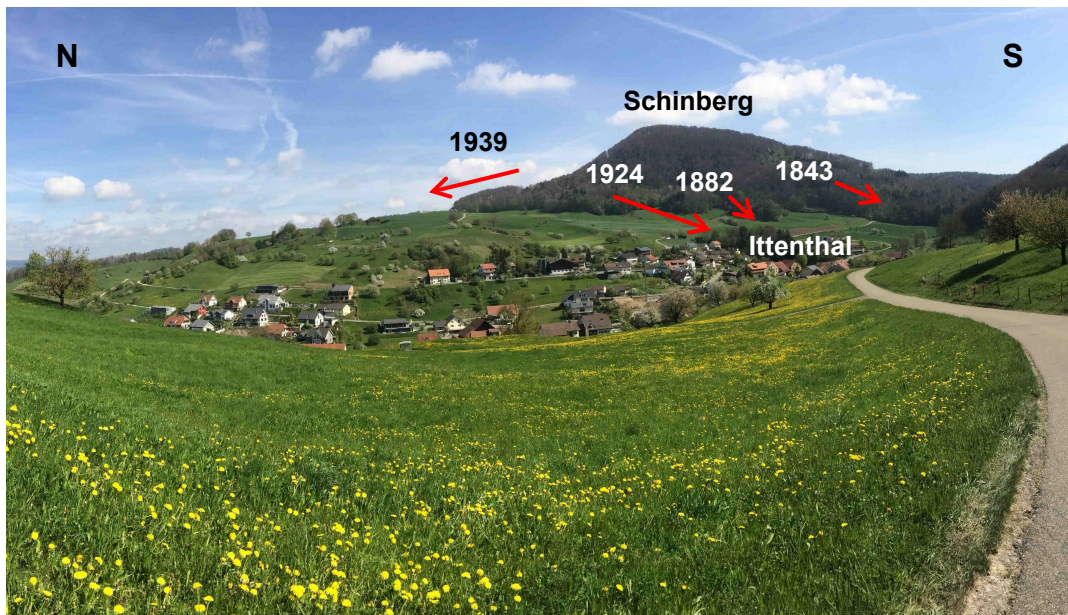


Fig. 15: Present-day situation at Schinberg, as seen from the west.

Location with one of the highest (recent) landslide activity in the study area. Approximate locations, direction and year of recorded landslides are indicated (according to Fig. 14 and Geological Atlas of Switzerland 1:25'000). For location, see Appendix I.A.



Fig. 16: Earthflow at Schinberg from February 1924 to 1926 (Hartmann 1928, p. 61). See approximate location in Fig. 15.



Fig. 17: Earthflow at Schinberg in spring 1939 (Haefeli 1940, p. 182).
See approximate location in Fig. 15.

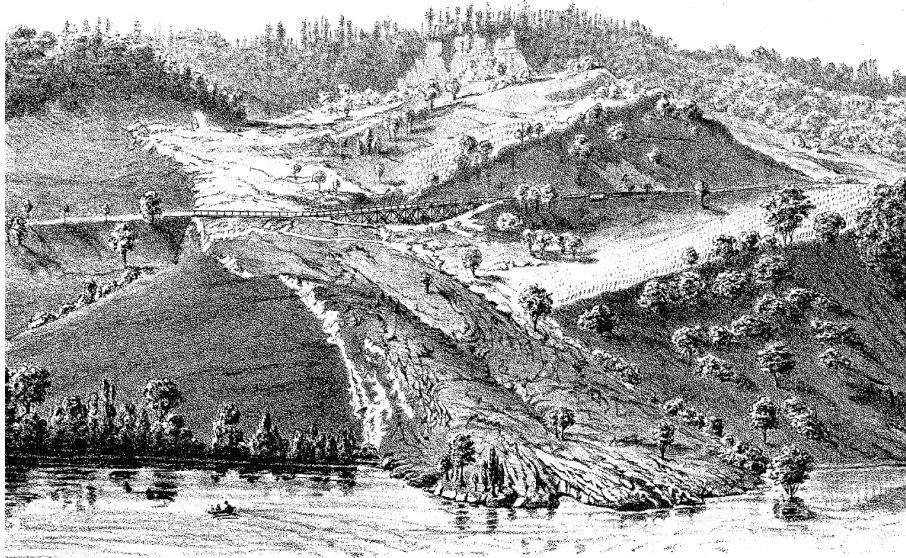


Fig. 18: Earthflow reaching the Aare near Böttstein in March 1876 (Baltzer 1876, p. 290).
This landslide is reported to have occurred within the Opalinus Clay. Probably, this spatially coincides with the location of a present-day clay pit south of Böttstein; for supposed location, see reference to this figure in Appendix 1.A.



Fig. 19: Interpreted (tongue-shaped) earthflow south of Böttstein, attributed to the Passwang-Formation according to the Geological Atlas of Switzerland 1:25'000.

This earthflow occurred on top of a large (potentially deep-seated) landslide on the south-flank of Nassberg. For location, see reference to this figure in Appendix 1.A.

4.2.3 Additional landslide types

While the large landslides (e.g. rock slope deformation, rock compound slide) and earthflows described above have already been interpreted as prominent hillslope processes of the study area, additional landslide types according to Tab. 3 (section 3.2.1) also contribute to total hillslope erosion. However, some of them may be less frequent or more difficult to detect and interpret by the remote mapping approach, e.g. due to i) small size of individual events, ii) weak surface expression of some shallow or diffuse landslide processes, iii) landslides being overprinted over time by other geomorphological processes or anthropogenic effects.

As pointed out in section 3.2.1, **rock fall** is certainly a relevant surface process for steep cliffs of more competent rock (particularly Villigen-Formation and Hauptrogenstein) along the boundary of plateaus (e.g. Geissberg, Frickberg).

The process type "slide" is also represented by smaller and potentially shallow landslides. This can for instance involve **planar or rotational slides** of soil or debris, triggered by heavy rainfall events or by fluvial erosion along channels. In some cases, near-surface bedrock may similarly be displaced by planar sliding along bedding planes, as interpreted from the example in Fig. 20.

Rock fall and the smaller slides described above can superimpose large, deep-seated landslides.

The process types "topple" and "spread" are not found to be relevant processes for landsliding in the study area, apart from possible small-scale toppling in rock fall source areas / cliffs.



Fig. 20: Head scarp of a medium-sized landslide ($\sim 0.07 \text{ km}^2$) within Wildegg-Formation, potentially representing sliding along a (nearly) planar rupture surface corresponding to well-defined bedding planes.

Red arrows indicate approximate dip direction of bedding planes and corresponding sense of movement of the landslide mass. The large trees within the scarp further suggest that the initiation of this landslide is rather old (several decades or even more). The location approximately corresponds to the coordinates 651'500 / 264'000; see also reference to this figure in Appendix 1.A.

4.3 Stream longitudinal profiles

The analysed stream profiles all contain anomalies, which are either expressed as distinct knick-points or as less obvious convex sections along the profile (Appendix 3). Apart from the shape and magnitude (vertical offsets in the range of a few meters up to several decameters) of these features, differences among the individual profiles can be observed with respect to the number of anomalies, their relative position along the profile (distance and elevation) and lithological substrate of the channel (alluvial vs. bedrock channels, lithostratigraphic units).

Where appropriate, an attempt is made here to group profiles with similar characteristics (profile geometry, main direction of drainage, lithostratigraphic units). The grouping pursues the following purposes:

- Identifying common signals (e.g. similar anomalies in the same lithostratigraphic units or at similar elevations): an interpretation can be expected to be more robust, if it is based on multiple observations. The latter can possibly also help "disentangle" signals of artificial vs. natural effects.
- Generalisation should help to gain a "greater picture": e.g. is the potential for future fluvial incision homogeneous for the entire study area, or is there a regional imbalance?

Subsequently, groups of stream profiles are described and interpreted in separate subsections. In the final section, the interpretation is synthesised with regard to the complete study area.

The geographical overview of the stream courses, together with the geographical position of anomalies indicated in the longitudinal profiles, is to be found in Appendix 1.G. The individual stream longitudinal profiles from Appendix 3 are additionally grouped and presented in Fig. 21.

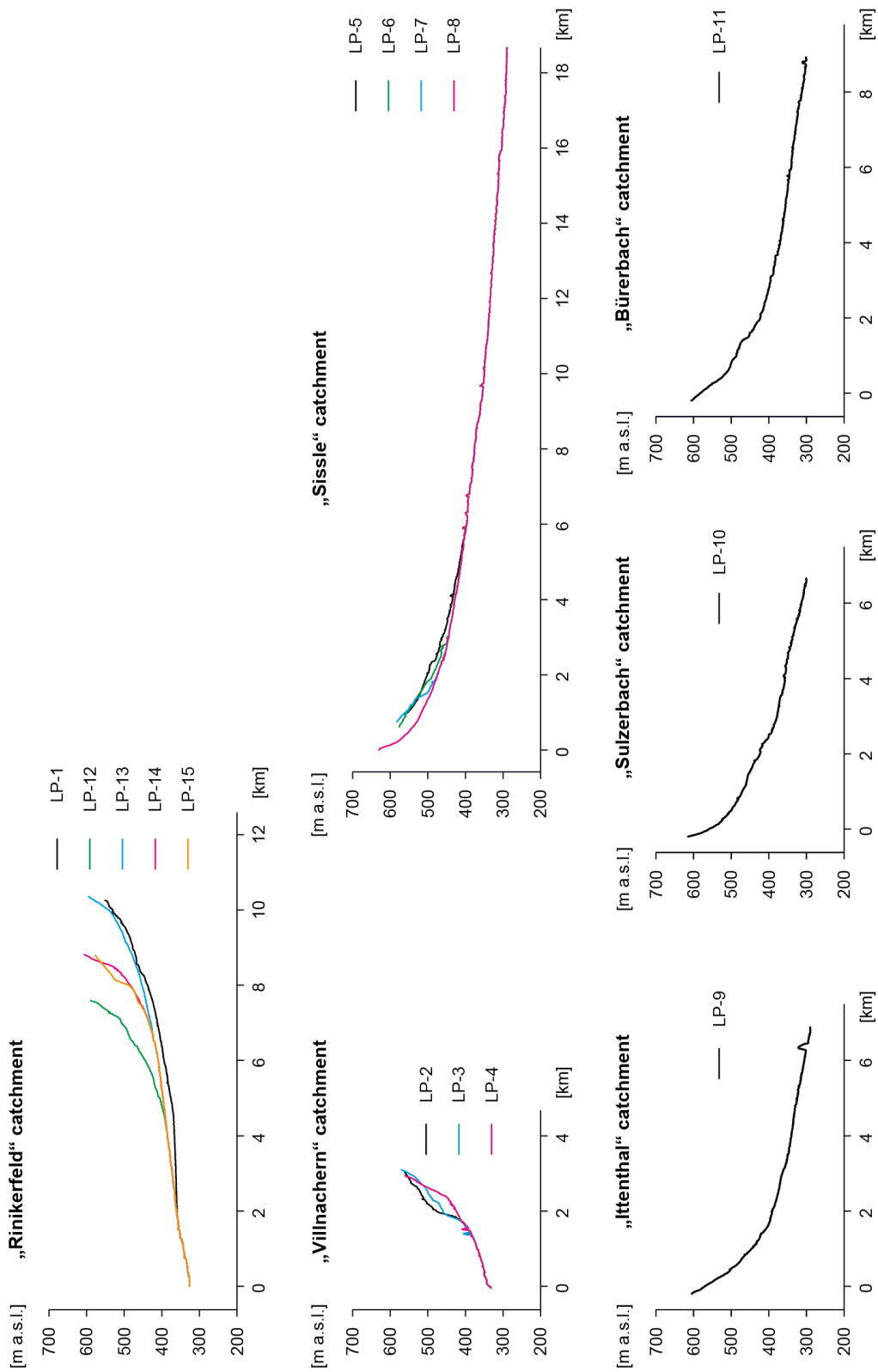


Fig. 21: Stream longitudinal profiles of the study area, grouped according to different catchments.

For detailed presentation of the individual profiles see Appendix 3. For the geographical location see Fig. 8 or Appendix 1.G.

4.3.1 "Rinikerfeld" catchment (LP-1, -12, -13, -14, -15)

These streams, located in the northeastern part of siting region, are characterised by a common outlet into the Aare river near Villigen. While the headwaters of LP-1 /-14 /-15 have incised into the Bözbergplateau, LP-12 /-13 originate from more northern areas near Mönthal and southwest of Geissberg.

In case of LP-12 /-13, the bedrock surface entirely corresponds to the Wildegg-Formation. In their most upper reaches (Bözbergplateau), the other profiles include shorter sections of Villigen-Formation and "Obere Süsswassermolasse" (Tertiary sediments). Alluvial channel sections prevail below an altitude of approximately 400 m a.s.l. These sections mostly correspond to the level of Late Pleistocene fluvial deposits (Fig. 22), which together with other Quaternary deposits fill the section of a former valley axis of the Aare river ("Paläo-Rinne Rinikerfeld"; see Schnellmann et al. 2014).

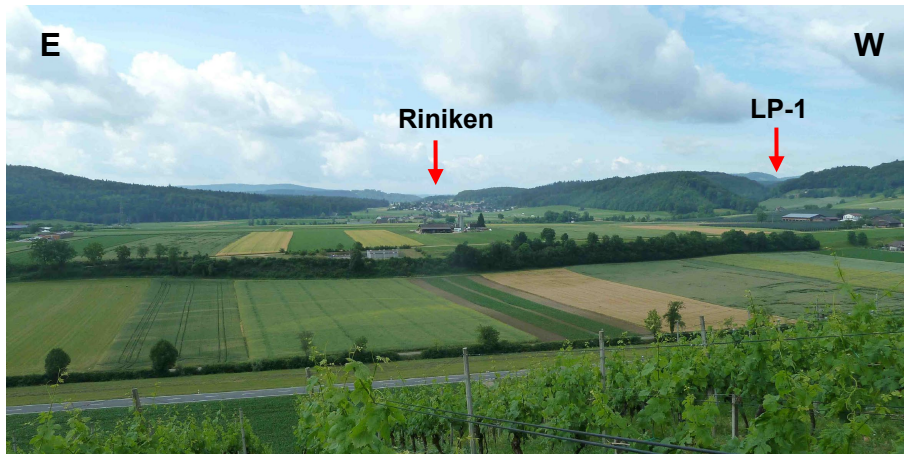


Fig. 22: View from southeastern hillslope of Geissberg (east of Remigen) towards Riniken.

The flat area represents the Rinikerfeld (former course of the Aare valley, filled with Quaternary deposits). Towards southwest, the upstream section of LP-1, which has incised into the inner regions of the Bözbergplateau, is indicated. For location of place names, see Appendix 1.A.

Between the outlet into the Aare River and the final confluence of LP-1 with the other streams, a steepening of the profile is observed as compared to the upstream sections. This results in a convex anomaly / knickpoint at an elevation of approximately 360 m a.s.l. At this location no obvious signal of lithological control, anthropogenic effects / artefacts or material input by lateral landslides can be identified. Therefore, the anomaly is attributed to the incision of the Aare relative to the level of the Late Pleistocene fluvial deposits. The anomaly thus potentially represents a migrating knickpoint in response to base level drop.

Above this knickpoint, LP-13 (entirely located in the domain of Wildegg-Formation) shows a concave profile without distinct anomalies. This suggests that its profile section above the Rinikerfeld has fully adjusted to the level of Late Pleistocene fluvial deposits.

In analogy to the lithostratigraphic setting of LP-13, LP-12 also shows a mostly concave profile above the anomaly at 360 m a.s.l. However, the profile is more irregular with local anomalies above 400 m a.s.l. This spatially coincides with the large landslide on the south flank of Geissberg (Fig. 23 and Appendix 4.A), which potentially counteracts fluvial incision in this section by lateral material input to the channel. Therefore, the adjustment to a graded stream profile geometry seems to be not fully completed yet.

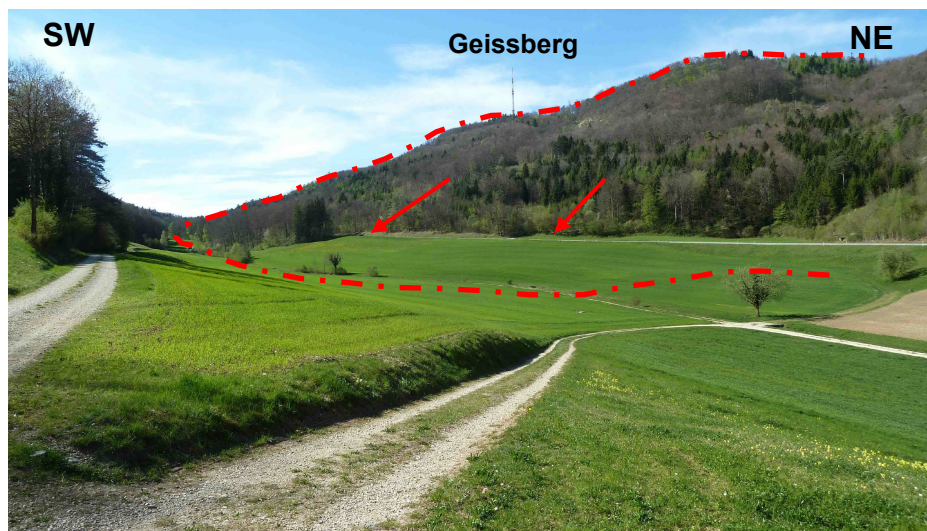


Fig. 23: Large landslide on south flank of Geissberg, potentially "counteracting" fluvial incision along stream longitudinal profile LP-12 by lateral material input.

For location, see reference to this figure in Appendix 1.A.

The remaining profiles LP-1 /-14 /-15 all show knickpoints in the headwater regions of the Bözbergplateau. These spatially coincide with profile sections of the Villigen-Formation, which here correspond to a lower altitude than in the more northerly regions of LP-12 and -13 (see also Appendix 4.A). The knickpoints suggest a lithological control by a higher substrate resistance in these calcareous rocks. Landsliding does not seem to be relevant. Following section 3.5.3, these knickpoints could represent fixed (or very slowly migrating) features.

4.3.2 "Villnachern" catchment (LP-2, -3, -4)

These streams in the southeastern part of the siting region are running from the Bözbergplateau near Linn towards the Aare River in the east. The bedrock mainly consists of Tertiary sediments, with only local outcrops of Upper Jurassic calcareous rocks (Villigen-Formation) that are mapped along LP-2 and possibly covered by debris in LP-3 and LP-4. All three profiles are characterised by a considerable elevation change (> 200 m) over relatively short distance (~ 3 km), thus forming the steepest streams of the study area.

Apart from anomalies next to the Aare, which are interpreted as anthropogenic effects, the lower reaches (< 400 m a.s.l.) indicate regularly concave shapes. Above 400 m a.s.l., convex sections and knickpoints are observed in each profile. The most prominent anomalies occur in LP-2 and LP-3, where they spatially coincide with the transition of "Obere Süswassermolasse" to lower lithostratigraphic units. In these steep transition zones, a lithological control by sections of more resistant substrate can be inferred (e.g. outcrop of Villigen-Formation in LP-2). Possibly, such more resistant sections are missing or less dominant in LP-4. This would explain the weaker expression of the signal in that profile.

In addition to the main knickpoints / anomalies, smaller ones can also be observed in the three profiles. Together, this turns the upper parts of the streams (> 400 m a.s.l.) into rather complexly shaped sections. According to the map of process domains (also displayed in Appendix 1.G as reference), this can partly be caused by material input from lateral landslides (see concepts in section 3.5.3).

Although less explicit in LP-4, the consistent occurrence of knickpoints / convex sections above 400 m a.s.l. in all three profiles could indicate knickpoint migration in response to base level drop. This explains the initiation of the mapped landslides, which in turn modify the shape of the stream profiles and decelerate (due to lateral material input to the channel) the upstream propagation of erosion.

Assuming that such migrating knickpoints in response to base level drop exist, it could be argued that the headwater sections (> ~ 500 m a.s.l.) preserve some of the geometry of a "perched low-relief landscape" (Fig. 9A), partly masked by landsliding. Considering its altitude, this "perched low-relief landscape" can potentially be related to the projected base level of TDS (see also intersection line with present topography in Appendix 1.D). In case of LP-4, the signal of base level drop has possibly been transmitted faster to the headwater region, due to the potential absence of more resistant sections along the channel. This gives a speculative explanation of why the "perched low-relief landscape" is hardly noticeable in this profile.

In conclusion, the three profiles are considered to be subject to ongoing knickpoint migration in response to base level drop. This is supported by observed landslides along the channels. The upstream propagation of erosion is partly decelerated and modified by material input from lateral landslides as well as lithological control. These factors may also explain differences in the geometries among the three profiles.

4.3.3 "Sissle" catchment (LP-5, -6, -7, -8)

These profiles belong to the "Sissle" catchment with its outlet to the Rhine River near Sisseln and headwater regions in the western part of the Bözbergplateau. The confluences of the different headwater sections are located in the region of Effingen. As a consequence, the stream profiles share an identical geometry over a relatively long distance. The lithostratigraphic setting of the upper stream sections is similar to the previously described Aare tributaries in the northeast of the siting region (see above). Again, the more southerly streams (LP-5, -6, -7) include short bedrock sections of the Villigen-Formation (calcareous rock) and "Obere Süßwassermolasse" (Tertiary sediments). In analogy to LP-13 and -14, the headwater section of the more northerly directed stream profile LP-8 has completely incised into the Wildegg-Formation.

Below an altitude of approximately 400 m a.s.l., the bedrock surface intersects with the various lithostratigraphic units from the Middle Jurassic (Ifenthal-Formation) to Triassic sediments (not differentiated here). However, the influence of lithological heterogeneities is reduced here, as the stream mostly consists of alluvial rather than bedrock channel sections (as indicated by the "top bedrock" surface projected in Appendix 3).

Weak convex anomalies can be interpreted at altitudes of ~ 305 and 370 m a.s.l. (identical for all four profiles). These could be related to incision of the Rhine relative to the level of Late Pleistocene fluvial deposits. The anomaly at 370 m a.s.l. spatially coincides with landslides on the south flank of Frickberg. However, these profile anomalies are not accentuated, and the interpretation therefore remains rather speculative.

In analogy to the streams of the northeastern part of the siting region ("Rinikerfeld" catchment), the geometry of the upper stream sections appears lithologically controlled. LP-8, which has completely incised into the Wildegge-Formation (same as LP-13) shows a graded profile up to the drainage divide above 600 m a.s.l. The other profiles (LP-5, -6, -7) again show knickpoints in the headwater regions of the Bözbergplateau. These are attributed to lithological control by more resistant substrate within the Villigen-Formation (Fig. 24). Again, these knickpoints are considered fixed (or very slowly moving). The projected base levels of HDS and TDS are poorly constrained and therefore more hypothetical in this region. As a consequence, it is difficult to judge, whether the "perched low-relief landscape" above these lithologically controlled knickpoints could possibly be linked to the base level of TDS.



Fig. 24: Knickpoint in LP-5 (northwest of Linn, 490 m a.s.l.), interpreted as lithologically controlled by higher substrate resistance within the Villigen-Formation (LP-5).

For exact location, see reference to this figure in Appendix 1.A.

4.3.4 "Ittenthal", "Sulzerbach", "Bürerbach" catchments (LP-9, -10, -11)

The streams considered here run more or less parallel along valleys from the northern boundary of the siting region to the Rhine river in the north. The lithostratigraphic setting is similar for all three streams. The drainage divide at about 600 m a.s.l. is situated within the Wildegge-Formation. The steepening of (southward directed) dip angles, associated with the Mandach thrust fault (see Appendix 4.A), results in a closely spaced sequence of Middle to Lower Jurassic units along the upper reaches of the channels (> ~ 400 m a.s.l.).

Below that altitude, the stream mostly corresponds to an alluvial channel in case of LP-9. The two other streams have longer bedrock channel sections.

All three profiles indicate convex anomalies at an altitude of about 340 m a.s.l., which however are not expressed very distinctly. In analogy to stream profiles described above, they could be interpreted as the result of the incision of the Rhine with respect to the level of Late Pleistocene fluvial deposits. Along LP-10 and LP-11 these anomalies spatially coincide with the observation of lateral landslides (indicated in hillshade base map of Appendix 1.G, however located outside

of process domain mapping extent). These landslides could have been triggered by the above inferred base level drop and associated knickpoint migration. However, the landslides could also have occurred independently and at a different time period.

An alternative explanation is offered in case of LP-10, where the steepening of the lowest section could be attributed to higher substrate resistance by Triassic sediments (Muschelkalk)¹⁵. However, this observation lacks confirmation by LP-9 and LP-11.

Convex sections with lateral landslides are also observed at higher altitudes (> ~ 400 m a.s.l.). This signal is confirmed by all three profiles, although less distinct in case of LP-9. Lithologically, the landslide-affected sections can be attributed to the closely spaced sequence of rather weak Jurassic sediments described above (Opalinus Clay, Passwang-Formation, Klingnau-Formation (LP-11), Ifenthal-Formation). For LP-9 and LP-10, this situation with lateral landslides is indicated in Appendix 4.B. Again, it is not clear, whether the landslides were initiated independently or as a direct result of knickpoint migration due to base level drop. At least in case of LP-10, the latter scenario is supported by the potential correlation of a "perched low-relief landscape" above approximately 450 m a.s.l. and the projected base level of TDS. However, such assumptions remain speculative.

4.3.5 Synthesis

As pointed out, the interpretation of stream longitudinal profiles is partly complicated by weakly expressed anomalies and the superposition of different signals (i.e. different natural and artificial / anthropogenic causes). However, some observations seem to be more reliable, since supported by a similar pattern in multiple profiles (Fig. 21):

- **Lithologically controlled knickpoints**, spatially coinciding with a) outcrops of Villigen-Formation around the Bözbergplateau and (possibly) b) the transition of "Obere Süßwassermolasse" to lower lithostratigraphic units in the Villnachern area
- **Convex anomalies associated with lateral landslides**, particularly observed in a) stream profiles draining the Bözbergplateau in the Villnachern area (Molasse), and b) stream sections between the northern boundary of the siting region and the Mandach thrust fault (Ifenthal-Formation to Opalinus Clay)
- **Knickpoint migration in response to the incision of the Rhine and Aare** with respect to the level of Late Pleistocene fluvial deposits

The latter is best expressed in LP-1, where future upstream migration of the convex anomaly at 360 m a.s.l. should be expected. The more distinct signal in comparison to the other profiles is probably attributed to the unique intersection of this stream course with the "Paläo-Rinne Rinikerfeld" (former Aare valley), where the former base level seems to be preserved along a nearly flat, approximately 2.5 km long profile section (Fig. 22). The transition from this flat section to the steepened channel section downstream of 360 m a.s.l. results in the distinct signal. In the absence of such a flat channel section, the other profiles show less distinct (or even no obvious) anomalies in their lower reaches, explainable by a lower contrast of channel steepness with respect to the upstream section.

¹⁵ Not differentiated in the profile illustration but inferred from the Geological Atlas of Switzerland 1:25'000.

Differences among the profile geometries in response to the incision of the Rhine and Aare after Late Pleistocene can further arise from various factors:

- Different timing / history of incision and aggradation (e.g. tributaries to the Aare experience later onset of incision associated with Rhine base level drop, as the signal first has to propagate along the Aare)
- Superposition of additional signals (anthropogenic, lateral landslides etc., see above)
- Variability in channel steepness of downstream sections due to cover effects from sediments of variable resistance along the channel bed (according to section 3.5.3 and Duvall et al. 2004)
- Variability in channel steepness between different profiles due to different catchment size and (consequently) runoff regime

Based on the signal in LP-1 (knickpoint migration of approximately 2 km horizontally and 30 m vertically) and less distinct signals recognisable in other profiles, it is inferred that stream profiles are still locally adjusting to incision of the Rhine and Aare after Late Pleistocene.

Considering their elevation, landslide initiation due to such "recent" knickpoint migration is a possibility in case of LP-10 and LP-11 (~ 340 m a.s.l.). However, these landslides may be older, implying that they could have been reactivated but not initiated by "recent" incision. Links between profile anomalies and lateral landslides seem to be more typical for profile sections at higher altitudes (> ~ 400 m a.s.l.; LP-2, -3, -4, -9, -10, -11, -12; Fig. 23). In these cases, it can be speculated, that convex profile anomalies (or "masked knickpoints") are more persistent in time, where relatively low runoff (due to proximity to water divide) competes with material input by lateral landslides, typically associated with weak lithologies. This material input may either occur as a "landslide dam" from a rather discrete event, or by more continuous sediment supply by ongoing landslide activity.

Profile anomalies within the Villigen-Formation along the Bözbergplateau can be interpreted as another form of temporally persistent knickpoints (lithologically controlled by higher substrate resistance). Considering their altitude, the "perched low-relief landscape" (e.g. Fig. 25) upstream of these knickpoints could nearly correspond to a steady-state situation at the time of base level of TDS (see Appendix 3, LP-1). In this case, the central regions of the Bözbergplateau might have seen only minor fluvial (and possibly glacial) incision over a relatively long time period.



Fig. 25: "Perched low-relief landscape" in headwater region of LP-1 (Kirchbözberg).
For location, see reference to this figure in Appendix 1.A. The approximate location and the topographic context is also indicated in the regional topographic profile of Appendix 4.A.

5 Conclusions

The analysis of hillslope / landslide processes and stream longitudinal profiles in the Jura Ost siting region and surrounding area indicates certain dynamics in the present (interglacial) landscape. It highlights that such dynamics are spatially modified by the geological and topographic setting in this eastern part of the Jura Mountains, dividing the study area into some rather "quiet" vs. "more active" areas. It is important to note, that the observed patterns and processes may be further modified in the future by different climatic conditions and/or by (base level) changes in the Aare-Rhine drainage system.

Key observations and implications for landscape evolution and exposure scenarios

A key indicator of recent landscape dynamics in the study area are landslides of various size and type. The analysis suggests, that both the "landslide susceptibility" of hillslopes and the associated landslide (process) types vary as a function of the geomechanical properties of the different lithostratigraphic units. Large (few 0.1 km² up to 1 km²) and potentially deep-seated (> 10 m) landslides are widely observed, where hillslopes have reached heights of 100 m up to ~ 300 m as a result of the past fluvial (and partly glacial) incision. For such "high relief" areas, multi-lithological hillslopes / landslides are the more typical observation than those restricted to a single lithostratigraphic unit. Concerning the initial motivation of this study, the following conclusions are drawn for scenarios of landscape evolution and a possible landslide-related exposure of the repository at its late stage:

- "Landslide susceptibility" and thus hillslope erodibility in the study area is temporally variable during landscape incision, given the mostly horizontally layered sequence of geomechanically heterogeneous (lithostratigraphic) units.
- Hillslope erodibility within a lithostratigraphic unit is not only depending on its own geomechanical properties, but also on those of its underlying unit(s); for instance, the Passwang-Formation seems to be often destabilised by large landslides, that have their basal rupture surface mainly located within the underlying (weaker) Opalinus Clay. With respect to the temporal scale mentioned above, this also implies that (hillslope) erosion of a lithostratigraphic unit may be significantly accelerated, once fluvial incision has reached an underlying weaker unit (e.g. Villigen-Formation to Wildegg-Formation; Hauptrogenstein / Passwang-Formation to Opalinus Clay). On the other hand, (hillslope) erosion may be slowed down again in the opposite case (e.g. Tertiary sediments (Molasse) to Villigen-Formation).
- Different landslide types, of various spatial and temporal scale, are often superimposing within large landslide complexes, which potentially complicates a quantification of hillslope erosion rates. Many lithostratigraphic units include weak rock types (marls, claystones), where slow but long-term acting landslides can evolve instead of discrete and rapid hillslope failures. The latter, however, are also represented in the study area by earthflows, shallow slides or rock fall, and possibly by some large bedrock slides (however, the latter being only interpreted and not evidenced by historic records).
- The positive correlation of landslide frequency and local relief confirms the basic assumption that future landslide activity will strongly depend on rates of fluvial (or glacial) incision. In this respect, the analysis of stream longitudinal profiles has revealed anomalies / knickpoints, which indicate upstream propagation of fluvial incision as another signal of landscape dynamics in the present system. While some of them at lower altitudes (< 400 m a.s.l.) are attributed to a base level drop with respect to the level of Late Pleistocene fluvial deposits (e.g.

Rinikerfeld), other convex anomalies are found at higher altitudes, where low runoff near the drainage divide seems to compete with material supply by lateral landslides within rather weak rock.

- This latter observation points to the question about the rate at which the fluvial system can remove material coming from lateral landslides, and how this relates to the drainage area. This problem is relevant with respect to linking hillslope erosion and subsequent (fluvial) transport in numerical landscape evolution models.
- Finally, the present study has shown, that hillslopes involving Opalinus Clay are often affected by large, potentially slow and deep-seated landslides. In a similar topographic and climatic setting, a landslide-related exposure of the repository at its late stage is therefore a plausible process that should be accounted for in corresponding scenario building. The latter effort may be supported by present-day analogies (as indicated by the reference from Appendix 4.A to Fig. 11 of this report).

Potential "hotspots" of landscape dynamics

While the conclusions above represent rather generic observations for landscape evolution and exposure scenarios, the analysis does also indicate potential "hotspots" of present or future landscape dynamics in the study area. This includes the "high-relief" zone between the northern boundary of the siting region and the Mandach thrust fault, where many (large) landslides / landslide complexes are observed on the hillslopes of Frickberg, Schinberg and a series of hilltops further towards the east. A second hotspot relates to the area west of Villnachern, where the drainage divide in the southern region of the Bözbergplateau might be shifted towards west, as suggested by comparison of stream longitudinal profiles on both sides of the plateau ("Villnachern" catchment vs. "Sissle" catchment; Fig. 21) and increased landslide occurrence on the eastern side.

Morphological implications

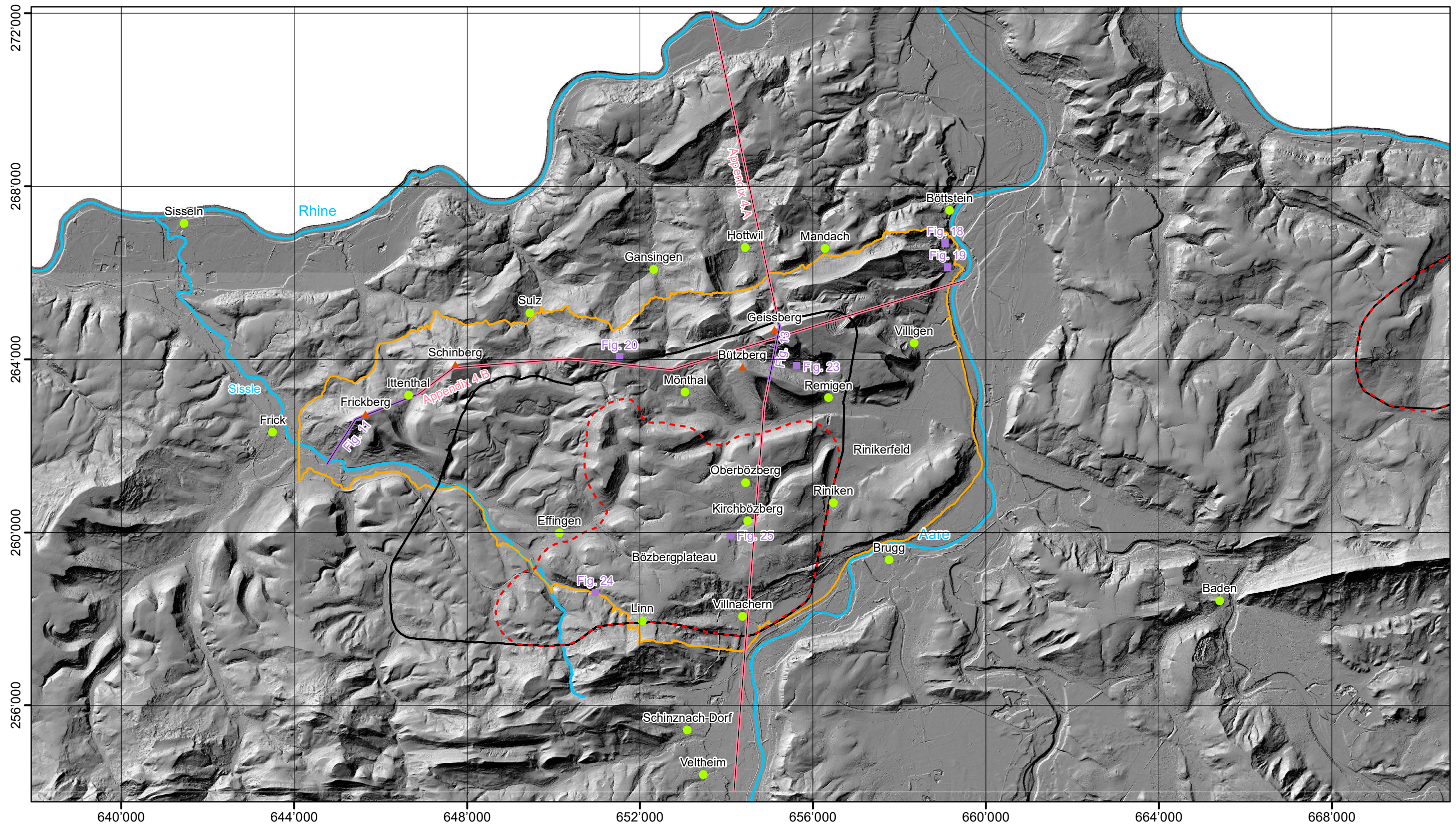
Apart from landscape dynamics and processes, terrain morphology, too, is spatially variable and modified by the different lithostratigraphic units within the study area. For instance, both slope gradients on hillslopes and stream gradients tend to be steeper within the more competent (calcareous) Villigen-Formation than within other (weaker) formations. Therefore, for a given depth of incision or local relief, valley width tends to increase from more competent calcareous, to marly and finally clay-rich formations. The same applies to stream gradients for a given drainage area, where steepening along channel sections of more competent lithostratigraphic units produces convex sections / knickpoints in stream longitudinal profiles. These lithologically controlled anomalies reduce the magnitude of fluvial incision in the upstream sections, which contributes to the conservation of the "upland low-relief area" of the Bözbergplateau (Fig. 25).

6 Literaturverzeichnis

- Baltzer, A. (1876): Der Erdschlipf von Böttstein. Vierteljahresschrift der Naturforschenden Gesellschaft Zürich 21/3, 285-290.
- Becker, A. (2000): The Jura Mountains – An active foreland fold-and-thrust belt? *Tectonophysics* 321, 381-406.
- Biaggi, D., Rust, S., Montani, S. & Wüthrich, E. (2014): Sachplan geologische Tiefenlager – Etappe 2. Standortsspezifische Baugrundmodelle für die Zugangsbauwerke: Geologische Profile nach SIA 199 (Rampen und Schächte). Nagra Arbeitsber. NAB 14-72.
- Blum, M.D. & Törnqvist, T.E. (2000): Fluvial responses to climate and sea-level change: a review and look forward. *Sedimentology* 47, 2-48.
- BWG / BUWAL (1995): Empfehlungen, Symbolbalken zur Kartierung der Phänomene. Reihe Naturgefahren, EDMZ. Bundesamt für Wasser und Geologie / Bundesamt für Umwelt, Wald und Landschaft, 3000 Bern.
- Bursztyn, N., Pederson, J.L., Tressler, C., Mackley, R.D. & Mitchell, K.J. (2015): Rock strength along a fluvial transect of the Colorado Plateau – quantifying a fundamental control on geomorphology. *Earth and Planetary Science Letters* 429, 90-100.
- Duval, A., Kirby, E. & Burbank, D. (2004): Tectonic and lithologic controls on bedrock channel profiles and processes in coastal California. *Journal of Geophysical Research* 109.
- Haefeli, R. (1940): Zur Mechanik aussergewöhnlicher Gletscherschwankungen. *Schweizerische Bauzeitung* 115/16, 179-184.
- Hartmann, A. (1928): Der Erdbeben von Ittenthal 1924-1926. *Mitteilungen der Aargauischen Naturforschenden Gesellschaft* 18, 53-70.
- Hartmann, A. (1950): Der untere braune Jura des Aargaus als wichtigster zukünftiger Tonlieferant der Schweiz. *Mitteilungen der Aargauischen Naturforschenden Gesellschaft* 23, 3-20.
- Heuberger, S. & Naef, H. (2014): Regionale GIS-Kompilation und -Analyse der Deckenschotter-Vorkommen im nördlichen Alpenvorland. Nagra Arbeitsber. NAB 12-35.
- Heuberger, S., Büchi, M. & Naef, H. (2014): Drainage system and landscape evolution of northern Switzerland since the Late Miocene. Nagra Arbeitsber. NAB 12-20.
- Hungr, O., Leroueil, S. & Picarelli, L. (2014): The Varnes classification of landslide types, an update. *Landslides* 11/2, 167-194. <https://doi.org/10.1007/s10346-013-0436-y>.
- Kirby, E. & Whipple, K.X. (2012): Expression of active tectonics in erosional landscapes. *Journal of Structural Geology* 44, 54-75.
- Korup, O., Densmore, A.L. & Schlunegger, F. (2010). The role of landslides in mountain range evolution. *Geomorphology* 120, 77-90.

- Madritsch, H. (2015): Geology of central Northern Switzerland: Overview and some key topics regarding Nagra's seismic exploration of the region. *Swiss Bulletin für angewandte Geologie* 20/2, 3-15.
- Madritsch, H., Schmid, S. & Fabbri, O. (2008): Interactions between thin- and thick-skinned tectonics at the northwestern front of the Jura fold-and-thrust belt (eastern France). *Tectonics* 27, 1-31.
- Mazurek, M. (2011): Aufbau und Auswertung der Gesteinsparameter-Datenbank für Opalinuston, den 'Braunen Dogger', Effinger Schichten und Mergel-Formationen des Helvetikums. *Nagra Arbeitsber. NAB* 11-20.
- McKean, J. & Roering, J. (2004). Objective landslide detection and surface morphology mapping using high-resolution airborne laser altimetry. *Geomorphology* 57, 331-351.
- Nagra (2008): Vorschlag geologischer Standortgebiete für das SMA- und das HAA-Lager. *Geologische Grundlagen. Nagra Tech. Ber. NTB* 08-04.
- Nagra (2014a): SGT Etappe 2: Vorschlag weiter zu untersuchender geologischer Standortgebiete mit zugehörigen Standortarealen für die Oberflächenanlage. *Geologische Grundlagen. Dossier II: Sedimentologische und tektonische Verhältnisse. Nagra Tech. Ber. NTB* 14-02.
- Nagra (2014b): SGT Etappe 2: Vorschlag weiter zu untersuchender geologischer Standortgebiete mit zugehörigen Standortarealen für die Oberflächenanlage. *Geologische Grundlagen. Dossier VI: Barriereneigenschaften der Wirt- und Rahmengesteine. Nagra Tech. Ber. NTB* 14-02.
- Nagra (2016): The Nagra Research, Development and Demonstration (RD&D) Plan for the Disposal of Radioactive Waste in Switzerland. *Nagra Tech. Ber. NTB* 16-02.
- Pietsch, J. & Jordan, P. (2014): Digitales Höhenmodell Basis Quartär der Nordschweiz – Version 2014 und ausgewählte Auswertungen. *Nagra Arbeitsber. NAB* 14-02.
- Preusser, F., Graf, H.R., Keller, O., Krayss, E. & Schlüchter, C. (2011): Quaternary glaciation history of northern Switzerland. *Quaternary Science Journal* 60/2-3, 282-305.
- Reichert, G. (1967): Die Rutschungen am Eichberg bei Achdorf (Wutach) - Erscheinungsformen, Mechanik, Ursachen. *Erdkunde* 21, 167-180.
- Schnellmann, M., Fischer, U., Heuberger, S. & Kober, F. (2014): Erosion und Landschaftsentwicklung der Nordschweiz. Zusammenfassung der Grundlagen im Hinblick auf die Beurteilung der Langzeitstabilität eines geologischen Tiefenlagers (SGT Etappe 2). *Nagra Arbeitsber. NAB* 14-25.
- Schumm, S.A. (1993): River Response to Baselevel Change: Implications for Sequence Stratigraphy. *The Journal of Geology* 101, 279-294.
- Van den Eeckhaut, M., Poesen, J., Verstraeten, G., Vanacker, V., Nyssen, J., Moeyersons, J., Van Beek, L.P.H. & Vandekerckhove, L. (2007): Use of LIDAR-derived images for mapping old landslides under forest. *Earth Surface Processes and Landforms* 32, 754-769.

- Van den Eeckhaut, M., Kerle, N., Poesen, J. & Hervás, J. (2012): Object-oriented identification of forested landslides with derivatives of single pulse LiDAR data. *Geomorphology* 173-174, 30-42.
- Whipple, K.X. & Tucker, G.E. (1999): Dynamics of the stream-power river incision model: Implications for height limits of mountain ranges, landscape response timescales, and research needs. *Journal of Geophysical Research* 104, 17'661-17'674.
- Yanites, B.J., Ehlers, T.A., Becker, J.K., Schnellmann, M. & Heuberger, S. (2013): High-magnitude and rapid incision from river capture: Rhine River, Switzerland. *Journal of Geophysical Research* 118, 1060-1084.
- Yanites, B.J., Becker, J.K., Madritsch, H., Schnellmann, M. & Ehlers, T.A. (2017): Lithologic effects on landscape response to base level changes: A modeling study in the context of the eastern Jura Mountains, Switzerland. *Journal of Geophysical Research: Earth Surface* 122, 2196-2222.
- Ziegler, P.A. & Fraefel, M. (2009): Response of drainage systems to Neogene evolution of the Jura fold-thrust belt and Upper Rhine Graben. *Swiss Journal of Geosciences* 102, 57-75.



Referenced Locations

- Village / town
- ▲ Hilltop
- Report figure

Profile Sampling Lines

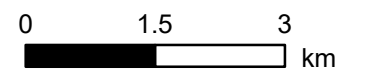
- Regional topographic / geological profile
- Subsection of regional profile, used for interpretation of landslide process types (report figures)

Drainage Network TLM

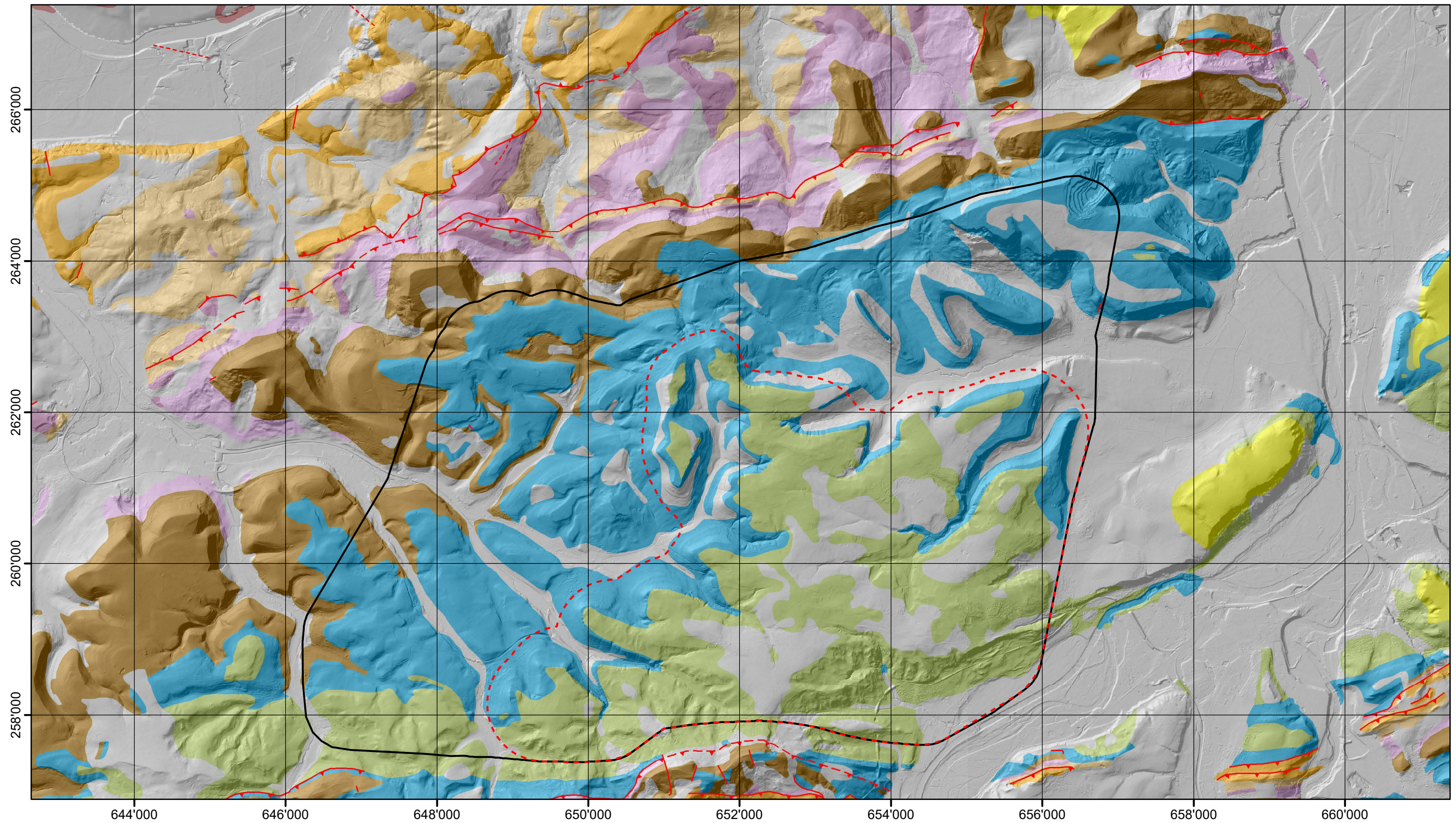
- Selected stream courses

Perimeters











- Extent of process domain mapping
- Siting region "Jura Ost": high-level waste
- Siting region "Jura Ost": low- and intermediate-level waste







nagra		NAB 17-42
Geographical Overview		
DAT.: Mar. 2018	Appendix 1.A	




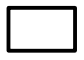
Geological Units

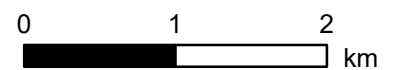
- | | | |
|---|--|--|
|  Quaternary (not differentiated) |  Middle and Upper Dogger (**) |  Muschelkalk |
|  Quaternary (Deckenschotter) |  Opalinus Clay |  Older Triassic and Paleozoic units (not differentiated) |
|  Tertiary |  Lias | <i>(*) Villigen- and Wildegg-Formation</i> |
|  Malm (*) |  Keuper | <i>(**) Ifenthal-Formation, Hauptrogenstein/Klingnau-Formation, Passwang-Form.</i> |

Tectonic Lineaments

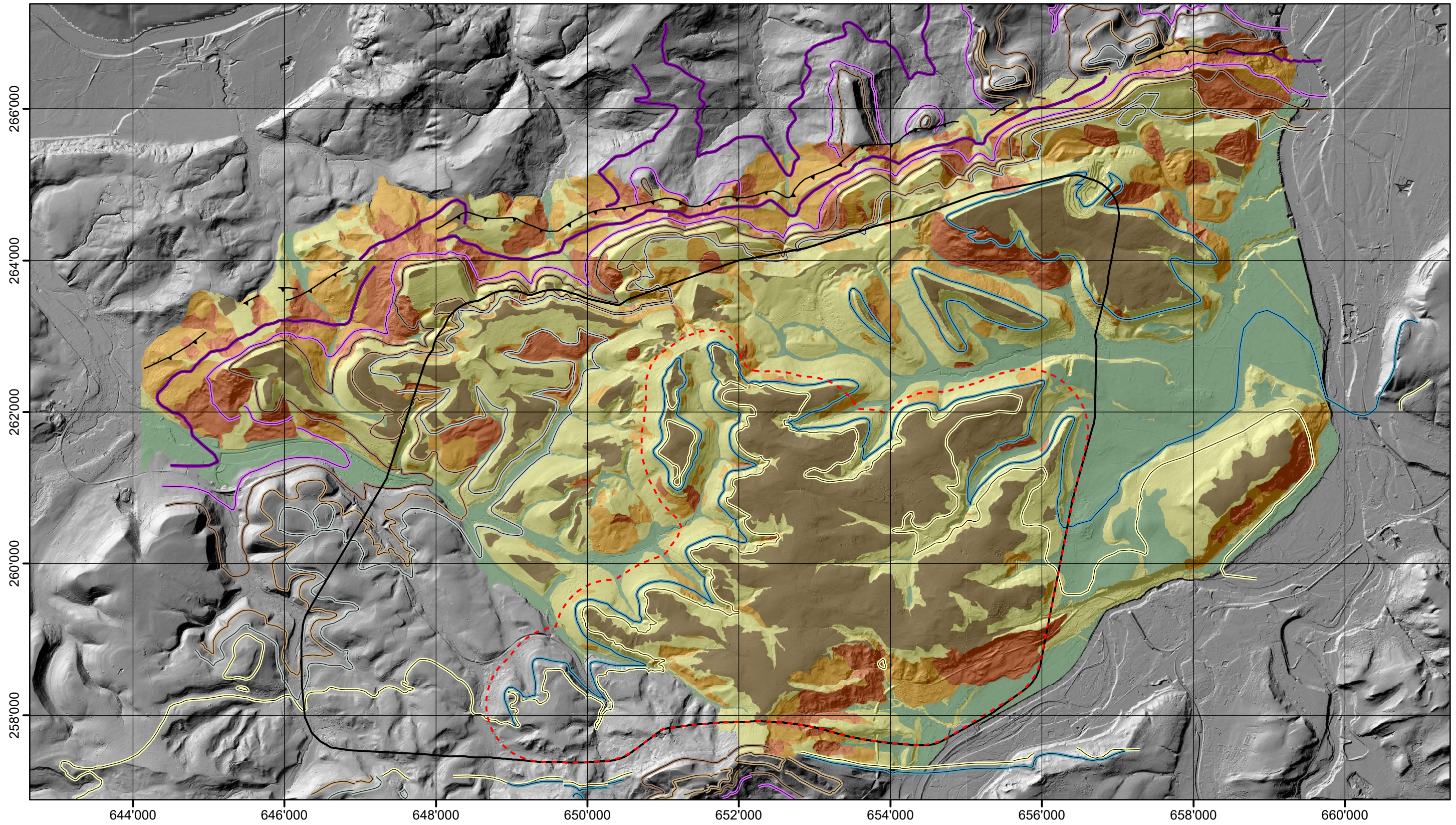
-  Thrust fault
-  Thrust fault (presumed)
-  Fault (not differentiated)
-  Fault (presumed; not differentiated)

Siting Region "Jura Ost"

-  High-level waste (perimeter)
-  Low- and intermediate-level waste (perimeter)



nagra		NAB 17-42
Geological Overview (based on Nagra, 2014a)		
	DAT.: Mar. 2018	Appendix 1.B



Process Domains

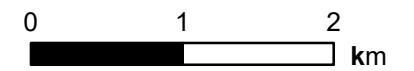
- Quaternary plains and terraces
- Upland low-relief areas
- Presumably unfailed hillslopes
- Presumed landslides
- Evident landslides

Geological Features

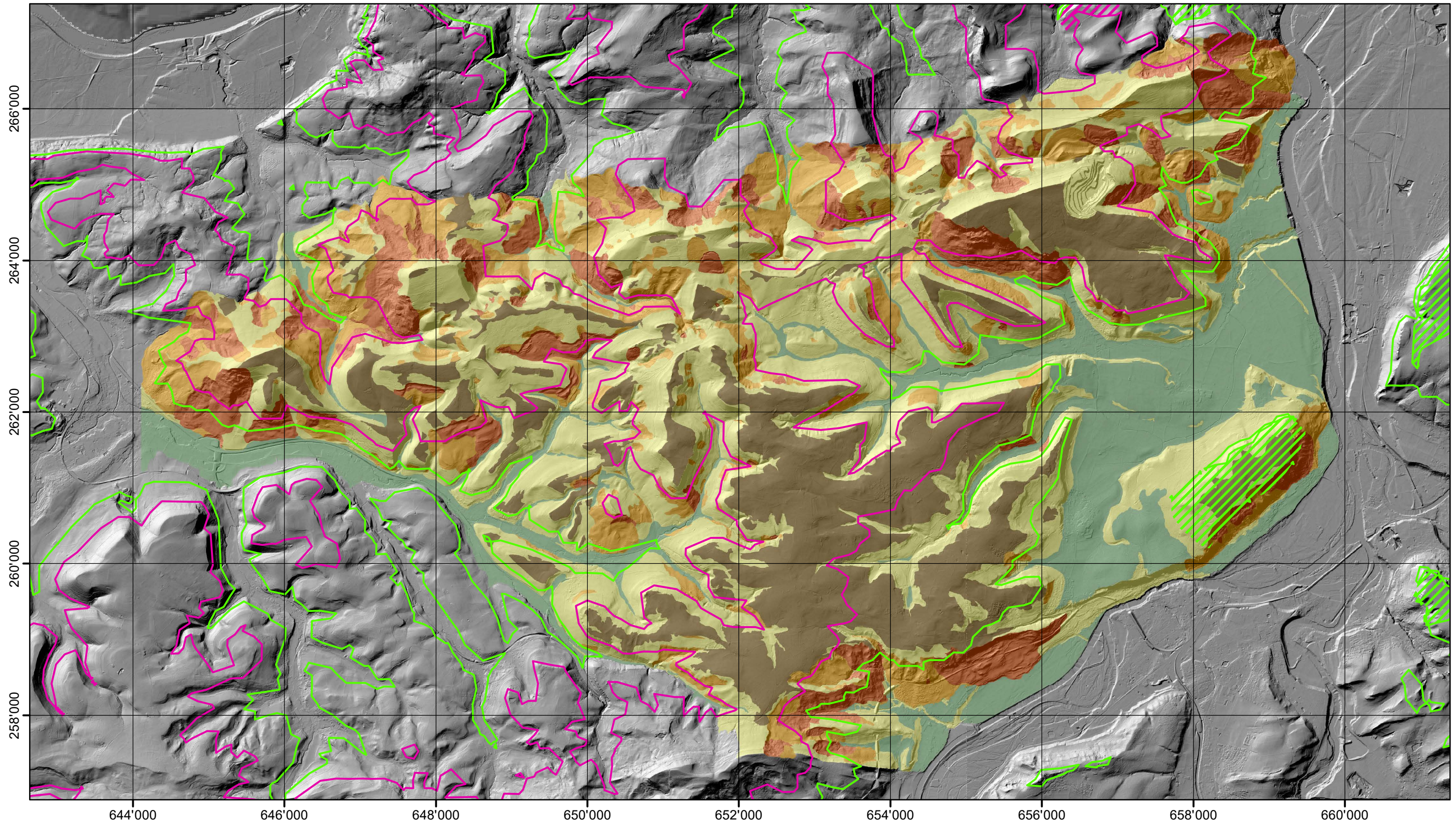
- Basis Tertiary (Molasse)
- Basis Villigen-Formation
- Basis Wildegg-Formation
- Top Hauptrogenstein / Klingnau-Formation
- Top Passwang-Formation
- Top Opalinus Clay
- Top Lias
- Mandach thrust fault (Nagra, 2014a)

Siting Region "Jura Ost"

- High-level waste (perimeter)
- Low- and intermediate-level waste (perimeter)



nagra	NAB 17-42
Map of (Hillslope) Process Domains (+ Geological Features)	
DAT.: Mar. 2018	Appendix 1.C



Process Domains

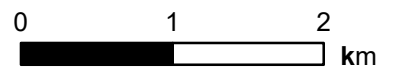
- Quaternary plains and terraces
- Upland low-relief areas
- Presumably unfailed hillslopes
- Presumed landslides
- Evident landslides

Quaternary Map (Extract)

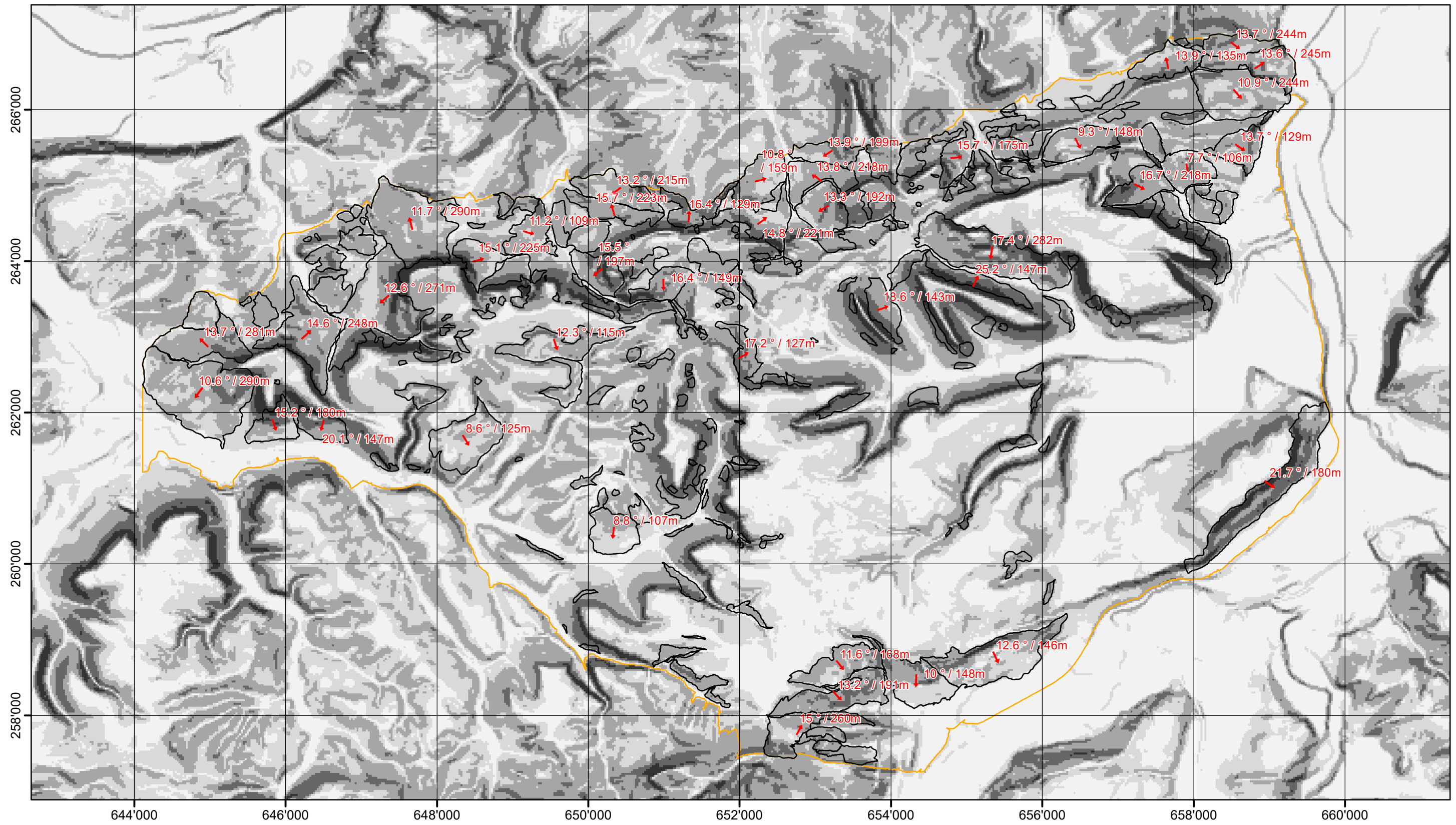
- "Höhere Deckenschotter" (HDS)
- "Tiefere Deckenschotter" (TDS)

Intersection of Projected Base Levels with DHM25

- Base level of "Höhere Deckenschotter" (HDS)
- Base level of "Tiefere Deckenschotter" (TDS)



nagra	NAB 17-42
Map of (Hillslope) Process Domains (+ Base Level HDS / TDS)	
DAT.: Mar. 2018	Appendix 1.D

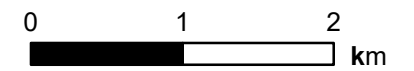


Landslide Inventory

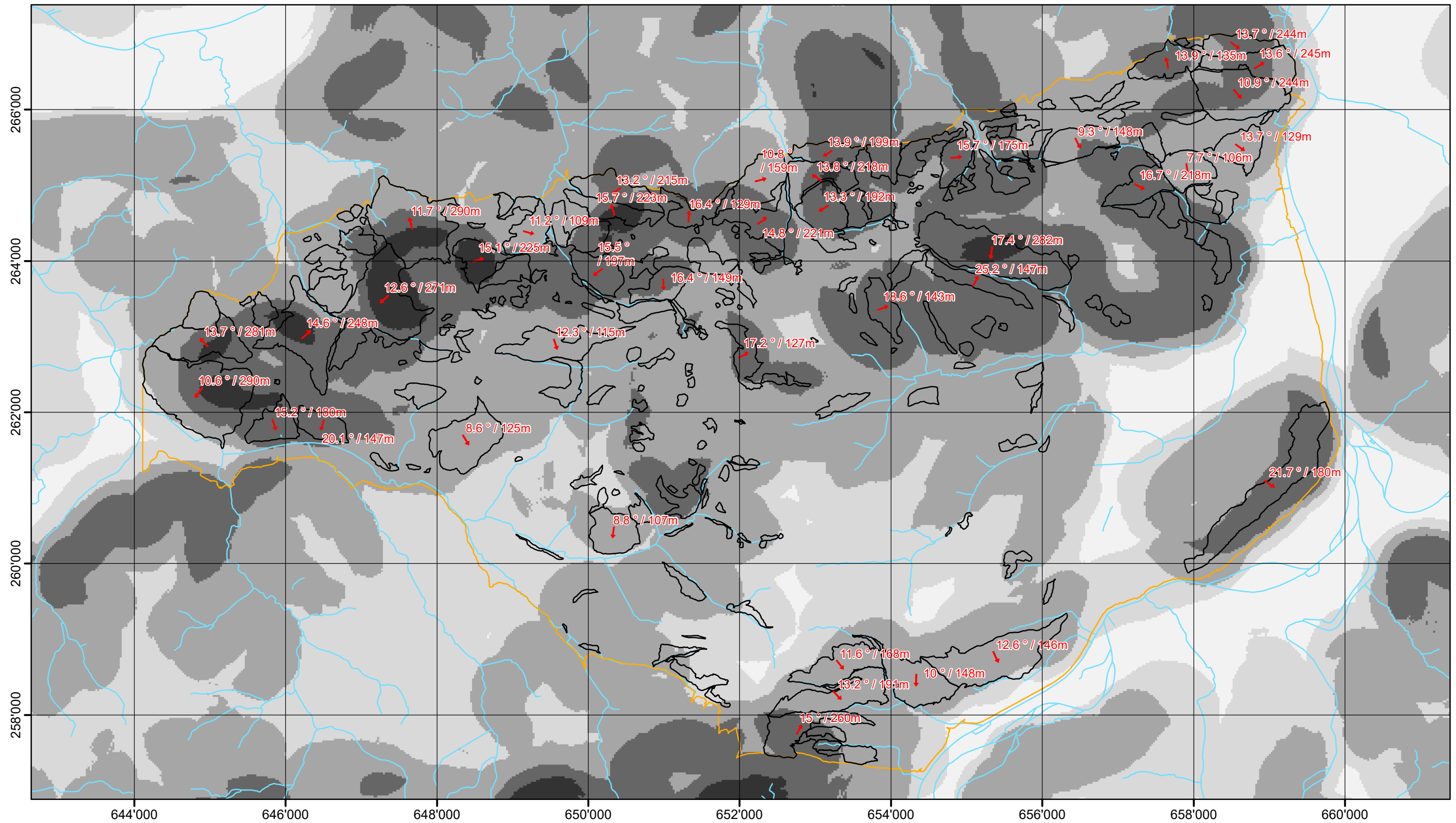
- Individual landslide / landslide complex (interpreted)
- ↑ Mean slope aspect of landslide surface, labelled with mean slope gradient [°] and internal relief [m], (only displayed for landslides > 0.2km²)
- Extent of process domain mapping (where not defined by landslide boundaries)

Slope Gradient (Based on DHM25)

- 0 - 5 °
- 5 - 10 °
- 10 - 20 °
- 20 - 30 °
- > 30 °



nagra	NAB 17-42
Landslide Map (+ Slope Gradient Map)	
DAT.: Mar. 2018	Appendix 1.E



Landslide Inventory

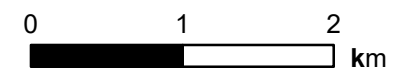
- Individual landslide / landslide complex (interpreted)
- ↑ Mean slope aspect of landslide surface, labelled with mean slope gradient [°] and internal relief [m], (only displayed for landslides > 0.2km²)
- Extent of process domain mapping (where not defined by landslide boundaries)

Local Relief (Based on DHM25, Search Radius = 500m)

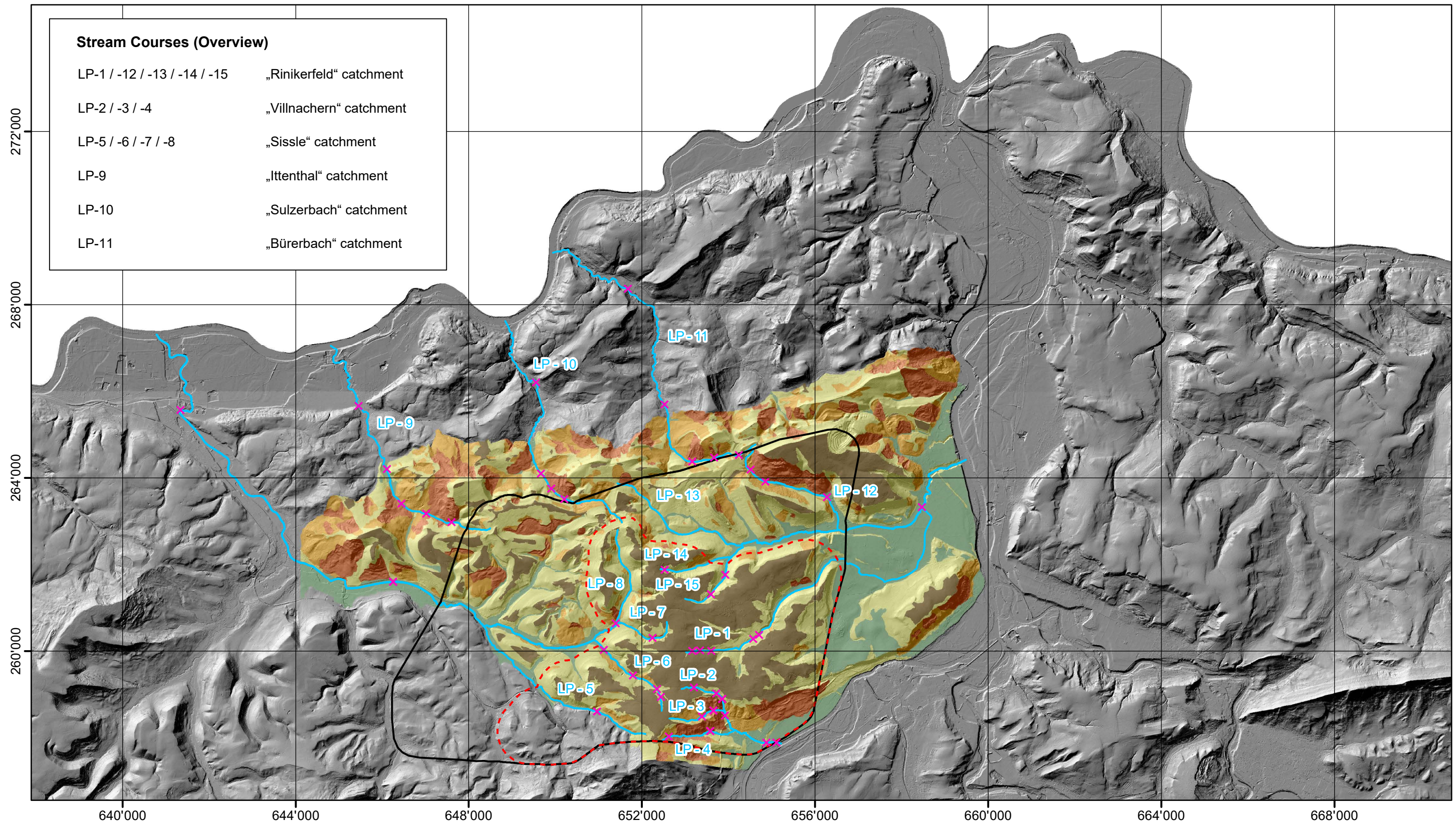
- 0 - 50m
- 50 - 100m
- 100 - 175m
- 175 - 250m
- > 250m

Drainage Network TLM

- Stream course



nagra		NAB 17-42
Landslide Map (+ Local Relief Map)		
DAT.: Mar. 2018	Appendix 1.F	



Process Domains

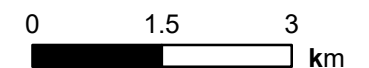
- Quaternary plains and terraces
- Upland low-relief areas
- Presumably unfailed hillslopes
- Presumed landslides
- Evident landslides

Analysis of Stream Longitudinal Profiles

- Stream course
- Location of anomalies referred to in Appendix 3

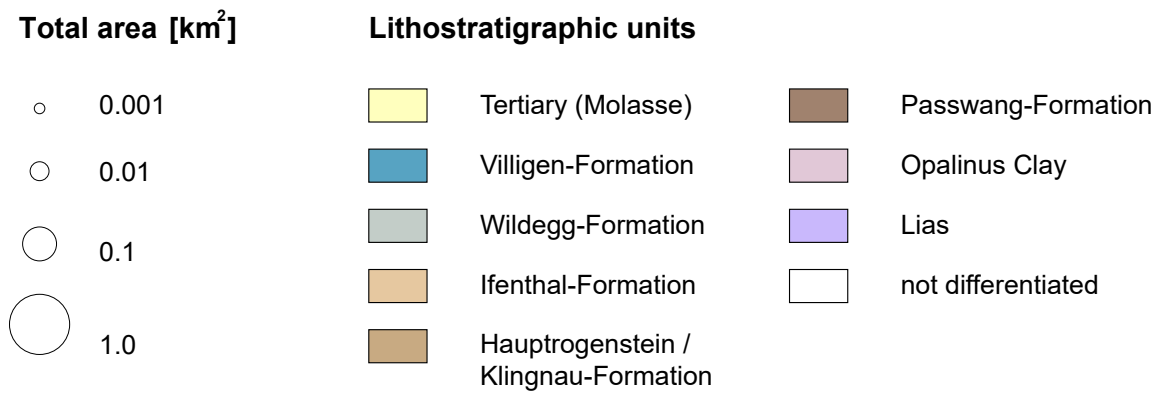
Siting Region "Jura Ost"

- High-level waste (perimeter)
- Low- and intermediate-level waste (perimeter)

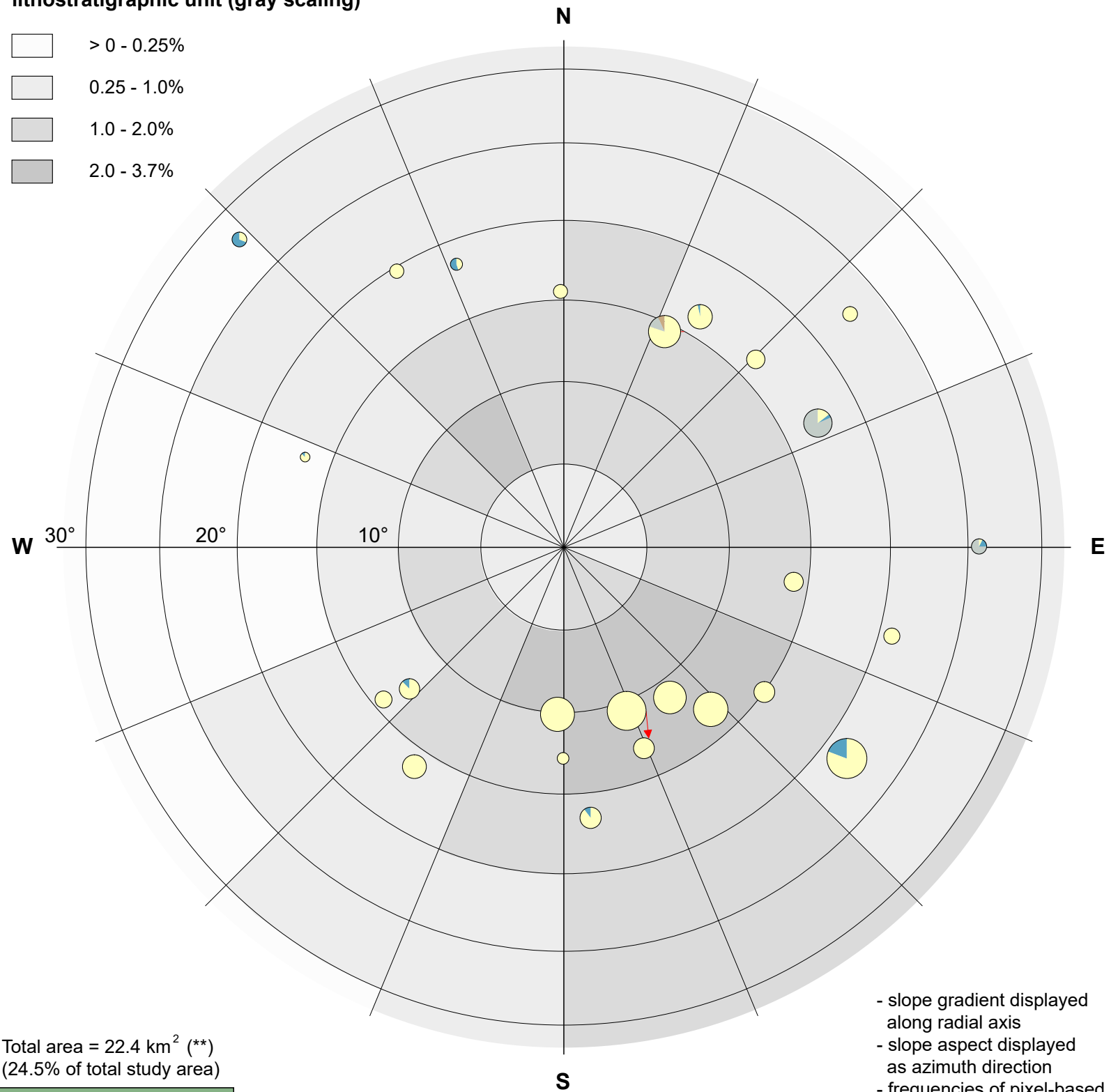
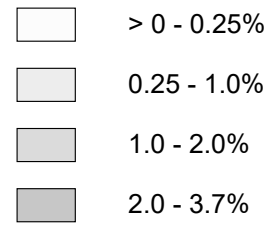


Surface characteristics of individual landslides intersecting with Tertiary (Molasse) (*)

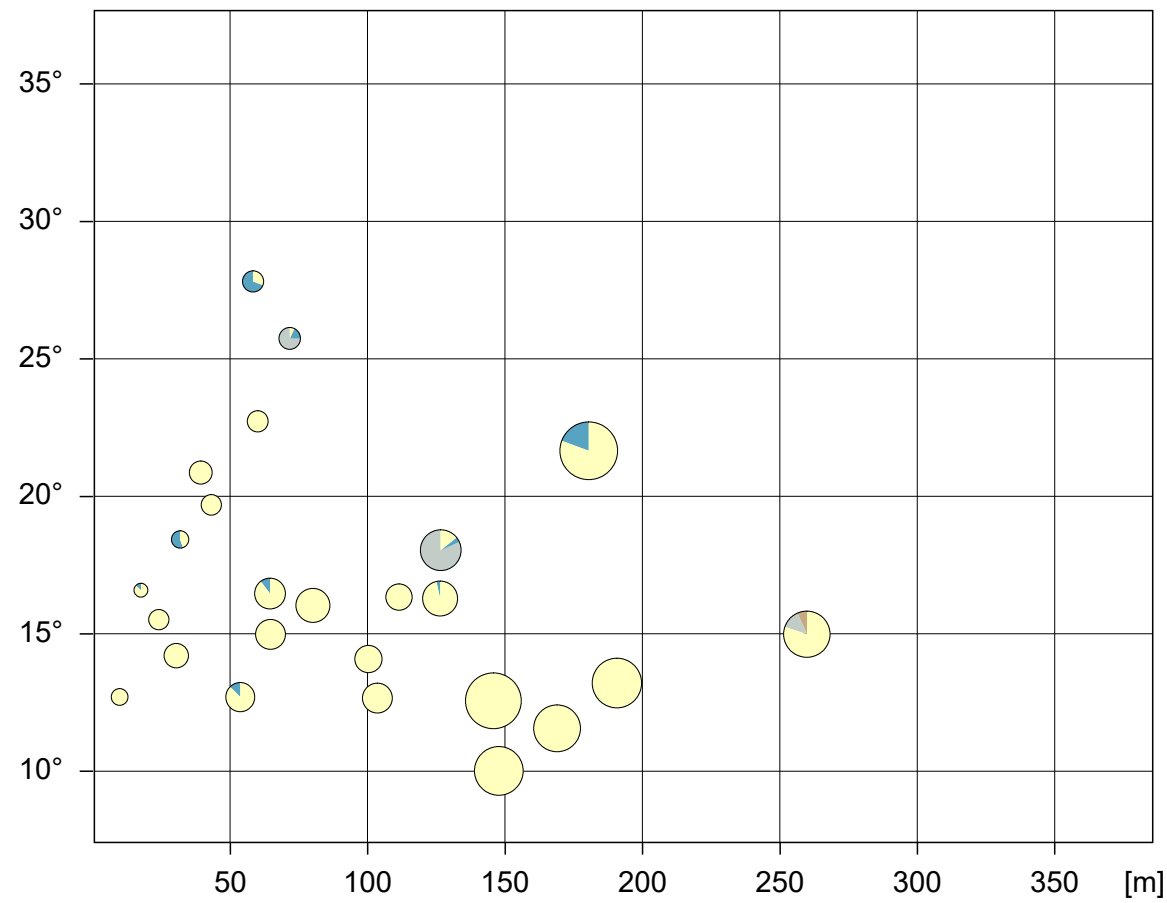
(*) where areal proportion of the lithostratigraphic unit is > 5% of the complete landslide surface



Mean surface orientation of landslides (pie charts) and frequency of pixel-based slope orientation within hillslope domain of the lithostratigraphic unit (gray scaling)



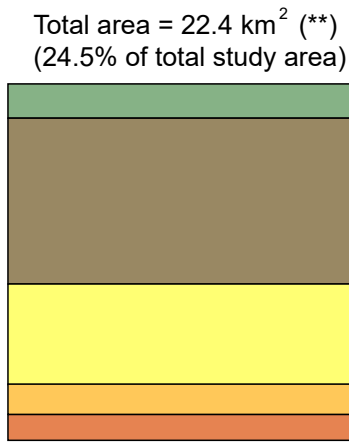
Mean slope gradient vs. maximum elevation difference (relief) of landslide surface



Areal proportion of different process domains intersecting with Tertiary (Molasse)

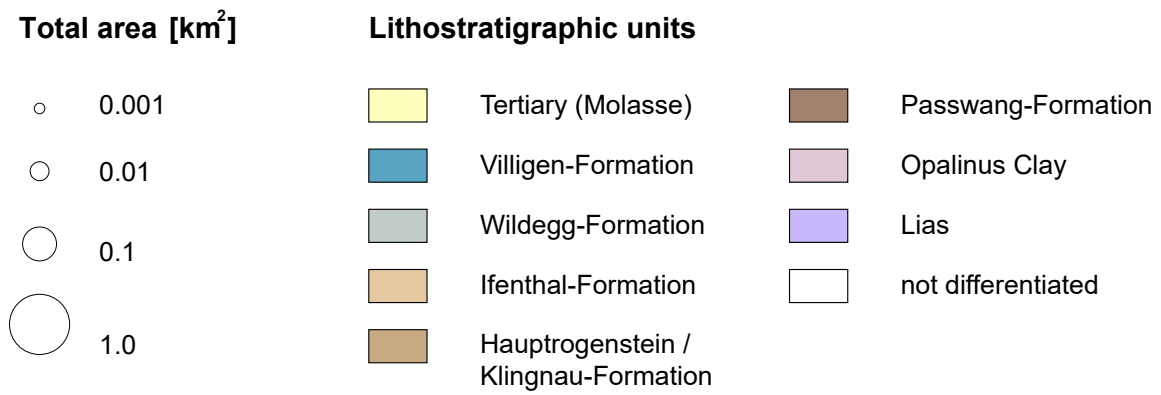
Process domains	[km ²]	[% of total area]	[% of hillslope area]
Quaternary plains and terraces	2.1	10%	
Upland low-relief areas	10.4	46%	
Presumably unfailed hillslopes	6.3	28%	63.5%
Presumed landslides	1.9	8%	19%
Evident landslides	1.7	8%	17.5%

36.5%

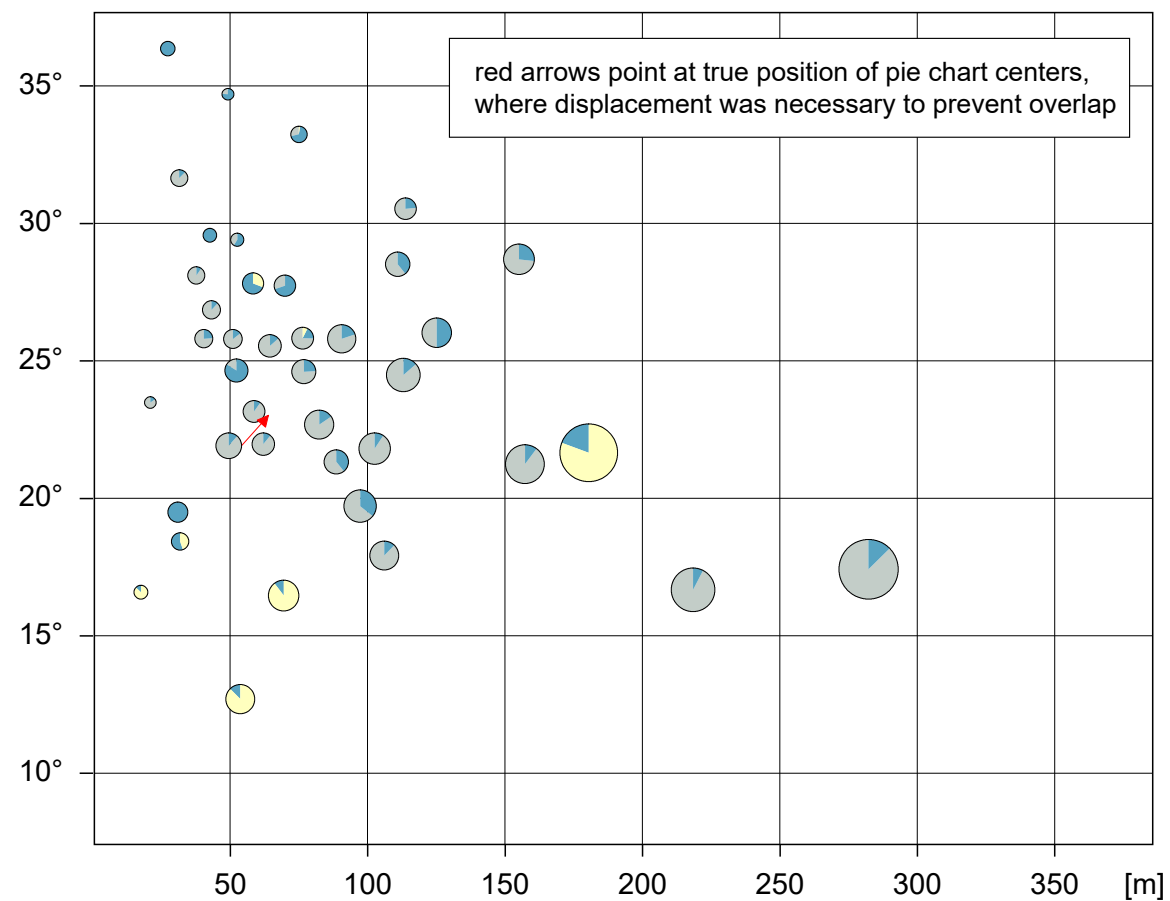


(**) box scaling proportional to absolute area

Surface characteristics of individual landslides intersecting with Villigen-Formation (*)



Mean slope gradient vs. maximum elevation difference (relief) of landslide surface

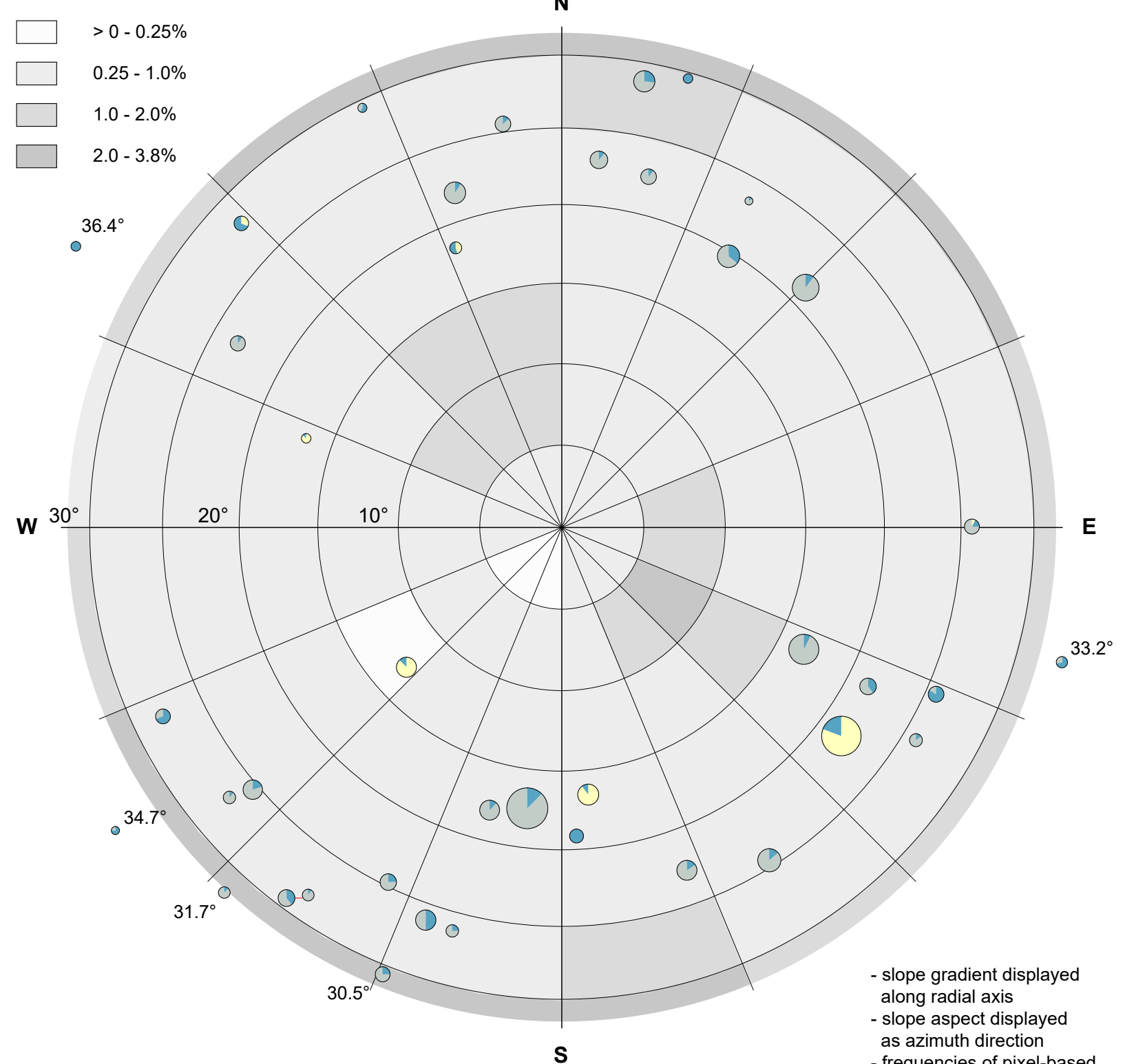


Areal proportion of different process domains intersecting with Villigen-Formation

Process domains	[km ²]	[% of total area]	[% of hillslope area]
Quaternary plains and terraces	2.1	19.5%	
Upland low-relief areas	3.3	31%	
Presumably unfailed hillslopes	4.6	43.5%	88%
Presumed landslides	0.2	2%	4%
Evident landslides	0.4	4%	8%

} 12%

Mean surface orientation of landslides (pie charts) and frequency of pixel-based slope orientation within hillslope domain of the lithostratigraphic unit (gray scaling)



(*) where areal proportion of the lithostratigraphic unit is > 5% of the complete landslide surface

Total area = 10.6 km² (**)
(11.6% of total study area)

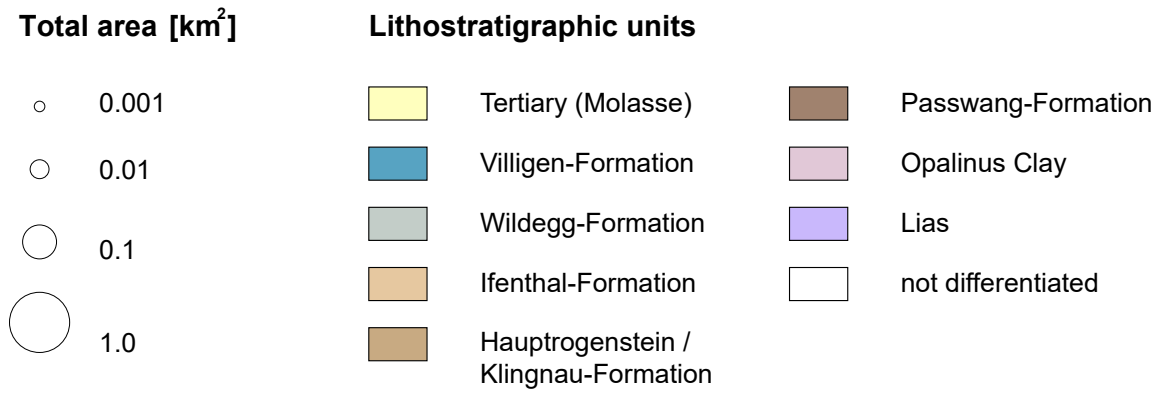


- red arrows point at true position of pie chart centers, where displacement was necessary to prevent overlap

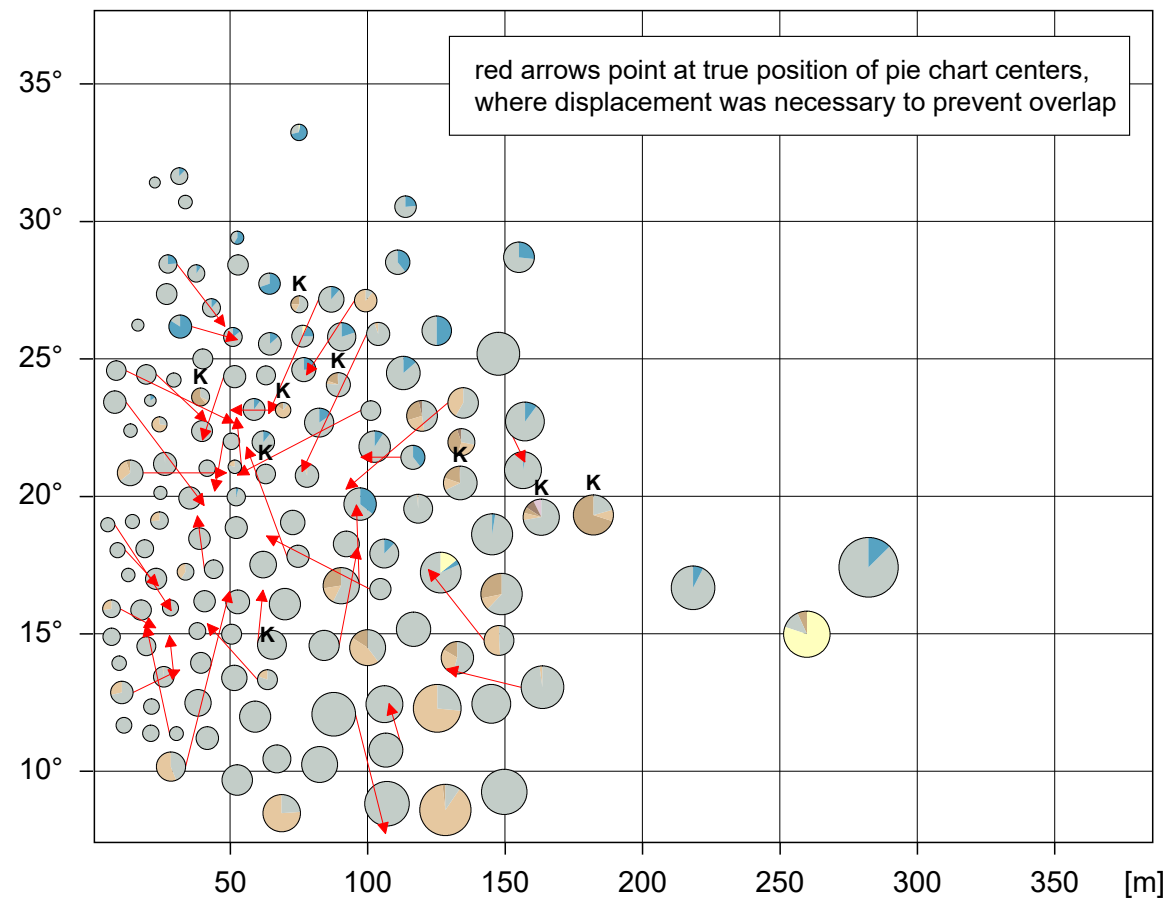
- slope gradient displayed along radial axis
- slope aspect displayed as azimuth direction
- frequencies of pixel-based values are summarized for slope gradients steeper than 30°

(**) box scaling proportional to absolute area

Surface characteristics of individual landslides intersecting with Wildegg-Formation (*)



Mean slope gradient vs. maximum elevation difference (relief) of landslide surface

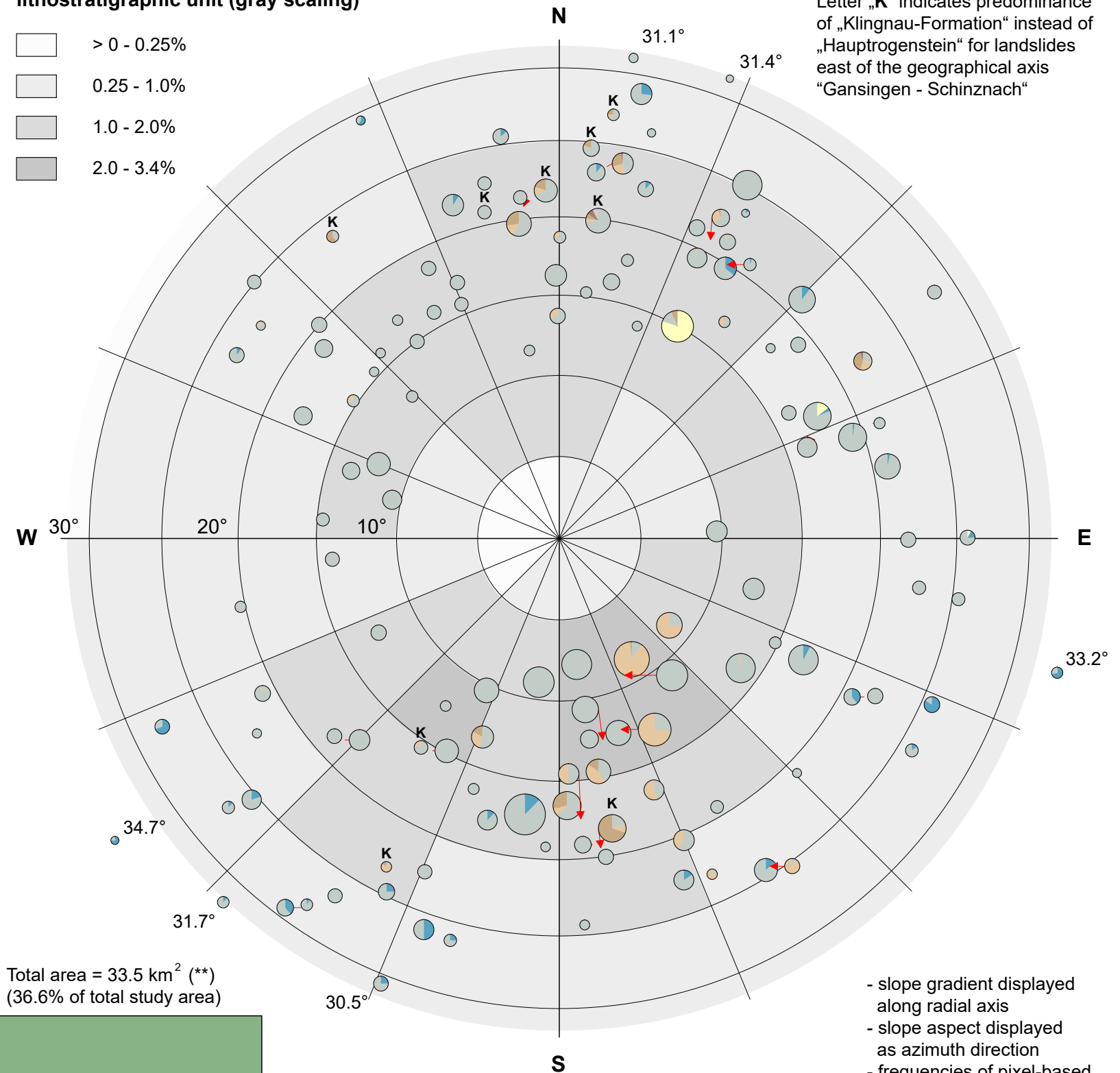
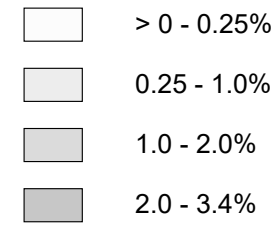


Areal proportion of different process domains intersecting with Wildegg-Form.

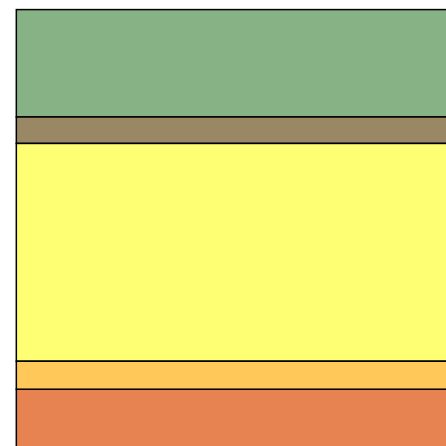
Process domains	[km ²]	[% of total area]	[% of hillslope area]
Quaternary plains and terraces	8.2	25%	
Upland low-relief areas	2.0	6%	
Presumably unfailed hillslopes	16.7	50%	72%
Presumed landslides	2.1	6%	9%
Evident landslides	4.5	13%	19%

28%

Mean surface orientation of landslides (pie charts) and frequency of pixel-based slope orientation within hillslope domain of the lithostratigraphic unit (gray scaling)



Total area = 33.5 km² (**)
(36.6% of total study area)

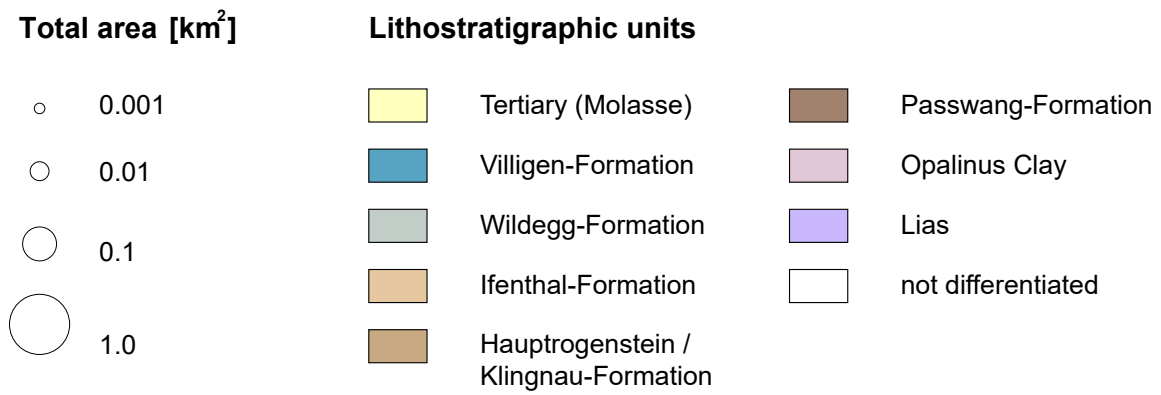


(**) box scaling proportional to absolute area

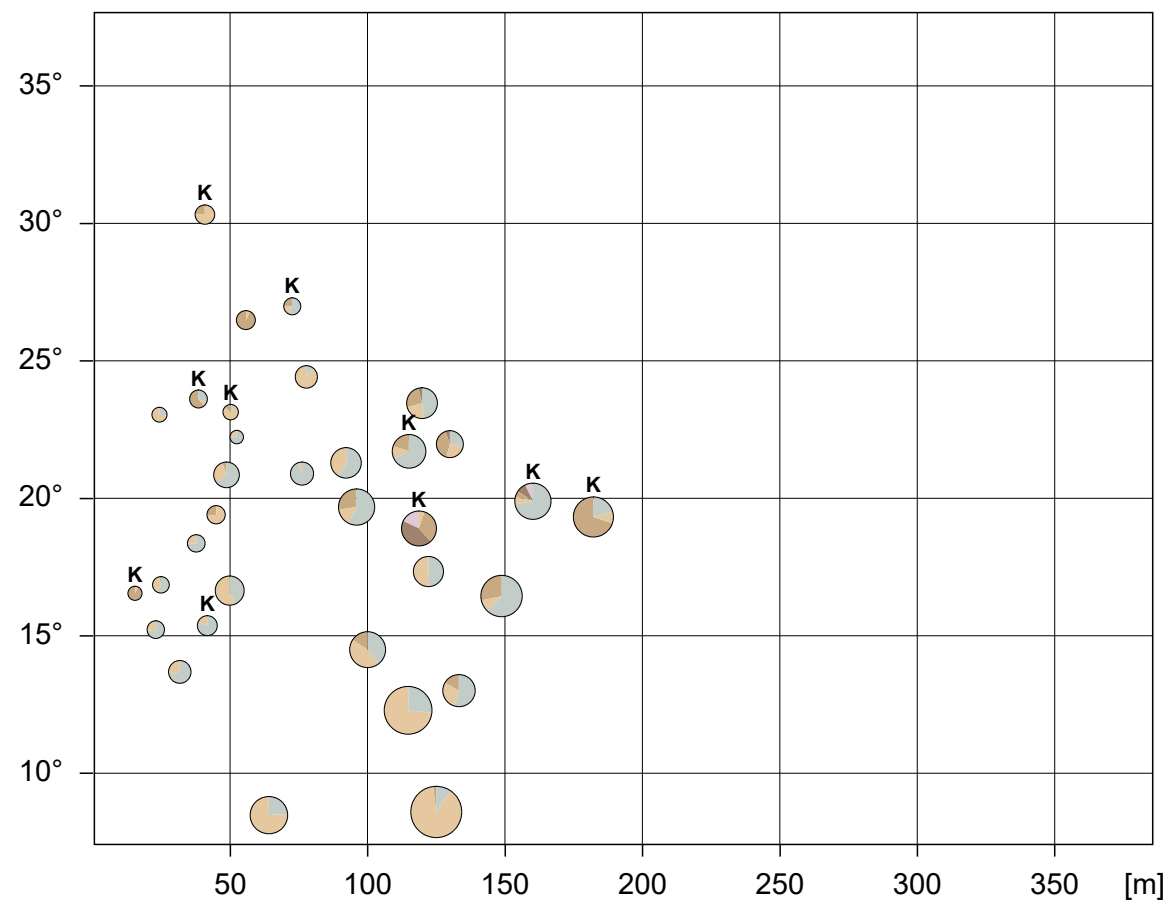
- slope gradient displayed along radial axis
- slope aspect displayed as azimuth direction
- frequencies of pixel-based values are summarized for slope gradients steeper than 30°

- red arrows point at true position of pie chart centers, where displacement was necessary to prevent overlap

Surface characteristics of individual landslides intersecting with Ifenthal-Formation (*)



Mean slope gradient vs. maximum elevation difference (relief) of landslide surface

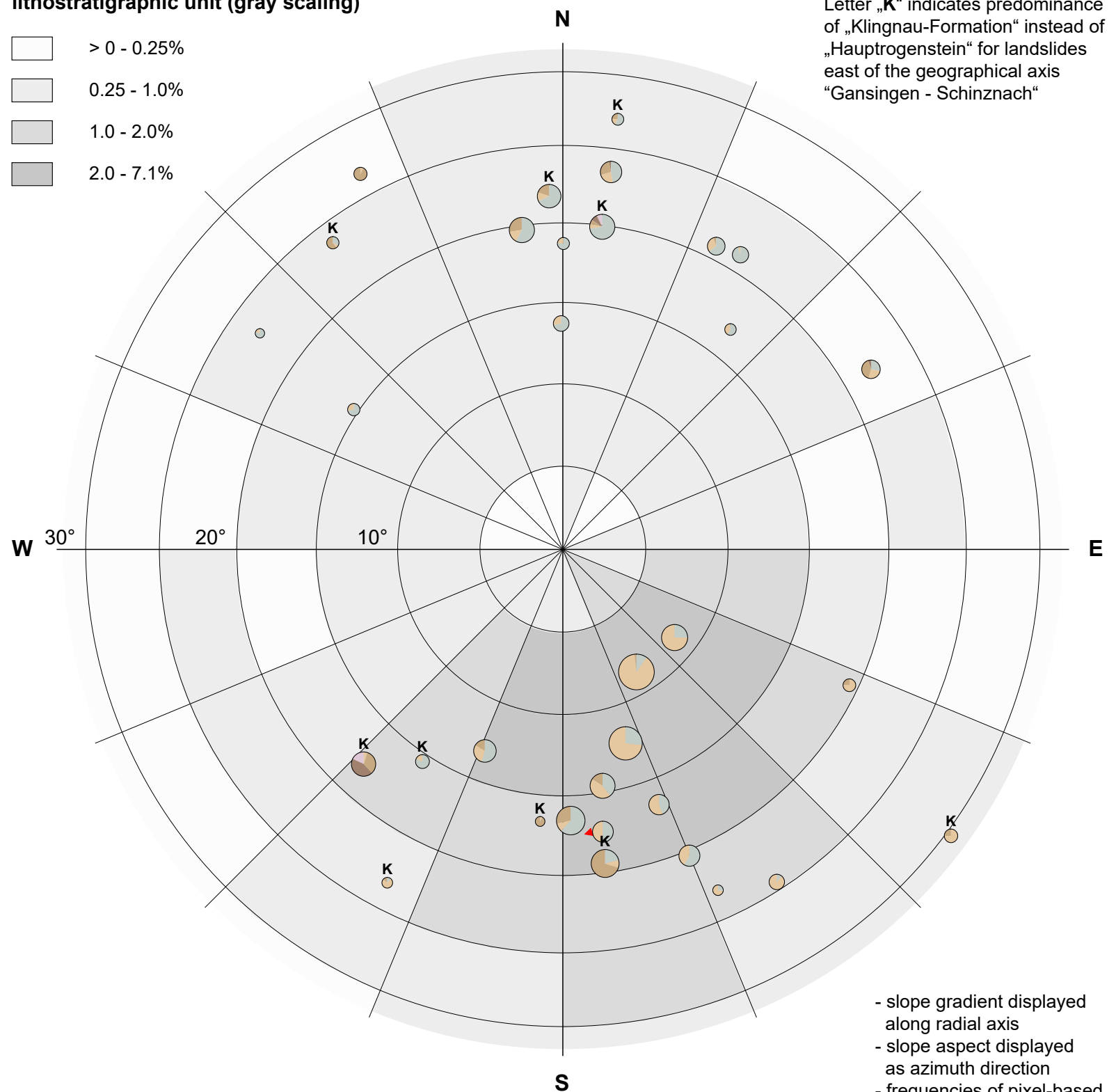
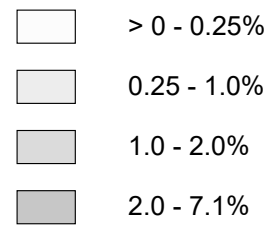


Areal proportion of different process domains intersecting with Ifenthal-Formation

Process domains	[km ²]	[% of total area]	[% of hillslope area]
Quaternary plains and terraces	0.45	13%	
Upland low-relief areas	0.5	13%	
Presumably unfailed hillslopes	1.4	38.5%	52%
Presumed landslides	0.65	18.5%	25%
Evident landslides	0.6	17%	23%

} 48%

Mean surface orientation of landslides (pie charts) and frequency of pixel-based slope orientation within hillslope domain of the lithostratigraphic unit (gray scaling)



(*) where areal proportion of the lithostratigraphic unit is > 5% of the complete landslide surface

Letter „K“ indicates predominance of „Klingnau-Formation“ instead of „Hauptrogenstein“ for landslides east of the geographical axis „Gansingen - Schinznach“

- red arrows point at true position of pie chart centers, where displacement was necessary to prevent overlap

- slope gradient displayed along radial axis
 - slope aspect displayed as azimuth direction
 - frequencies of pixel-based values are summarized for slope gradients steeper than 30°

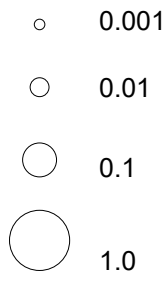
Total area = 3.6 km² (**)
 (3.9% of total study area)



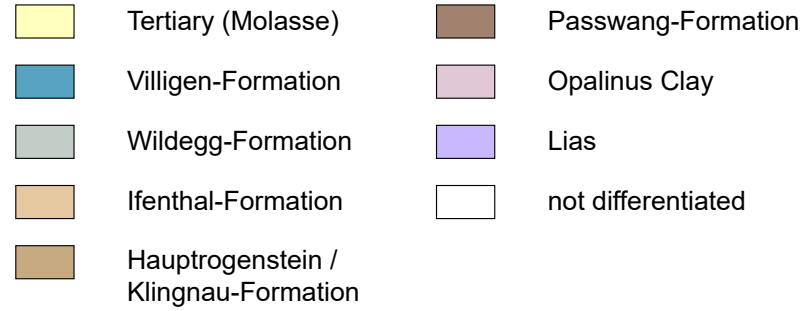
(**) box scaling proportional to absolute area

Surface characteristics of individual landslides intersecting with Hauptrogenstein / Klingnau-Formation (*)

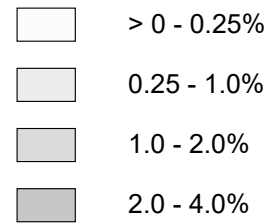
Total area [km²]



Lithostratigraphic units

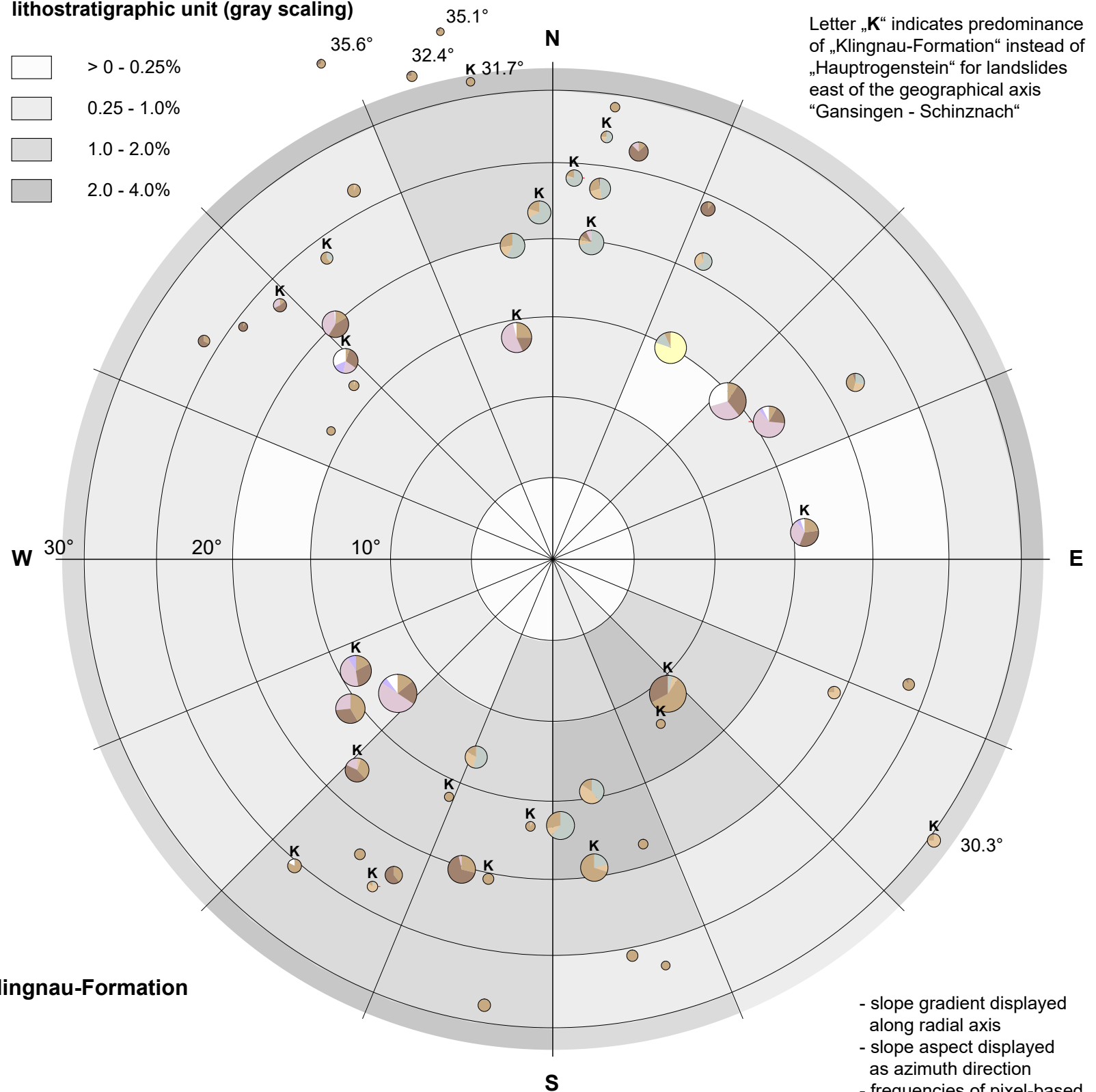


Mean surface orientation of landslides (pie charts) and frequency of pixel-based slope orientation within hillslope domain of the lithostratigraphic unit (gray scaling)

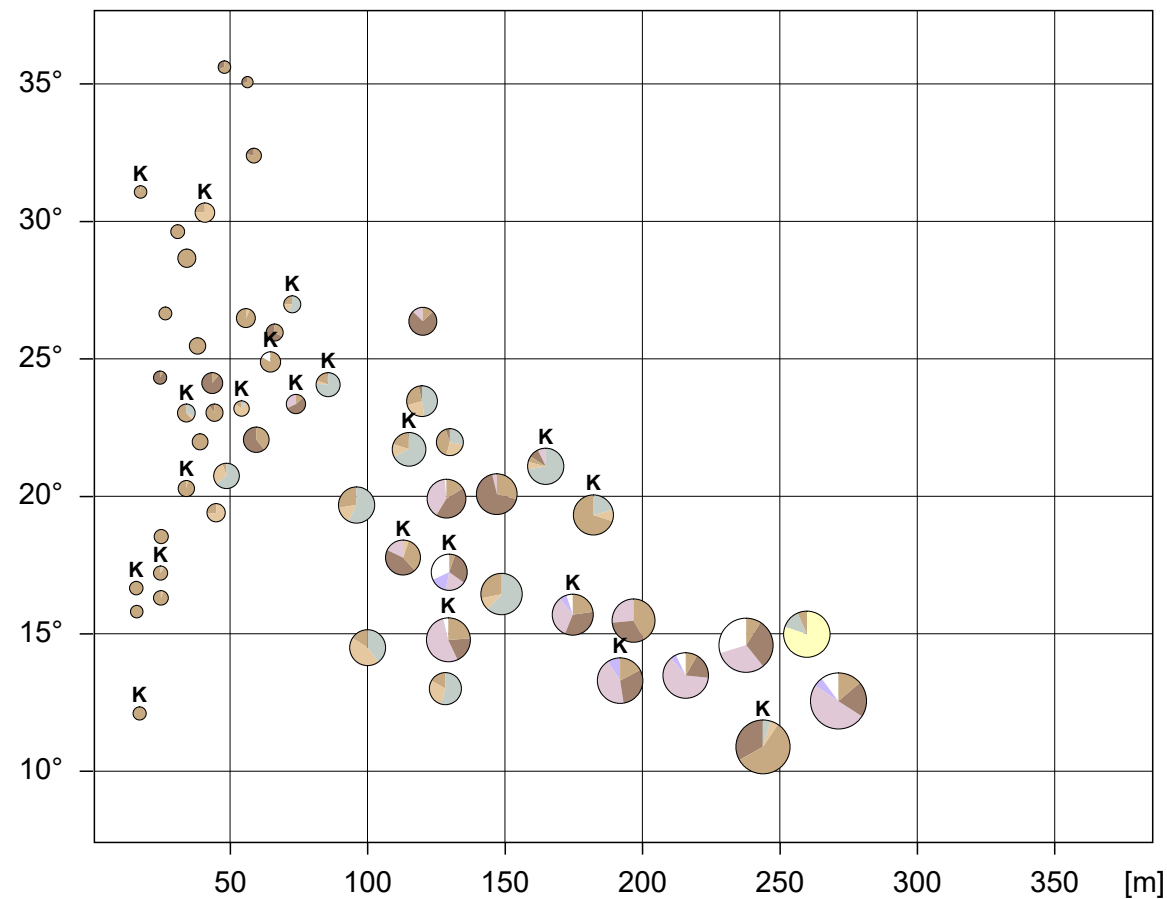


(*) where areal proportion of the lithostratigraphic unit is > 5% of the complete landslide surface

Letter „K“ indicates predominance of „Klingnau-Formation“ instead of „Hauptrogenstein“ for landslides east of the geographical axis „Gansingen - Schinznach“



Mean slope gradient vs. maximum elevation difference (relief) of landslide surface

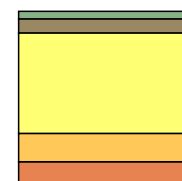


Areal proportion of different process domains intersecting with Hauptrogenstein / Klingnau-Formation

Process domains	[km ²]	[% of total area]	[% of hillslope area]
Quaternary plains and terraces	0.2	4.5%	
Upland low-relief areas	0.4	8%	
Presumably unfailed hillslopes	3.0	58%	66%
Presumed landslides	0.9	16.5%	19%
Evident landslides	0.7	13%	15%

} 34%

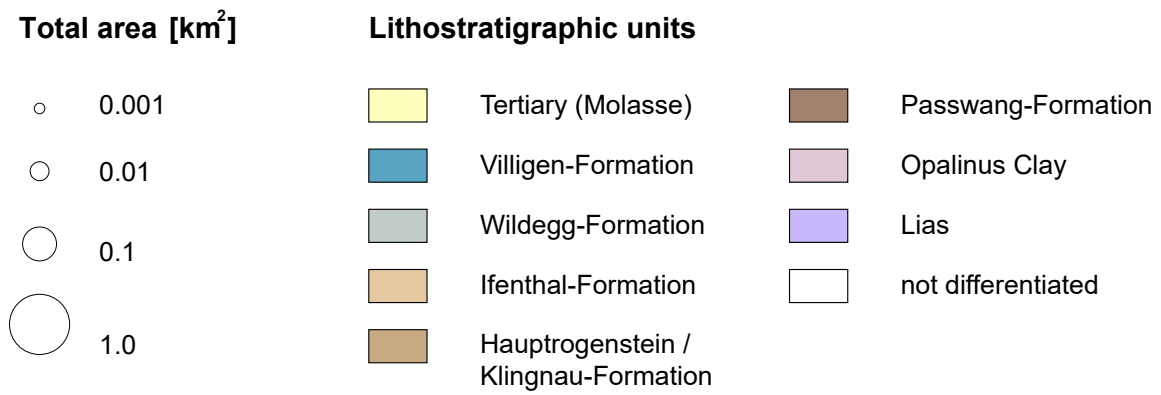
Total area = 5.2 km² (**)
(5.7% of total study area)



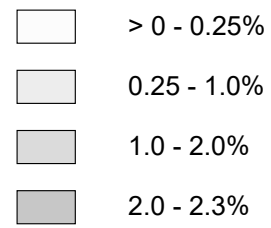
(**) box scaling proportional to absolute area

- slope gradient displayed along radial axis
- slope aspect displayed as azimuth direction
- frequencies of pixel-based values are summarized for slope gradients steeper than 30°

Surface characteristics of individual landslides intersecting with Passwang-Formation (*)

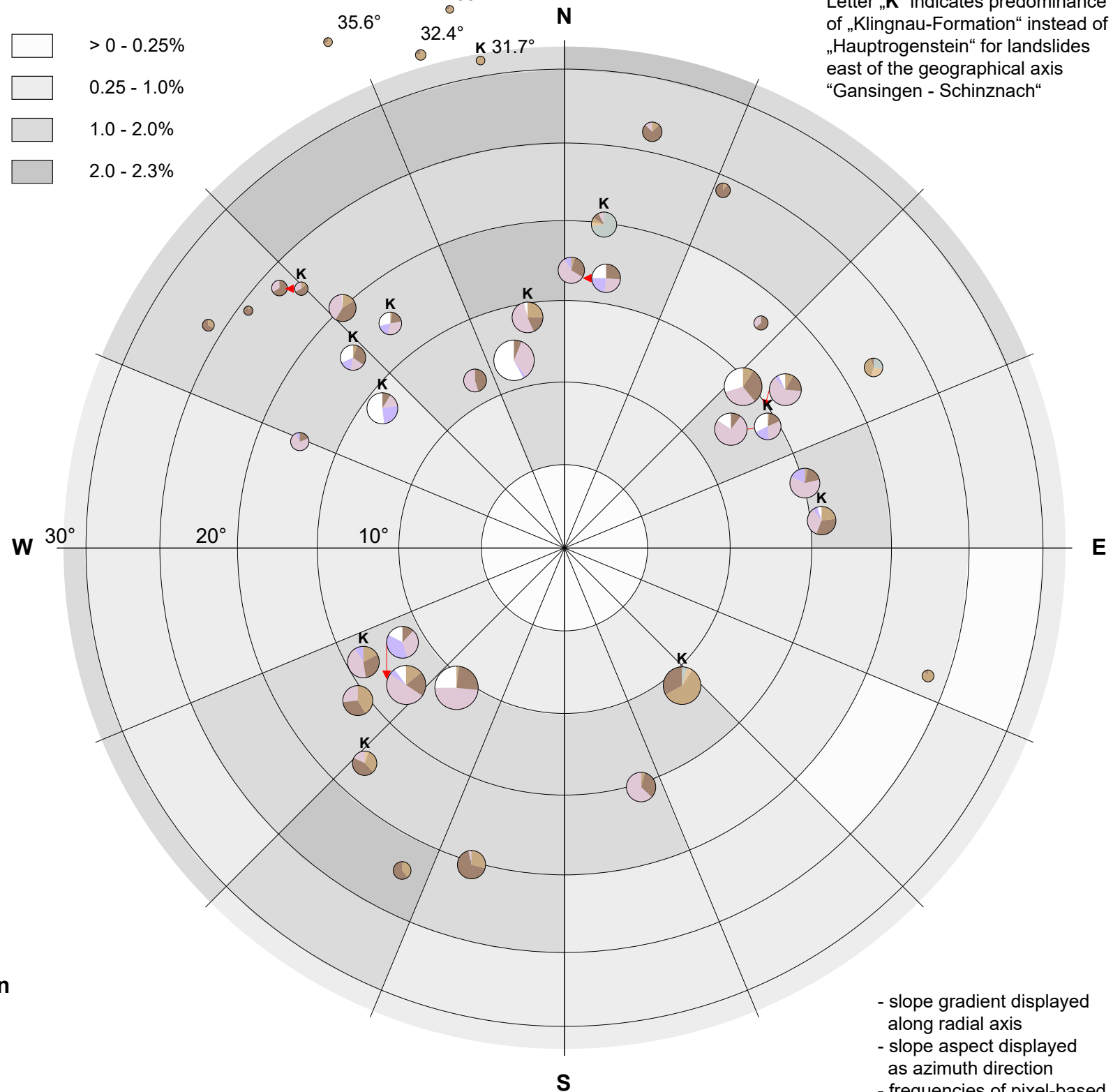


Mean surface orientation of landslides (pie charts) and frequency of pixel-based slope orientation within hillslope domain of the lithostratigraphic unit (gray scaling)

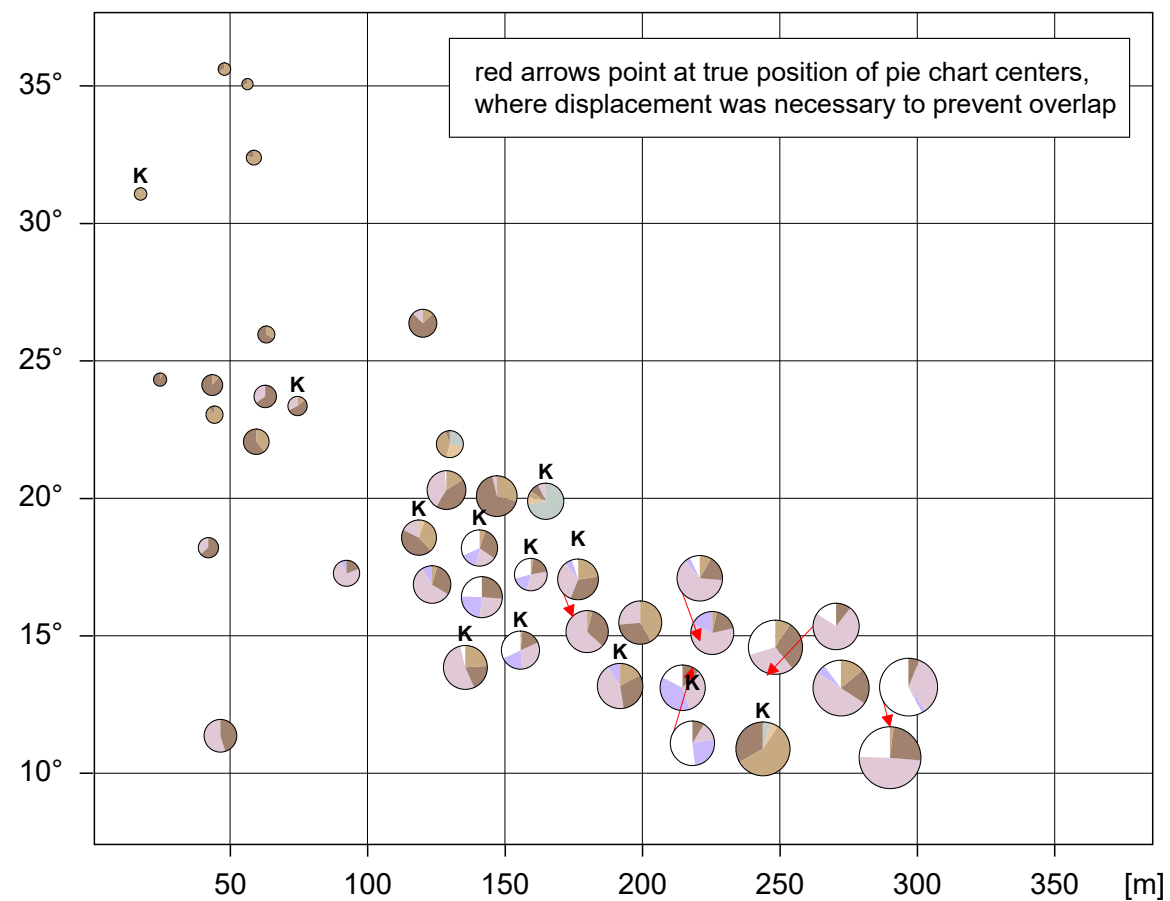


(*) where areal proportion of the lithostratigraphic unit is > 5% of the complete landslide surface

Letter „K“ indicates predominance of „Klingnau-Formation“ instead of „Hauptrogenstein“ for landslides east of the geographical axis „Gansingen - Schinznach“



Mean slope gradient vs. maximum elevation difference (relief) of landslide surface



Areal proportion of different process domains intersecting with Passwang-Formation

Process domains	[km ²]	[% of total area]	[% of hillslope area]
Quaternary plains and terraces	0.4	11%	
Upland low-relief areas	0	0%	
Presumably unfailed hillslopes	0.9	27%	30%
Presumed landslides	1.2	36%	40%
Evident landslides	0.9	26%	30%

70%

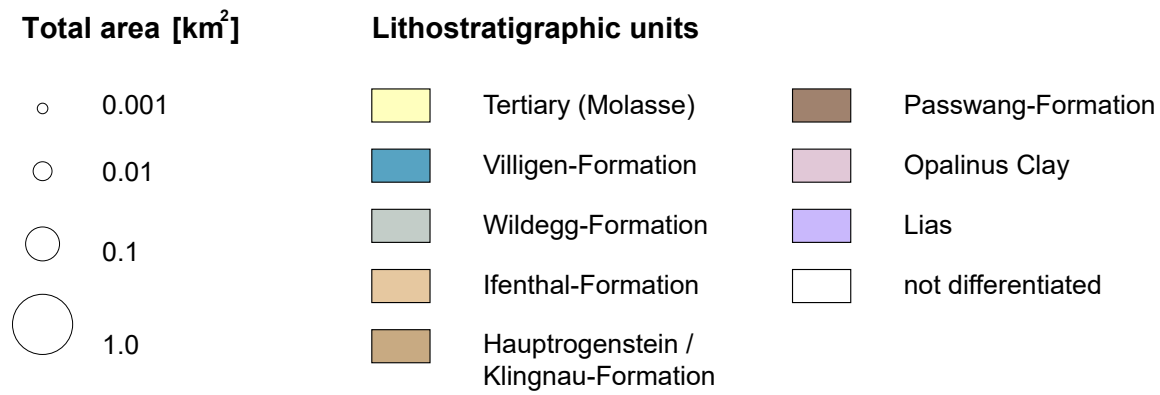
Total area = 3.4 km² (**)
(3.8% of total study area)



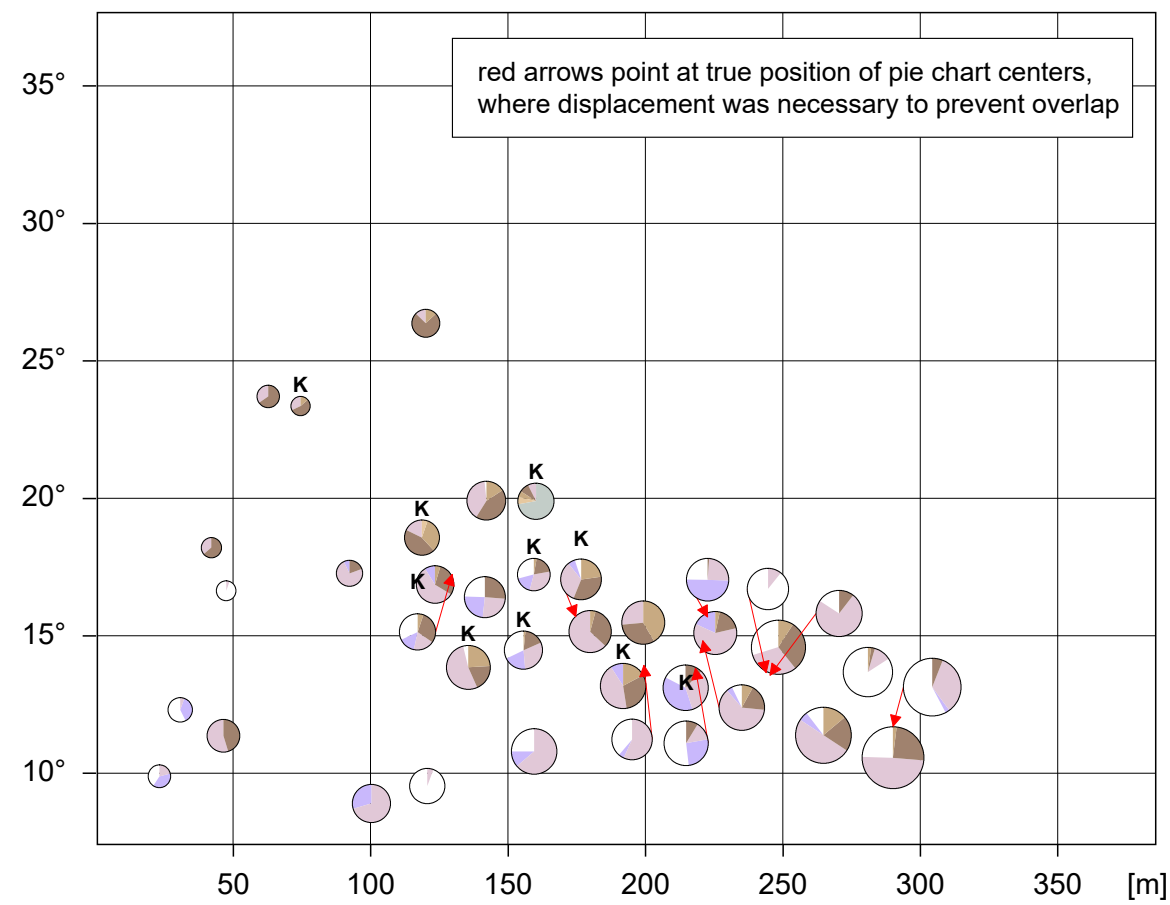
(**) box scaling proportional to absolute area

- slope gradient displayed along radial axis
- slope aspect displayed as azimuth direction
- frequencies of pixel-based values are summarized for slope gradients steeper than 30°

Surface characteristics of individual landslides intersecting with Opalinus Clay (*)



Mean slope gradient vs. maximum elevation difference (relief) of landslide surface

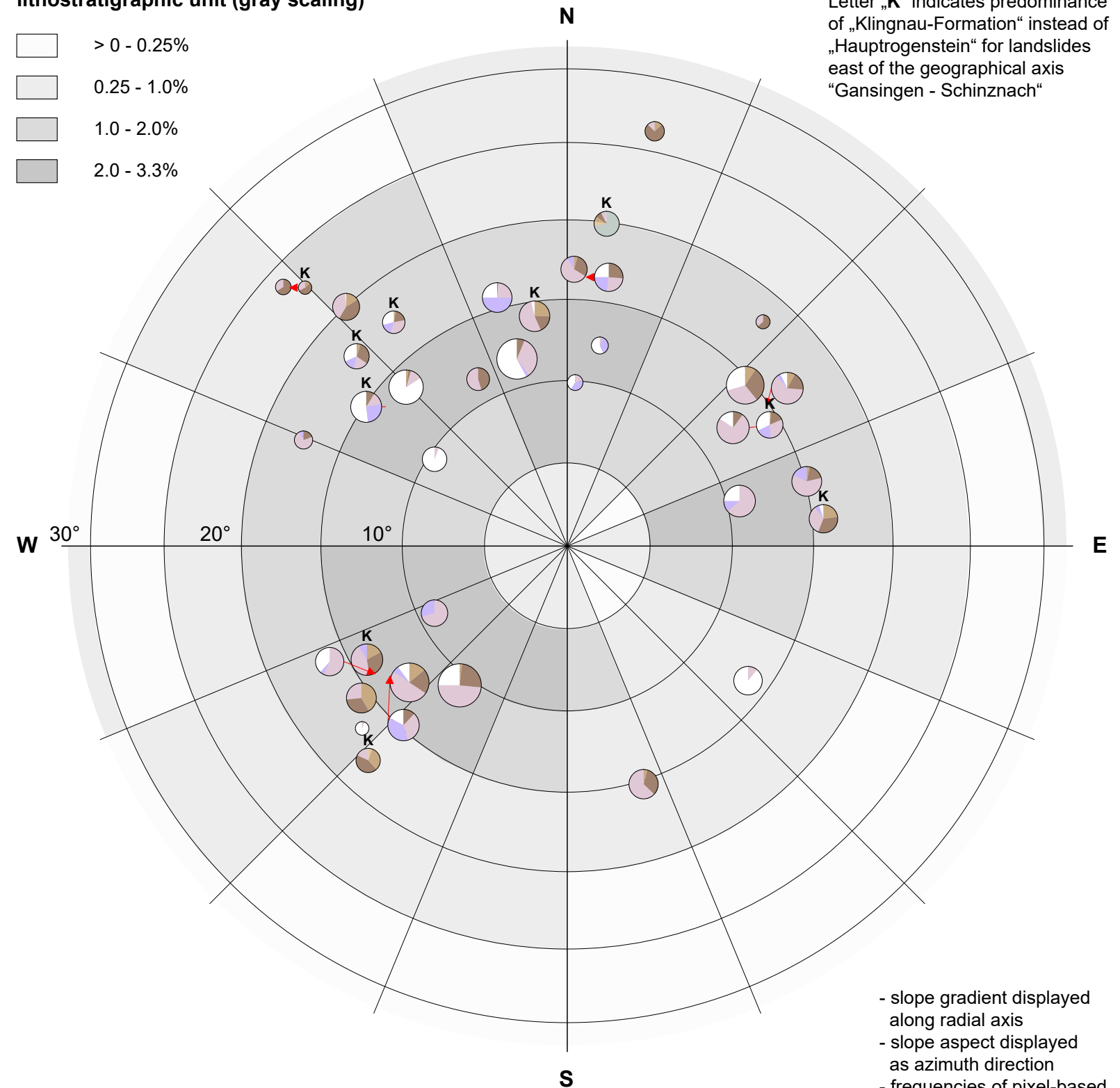
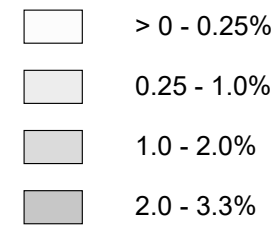


Areal proportion of different process domains intersecting with Opalinus Clay

Process domains	[km ²]	[% of total area]	[% of hillslope area]
Quaternary plains and terraces	0.7	12%	
Upland low-relief areas	0.1	1.5%	
Presumably unfailed hillslopes	0.9	16%	19%
Presumed landslides	1.8	34%	39%
Evident landslides	2.0	36.5%	42%

81%

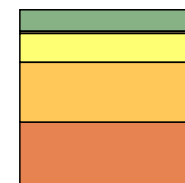
Mean surface orientation of landslides (pie charts) and frequency of pixel-based slope orientation within hillslope domain of the lithostratigraphic unit (gray scaling)



- red arrows point at true position of pie chart centers, where displacement was necessary to prevent overlap

- slope gradient displayed along radial axis
 - slope aspect displayed as azimuth direction
 - frequencies of pixel-based values are summarized for slope gradients steeper than 30°

Total area = 5.5 km² (**)
 (6.0% of total study area)



(**) box scaling proportional to absolute area

Stream analysis „Jura Ost“: longitudinal profile LP-1, „Rinikerfeld“ catchment (vertical axis scaled by factor 10)

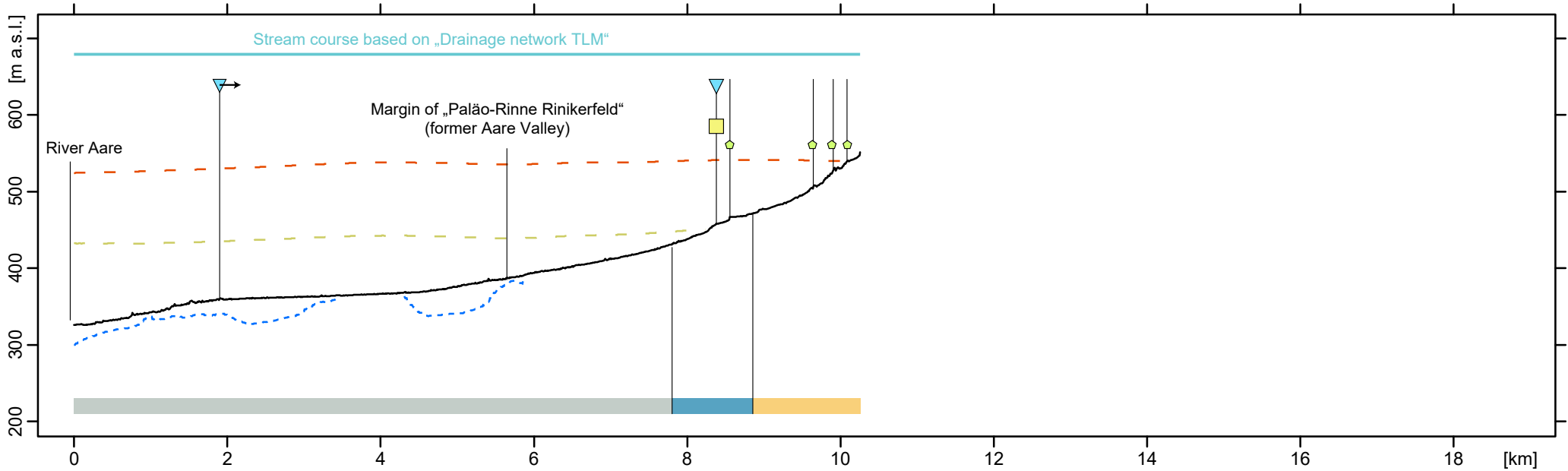
Extracted surfaces

- - - Base level of „Höhere Deckenschotter“ (HDS) } Heuberger & Naef (2014)
- - - Base level of „Tiefere Deckenschotter“ (TDS) } *(regionally interpolated surfaces (!):*
- Present topography (DTM-AV) } *poorly constrained / hypothetical*
- - - Top bedrock (where Quaternary deposits > 5m) } Pietsch & Jordan (2014)

Interpretation of profile anomalies (*)

- ↘ / ▽ Base level drop with knickpoint (migrating / fixed)
- ★ Lateral landsliding with material input to channel
- Lithological control
- ◇ Anthropogenic effect / artefact

(*) where multiple options are indicated, they may be superimposing.



Lithostratigraphic units of bedrock surface

- Obere Süßwassermolasse
- Villigen-Formation
- Wildeggen-Formation

nagra		NAB 17-42
Stream Analysis „Jura Ost“		
	DAT.: Mar. 2018	Appendix 3.A

Stream analysis „Jura Ost“: longitudinal profile LP-2, „Villnachern“ catchment (vertical axis scaled by factor 10)

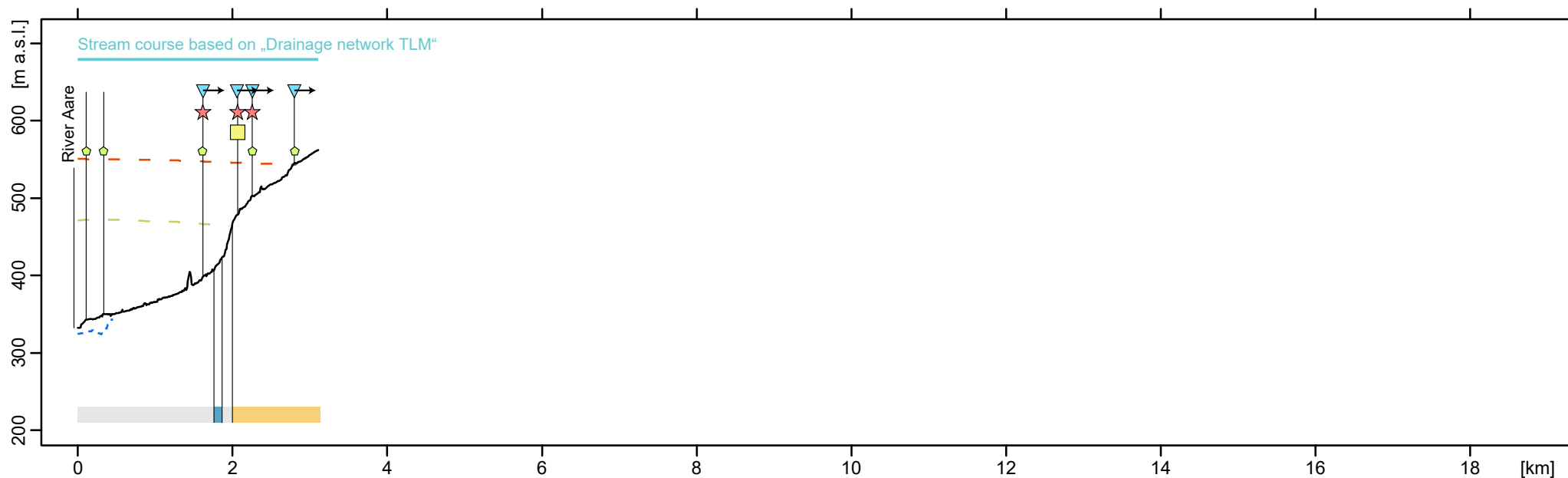
Extracted surfaces

- - - Base level of „Höhere Deckenschotter“ (HDS) } Heuberger & Naef (2014)
- - - Base level of „Tiefere Deckenschotter“ (TDS) } *(regionally interpolated surfaces (!):*
- Present topography (DTM-AV) } *poorly constrained / hypothetical*
- - - Top bedrock (where Quaternary deposits > 5m) } Pietsch & Jordan (2014)

Interpretation of profile anomalies (*)

- ↘ / ▽ Base level drop with knickpoint (migrating / fixed)
- ★ Lateral landsliding with material input to channel
- Lithological control
- ◇ Anthropogenic effect / artefact

(*) where multiple options are indicated, they may be superimposing.



Lithostratigraphic units of bedrock surface

- Obere Süßwassermolasse
- Villigen-Formation
- not differentiated

nagra	NAB 17-42	
Stream Analysis „Jura Ost“		
	DAT.: Mar. 2018	Appendix 3.B

Stream analysis „Jura Ost“: longitudinal profile LP-3, „Villnachern“ catchment (vertical axis scaled by factor 10)

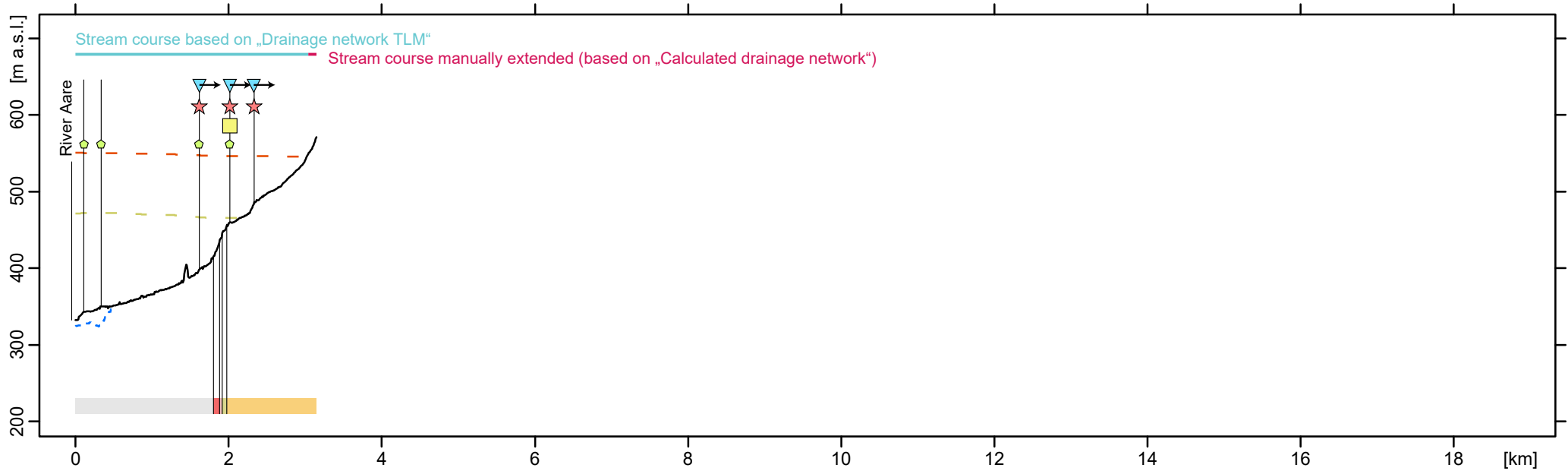
Extracted surfaces

- - - Base level of „Höhere Deckenschotter“ (HDS) } Heuberger & Naef (2014)
 - - - Base level of „Tiefere Deckenschotter“ (TDS) } *(regionally interpolated surfaces (!):*
 - Present topography (DTM-AV) } *poorly constrained / hypothetical*
 - - - Top bedrock (where Quaternary deposits > 5m) } *towards interior valleys)*
- Pietsch & Jordan (2014)

Interpretation of profile anomalies (*)

- ↘ / ▽ Base level drop with knickpoint (migrating / fixed)
- ★ Lateral landsliding with material input to channel
- Lithological control
- ◇ Anthropogenic effect / artefact

(*) where multiple options are indicated, they may be superimposing.



Lithostratigraphic units of bedrock surface

- Obere Süßwassermolasse
- Obere Meeresmolasse
- Untere Süßwassermolasse
- Siderolithikum
- not differentiated

nagra		NAB 17-42
Stream Analysis „Jura Ost“		
	DAT.: Mar. 2018	Appendix 3.C

Stream analysis „Jura Ost“: longitudinal profile LP-4, „Villnachern“ catchment (vertical axis scaled by factor 10)

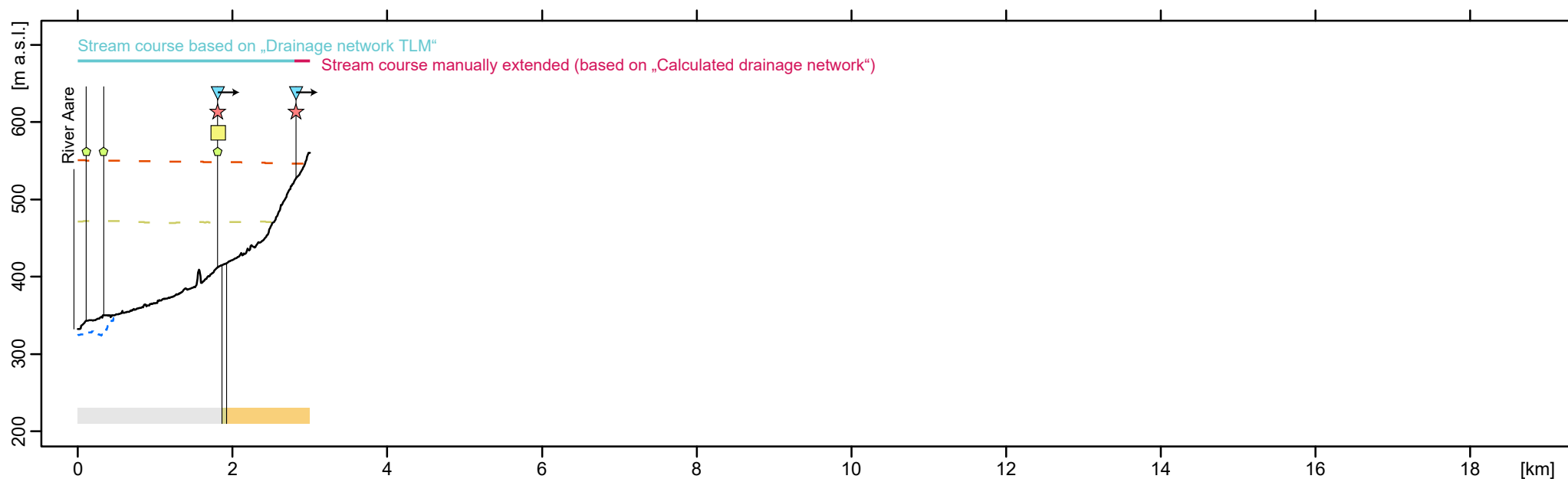
Extracted surfaces

- - - Base level of „Höhere Deckenschotter“ (HDS) } Heuberger & Naef (2014)
 - - - Base level of „Tiefere Deckenschotter“ (TDS) } *(regionally interpolated surfaces (!):*
 - Present topography (DTM-AV) } *poorly constrained / hypothetical*
 - - - Top bedrock (where Quaternary deposits > 5m) } *towards interior valleys)*
- Pietsch & Jordan (2014)

Interpretation of profile anomalies (*)

- ↘ / ▽ Base level drop with knickpoint (migrating / fixed)
- ★ Lateral landsliding with material input to channel
- Lithological control
- ◇ Anthropogenic effect / artefact

(*) where multiple options are indicated, they may be superimposing.



Lithostratigraphic units of bedrock surface

- Obere Süßwassermolasse
- Obere Meeresmolasse
- not differentiated

nagra		NAB 17-42
Stream Analysis „Jura Ost“		
	DAT.: Mar. 2018	Appendix 3.D

Stream analysis „Jura Ost“: longitudinal profile LP-5, „Sissle“ catchment (vertical axis scaled by factor 10)

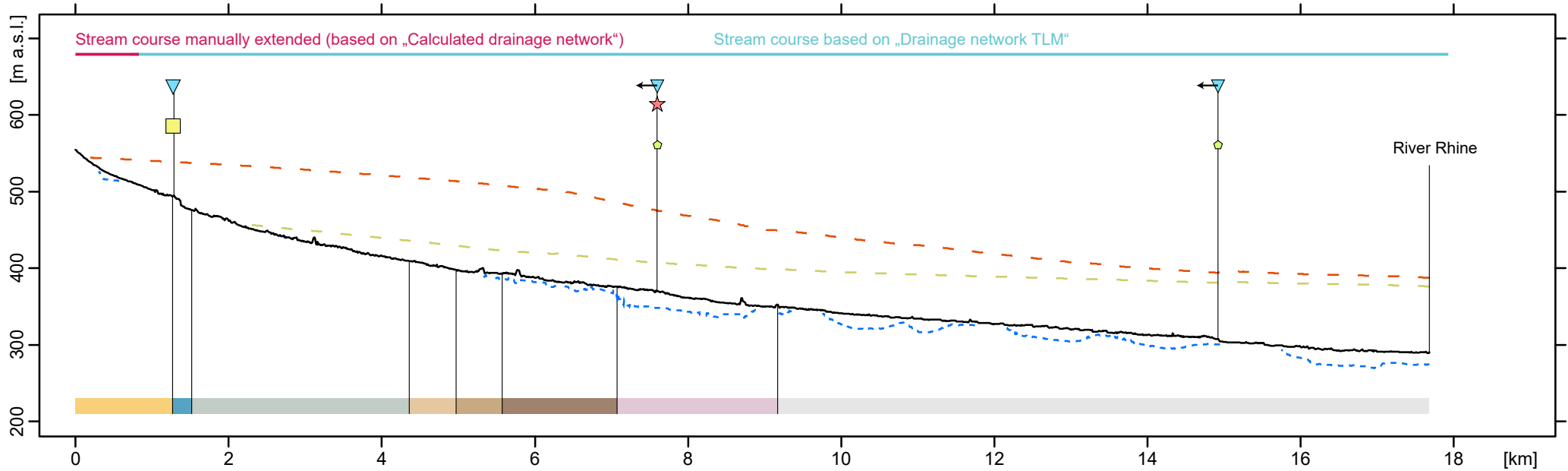
Extracted surfaces

- - - Base level of „Höhere Deckenschotter“ (HDS) } Heuberger & Naef (2014)
- - - Base level of „Tiefere Deckenschotter“ (TDS) } *(regionally interpolated surfaces (!):*
- Present topography (DTM-AV) } *poorly constrained / hypothetical*
- - - Top bedrock (where Quaternary deposits > 5m) } Pietsch & Jordan (2014)
- } *towards interior valleys)*

Interpretation of profile anomalies (*)

- ↔ / ▼ Base level drop with knickpoint (migrating / fixed)
- ★ Lateral landsliding with material input to channel
- Lithological control
- ◇ Anthropogenic effect / artefact

(*) where multiple options are indicated, they may be superimposing.



Lithostratigraphic units of bedrock surface

- | | |
|---------------------------|----------------------|
| ■ Obere Süsswassermolasse | ■ Hauptrogenstein |
| ■ Villigen-Formation | ■ Passwang-Formation |
| ■ Wildegg-Formation | ■ Opalinus Clay |
| ■ Ifenthal-Formation | ■ not differentiated |

nagra		NAB 17-42
Stream Analysis „Jura Ost“		
	DAT.: Mar. 2018	Appendix 3.E

Stream analysis „Jura Ost“: longitudinal profile LP-6, „Sissle“ catchment (vertical axis scaled by factor 10)

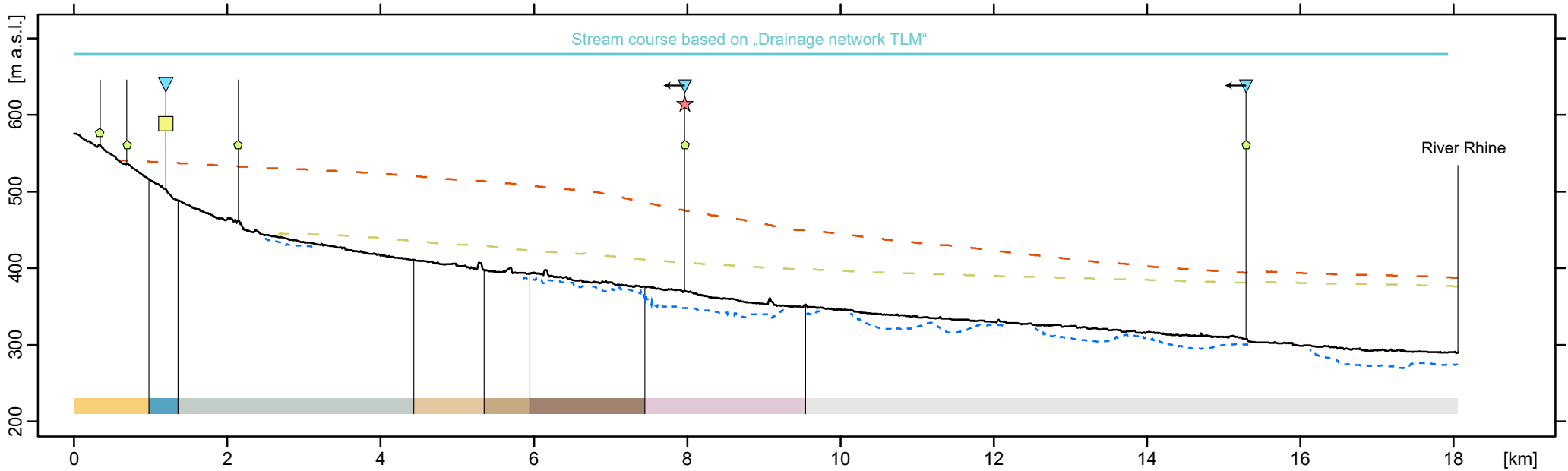
Extracted surfaces

- - - Base level of „Höhere Deckenschotter“ (HDS) } Heuberger & Naef (2014)
(regionally interpolated surfaces (!):
poorly constrained / hypothetical
towards interior valleys)
- - - Base level of „Tiefere Deckenschotter“ (TDS) }
- Present topography (DTM-AV)
- - - Top bedrock (where Quaternary deposits > 5m) Pietsch & Jordan (2014)

Interpretation of profile anomalies (*)

- ↔ / ▼ Base level drop with knickpoint (migrating / fixed)
- ★ Lateral landsliding with material input to channel
- Lithological control
- ◇ Anthropogenic effect / artefact

(*) where multiple options are indicated, they may be superimposing.



Lithostratigraphic units of bedrock surface

- | | |
|---------------------------|----------------------|
| ■ Obere Süsswassermolasse | ■ Hauptrogenstein |
| ■ Villigen-Formation | ■ Passwang-Formation |
| ■ Wildegg-Formation | ■ Opalinus Clay |
| ■ Ifenthal-Formation | ■ not differentiated |

nagra		NAB 17-42
Stream Analysis „Jura Ost“		
	DAT.: Mar. 2018	Appendix 3.F

Stream analysis „Jura Ost“: longitudinal profile LP-7, „Sissle“ catchment (vertical axis scaled by factor 10)

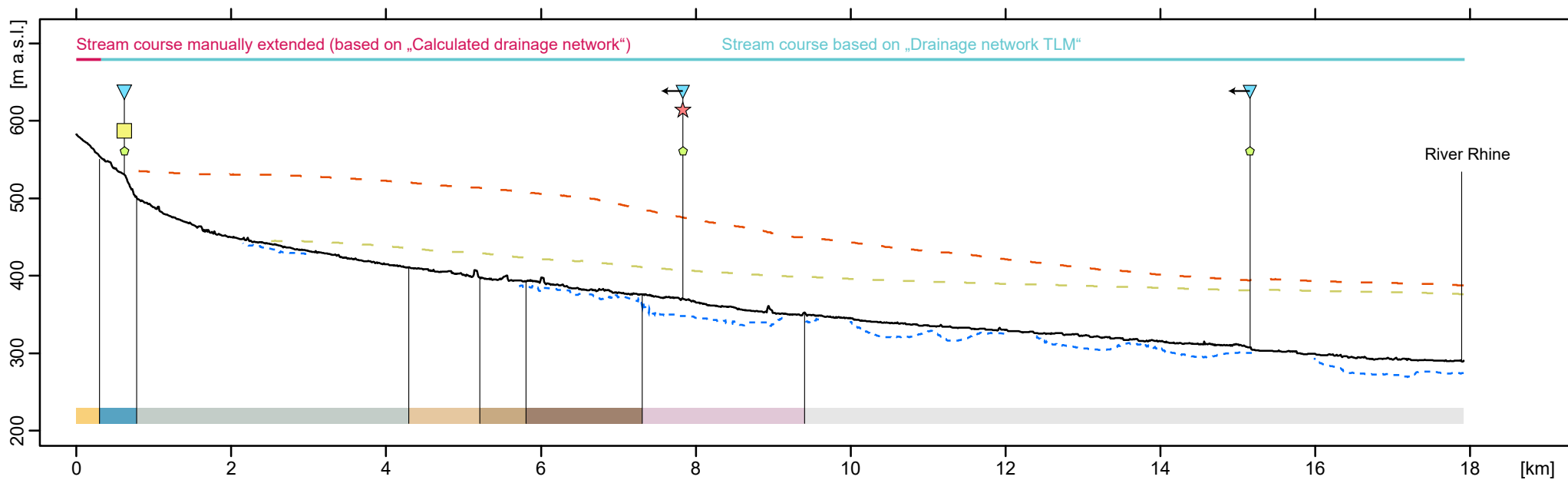
Extracted surfaces

- - - Base level of „Höhere Deckenschotter“ (HDS) } Heuberger & Naef (2014)
- - - Base level of „Tiefere Deckenschotter“ (TDS) } *(regionally interpolated surfaces (!):*
- Present topography (DTM-AV) } *poorly constrained / hypothetical*
- - - Top bedrock (where Quaternary deposits > 5m) } *towards interior valleys)*
- } Pietsch & Jordan (2014)

Interpretation of profile anomalies (*)

- ↖ / ▼ Base level drop with knickpoint (migrating / fixed)
- ★ Lateral landsliding with material input to channel
- Lithological control
- ◇ Anthropogenic effect / artefact

(*) where multiple options are indicated, they may be superimposing.



Lithostratigraphic units of bedrock surface

- | | |
|---|---|
| ■ Obere Süsswassermolasse | ■ Hauptrogenstein |
| ■ Villigen-Formation | ■ Passwang-Formation |
| ■ Wildegg-Formation | ■ Opalinus Clay |
| ■ Ifenthal-Formation | ■ not differentiated |

nagra	NAB 17-42
Stream Analysis „Jura Ost“	
DAT.: Mar. 2018	Appendix 3.G

Stream analysis „Jura Ost“: longitudinal profile LP-8, „Sissle“ catchment (vertical axis scaled by factor 10)

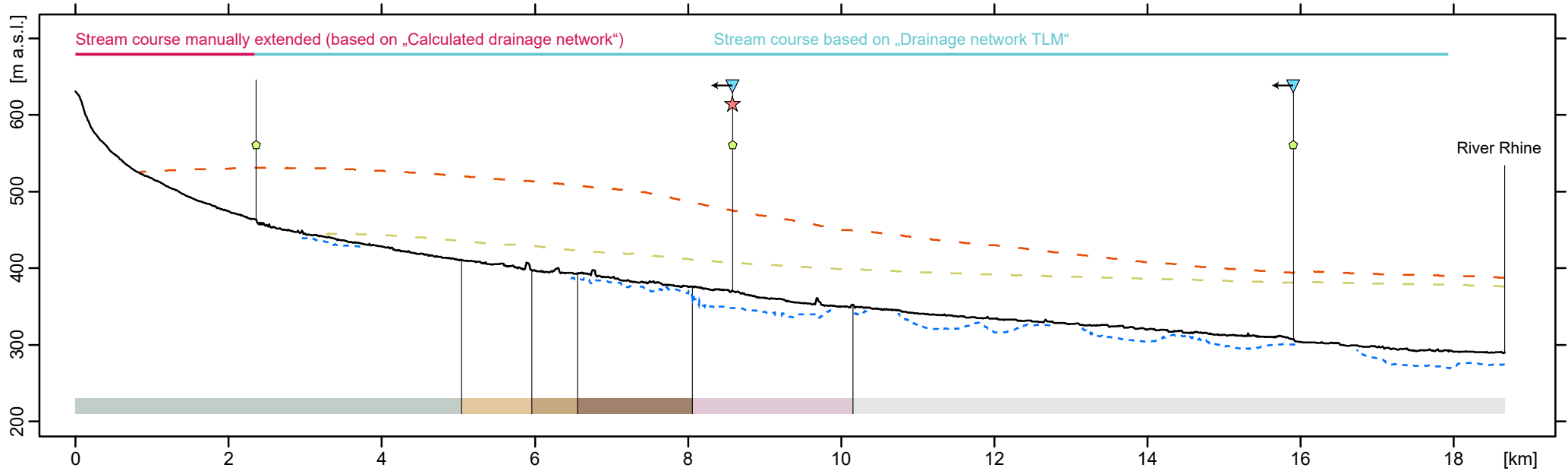
Extracted surfaces

- - - Base level of „Höhere Deckenschotter“ (HDS) } Heuberger & Naef (2014)
- - - Base level of „Tiefere Deckenschotter“ (TDS) } *(regionally interpolated surfaces (!):*
- Present topography (DTM-AV) } *poorly constrained / hypothetical*
- - - Top bedrock (where Quaternary deposits > 5m) Pietsch & Jordan (2014) } *towards interior valleys)*

Interpretation of profile anomalies (*)

- ↔ / ▽ Base level drop with knickpoint (migrating / fixed)
- ★ Lateral landsliding with material input to channel
- Lithological control
- ◇ Anthropogenic effect / artefact

(*) where multiple options are indicated, they may be superimposing.



Lithostratigraphic units of bedrock surface

- Wildegg-Formation
- Ifenthal-Formation
- Hauptrogenstein
- Passwang-Formation
- Opalinus Clay
- not differentiated

nagra		NAB 17-42
Stream Analysis „Jura Ost“		
	DAT.: Mar. 2018	Appendix 3.H

Stream analysis „Jura Ost“: longitudinal profile LP-9, „Ittenthal“ catchment (vertical axis scaled by factor 10)

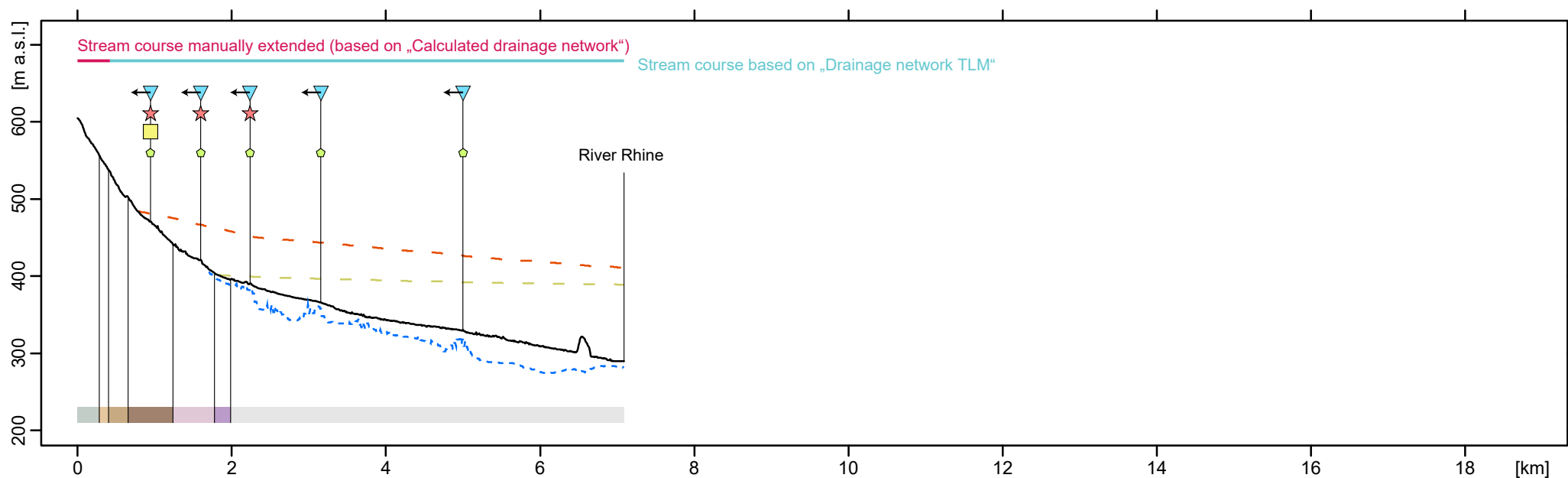
Extracted surfaces

- - - Base level of „Höhere Deckenschotter“ (HDS) } Heuberger & Naef (2014)
- - - Base level of „Tiefere Deckenschotter“ (TDS) } (regionally interpolated surfaces (!):
- Present topography (DTM-AV) } poorly constrained / hypothetical
- - - Top bedrock (where Quaternary deposits > 5m) } towards interior valleys)
- Top bedrock (where Quaternary deposits > 5m) Pietsch & Jordan (2014)

Interpretation of profile anomalies (*)

- ↔ / ▽ Base level drop with knickpoint (migrating / fixed)
- ★ Lateral landsliding with material input to channel
- Lithological control
- ◇ Anthropogenic effect / artefact

(*) where multiple options are indicated, they may be superimposing.



Lithostratigraphic units of bedrock surface

- | | |
|--|---|
| Wildeggen-Formation | Opalinus Clay |
| Ifenthal-Formation | Lias |
| Hauptrogenstein | not differentiated |
| Passwang-Formation | |

nagra

NAB 17-42

Stream Analysis „Jura Ost“

DAT.: Mar. 2018

Appendix 3.J

Stream analysis „Jura Ost“: longitudinal profile LP-10, „Sulzerbach“ catchment (vertical axis scaled by factor 10)

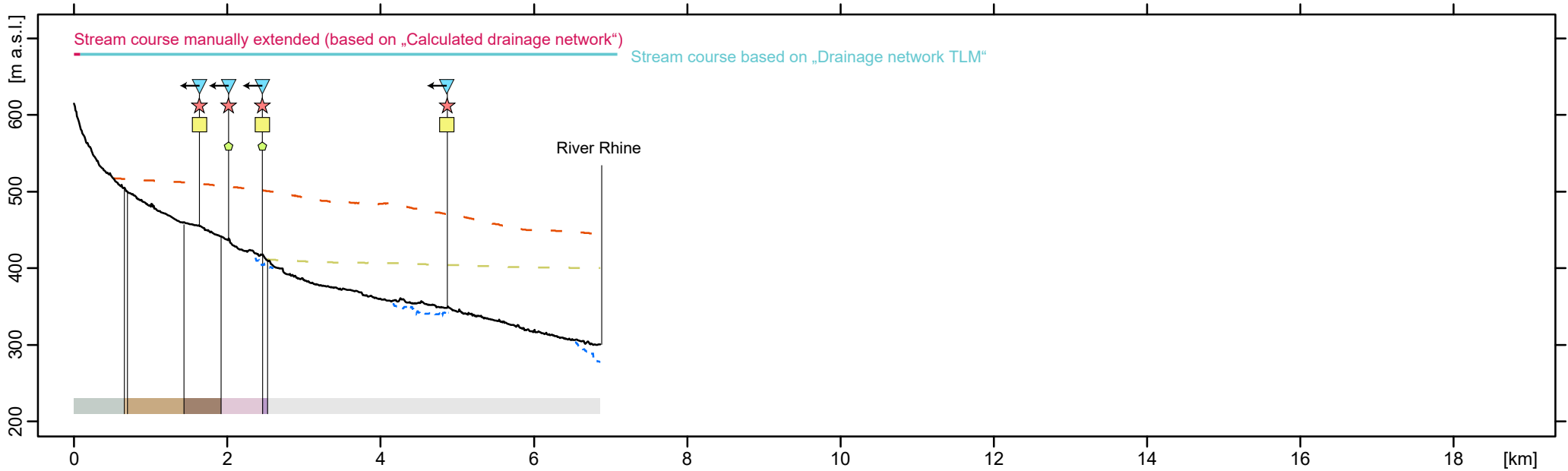
Extracted surfaces

- - - Base level of „Höhere Deckenschotter“ (HDS) } Heuberger & Naef (2014)
- - - Base level of „Tiefere Deckenschotter“ (TDS) } *(regionally interpolated surfaces (!):*
- Present topography (DTM-AV) } *poorly constrained / hypothetical*
- - - Top bedrock (where Quaternary deposits > 5m) } *towards interior valleys)*
- Top bedrock (where Quaternary deposits > 5m) Pietsch & Jordan (2014)

Interpretation of profile anomalies (*)

- ↔ / ▽ Base level drop with knickpoint (migrating / fixed)
- ★ Lateral landsliding with material input to channel
- Lithological control
- ◇ Anthropogenic effect / artefact

(*) where multiple options are indicated, they may be superimposing.



Lithostratigraphic units of bedrock surface

- | | |
|----------------------|----------------------|
| ■ Wildegg-Formation | ■ Opalinus Clay |
| ■ Ifenthal-Formation | ■ Lias |
| ■ Hauptrogenstein | ■ not differentiated |
| ■ Passwang-Formation | |

nagra		NAB 17-42
Stream Analysis „Jura Ost“		
	DAT.: Mar. 2018	Appendix 3.K

Stream analysis „Jura Ost“: longitudinal profile LP-11, „Bürerbach“ catchment (vertical axis scaled by factor 10)

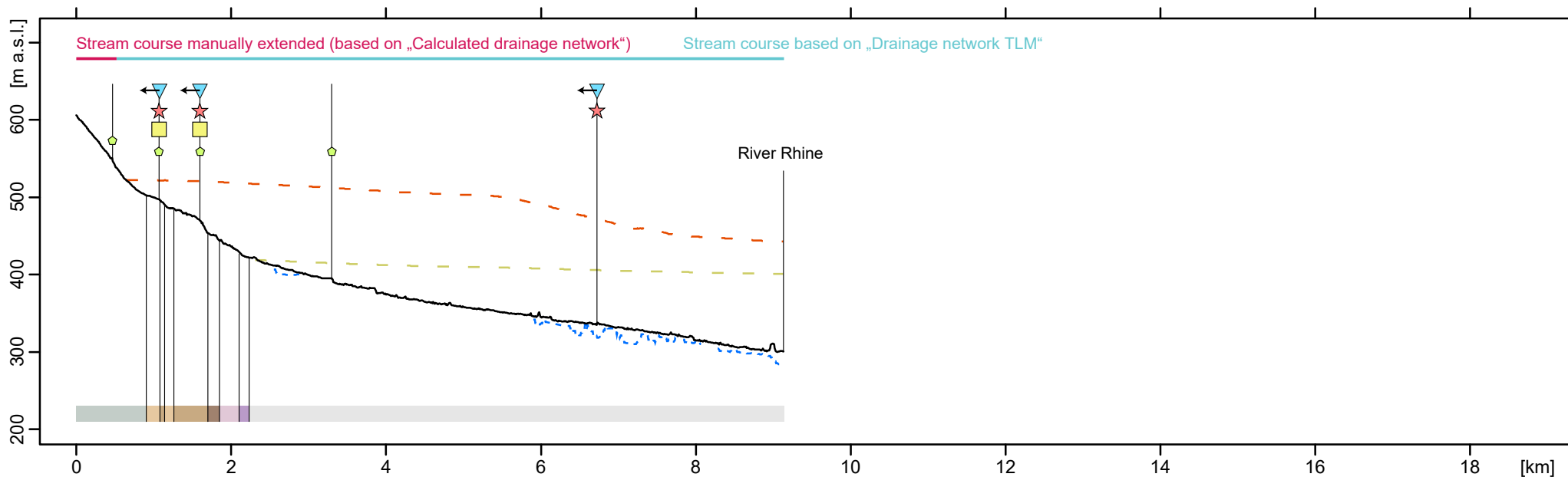
Extracted surfaces

- - - Base level of „Höhere Deckenschotter“ (HDS) } Heuberger & Naef (2014)
- - - Base level of „Tiefere Deckenschotter“ (TDS) } (*regionally interpolated surfaces (!):*
- poorly constrained / hypothetical*
- towards interior valleys*)
- Present topography (DTM-AV)
- - - Top bedrock (where Quaternary deposits > 5m) Pietsch & Jordan (2014)

Interpretation of profile anomalies (*)

- ↖ / ▽ Base level drop with knickpoint (migrating / fixed)
- ★ Lateral landsliding with material input to channel
- Lithological control
- ◇ Anthropogenic effect / artefact

(*) where multiple options are indicated, they may be superimposing.



Lithostratigraphic units of bedrock surface

- | | |
|--|--|
| Wildeggen-Formation | Opalinus Clay |
| Ifenthal-Formation | Lias |
| (Hauptrogenstein) / Klingnau-Formation | not differentiated |
| Passwang-Formation | |

nagra	NAB 17-42
Stream Analysis „Jura Ost“	
DAT.: Mar. 2018	Appendix 3.L

Stream analysis „Jura Ost“: longitudinal profile LP-12, „Rinikerfeld“ catchment (vertical axis scaled by factor 10)

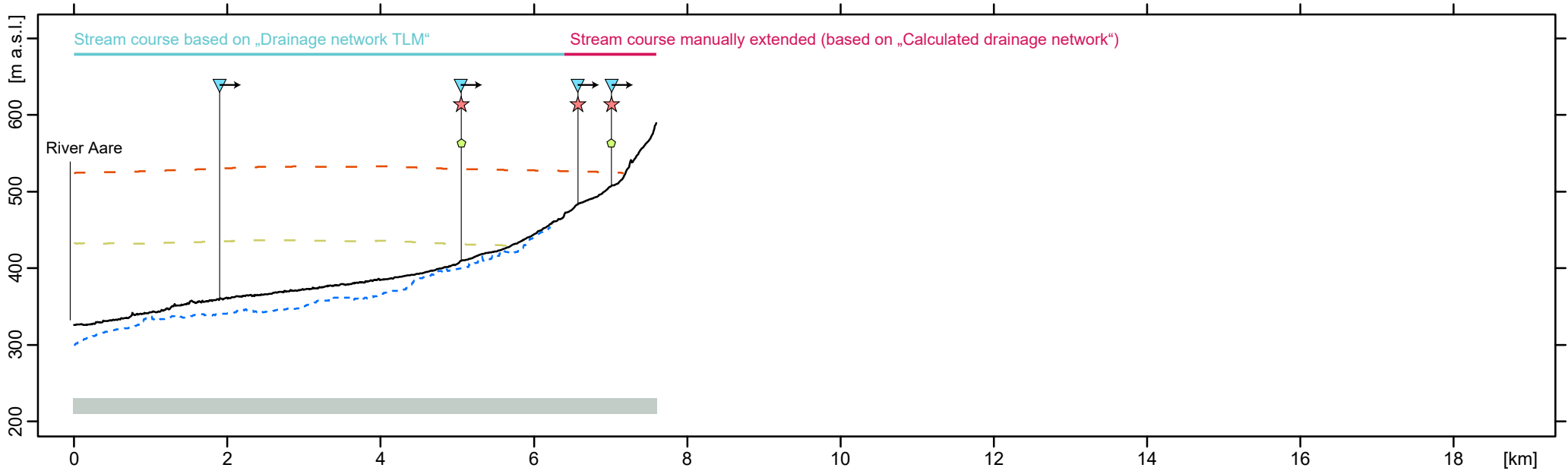
Extracted surfaces

- - - Base level of „Höhere Deckenschotter“ (HDS) } Heuberger & Naef (2014)
- - - Base level of „Tiefere Deckenschotter“ (TDS) } (*regionally interpolated surfaces (!):*
poorly constrained / hypothetical
towards interior valleys)
- Present topography (DTM-AV)
- - - Top bedrock (where Quaternary deposits > 5m) Pietsch & Jordan (2014)

Interpretation of profile anomalies (*)

- ↘ / ▽ Base level drop with knickpoint (migrating / fixed)
- ★ Lateral landsliding with material input to channel
- Lithological control
- ◇ Anthropogenic effect / artefact

(*) where multiple options are indicated, they may be superimposing.



Lithostratigraphic units of bedrock surface

- Wildegg-Formation

nagra		NAB 17-42
Stream Analysis „Jura Ost“		
	DAT.: Mar. 2018	Appendix 3.M

Stream analysis „Jura Ost“: longitudinal profile LP-13, „Rinikerfeld“ catchment (vertical axis scaled by factor 10)

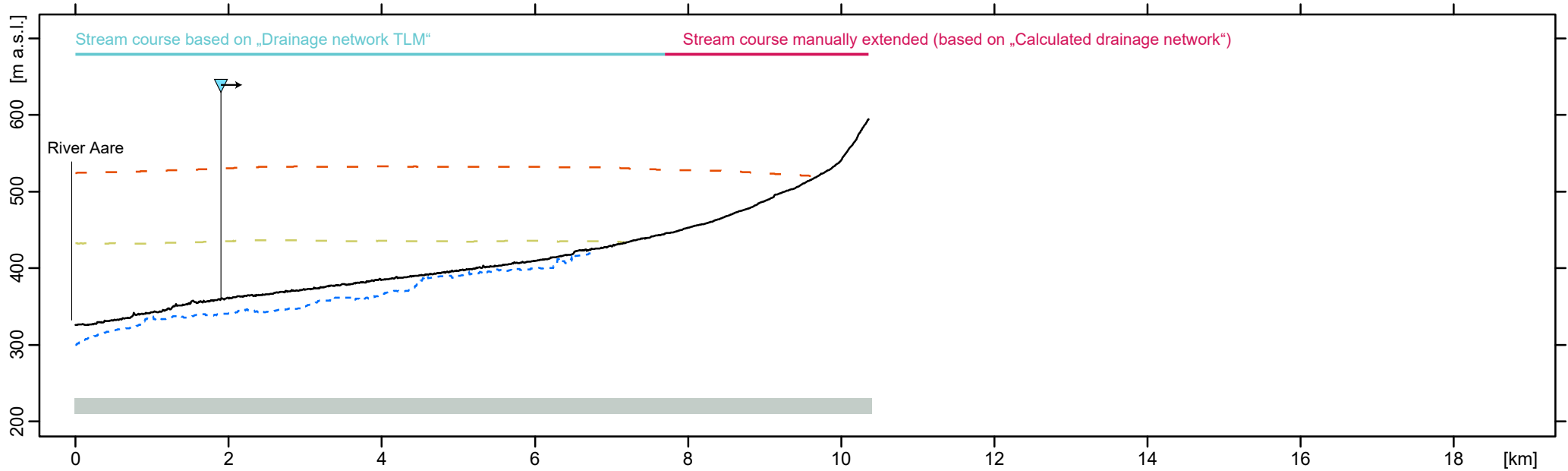
Extracted surfaces

- - - Base level of „Höhere Deckenschotter“ (HDS) } Heuberger & Naef (2014)
 - - - Base level of „Tiefere Deckenschotter“ (TDS) } *(regionally interpolated surfaces (!):*
 - Present topography (DTM-AV) } *poorly constrained / hypothetical*
 - - - Top bedrock (where Quaternary deposits > 5m) } *towards interior valleys)*
- Pietsch & Jordan (2014)

Interpretation of profile anomalies (*)

- ↘ / ▽ Base level drop with knickpoint (migrating / fixed)
- ★ Lateral landsliding with material input to channel
- Lithological control
- ◇ Anthropogenic effect / artefact

(*) where multiple options are indicated, they may be superimposing.



Lithostratigraphic units of bedrock surface

- Wildegg-Formation

nagra		NAB 17-42
Stream Analysis „Jura Ost“		
	DAT.: Mar. 2018	Appendix 3.N

Stream analysis „Jura Ost“: longitudinal profile LP-14, „Rinikerfeld“ catchment (vertical axis scaled by factor 10)

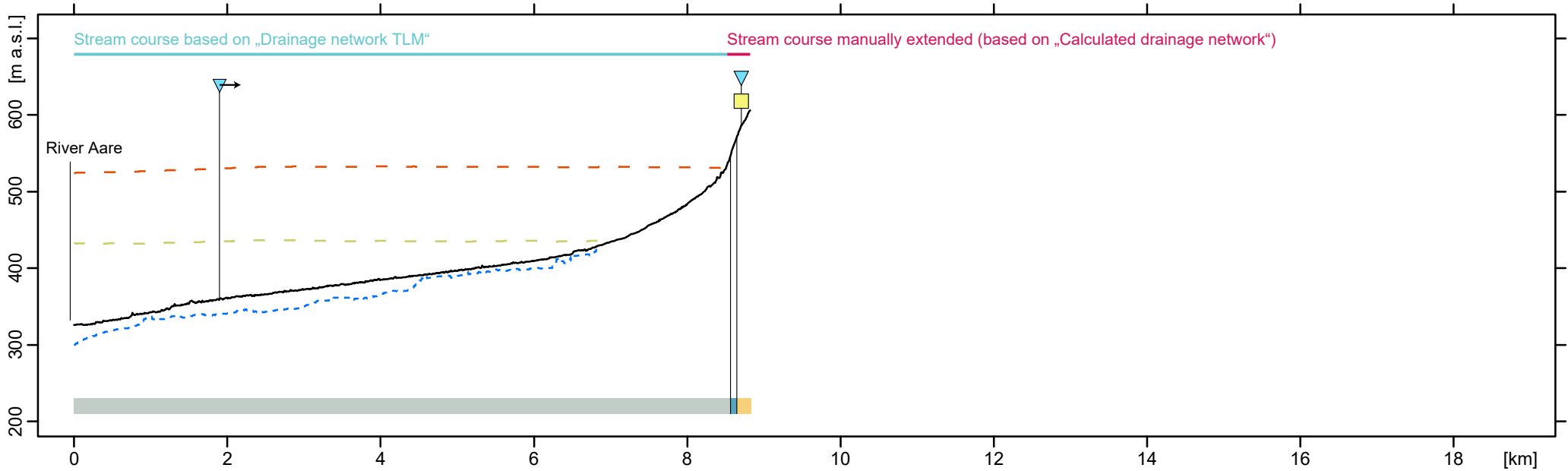
Extracted surfaces

- - - Base level of „Höhere Deckenschotter“ (HDS) } Heuberger & Naef (2014)
- - - Base level of „Tiefere Deckenschotter“ (TDS) } *(regionally interpolated surfaces (!):*
- Present topography (DTM-AV) } *poorly constrained / hypothetical*
- - - Top bedrock (where Quaternary deposits > 5m) } Pietsch & Jordan (2014)
- } *towards interior valleys)*

Interpretation of profile anomalies (*)

- ↘ / ▽ Base level drop with knickpoint (migrating / fixed)
- ★ Lateral landsliding with material input to channel
- Lithological control
- ◇ Anthropogenic effect / artefact

(*) where multiple options are indicated, they may be superimposing.



Lithostratigraphic units of bedrock surface

- Obere Süsswassermolasse
- Villigen-Formation
- Wildeggen-Formation

nagra		NAB 17-42
Stream Analysis „Jura Ost“		
	DAT.: Mar. 2018	Appendix 3.0

Stream analysis „Jura Ost“: longitudinal profile LP-15, „Rinikerfeld“ catchment (vertical axis scaled by factor 10)

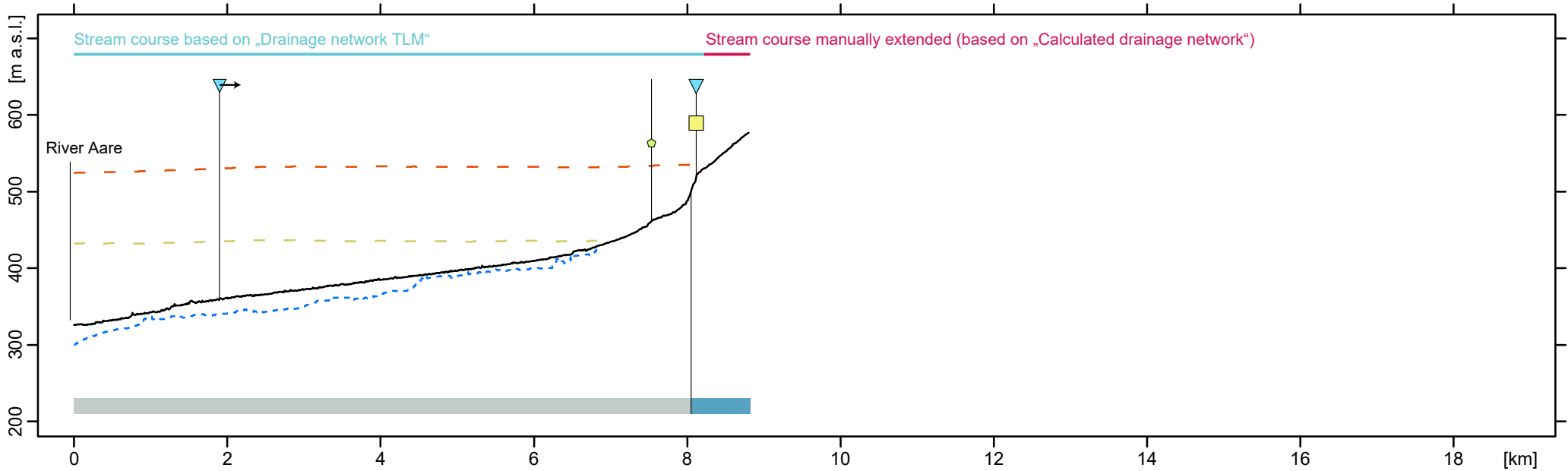
Extracted surfaces

- - - Base level of „Höhere Deckenschotter“ (HDS) } Heuberger & Naef (2014)
 - - - Base level of „Tiefere Deckenschotter“ (TDS) } *(regionally interpolated surfaces (!):*
 - Present topography (DTM-AV) } *poorly constrained / hypothetical*
 - - - Top bedrock (where Quaternary deposits > 5m) } *towards interior valleys)*
- Pietsch & Jordan (2014)

Interpretation of profile anomalies (*)

- ↘ / ▽ Base level drop with knickpoint (migrating / fixed)
- ★ Lateral landsliding with material input to channel
- Lithological control
- ◇ Anthropogenic effect / artefact

(*) where multiple options are indicated, they may be superimposing.



Lithostratigraphic units of bedrock surface

- Villigen-Formation
- Wildegg-Formation

nagra		NAB 17-42
Stream Analysis „Jura Ost“		
	DAT.: Mar. 2018	Appendix 3.P

Regional topographic / geological profile „Jura Ost“, north-south directed (vertical axis scaled by factor 10)

Extracted surfaces

- - - Base level of „Höhere Deckenschotter“ (HDS) } Heuberger & Naef (2014)
- - - Base level of „Tiefere Deckenschotter“ (TDS) } Regionally interpolated surfaces (!): poorly constrained / hypothetical towards interior valleys
- Present topography (DTM-AV)
- - - Top bedrock (where Quaternary deposits > 5m) Pietsch & Jordan (2014)

This study

- ↙ Landslides } Schematic illustration according to map of process domains / visual inspection of DTM-AV hillshade and GeoCover (Geological Atlas of Switzerland 1:25'000) for sections outside of the map extent
- ↘ Landslides (oblique to profile direction)
- LP-1 Intersection with stream longitudinal profile Appendix 3

Lithostratigraphic boundaries

- a) Intersection with subsurface model NTB 14-02 (Nagra, 2014a), simplified at depth
- - - b) Manually aligned with (a) and lithostratigraphic boundaries at terrain surface (as derived from GeoCover, Geological Atlas of Switzerland 1:25'000)

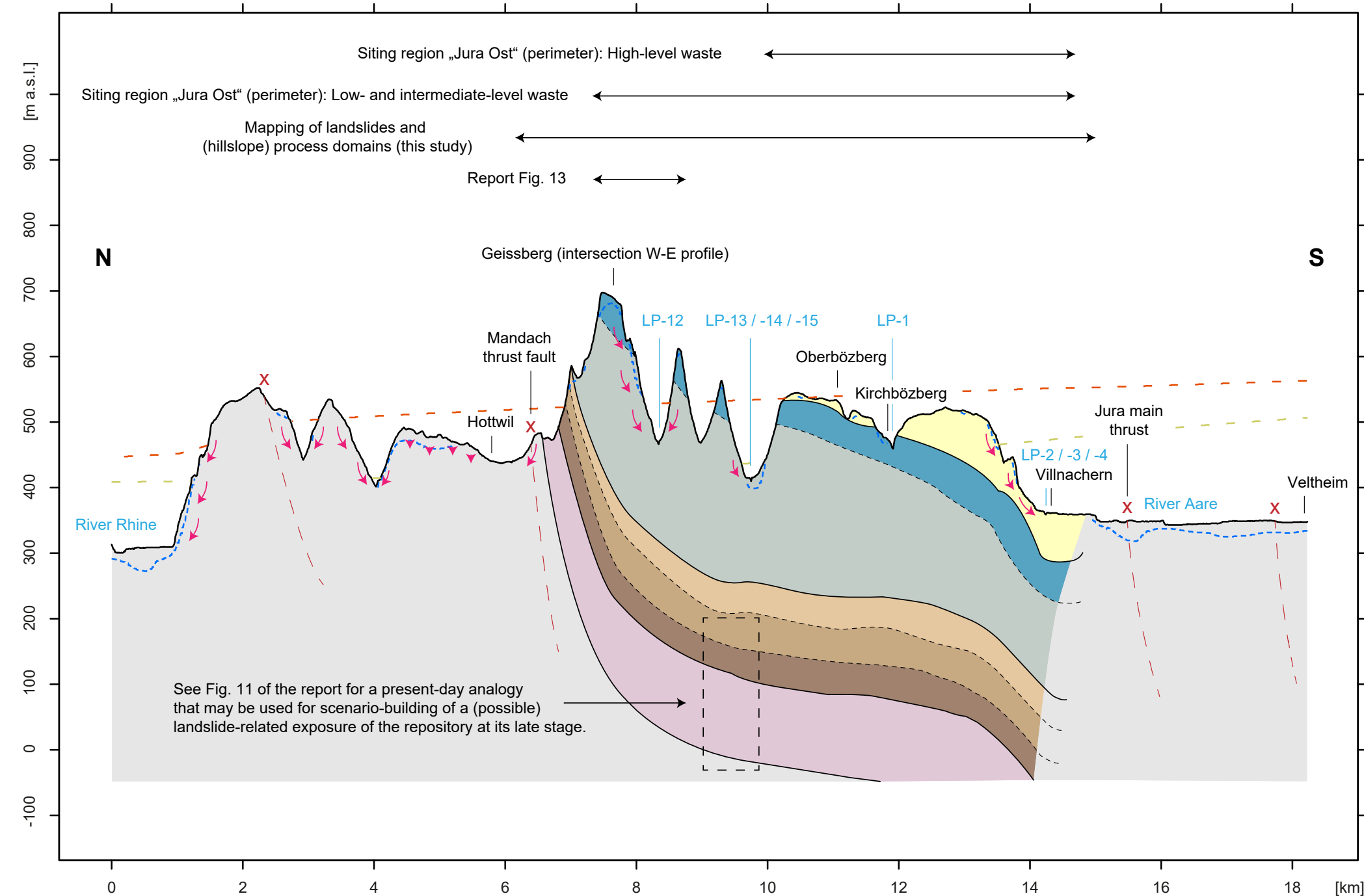
Lithostratigraphic units

- Tertiary (Molasse)
- Villigen-Formation
- Wildeggen-Formation
- Ifenthal-Formation
- (Hauptrogenstein) / Klingnau-Formation
- Passwang-Formation
- Opalinus Clay
- not differentiated (*)

(*) Section between Mandach thrust fault and Rhine is characterized by surface outcrops of Lias, Opalinus Clay and Triassic sediments.

Tectonic lineaments NTB 14-02

- X Thrust fault; projection at depth only indicative (based on Nagra, 2014a; enclosure A3-1)



See Fig. 11 of the report for a present-day analogy that may be used for scenario-building of a (possible) landslide-related exposure of the repository at its late stage.

Regional topographic / geological profile „Jura Ost“, west-east directed (vertical axis scaled by factor 10)

Extracted surfaces

- - - Base level of „Höhere Deckenschotter“ (HDS) } Heuberger & Naef (2014)
- - - Base level of „Tiefere Deckenschotter“ (TDS) } Regionally interpolated surfaces (!): poorly constrained / hypothetical towards interior valleys
- Present topography (DTM-AV)
- - - Top bedrock (where Quaternary deposits > 5m) Pietsch & Jordan (2014)

This study

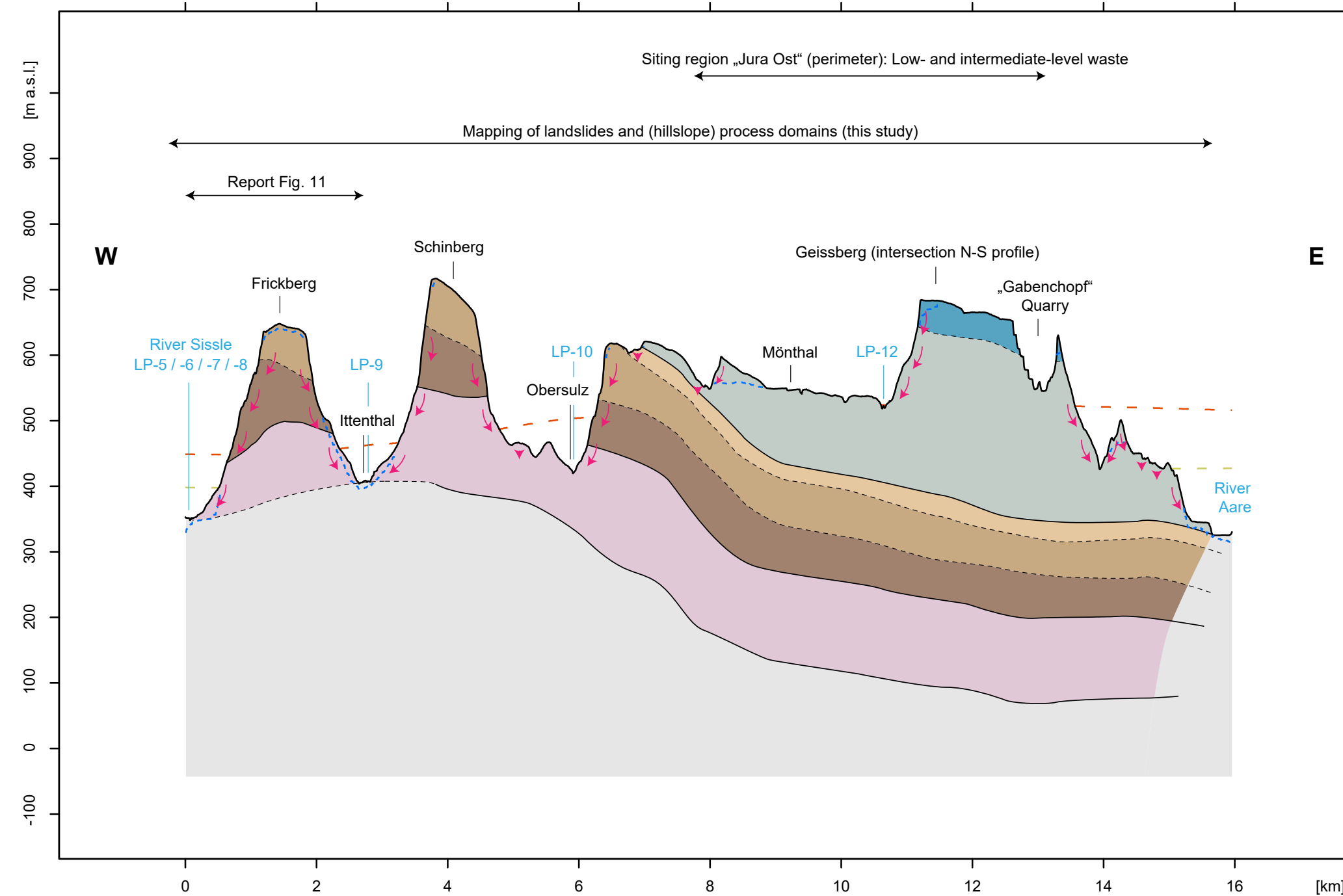
- ↘ Landslides } Schematic illustration according to map of process domains
- ▼ Landslides (oblique to profile direction) }
- LP-9 Intersection with stream longitudinal profile Appendix 3

Lithostratigraphic boundaries

- a) Intersection with subsurface model NTB 14-02 (Nagra, 2014a), simplified at depth
- - - b) Manually aligned with (a) and lithostratigraphic boundaries at terrain surface (as derived from GeoCover, Geological Atlas of Switzerland 1:25'000)

Lithostratigraphic units

- Villigen-Formation
- Wildeggen-Formation
- Ifenthal-Formation
- Hauptrogenstein / Klingnau-Formation
- Passwang-Formation
- Opalinus Clay
- not differentiated



Dataset (as referenced in report)	Data source	Type	Filename(s)	Supplementary information
DHM25	Swisstopo	Raster	dhm25_mosaic	25m grid size
DTM-AV	Swisstopo	Raster	dtm1049; dtm1050; dtm1069; dtm1070;	2m grid size; for data processing, a "DTM-AV (Jura Ost)" is created by merging the original map tiles (dtm1049; dtm1050; dtm1069; dtm1070), see Appendix 5.B
DTM Jura Ost	Nagra	Raster	dtm_jo_3dseis	0.5m grid size
DTM-AV hillshade	Swisstopo (processed)	Raster	dtm1049_hs; dtm1050_hs; dtm1069_hs; dtm1070_hs	2m grid size; azimuth angle of the light source = 315°; additionally, hillshades with azimuth angle of 45°, 135° and 225° have been calculated for "DTM-AV (Jura Ost)", see Appendix 5.B
DTM-AV slope gradient map	Swisstopo (processed)	Raster	temporary project files; processed to "dtm_av_jo_slope", see output dataset (Appendix 5.B)	2m grid size
DTM Jura Ost hillshade	Nagra	Raster	hst_jo_3dseis	Hillshade map calculated from "DTM Jura Ost", 0.5m grid size
GeoCover (Geological Atlas of Switzerland 1:25'000)	Swisstopo	Polygon-, Polyline-, Point-Shapefiles	FRICK_POLYGON_MAIN.shp; FRICK_LINE_AUX.shp etc.	+ analogous datasets for map tiles "Baden" and "Zurzach"
Quaternary map	Heuberger et al. 2014 (NAB 12-20)	Polygon-Shapefile	quartaer_NCH100_20121110.shp	
Base level of HDS	Heuberger & Naef 2014 (NAB 12-35)	Raster	bhds_130813	25m grid size; HDS = Höhere Deckenschotter
Base level of TDS	Heuberger & Naef 2014 (NAB 12-35)	Raster	bt ds_130813	25m grid size; TDS = Tiefere Deckenschotter
Top bedrock	Pietsch & Jordan 2014 (NAB 14-02)	Raster	bqu_140612	25m grid size
Thickness of Quaternary deposits	Pietsch & Jordan 2014 (NAB 14-02)	Raster	mqu_140612	25m grid size
Subsurface model NTB 14-02	Nagra 2014a (NTB 14-02, Dossier II)	Raster	BTe_union_20140930; BMa_union_20140930; TOp_union_20140930; TLi_union_20140930	25m grid size
Tectonic lineaments NTB 14-02	Nagra 2014a (NTB 14-02, Dossier II)	Polyline-Shapefile	verwerfungen.shp; Ergaenzung_Stoerungen2014.shp	As published in NTB 14-02, Dossier II, Enclosure A3-1 ("Geologische Karte für das Standortgebiet Jura Ost")
Geological units NTB 14-02	Nagra 2014a (NTB 14-02, Dossier II)	Polygon-Shapefile	nordschweiz.shp	As published in NTB 14-02, Dossier II, Enclosure A3-1 ("Geologische Karte für das Standortgebiet Jura Ost"); here only used for map representations
Drainage network TLM	Swisstopo	Polyline-Shapefile	ExtractedData_TLM_FLIESSGEWAESSER.shp	TLM = Topographic landscape model
Topographic map	Swisstopo	Raster	PK25	
Orthophotos	Swisstopo	Raster	645_265_r.tif etc.	+ adjacent map tiles of study area
Geological siting region	Nagra 2008 (NTB 08-03)	Polygon-Shapefile	regio090129n.shp	Here only used for map representations and manual intersection with topographic / geological profiles

Dataset (as referenced in report)	Chapter NAB 17-42	Type	Filename(s)	Supplementary information
Location names		Point Feature Class	Location_Names	Manually digitized according to input dataset "Topographic map" (PK25) and field observations
DTM-AV (Jura Ost)	3.2	Raster	dtm_av_jo_clip	Raster Mosaic of input dataset "DTM-AV", tiles "dtm1049"; "dtm1050"; "dtm1069"; "dtm1070"
DTM-AV slope gradient map (Jura Ost)	3.2	Raster	dtm_av_jo_slope	Slope gradient map calculated from "DTM-AV (Jura Ost)"
DTM-AV hillshade (lightsource azimuth 45°)	3.2	Raster	dtm_av_jo_hs_045	Hillshade map calculated from "DTM-AV (Jura Ost)"
DTM-AV hillshade (lightsource azimuth 135°)	3.2	Raster	dtm_av_jo_hs_135	Hillshade map calculated from "DTM-AV (Jura Ost)"
DTM-AV hillshade (lightsource azimuth 225°)	3.2	Raster	dtm_av_jo_hs_225	Hillshade map calculated from "DTM-AV (Jura Ost)"
Process domains	3.2	Polygon Feature Class	Process_Domains	
Process domains (raster)	3.3	Raster	process_domains_2m	
Extent of process domain mapping	3.3	Polygon Feature Class	Mapping_Extent	
Lithostratigraphic boundaries (extended from Geological Atlas of Switzerland 1:25'000)	3.3	Polyline-Shapefile	Ausstrich_Schichtgrenzen_20171016.shp	Provided to Nagra by P. Jordan (16.10.2017)
Tectonic lineaments (extended from Geological Atlas of Switzerland 1:25'000)	3.3	Polyline-Shapefile	Tekto_Linien_geol-Atlas_mod_20171016.shp	Provided to Nagra by P. Jordan (16.10.2017)
Lithostratigraphic boundaries (completed)	3.3	Polyline Feature Class	Litho_Boundaries	Manually completed, based on datasets "Lithostratigraphic boundaries (extended from Geological Atlas of Switzerland 1:25'000)" and "Tectonic lineaments (extended from Geological Atlas of Switzerland 1:25'000)"
Lithostratigraphic domains	3.3	Polygon Feature Class	Litho_Domains	
Lithostratigraphic domains (raster)	3.3	Raster	litho_domains_2m	
DTM-AV (Extent of process domain mapping)	3.3	Raster	dtm_av_pd_clip	"DTM-AV (Jura Ost)" clipped to "Extent of process domain mapping"
X-component of local normal vectors on terrain surface (DTM-AV)	3.3	Raster	dtm_av_pd_norm_vec_x	Calculated by separate Java-Script (A. Ludwig); based on same algorithms for calculation of slope gradient and slope aspect as ArcGIS + subsequent conversion to x-/y-/z-coordinate system by trigonometric functions
Y-component of local normal vectors on terrain surface (DTM-AV)	3.3	Raster	dtm_av_pd_norm_vec_y	Calculated by separate Java-Script (A. Ludwig); based on same algorithms for calculation of slope gradient and slope aspect as ArcGIS + subsequent conversion to x-/y-/z-coordinate system by trigonometric functions
Z-component of local normal vectors on terrain surface (DTM-AV)	3.3	Raster	dtm_av_pd_norm_vec_z	Calculated by separate Java-Script (A. Ludwig); based on same algorithms for calculation of slope gradient and slope aspect as ArcGIS + subsequent conversion to x-/y-/z-coordinate system by trigonometric functions
Sampling points (20m grid spacing)	3.3	Point Feature Class	Sampling_Points_20m	Created as regular grid (20m spacing) in the area of "DTM-AV (Extent of process domain mapping)"
Hillslopes	3.3	Polygon Feature Class	Hillslope_Polygons	Polygons of the classes 'Presumably unfailed hillslopes'; 'Presumed landslides' and 'Evident landslides' extracted from "Process domains"
Hillslope sampling points (20m grid spacing)	3.3	Point Feature Class	Hillslope_Sampling_Points_20m	Result of intersecting "Sampling points (20m grid spacing)" with "Hillslopes"
Landslides	3.3	Polygon Feature Class	Landslide_Polygons	Aggregated manually from "Process domains"
Landslide centroids	3.3	Point Feature Class	Landslide_Centroids	Manually moved inside landslide polygons, where the centroid is located outside (in case of "irregularly" shaped landslides)
Landslides (raster)	3.3	Raster	landslides_2m	
Mean x-component of local normal vectors on landslide surfaces (DTM-AV)	3.3	Raster	landslides_norm_vec_x	
Mean y-component of local normal vectors on landslide surfaces (DTM-AV)	3.3	Raster	landslides_norm_vec_y	
Mean z-component of local normal vectors on landslide surfaces (DTM-AV)	3.3	Raster	landslides_norm_vec_z	
Internal relief within landslide surfaces	3.3	Raster	landslides_relief	Maximum elevation range within surface of individual landslides / landslide complexes
Quaternary map (TDS polygons)	3.4	Polygon Feature Class	Quartaer_geologische_KarteNCH100_TDS_20121110.shp	Extract from input dataset "Quaternary map"
Quaternary map (TDS raster)	3.4	Raster	nch100_tds25m	
Intersection of projected base level TDS with present topography (raster with -9999 values)	3.4	Raster	dhm25_bt ds_o	Intersecting former base levels of erosion with present topography: resulting raster with "-9999" raster values
Intersection of projected base level TDS with present topography (raster with NoData values)	3.4	Raster	dhm25_bt ds_nd	Intersecting former base levels of erosion with present topography: resulting raster with "NoData" raster values
Intersection of projected base level TDS with present topography (bitmap)	3.4	Raster	dhm25_bt ds_bm	Bitmap representation of dhm25_bt ds_nd

Dataset (as referenced in report)	Chapter NAB 17-42	Type	Filename(s)	Supplementary information
Intersection of projected base level TDS with present topography	3.4	Polygon Feature Class	Intersect_dhm25_btlds	dhm25_btlds_bm converted to polygon feature class
Quaternary map (HDS polygons)	3.4	Polygon Feature Class	Quartaer_geologische_KarteNCH100_HDS_20121110.shp	Extract from input dataset "Quaternary map"
Quaternary map (HDS raster)	3.4	Raster	nch100_hds25m	
Intersection of projected base level HDS with present topography (raster with -9999 values)	3.4	Raster	dhm25_bhds_o	Intersecting former base levels of erosion with present topography: resulting raster with "-9999" raster values
Intersection of projected base level HDS with present topography (raster with NoData values)	3.4	Raster	dhm25_bhds_nd	Intersecting former base levels of erosion with present topography: resulting raster with "NoData" raster values
Intersection of projected base level HDS with present topography (bitmap)	3.4	Raster	dhm25_bhds_bm	Bitmap representation of dhm25_bhds_nd
Intersection of projected base level HDS with present topography	3.4	Polygon Feature Class	Intersect_dhm25_bhds	dhm25_bhds_bm converted to polygon feature class
Top bedrock (where Quaternary deposits > 5m)	3.5	Raster	bqu_25m_nd5	Input dataset "Top bedrock", with "NoData" value where input dataset "Thickness of Quaternary deposits" < 5m
Stream courses	3.5	Polyline Feature Class	Stream_Profile_Lines_JO	Extracted and partly manually extended from input dataset "Drainage network TLM"
Stream network	3.5	Polyline Feature Class	Stream_Network_JO	Merged "Stream courses"
Calculated drainage network	3.5	Polyline-Shapefile	Stream_Network_JO_Calculated	Provided to Nagra for this study by M. Foster and R. Arrowsmith (Arizona State University); dataset for this study was generated by merging original datasets (subbasins) "f39m3_ksn_1e5.shp", "f38m3_ksn_1e5.shp", "f37m3_ksn_1e5.shp" and "f36m3_ksn_1e5.shp"
Stream points (10m)	3.5	Point Feature Class	Stream_Profile_Points_JO_10m	Sampling points to extract elevation values along "Stream network"
Stream courses (routes)	3.5	Polyline Feature Class	Stream_Profile_Routes_JO	"Stream courses" converted to routes
Stream profile anomalies	3.5	Point Feature Class	Stream_Profile_Anomalies_JO	Location of anomalies as identified in stream longitudinal profiles and manually projected on map
Topographic profiles (sampling lines)	3.6	Polyline Feature Class	Topo_Profile_Lines	Manually defined sampling lines for extraction of topographic profiles
Topographic profiles (sampling points 10m)	3.6	Point Feature Class	Topo_Profile_Points_10m	Sampling points to extract elevation values along "Topographic profiles (sampling lines)"
Topographic profiles (routes)	3.6	Polyline Feature Class	Topo_Profile_Routes	"Topographic profiles (sampling lines)" converted to routes
Intersection points of topographic profiles and lithostratigraphic boundaries at surface	3.6	Point Feature Class	Topo_Profile_Points_Litho	Intersection points of "Topographic profiles (sampling lines)" and "Lithostratigraphic boundaries" at surface
Basis Tertiary	3.6	Raster	basis_tertiaer_ntb14_02_o	Basis Tertiary according to input dataset "Subsurface model NTB 14-02", with "NoData" values replaced by "-9999"
Basis Malm (Wildeggen-Formation)	3.6	Raster	basis_malm_ntb14_02_o	Basis Malm according to input dataset "Subsurface model NTB 14-02", with "NoData" values replaced by "-9999"
Top Opalinus Clay	3.6	Raster	top_opalinus_ntb14_02_o	Top Opalinus Clay according to input dataset "Subsurface model NTB 14-02", with "NoData" values replaced by "-9999"
Top Lias	3.6	Raster	top_lias_ntb14_02_o	Top Lias according to input dataset "Subsurface model NTB 14-02", with "NoData" values replaced by "-9999"
DHM25 (Jura Ost)	3.7	Raster	dhm25_jo_clip	Input dataset "DHM25" clipped to extent of "DTM-AV (Jura Ost)"
DHM25 slope gradient map (Jura Ost)	3.7	Raster	dhm25_jo_slope	Slope gradient map calculated from "DHM25 (Jura Ost)"
DHM25 local relief map (search radius 500m)	3.7	Raster	dhm25_relief_r500m	Pixel-based local relief map, based on input dataset "DHM25" and calculated within circular neighbourhood with radius 500m
Areal proportion table	3.3.1	Excel Table	Areal_Proportion_Process_Domains_Litho_Domains.xlsx	Output data table from Chapter 3.3.1
Hillslope orientation table	3.3.2	Excel Table	Hillslope_Orientation_Pixel_based.xlsx	Output data table from Chapter 3.3.2
Landslide surface table	3.3.3	Excel Table	Landslide_Surface_Characteristics.xlsx	Output data table from Chapter 3.3.3
Stream profile table	3.5.2	Excel Table	Stream_Analysis_JO_Output_Event_Table.xlsx	Output data table from Chapter 3.5.2
Topographic profile table	3.6	Excel Table	Topo_Profiles_JO_Output_Event_Table.xlsx	Output data table from Chapter 3.6
Topographic profile table (intersection points of topographic profiles and lithostratigraphic boundaries at surface)	3.6	Excel Table	Topo_Profiles_Litho_Surface_JO_Output_Event_Table.xlsx	Output data table from Chapter 3.6

Technical documentation (NAB-17-42)

Introduction

This appendix is a detailed documentation of the technical processing steps in ArcGIS, related to the tasks outlined in sections 3.3 to 3.6 of the report.

- Quantitative synthesis of mapping results (section 6.A)
- Intersecting former base levels of erosion with present topography (section 6.B)
- Extracting stream longitudinal profiles (section 6.C)
- Extracting topographic / geological profiles (section 6.D)

Section 3.2 "Manual mapping of landslides and (hillslope) process domains" does not involve any particular ArcGIS function other than the standard editing tools. Therefore, no additional explanations are necessary in that case. Similarly, section 3.7 "Calculation of topographic parameters for map representations" does not require additional explanations here.

To provide some context, each of the sections A to D contains excerpts or summaries from the corresponding sections of the report. The reader is referred to the main report for further background.

Datasets are referenced according to their reference names given in Appendix 5 and Fig. 3 of the main report. As to the descriptions below, it should be noted that "output datasets" of this study according to Appendix 5.B can also appear as "input datasets", if they are used for subsequent processing steps. Temporary data outputs are labelled as such.

Filenames appearing in the screenshots can deviate from the finally assigned filenames as listed in Appendix 5. However, based on the descriptions of processing steps in the tables of this appendix, the corresponding datasets according to Appendix 5 remain traceable.

6.A Quantitative synthesis of mapping results

Introduction (summarised from section 3.3):

The mapping results have been quantitatively analysed as follows:

- Calculation of areal proportion of each process domain intersecting with a lithostratigraphic unit: This should indicate, whether certain lithostratigraphic units within the study area are rather dominated by the "hillslope" vs. "non-hillslope" domain and to what degree hillslopes tend to be landslide-affected (~ "landslide susceptibility" of lithostratigraphic units).
- Distribution of pixel-based slope orientation within hillslope domain, separated for different lithostratigraphic units: This should indicate dependences of slope gradients on lithology and slope aspect. Additionally, it forms a "reference frame" for analysing slope orientations of landslide surfaces.
- Calculation of surface characteristics of individual landslides / landslide complexes: This includes topographic characteristics (area, mean slope orientation (gradient and aspect) and internal relief) and the lithostratigraphic composition, which should help to identify topographic and lithological controls on landslides.

Appendix 6**Data processing: 1) Areal proportion of process domains within lithostratigraphic units**

To calculate the areal proportion of different process domains within each lithostratigraphic unit, the "Zonal Histogram" tool in ArcGIS was used. As input for this, two raster datasets, representing both the process domains and lithostratigraphic domains, were required. The raster representing the "lithostratigraphic domains" is based on the dataset "lithostratigraphic boundaries", that in turn was manually extracted and partly interpolated based on the Geological Atlas of Switzerland 1:25'000. The corresponding working steps in ArcGIS are listed in Tab. A6-1.

Tab. A6-1: Calculating areal proportion of process domains within lithostratigraphic units (with preprocessing).

Nr.	Processing step	Input dataset(s)	ArcGIS
1	Manual completion of lithostratigraphic boundaries	Lithostratigraphic boundaries Tectonic lineaments (GeoCover)	Editing Tool > Create Features Editing Tool > Merge
2	Creating a mask (feature class) that represents the extent of process domain mapping	Process domains	"Select Features" tools Right-click on layer in TOC > Data > Export Data (copy of "process domains") Editing Tool > Merge
3	Creating polygons of "lithostratigraphic domains" within mapping extent	Lithostratigraphic boundaries (completed) Extent of process domain mapping	Editing Tool > More Editing Tools > Advanced Editing > Split Polygons (Details in Fig. A6-1)
4	Conversion of lithostratigraphic domains to raster (cell size = 2 m)	Lithostratigraphic domains	Conversion Tools > To Raster > Feature to Raster
5	Conversion of process domains to raster (cell size = 2 m)	Process domains	Conversion Tools > To Raster > Feature to Raster
6	Calculating areal proportions	Lithostratigraphic domains (raster) Process domains (raster)	Spatial Analyst Tools > Zonal > Zonal Histogram (Details in Fig. A6-2)

The results of the "Zonal Histogram" tool were subsequently processed in Excel as "Areal proportion table" ¹ and illustrated in Adobe Illustrator.

¹ Filepath within directory NAB 17-42: .../Data/Quantitative_Synthesis/Areal_Proportion_Process_Domains_Litho_Domains.xlsx

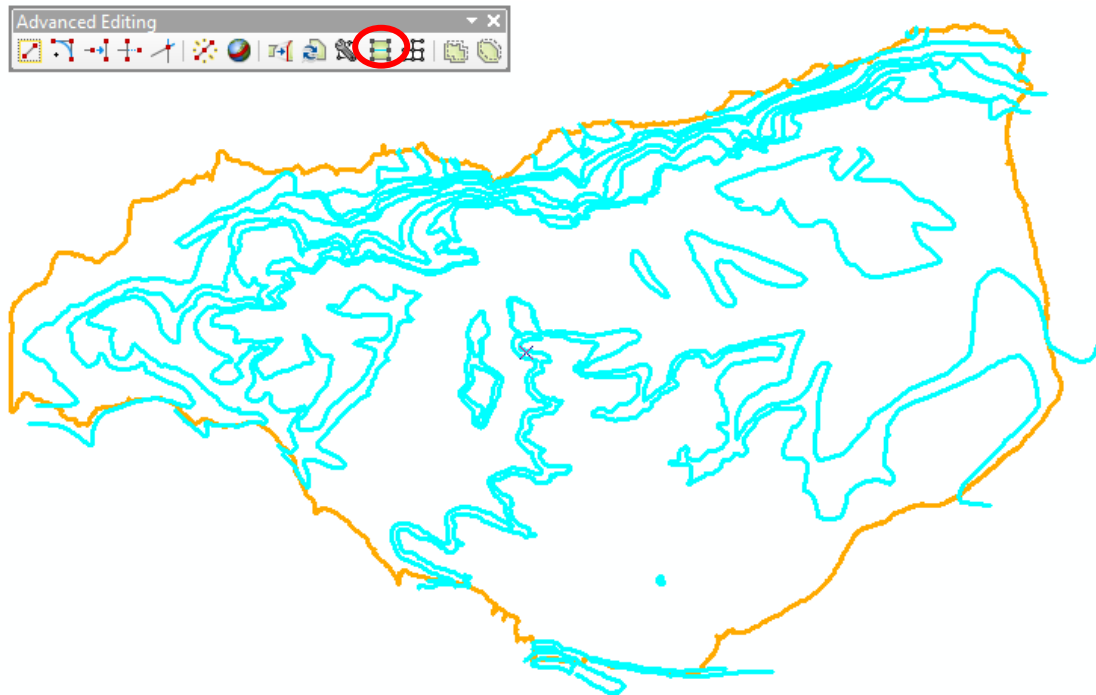


Fig. A6-1: Creating polygons of "lithostratigraphic domains".

First, all polylines of the dataset "lithostratigraphic boundaries (completed)" are selected (blue) within an editing session. By using "Split Polygons" (Advanced Editing toolbar, red circle), the "Extent of process domain mapping" (orange polygon) is dissected along the lithostratigraphic boundaries, resulting in polygons of "lithostratigraphic domains".

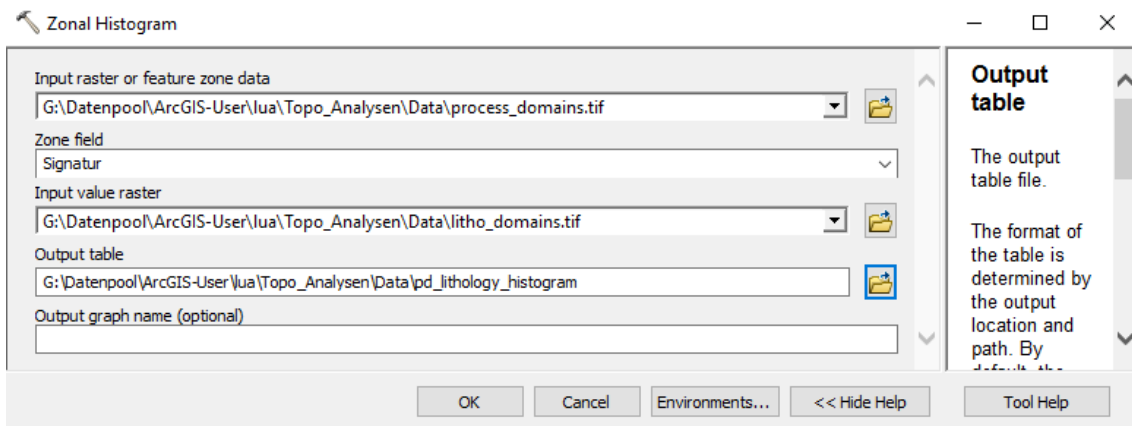


Fig. A6-2: Calculating the areal proportion of different process domains within each lithostratigraphic domain with the "Zonal Histogram" tool.

The result is a table, which has then been further processed in Excel as "Areal_Proportion_Process_Domains_Litho_Domains.xlsx" file.

Appendix 6**Data processing: 2) Distribution of pixel-based slope orientation within hillslope domain**

This analysis was based on derivatives of DTM-AV at a grid size of 2 m. To represent slope orientation, three raster datasets were calculated which store the x-, y- and z-components of local normal vectors on terrain surface, respectively. These were derived from pixel-wise calculations of slope gradient and slope aspect and transformation by trigonometric functions in a separate Java-Script (A. Ludwig).

The procedure of extracting the slope orientation and the lithostratigraphic unit for a dataset of subsampling points is outlined in Tab. A6-2.

Tab. A6-2: Extracting slope orientation and lithostratigraphic unit for subsampling points within the hillslope domain.

Nr.	Processing step	Input dataset(s)	ArcGIS
1	Calculating x-, y- and z-components of local normal vectors on terrain surface	DTM-AV (Extent of process domain mapping)	Separate JAVA-Script (A. Ludwig)
2	Creating sampling points at a regular grid spacing of 20 m	DTM-AV (Extent of process domain mapping)	Data Management Tools > Feature Class > Create Fishnet (Details in Fig. A6-3)
3	Extracting hillslope polygons from "process domains"	Process domains	Attribute Table > Select By Attributes Right-click on layer in TOC > Data > Export Data
4	Intersecting sampling points with hillslope domain ²	Sampling points (20 m grid spacing) Hillslopes	Analysis Tools > Overlay > Intersect (Details in Fig. A6-4)
5	Sampling the following attributes for each hillslope sampling point: x- and y-component of local normal vectors on terrain surface lithostratigraphic unit	Hillslope sampling points (20m grid spacing) X-component of local normal vectors on terrain surface (DTM-AV) Y-component of local normal vectors on terrain surface (DTM-AV) Lithostratigraphic domains (raster)	Spatial Analyst Tools > Extraction > Sample (Details in Fig. A6-5)

² The point features resulting from this intersection also store the information about the (hillslope) process domain each sampling point belongs to (i.e. "Presumably unfailed hillslopes", "Presumed landslides", "Evident landslides"). This is ensured by the setting "JoinAttributes (optional)" = ALL, as shown in Fig. A6-4.

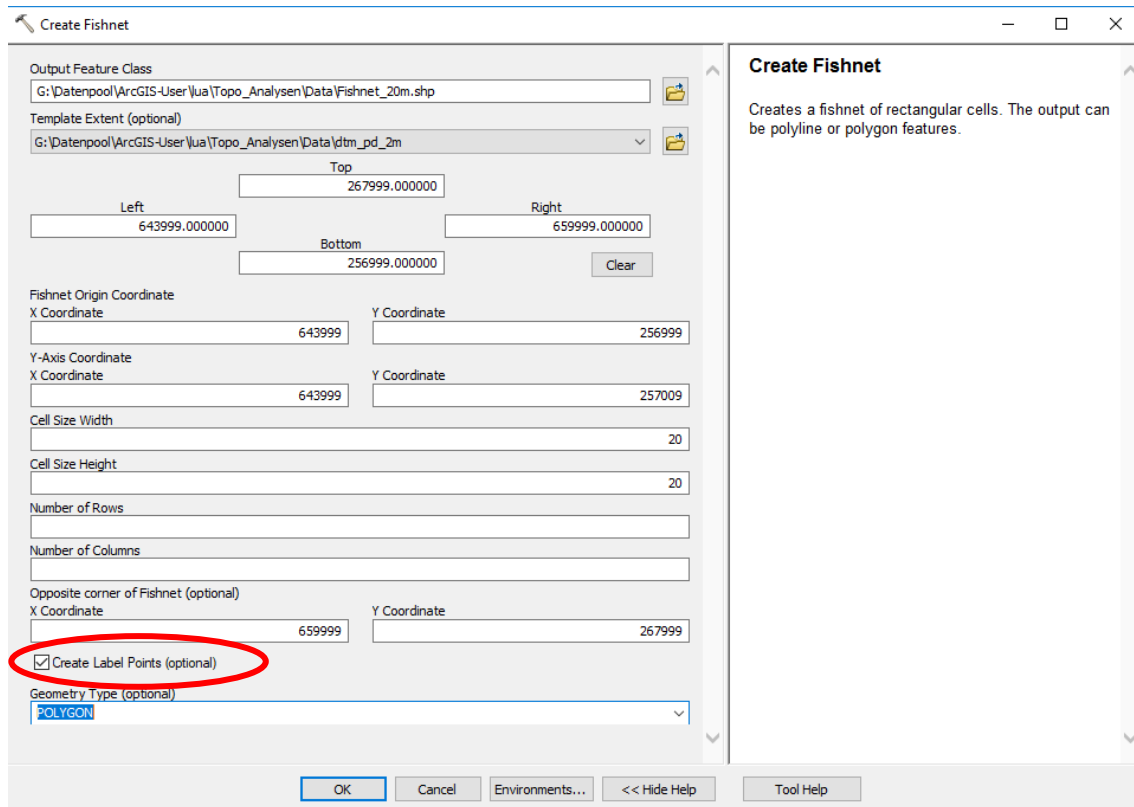


Fig. A6.3: Using the "Create Fishnet" tool to create subsampling points at regular grid spacing of 20 m within "Extent of process domain mapping".

The polygon output file "Fishnet_20m.shp" can be deleted after execution of the tool. The "Label points" (red circle) return the dataset, that is subsequently used as "Sampling points (20 m grid spacing)".

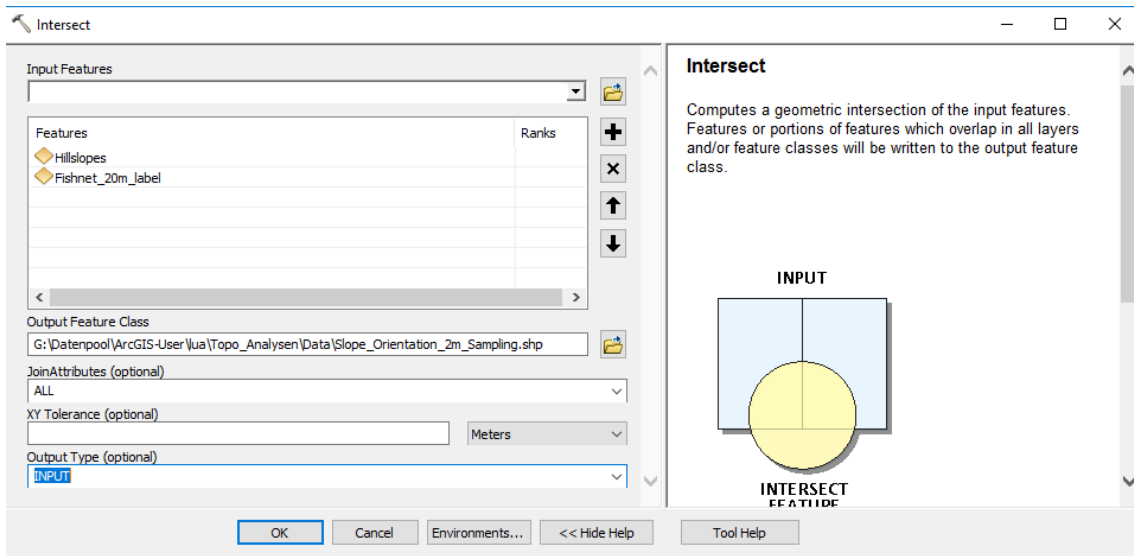


Fig. A6-4: Intersecting the "Sampling points (20 m grid spacing)" (here named "Fishnet_20m_label") with "hillslopes" (polygons).

The setting of "JoinAttributes (optional)" as "ALL" ensures that the resulting point features also store the information about the (hillslope) process domain each sampling point belongs to (i.e. "Presumably unfailed hillslopes", "Presumed landslides", "Evident landslides").

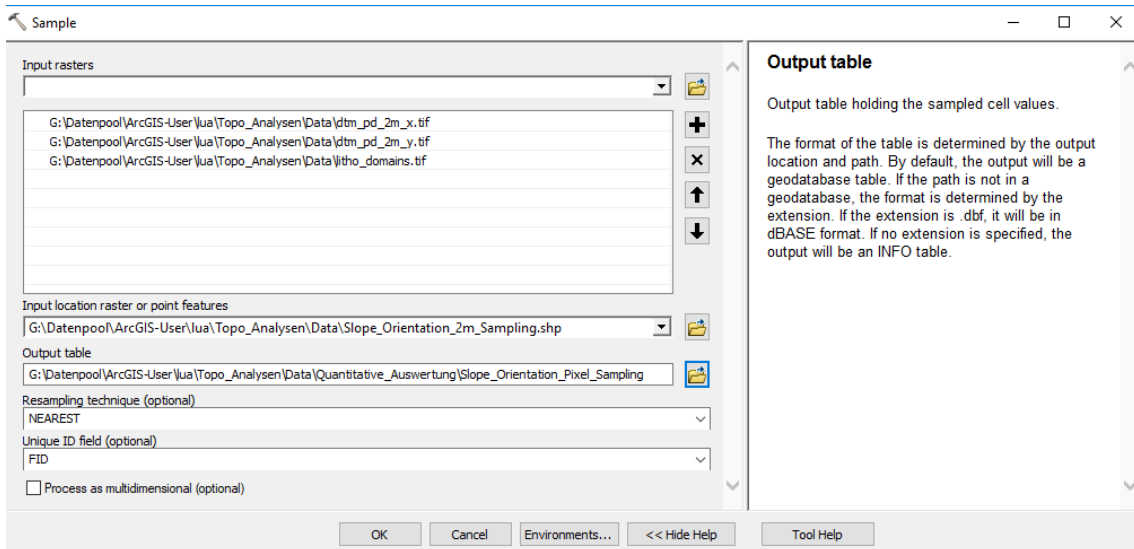


Fig. A6-5: Creating a table that contains the x- and y-component of local normal vectors on terrain surface (based on DTM-AV) as well as the lithostratigraphic unit for sub-sampling points (20 m grid spacing) within hillslope domain.

The resulting table has been further processed in Excel as "Hillslope_Orientation_Pixel_based.xlsx" file.

The resulting table of the sampling tool was then imported in Excel ("Hillslope orientation table" ³). The data were used for illustrations, that were first prepared in ArcGIS according to the explanations below and finally presented in Adobe Illustrator. This involved the creation of various shapefiles in ArcGIS that do not represent "real" geographic datasets and have therefore not been included in Appendix 5.B. However, the shapefiles can be found via filepath: .../Data/Quantitative_Synthesis/ of the NAB 17-42 directory.

Based on the x- and y-components in the "Hillslope orientation table", data points were projected on a radial diagram in ArcGIS, where slope gradients are indicated along the radial axis and slope aspect is represented by the azimuth direction. Filtering of the data points is possible by lithostratigraphic units, which were previously assigned to the dataset (see Tab. A6-2).

For the final illustration, points have been counted within subsections of the radial diagram (regularly divided by intervals of slope gradients (5°) and aspect (22.5°). This allowed for displaying the frequencies of slope orientations for given lithostratigraphic units intersecting with the hillslope domain (see Appendix 2 for graphical results).

Tab. A6-3 explains how the (empty) radial diagram has been created. Tab. A6-4 explains how the hillslope orientation data was subsequently illustrated in the radial diagram.

³ Filepath within directory NAB 17-42: .../Data/Quantitative_Synthesis/Hillslope_Orientation_Pixel_based.xlsx

Appendix 6

Tab. A6-3: Creating an (empty) radial diagram.

Nr.	Processing step	Input dataset(s)	ArcGIS
1	Projecting radii of slope gradients at 5°-intervals ("Construction_Slope_Gradient_Radii.shp")	Temporary table according to Fig. A6-6	ArcCatalog > Create Feature Class > From XY Table... (analogous to Fig. A6-35 and Fig. A6-36)
2	Creating circular disks with corresponding radii ("Construction_Slope_Gradient_Ringe.shp")	"Construction_Slope_Gradient_Radii.shp" (as snapping points)	Editing Tool > Create Features > Construction Tools > Circles
3	Creating "rings" of 5°-intervals from internally overlapping circular disks	"Construction_Slope_Gradient_Ringe.shp"	Editing Tool: Select smallest disk Editor > Clip Discard the area that intersects (repeat iteratively from smallest to largest disk)
4	Draw lines to divide segments of slope aspect at intervals of 22.5° ("Construction_Slope_Aspect_Lines.shp")		Editing Tool > Create Features
5	Intersecting circular intervals of slope gradients with segment lines of slope aspect to define "subsections" of radial diagram ("Hillslope_Orientation_Segments.shp")	"Construction_Slope_Gradient_Ringe.shp" "Construction_Slope_Aspect_Lines.shp"	Editing Tool > More Editing Tools > Advanced Editing > Split Polygons (analogous to Fig. A6-1)
6	Aggregating subsections from 30° to 90° for graphic illustration in Appendix 2 ("Hillslope_Orientation_Segments_Aggregated_30deg_90deg.shp")	"Hillslope_orientation_segments.shp"	Editing Tool > Merge

Tab. A6-4: Illustrating hillslope orientation in radial diagram.

Nr.	Processing step	Input dataset(s)	ArcGIS
1	Creating data points that represent hillslope orientation by x- and y-components of local normal vectors on terrain surface	"Hillslope orientation table"	ArcCatalog > Create Feature Class > From XY Table... (Analogy in Fig. A6-35 and Fig. A6-36).
2	Creating separate shapefiles for each lithostratigraphic unit	"Hillslope_Orientation_Points_All.shp"	Attribute Table > Select By Attributes Right-click on layer in TOC > Data > Export Data
3a 3b	Counting number of data points within each subsection of the radial diagram by a spatial join Storing the resulting "Count" column after each spatial join in a new attribute field (named according to the lithostratigraphic unit)	"Hillslope_Orientation_Segments_Aggregated_30deg_90deg.shp" "Hillslope_Orientation_Points_Opalinus.shp" etc.	Right-click on layer in TOC > Joins and Relates > Joins > ... + "spatial join" according to Fig. A6-7 Attribute Table > Add Field (Long)... + Field Calculator ... + Details Fig. A6-8 (repeat for each lithostratigraphic unit)
4	Visualising the (classified) percentage of data points within subsections of the radial diagram	"Hillslope_Orientation_Segments_Aggregated_30deg_90deg.shp"	Layer Symbology + settings according to Fig. A6-9 (repeat for each lithostratigraphic unit)

FID	Shape *	Grad	Y	X
0	Point	0	0	0
1	Point	5	0	0.087156
2	Point	10	0	0.173648
3	Point	15	0	0.258819
4	Point	20	0	0.34202
5	Point	25	0	0.422618
6	Point	30	0	0.5
7	Point	35	0	0.573576
8	Point	40	0	0.642788
9	Point	45	0	0.707107
10	Point	50	0	0.766044
11	Point	55	0	0.819152
12	Point	60	0	0.866025
13	Point	65	0	0.906308
14	Point	70	0	0.939693
15	Point	75	0	0.965926
16	Point	80	0	0.984808
17	Point	85	0	0.996195
18	Point	90	0	1

Fig. A6-6: Attribute table of shapefile "Construction_Slope_Gradient_Radii.shp".

The column "X" stores the x-coordinate of the points that represent the radii of "slope gradient circles" at intervals of 5° in the radial diagram (radius = sin(slope gradient)).

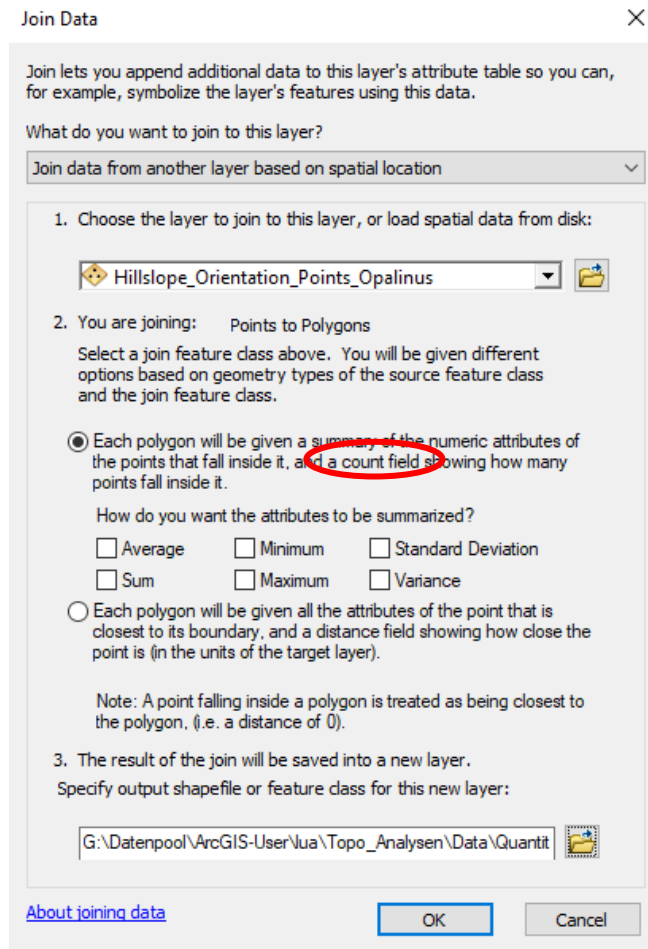


Fig. A6-7: Spatial join to count the number of data points (hillslope orientation) within each subsection of the radial diagram ("Hillslope_Orientation_Segments_Aggregated_30deg_90deg.shp").

The result is saved into a new layer, whose attribute table contains an additional attribute field "Count" (see Fig. A6-8). The latter stores the number of data points within each subsection of the radial diagram. This procedure is repeated for each lithostratigraphic unit.

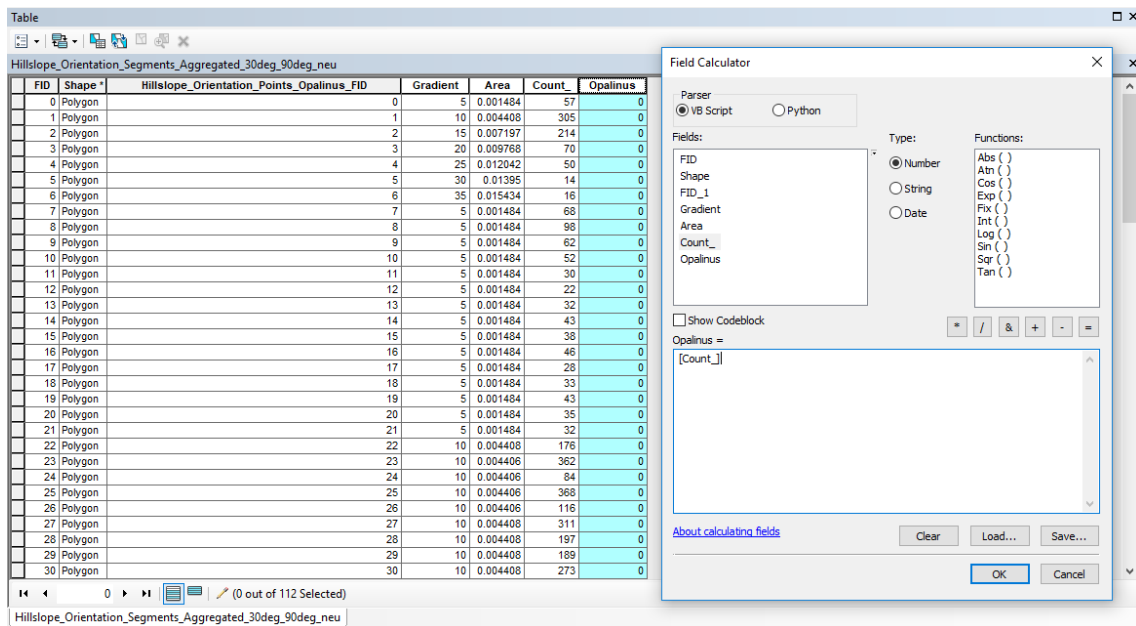


Fig. A6-8: Storing the resulting "Count" column after each spatial join in a new attribute field, named according to the lithostratigraphic unit (here "Opalinus").

After running the "Field Calculator", the original field "Count" should be deleted.

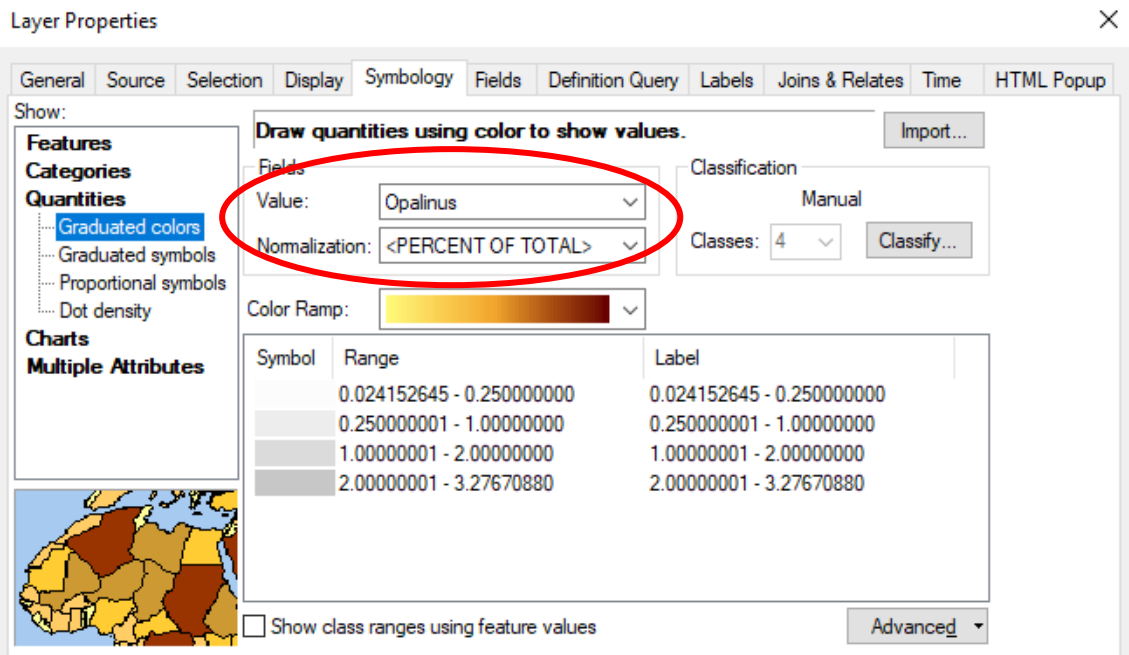


Fig. A6-9: Symbology setting of the layer "Hillslope_Orientation_Segments_Aggregated_30deg_90deg.shp" to illustrate the distribution of hillslope orientation in a radial diagram (filtered by lithostratigraphic unit).

With the presented setting, the radial diagram is displayed for Opalinus Clay, by selecting the corresponding attribute field in the symbology setting (see red circle). By selecting "< Percent of Total >" the number of points within each subsection of the diagram is normalised by the total number of subsampling points within the lithostratigraphic unit.

Data processing: "Surface characteristics of individual landslides / landslide complexes"

An attempt is here made, to separate individual landslides / landslide complexes within the map of process domains. The basic idea is to aggregate adjacent segments of the classes "Evident landslides" and "Presumed landslides", if their deformation likely occurs interdependently.

Once individual landslides have been merged and converted into a raster dataset, their topographic and lithostratigraphic surface characteristics are calculated from other raster datasets and displayed in a number of ways. This whole procedure is outlined by the subsequent series of tables and figures.

Tab. A6-5: Preparing different datasets to represent individual landslides / landslide complexes.

Nr.	Processing step	Input dataset(s)	ArcGIS
1	Manually aggregating segments of process domains into individual landslides / landslide complexes	Process domains [copy]	ArcCatalog > Copy Feature (Process Domains) Editing Tool > Merge
2	Adding additional attribute "Area" to "Landslides" (polygons), to convert default attribute "SHAPE_Area" [m ²] into [km ²]	Landslides	Attribute Table > Add Field (Double)... + Field Calculator "Area" = "SHAPE_Area" / 1'000'000
3	Calculating centroid coordinates of each individual landslide / landslide complex	Landslides	Attribute Table > Add Field (Double)... + Calculate Geometry (Details in Fig. A6-10)
4	Creating a feature class of "Landslide centroids" (points)	Landslides	a) Attribute Table > Table Options > Export (as Text File, temporary) b) ArcCatalog > Create Feature Class > From XY Table... (Analogy in Figs. A6-35 and A6-36).
5	Manually moving landslide centroids into landslide polygons, if located outside (observed in case of "irregularly" shaped landslides)	Landslide Centroids	Editing Tool > Move
6	Conversion of landslides (polygons) to raster (cell size = 2 m)	Landslides	Conversion Tools > To Raster > Feature to Raster

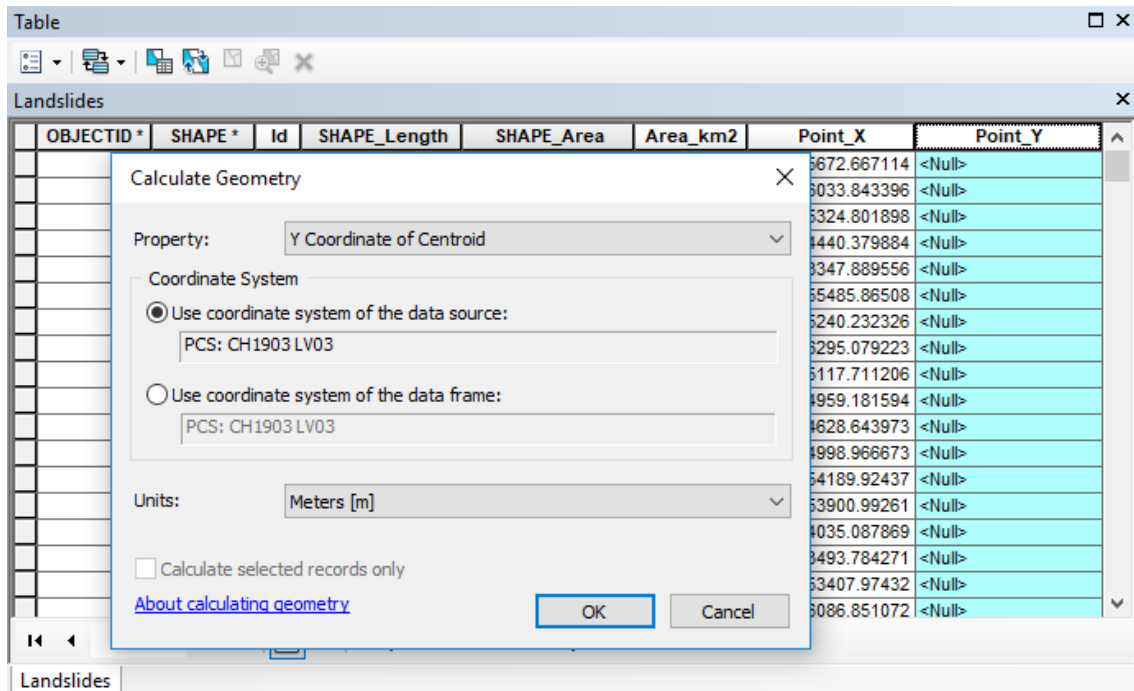


Fig. A6-10: Calculating the centroid coordinates of each individual landslide / landslide complex.

As a first step, empty attribute fields "Point_X" and "Point_Y" of type "Double" have to be added to the attribute table. The centroid coordinates are then assigned to the corresponding columns by the "Calculate Geometry" function. Depending on the geometry of the landslide polygon, the centroid coordinates may be located outside the landslide boundaries. In these cases, the "Landslide centroids" were later moved manually to a location inside the landslide boundaries.

Tab. A6-6: Calculating and extracting landslide surface characteristics.

Nr.	Processing step	Input dataset(s)	ArcGIS
1	Calculating three raster datasets that represent the mean x-, y- and z-component of local normal vectors on landslide surfaces.	Landslides (raster) X-component of local normal vectors on terrain surface (DTM-AV) Y-component of local normal vectors on terrain surface (DTM-AV) Z-component of local normal vectors on terrain surface (DTM-AV)	Spatial Analyst Tools > Zonal > Zonal Statistics (Details in Fig. A6-11)
2	Calculating a raster dataset that represents the internal relief (maximum elevation range) within surface of each landslide.	Landslides (raster) DTM-AV (Extent of process domain mapping)	Spatial Analyst Tools > Zonal > Zonal Statistics (Details in Fig. A6-12)
3	Extracting surface characteristics to landslide centroids (Normal vector representing the mean surface orientation of the landslide surface + internal relief within landslide surface)	Landslide centroids Mean x-component of local normal vectors on landslide surfaces (DTM-AV) Mean y-component of local normal vectors on landslide surfaces (DTM-AV) Mean z-component of local normal vectors on landslide surfaces (DTM-AV) Internal relief within landslide surfaces	Spatial Analyst Tools > Extraction > Extract Multi Values to Points (Details in Fig. A6-13).
4	Calculating mean slope aspect of landslide surface	Landslide centroids	Attribute Table > Add Field ("mean_aspect", type Double) + Field Calculator (Details in Fig. A6-14)
5	Calculating mean slope gradient of landslide surface	Landslide centroids	Attribute Table > Add Field ("mean_slope", type Double) + Field Calculator (Details in Fig. A6-15)
6	Displaying mean slope orientation of landslide surfaces on a map	Landslide centroids	Layer Symbology + setting according to Fig. A6-16

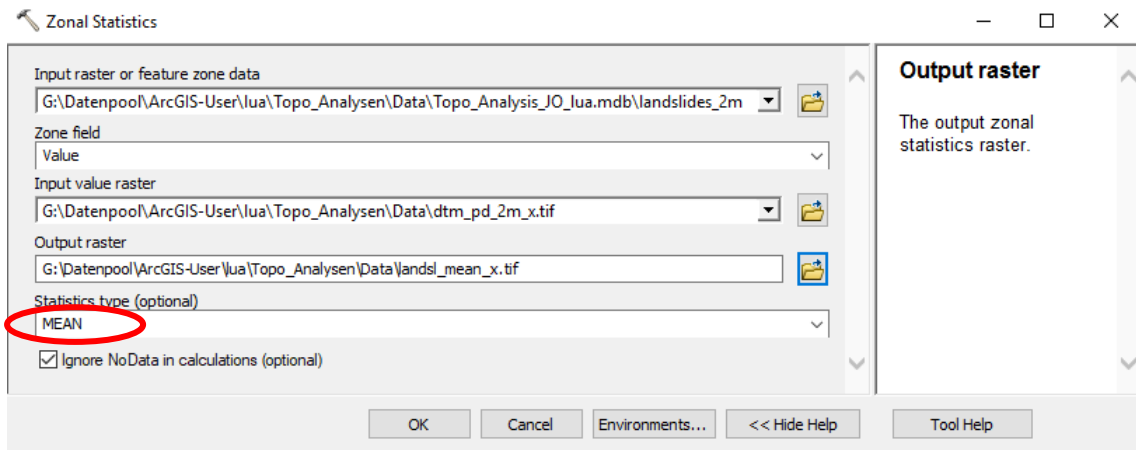


Fig. A6-11: Calculating a raster dataset that shows the mean x-component of local normal vectors on individual landslide surfaces.

This procedure is repeated analogously for the y- and z-component. Together, the three resulting datasets indicate the mean surface orientation of each landslide.

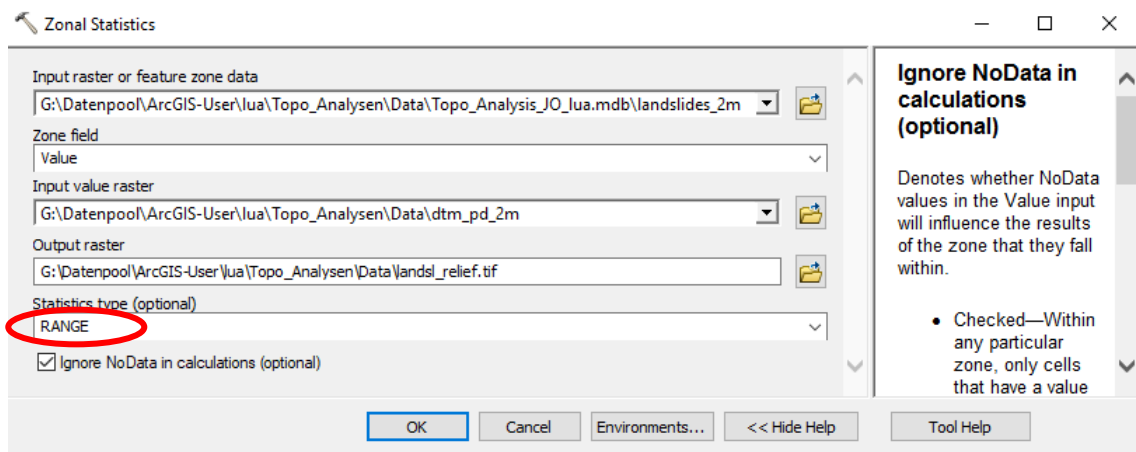


Fig. A6-12: Calculating a raster dataset that shows the internal relief (maximum elevation difference) within individual landslide surfaces.

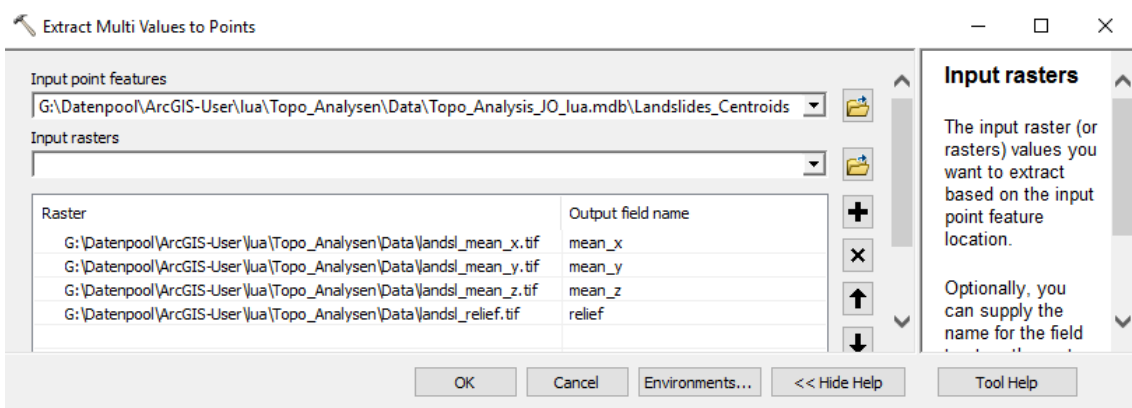


Fig. A6-13: Extracting landslide surface characteristics to landslide centroids.

The selected input rasters correspond to temporary file versions of: 1) – 3) Mean x/-y/-z-component of local normal vectors on landslide surfaces (DTM-AV); this describes the mean surface orientation of each individual landslide / landslide complex 4) Internal relief within landslide surfaces.

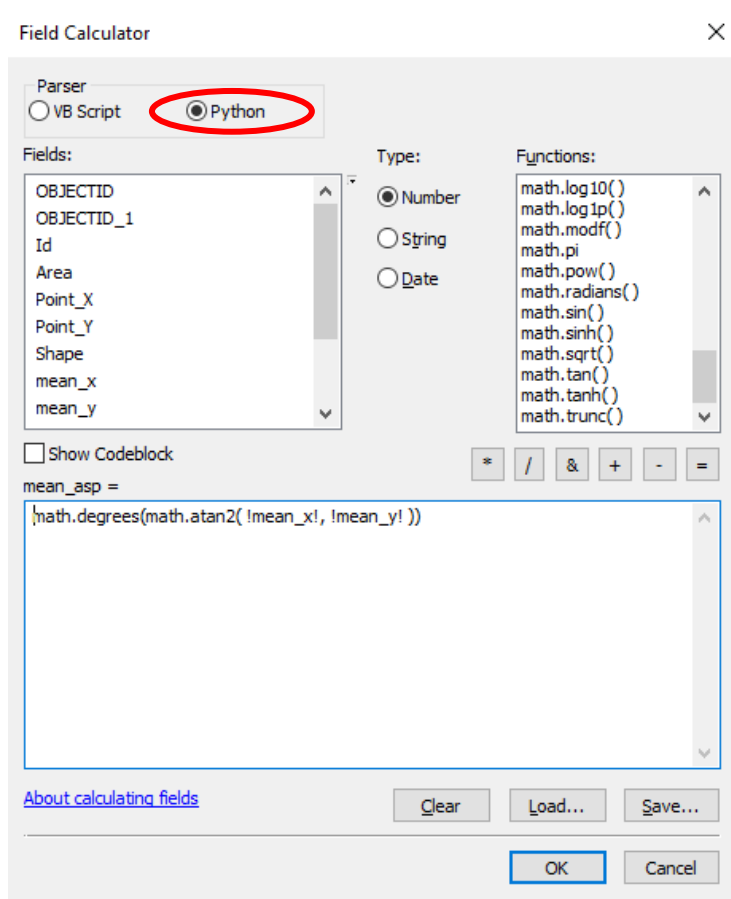


Fig. A6-14: Calculating mean slope aspect of landslide surfaces in attribute table of "Landslide centroids".

Mean slope aspect is calculated by trigonometric functions from the mean x- and y-components of local normal vectors on landslide surfaces (as derived according to Tab. A6-6 and Fig. A6-11).

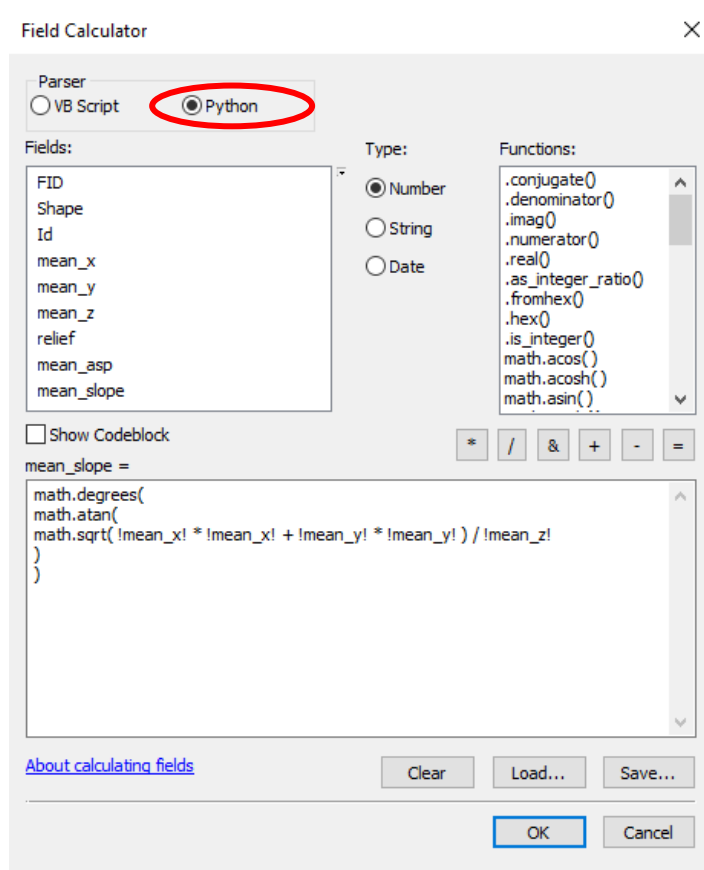


Fig. A6-15: Calculating mean slope gradient of landslide surfaces in the attribute table of "Landslide centroids".

Mean slope gradient is calculated by trigonometric functions from the mean x-, y- and z-components of local normal vectors on landslide surfaces (as derived according to Tab. A6-6 and Fig. A6-11).

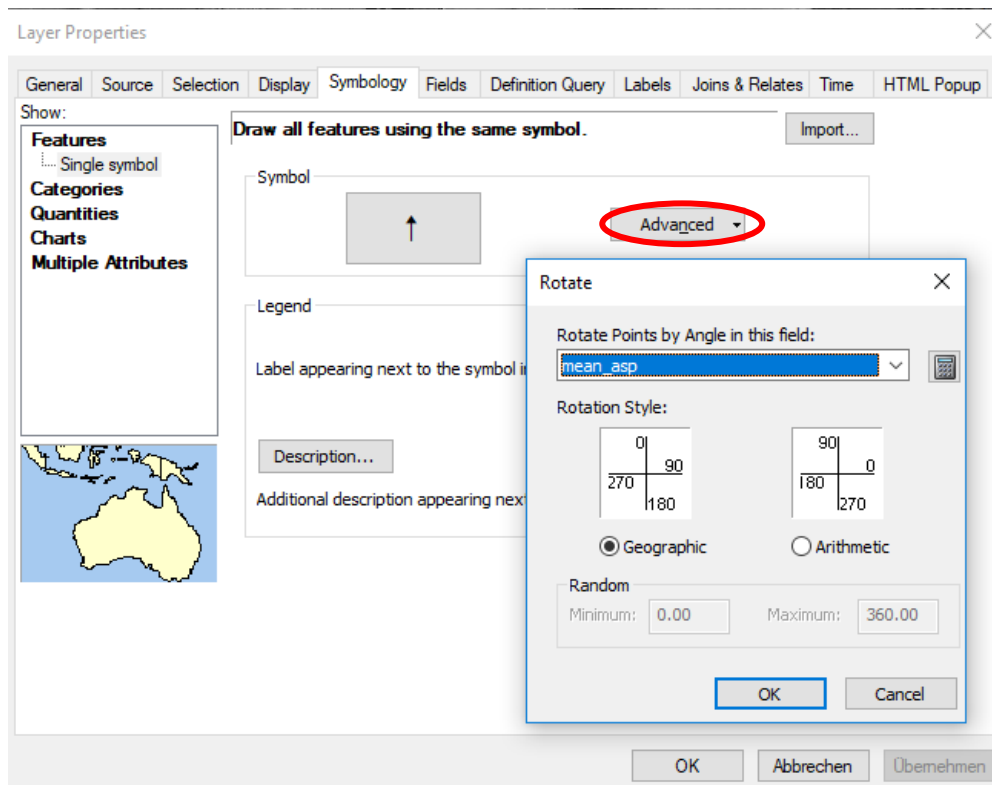


Fig. A6-16: Symbology setting to display the mean slope orientation of landslide surfaces on a map.

The mean slope aspect of the landslide surface is thus displayed by a rotated arrow (the mean slope gradient can be displayed by a label).

While the mean x-, y- and z-components of local normal vectors on the individual landslide surfaces are valid parameters to calculate the mean slope aspect and slope gradient (Figs. A6-14 and A6-15), they can not immediately be used to be plotted on a radial diagram as introduced in Tabs. A6-3 and A6-4 (and illustrated in Appendix 2).

This arises from the following fact:

- Each local normal vector on the surface is defined by unit length = 1. If all local normal vectors within a (landslide) surface were directed exactly in the same direction (i.e. representing a planar surface), the mean normal vector (vector sum rescaled by number n vectors) would also have a length = 1.
- However, since the landslide surfaces are not planar, the resulting mean normal vector has a length < 1. Proportionally to this length, the x-, y- and z- components are also shorter, than would be the case if vector length = 1.

Therefore, the x- and y- components need to be rescaled according to the length of the mean normal vector, in order that they can be correctly plotted in the radial diagram. This step is described in Tab. A6-7.

Appendix 6

Tab. A6-7: Rescaling the mean x- and y- components of local normal vectors on the individual landslide surfaces, to be plotted correctly in the radial diagram.

Nr.	Processing step	Input dataset(s)	ArcGIS
1	Calculating the length of the mean vector of local normal vectors on landslide surface	Landslide centroids	Attribute Table > Add Field ("mean_vecl", type Double) + Field Calculator (Details in Fig. A6-17)
2	Rescaling the x- and y- components in new attribute fields (dividing by vector length)	Landslide centroids	Attribute Table > Add Field ("mean_x_cor" and "mean_y_cor", type Double) + Field Calculator

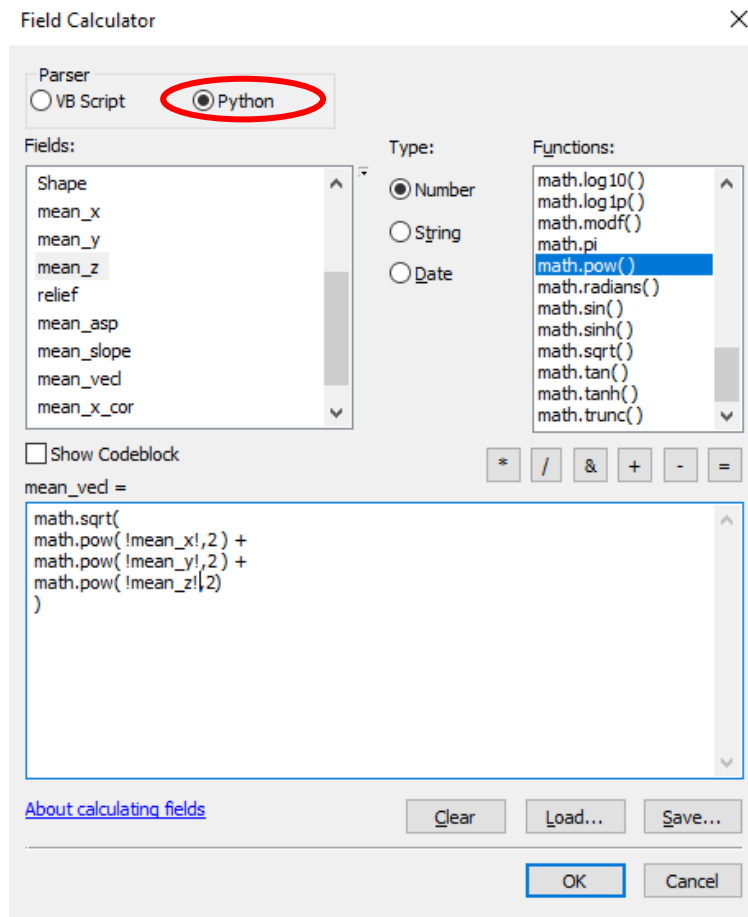


Fig. A6-17: Calculating the length of the mean vector of local normal vectors on landslide surfaces.

Tab. A6-8: Extending the list of landslide surface characteristics by the lithostratigraphic composition.

Nr.	Processing step	Input dataset(s)	ArcGIS
1	Calculating the areal proportion of different lithostratigraphic units intersecting with the landslide surface	Landslides (raster) Lithostratigraphic domains (raster)	Spatial Analyst Tools > Zonal > Zonal Histogram (Details in Fig. A6-18)
2	Extending the resulting table with a numeric attribute field to store the "landslide ID"	Temporary table	Attribute Table > Add Field ("Nr", type Short Integer) + Field Calculator (Details in Fig. A6-19)
3	Joining the lithostratigraphic surface characteristics with the topographic ones (as derived in Tabs. A6-6 and A6-7)	Temporary table Landslide centroids	Right-click on layer in TOC > Joins and Relates > Joins > ... + "relational join" according to Fig. A6-7
4	Export the joint attribute table with all landslide surface characteristics	Landslide centroids	Attribute Table > Table Options > Export (as Text File)

The exported table is subsequently processed in Excel as "Landslide surface table" ⁴ and used for further illustrations (Tab. A6-9).

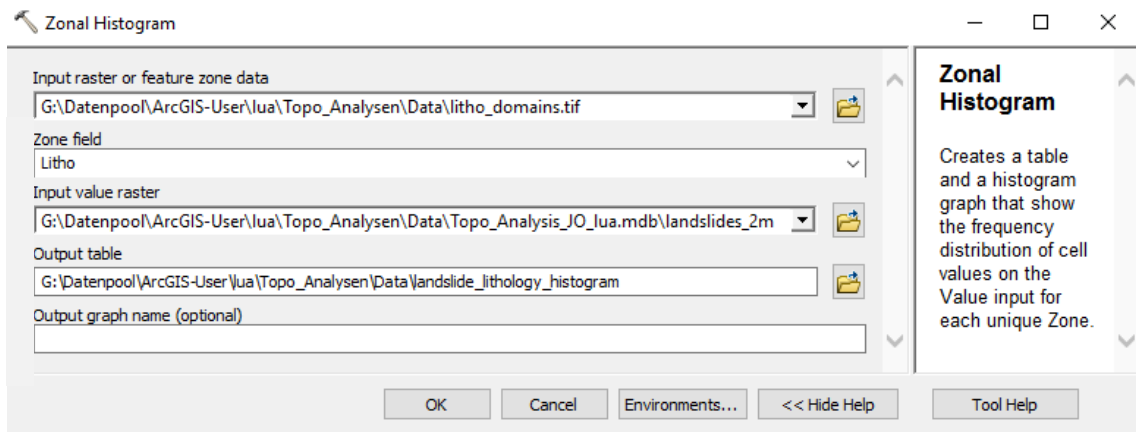


Fig. A6-18: Calculating the areal proportion of different lithostratigraphic units intersecting with the landslide surface, by "Zonal histogram".

⁴ Filepath within directory NAB 17-42: .../Data/Quantitative_Synthesis/Landslide_Surface_Characteristics.xlsx

Rowid	LABEL	NR	NOT_DIFFERENTIAT	HAUPTROGENSTE	LIAS	OPALINUSTON	VILLIGEN-FORMATI	PASSWANG-FOR	WILDEGG-FORMATIO	TERTIAR	IFENTHAL-FORMATI
1	1	1	0	0	0	0	2101	0	11477	0	0
2	8	8	0	0	0	0	0	0	3043	0	0
3	15	15	0	0	0	0	30047	0	210494	0	0
4	20	20	0	0	0	0	66	0	18218	0	0
5	22	22	0	0	0	0	3331	0	21165	0	0
6	26	26	0	0	0	0	496	0	1596	0	0
7	27	27	0	0	0	0	1602	0	11487	0	0

Fig. A6-19: The resulting (temporary) table stores the "landslide ID" in a text field ("LABEL").

A numeric field ("NR") is therefore added to the table and the IDs are assigned to this new field via Field Calculator (= "LABEL").

This step allows for the table to be used in a subsequent relational join (Fig. A6-20).

Fig. A6-20: Joining the lithostratigraphic characteristics of the landslide surfaces with the topographic ones (as derived in Tabs. A6-6 and A6-7).

Tab. A6-9: Illustrating landslide surface characteristics in diagrams.

Nr.	Processing step	Input dataset(s)	(Excel) / ArcGIS
1	Rescaling "mean_slope" by factor 10 for later illustration	Landslide surface table	Excel formula in a separately added column "mean_slope_10x"
2	Creating data points that represent mean slope gradient (scaled by factor 10, y-axis) vs. internal relief (x-axis) of landslide surfaces	Landslide surface table (coordinates defined by attribute fields "mean_slope_10x" and "relief")	ArcCatalog > Create Feature Class > From XY Table... (Analogy in Figs. A6-35 and A6-36).
3	Creating data points that represent mean orientation of landslide surfaces by mean x- and y-components of local normal vectors on terrain surface (to be displayed in radial diagram)	Landslide surface table (coordinates defined by attribute fields "mean_x_cor" and "mean_y_cor" according to Tab. A6-7)	ArcCatalog > Create Feature Class > From XY Table... (Analogy in Figs. A6-35 and A6-36)
4	Adding artificial data points to manipulate the dataset in a way, that the symbol scaling (as a function of landslide area, step 5) is identical for all lithostratigraphic units	"Landslides_Slope_Relief_Data_Points.shp" "Landslides_Litho_Morpho_Data_Points.shp"	Editing Tool > Create Features (Details in Fig. A6-22)
5	Plotting the data points from steps 2 and 3 in separate diagrams. Each data point (landslide) represented by a pie chart, to show the lithostratigraphic composition of its surface. Size of the pie chart is scaled as a function of the landslide area.	"Landslides_Slope_Relief_Data_Points.shp" "Landslides_Litho_Morpho_Data_Points.shp"	Attribute Table > Add Field ("Pie_Size", type Double) + Field Calculator (Details in Fig. A6-21) Layer Symbology + setting according to Fig. A6-23.

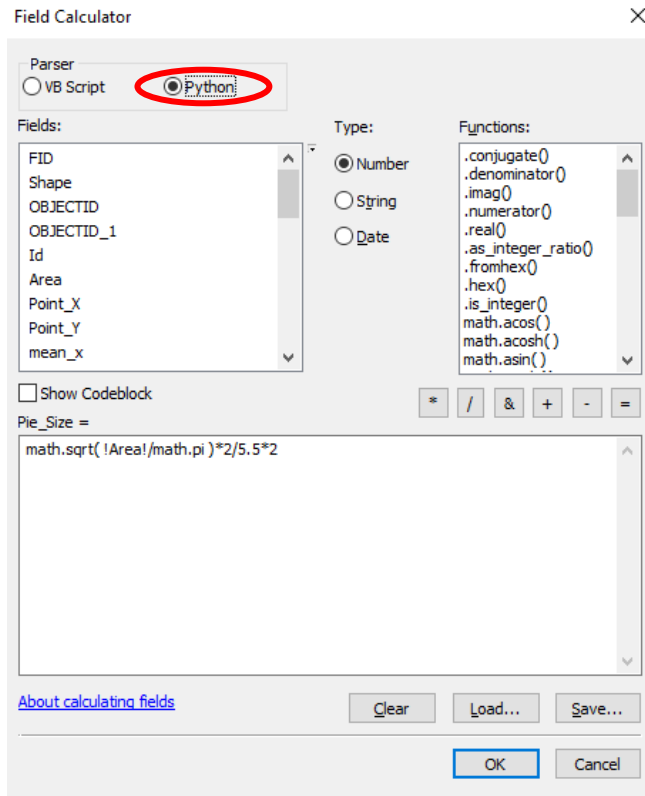


Fig. A6-21: Calculating a field to be used for size scaling of pie chart representations of individual landslides (function of the landslide surface area and layout scale, arbitrary).

FID	Shape *	OBJECTID	OBJECTID_1	Id	Area	Pie_Radius	TERTIAR	VILLIGEN_F	WILDEGG_F0	IFENTHAL_F	HAUPTROGEN	PASSWANG_F	OPALINUSTO	LIAS
244	Point	0	0	0	0.001	0.012975	999999	0	0	0	0	0	0	0
245	Point	0	0	0	0.001	0.012975	0	999999	0	0	0	0	0	0
246	Point	0	0	0	0.001	0.012975	0	0	999999	0	0	0	0	0
247	Point	0	0	0	0.001	0.012975	0	0	0	999999	0	0	0	0
248	Point	0	0	0	0.001	0.012975	0	0	0	0	999999	0	0	0
249	Point	0	0	0	0.001	0.012975	0	0	0	0	0	999999	0	0
250	Point	0	0	0	0.001	0.012975	0	0	0	0	0	0	999999	0
251	Point	0	0	0	0.001	0.012975	0	0	0	0	0	0	0	999999
17	Point	18	1785	0	0.001085	0.013517	0	0	276	0	0	0	0	0
104	Point	105	1372	0	0.00124	0.014446	0	0	0	0	222	90	0	0
215	Point	216	211	0	0.001331	0.014971	0	54	281	211	0	0	0	0
177	Point	178	246	0	0.001487	0.015821	0	278	88	0	0	0	0	0
118	Point	119	1380	0	0.001607	0.016451	0	0	398	0	0	0	0	0
26	Point	27	1782	0	0.001882	0.0178	0	0	0	0	450	26	0	0
130	Point	131	1325	0	0.00189	0.01784	0	0	0	0	476	0	0	0
78	Point	79	2306	0	0.002015	0.018419	0	0	0	0	345	158	0	0
197	Point	198	1075	0	0.00208	0.018713	0	0	0	0	525	0	0	0

Fig. A6-22: Adding one artificial data point per lithostratigraphic unit to the datasets "Landslides_Slope_Relief_Data_Points.shp" and "Landslides_Litho_Morpho_Data_Points.shp".

The identical area of 0.001 km², which is slightly smaller than the smallest mapped landslide, defines an equal minimum of symbol size for all lithostratigraphic units and thus ensures a consistent size scaling in Appendix 2.

These data points are created at artificial locations / coordinates outside the scope of the actual data points. A more sophisticated method for this workaround may be implemented in future applications.

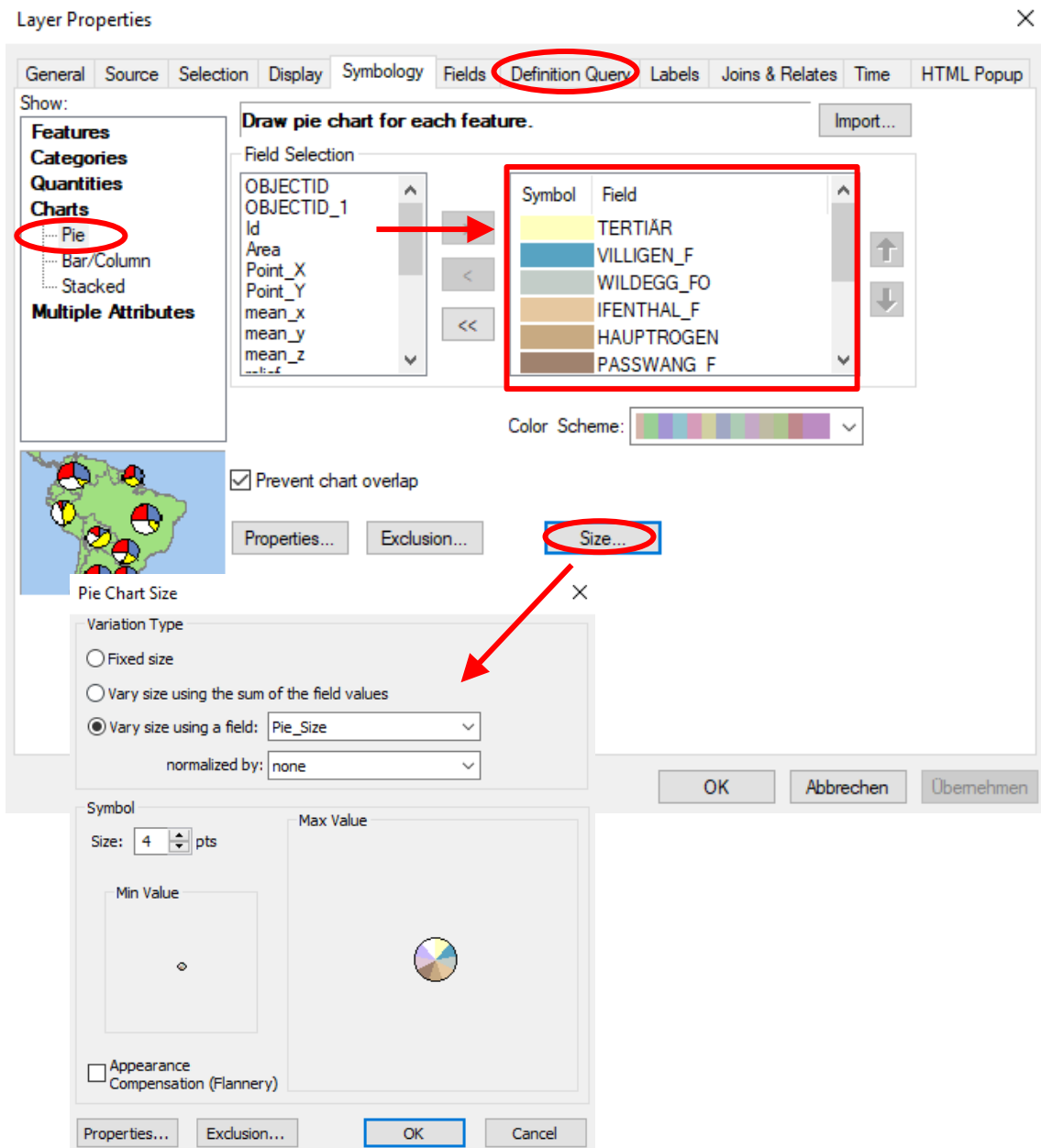


Fig. A6-23: Symbology setting of the layer "Landslides_Litho_Morpho_Data_Points.shp" to show individual landslides as pie charts with the following properties: i) size of pie chart indicates landslide area; ii) segments of pie charts indicate areal proportion of the different lithostratigraphic units intersecting with the landslide surface.

The attribute fields (red box) defining the pie chart segments have to be selected from the left-hand side "Field Selection" list. The definition query can be used to apply a "lithostratigraphic" filter, e.g. displaying only landslides where areal proportion of a lithostratigraphic unit is $> 5\%$ of the complete landslide surface ($(\text{"PASSWANG_F"} * 4 / (\text{"Area"} * 1000000)) > 0.05$; factor 4 is used to multiply the number of raster cells by the cell size of $2\text{ m} \times 2\text{ m}$). The dataset "Landslides_Slope_Relief_Data_Points.shp" is displayed in the same way.

6.B Intersecting former base levels of erosion with present topography

Introduction (summarised from section 3.4):

The aim of this processing step is to indicate a simplified minimum terrain elevation at the time of the former base levels "Höhere Deckenschotter" (HDS) and "Tiefere Deckenschotter" (TDS).

The two input datasets "Base level of HDS" and "Base level of TDS" represent regionally interpolated (nearly planar) surfaces. These interpolated surfaces technically "undercut" the present topography, if the latter is higher. While this represents a real situation in regions presently covered by the corresponding Quaternary deposit (e.g. HDS), such "undercutting surfaces" are of course only theoretical in the absence of these deposits.

Therefore, new raster datasets have been created, where these "undercutting" surfaces are excluded in the absence of HDS or TDS deposits, respectively. For illustration purposes, the resulting raster datasets are finally converted into polygon feature classes. On the map, these polygon feature classes display the intersection of the projected base levels of HDS and TDS with present topography (DHM25).

Data processing: "Intersecting former base levels of erosion with present topography"

The detailed working steps of intersecting former base levels of erosion with the present topography in ArcGIS are listed in Tab. A6-10 (example HDS; analogously for TDS). Additional explanations are given below.

Tab. A6-10: Intersecting former base levels of erosion (example "Höhere Deckenschotter" = HDS) with present topography.

Nr.	Processing step	Input dataset(s)	ArcGIS
1.	Extracting HDS-polygons from shapefile	Quaternary map	Attribute Table > Select By Attributes Right-click on layer in TOC > Data > Export Data
2.	Conversion of HDS-shapefile to raster (cell size = 25 m)	Quaternary map (HDS polygons)	Conversion Tools > To Raster > Feature to Raster
3.	Intersecting base level of HDS with present topography	DHM25 Base level of HDS Quaternary map (HDS raster)	Spatial Analyst Tools > Map Algebra > Raster Calculator (Details in Fig. A6-24 and explanations in text)
4.	Replacing "-9999" values by "NoData" in the resulting raster	Intersection of projected base level HDS with present topography (raster with -9999 values) (dhm25_bhds_o)	Spatial Analyst Tools > Conditional > Set Null (Details in Fig. A6-25)
5.	Converting raster to bitmap	Intersection of projected base level HDS with present topography (raster with NoData values) (dhm25_bhds_nd)	Spatial Analyst Tools > Conditional > Con (Details in Fig. A6-26)
6.	Converting bitmap to polygon feature	Intersection of projected base level HDS with present topography (bitmap) (dhm25_bhds_bm)	Conversion Tools > From Raster > Raster to Polygon (Details in Fig. A6-27)

Appendix 6

Step 3 of Tab. A6-10 uses the following criteria, to create a raster dataset without "undercutting" surfaces:

- Elevation value of "base level of HDS", where deposits of HDS are indicated in "Quaternary map"
- Else: Elevation value of "base level of HDS", where higher than present topography ("DHM25")
- Else: -9999 (no HDS deposits and DHM25 > "base level of HDS")

These conditions are summarised in the ArcGIS Raster Calculator expression of Fig. A6-24.

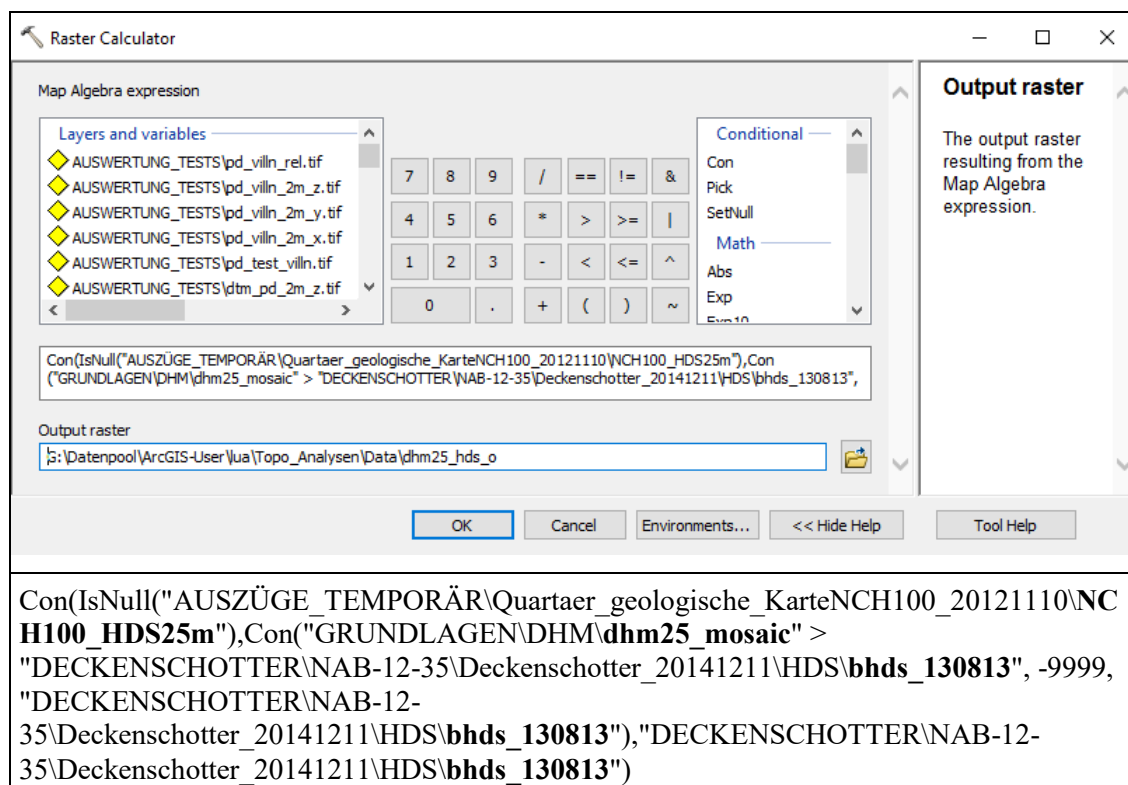


Fig. A6-24: Using Raster Calculator to intersect base level of HDS with present topography.

The complete expression used in the Raster Calculator is inserted as text at the bottom. See text of this section for explanations. Bold elements indicate filenames according to Appendix 5. For base level of TDS, the procedure is analogous.

For further processing, an additional raster has been created (Tab. A6-10, step 4) where the "-9999" values in the output dataset of step 3 are replaced by "NoData" values (Fig. A6-25). "NoData" raster values are displayed transparently in ArcGIS. The resulting raster datasets can be displayed in combination with the DTM hillshade of the present topography. This allows for visualisation of how a simplified minimum terrain surface at the time of the former base level could have looked like.

Similarly, steps 5 and 6 are used to create a polygon feature class that spatially displays the intersection of the projected base level of HDS with present topography (DHM25).

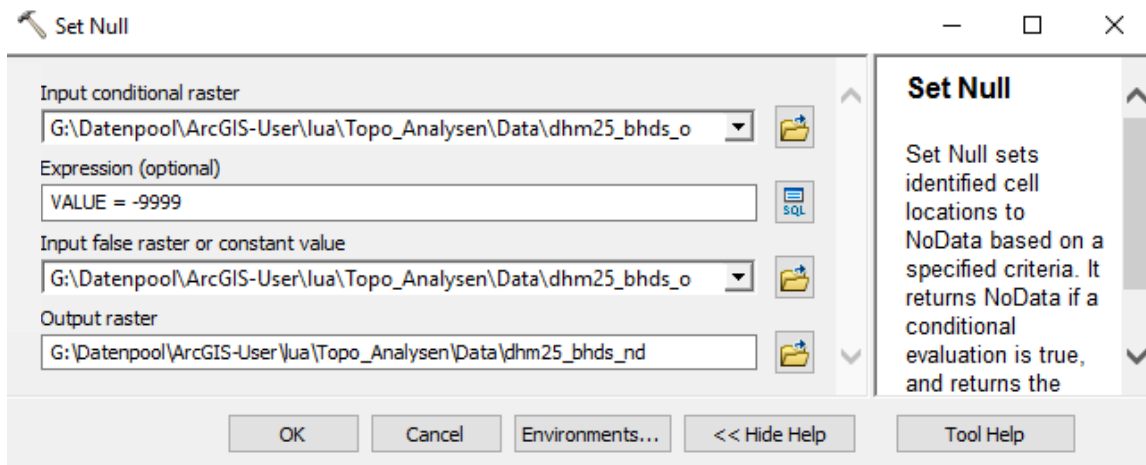


Fig. A6-25: Replacing "-9999" raster values by "NoData".

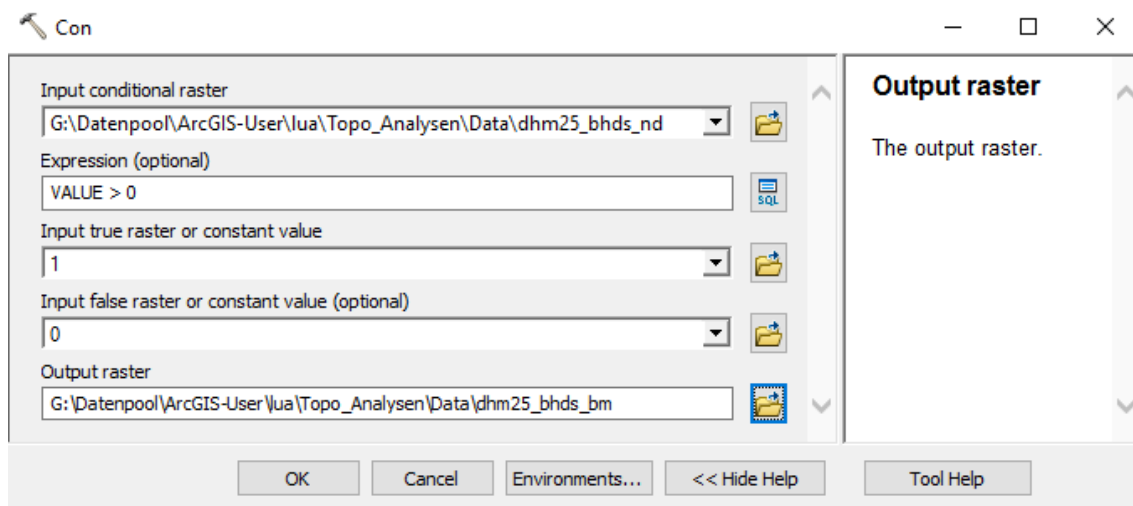


Fig. A6-26: Converting raster to "bitmap".

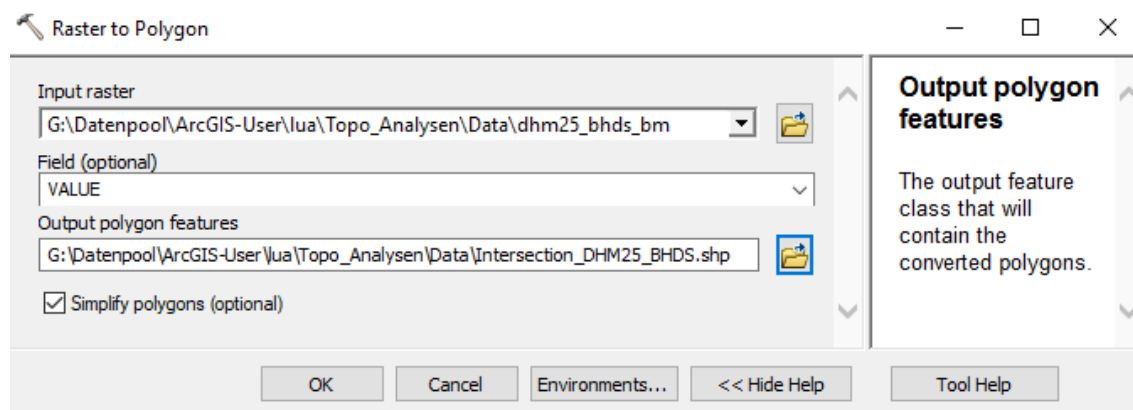


Fig. A6-27: Converting "bitmap" into polygon feature class for final illustration.

Appendix 6**6.C Extracting stream longitudinal profiles****Introduction (summarised from section 3.5):**

Stream longitudinal profiles are extracted here for 15 tributaries to the Aare and Rhine with headwaters in the central Jura Ost siting region (Fig. A6-28). Apart from the present topography, the resulting profiles display the following information:

- Base level of HDS
- Base level of TDS
- Top bedrock (where Quaternary deposits > 5 m)
- Lithostratigraphic units of bedrock surface

The following sections outline the technical procedure of their extraction.

Data processing: "Selection of stream courses"

For extraction of stream longitudinal profiles, stream courses have been selected from the input dataset "drainage network TLM" (Fig. A6-28). These data are part of the Topographic Landscape Model 'TLM' by swisstopo.

In some cases, the polylines of the "drainage network TLM" had to be extended manually for the headwater regions (Fig. A6-28). This was done by visually following a drainage network that was calculated with the "Hydrology" toolbox in ArcGIS and Matlab from a resampled (3 m-grid) version of DTM-AV (hence referred to as "calculated drainage network"; provided to Nagra by M. Foster and R. Arrowsmith / Arizona State University). The DTM-AV hillshade was used to check, that these sections are not affected by major artefacts.

Each stream (longitudinal profile) has been assigned a number (LP-1 to LP-15) according to Fig. A6-28.

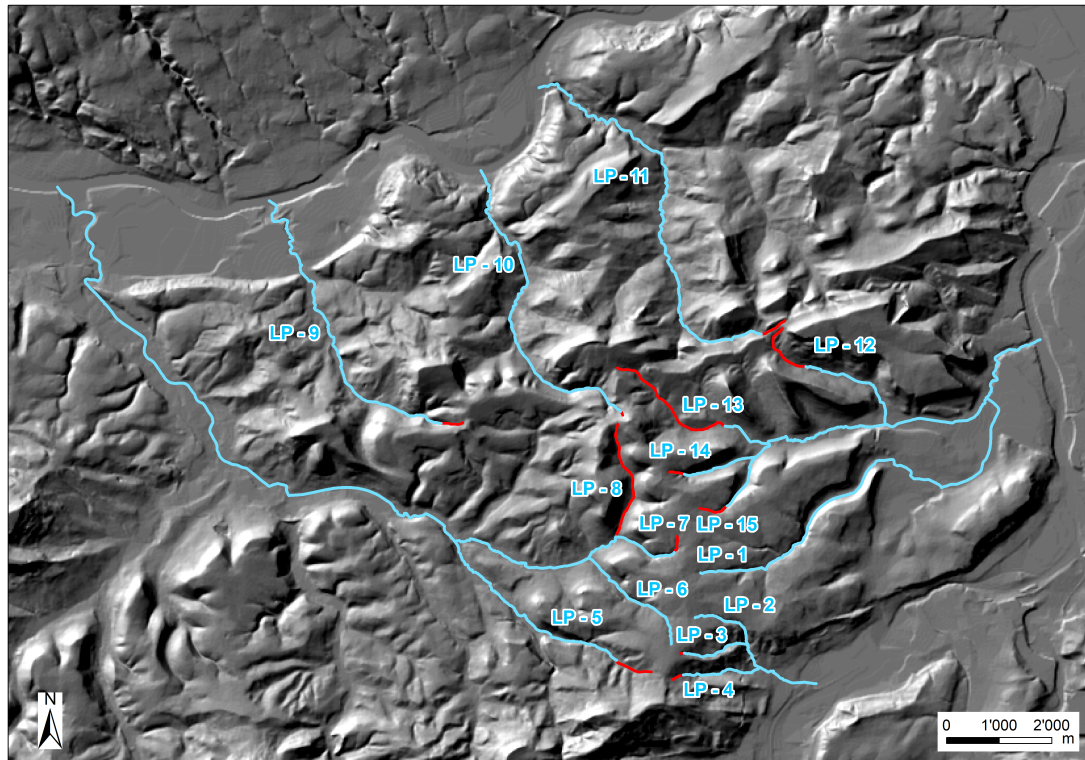


Fig. A6-28: Selected stream courses for stream longitudinal profiles (LP).

Blue sections correspond to the dataset "drainage network TLM", red sections have been extended manually based on the visual inspection of the "calculated drainage network" (provided to Nagra by M. Foster and R. Arrowsmith / Arizona State University) and "DTM-AV hillshade".

Appendix 6

Tab. 11: Selection of stream courses.

Nr.	Processing step	Input dataset(s)	ArcGIS
1.	Extraction of stream sections (polylines) belonging to an individual stream and export as a separate (temporary) shapefile	Drainage network TLM	"Select Features" tools Right-click on layer in TOC > Data > Export Data
2.	If necessary: manually extending the stream course by additional section towards headwater region	Temporary shapefile (step 1) "Base map": Calculated drainage network DTM-AV hillshade	Editing Tool > Create Features
3.	Merge all sections	Temporary shapefile (step 1/2)	Editing Tool > Merge
4.	Creating one permanent feature class, that contains all individual stream courses as single features	Temporary shapefiles (one for each individual stream course) from step 3	Data Management Tools > General > Merge
5.	Manually assigning reference numbers (1 to 15) to stream courses	Stream courses	Attribute Table > Add Field ("StreamA_Nr") (see Fig. A6-28)

Data processing: "Extraction of elevation values"

For each stream course, points have been generated along the polyline at horizontal distances of 10 m. Then, elevation values of different surfaces (present topography, base level of HDS, base level of TDS, top bedrock) have been extracted at these point locations, to be projected on the stream longitudinal profiles. Tab. A6-12 and corresponding figures summarise the processing steps in detail.

Tab. A6-12: Projection of sampling points (Stream points (10 m)) on profile lines (Stream courses (routes)).

Nr.	Processing step	Input dataset(s)	ArcGIS
1.	Preprocessing input raster Top bedrock	Top bedrock Thickness of Quaternary deposits	Spatial Analyst Tools > Conditional > Set Null (Details in Fig. A6-29)
2.	Creating stream network (without overlapping polyline sections)	Stream courses	Data Management Tools > Generalisation > Dissolve
3.	Creating sampling points along stream network (at regular distances of 10m)	Stream network	Data Management Tools > Sampling > Generate Points Along Lines (Details in Fig. A6-30)
4.	Extracting elevation values at sampling point locations	Stream points (10 m) DTM-AV Base level of HDS Base level of TDS Top bedrock } (*)	Spatial Analyst Tools > Extraction > Extract Multi Values to Points (Details in Fig. A6-31)
5.	Convert stream courses to route elements (for linear referencing)	Stream courses	Linear Referencing Tools > Create Routes (Details in Fig. A6-32)
6.	Locating points along routes (measures distance of sampling points along stream courses)	Stream points (10 m) Stream courses (routes)	Linear Referencing Tools > Locate Features Along Routes (Details in Fig. A6-33)
(*) preprocessed according to Tab. A6-10 (HDS, TDS) and step 1 of this table (Top bedrock) resp.			

As shown in Fig. A6-34, elevation values are finally scaled by factor 10, to accentuate changes in channel gradient in the resulting illustrations.

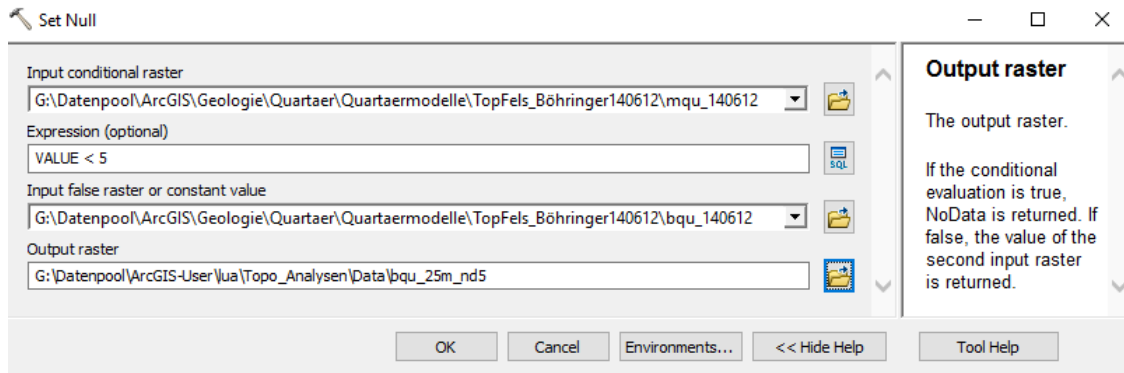


Fig. A6-29: Preprocessing input raster "Top bedrock" with Raster Calculator.

A copy of the input dataset "Top bedrock" (bqu_140612) is created here. However, cell values are set to "NoData", where Quaternary deposits have a thickness of less than 5 m. With this condition, the stream longitudinal profiles will only display "Top bedrock" in sections of thicker Quaternary deposits.

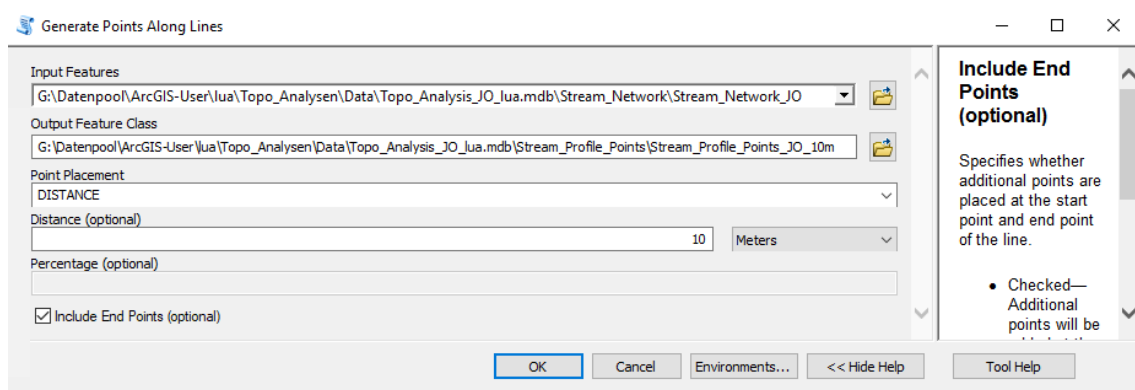


Fig. A6-30: Creating sampling points for profile extraction along the stream network.

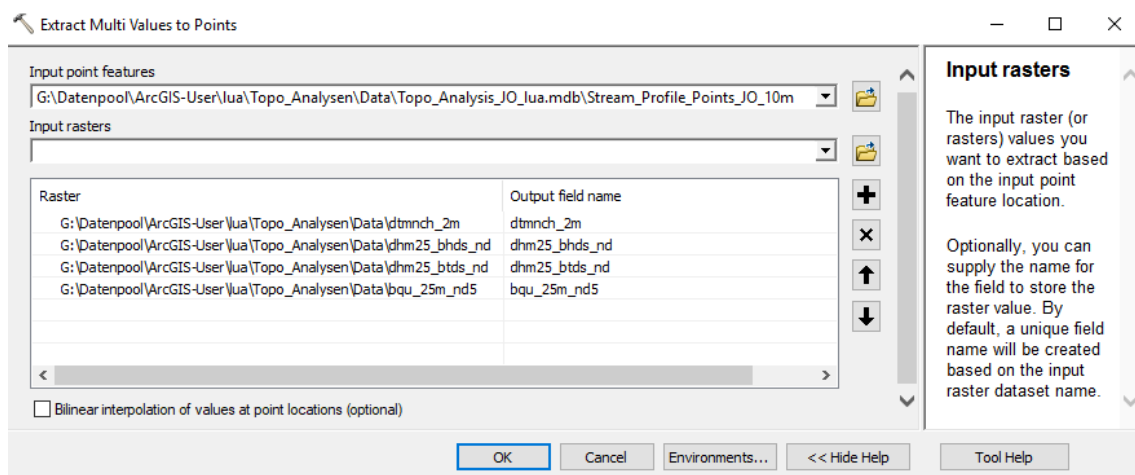


Fig. A6-31: Extracting elevation values at sampling point locations.

The selected input rasters correspond to: 1) DTM-AV (here named "dtmnch_2m"); 2) Base level of HDS; 3) Base level of TDS; 4) Top bedrock (with 2, 3 and 4 modified according to Tabs. A6-10 and A6-12).

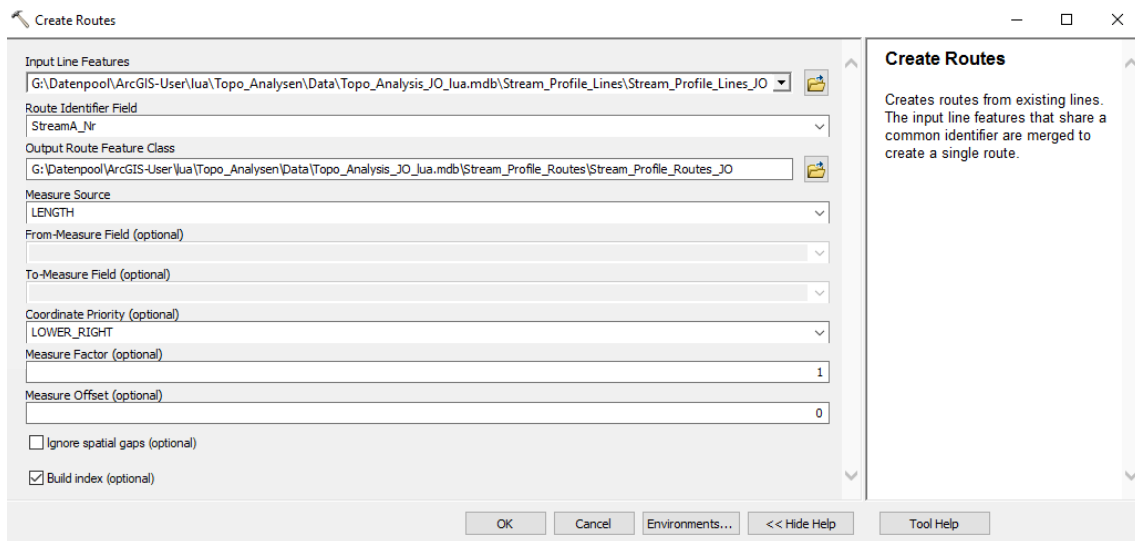


Fig. A6-32: Convert stream courses to route elements (for linear referencing).

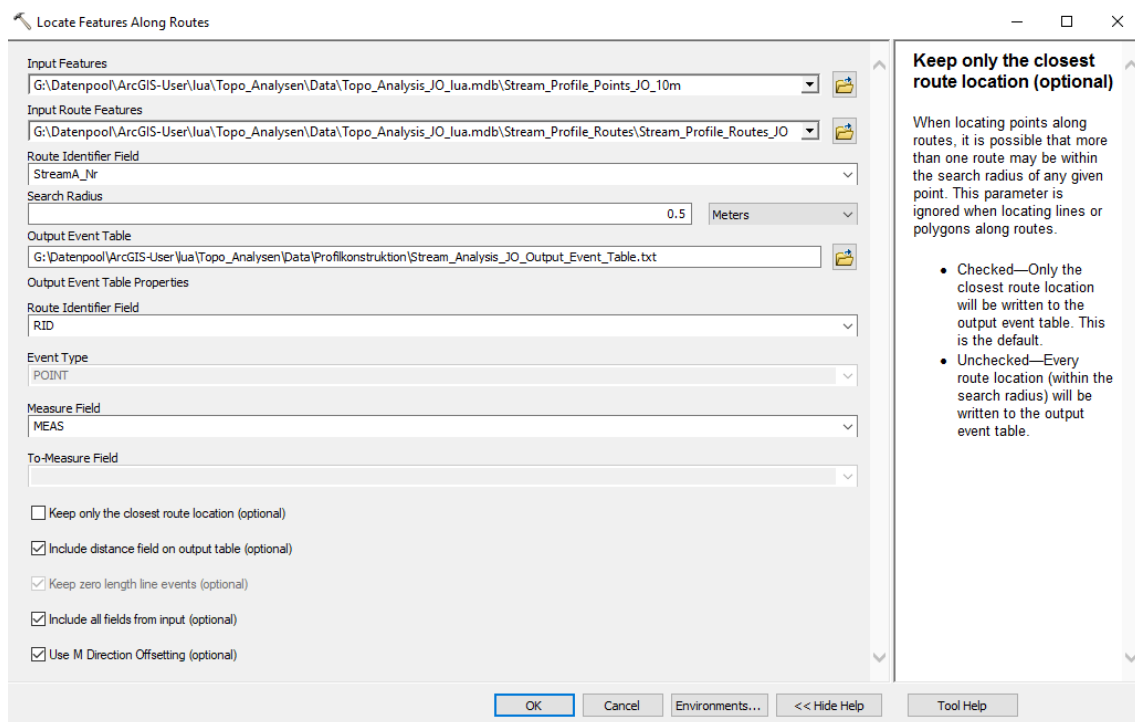


Fig. A6-33: Locating points along routes (measures distance of sampling points along stream courses).

The output is a txt-file containing elevation values and distance of sampling points along stream courses. The table has been exported and processed in Excel as "Stream profile table"⁵ (see Fig. A6-34).

⁵ Filepath within directory NAB 17-42: .../Data/Profile_Construction_Stream_Profiles/Stream_Analysis_JO_Output_Event_Table.xlsx



Fig. A6-34: "Stream profile table": Editing the resulting txt-file from point projections (Tab. A6-12 and Fig. A6-33) in MS Excel, as input for subsequent plotting of stream longitudinal profiles.

For subsequent illustration purposes, additional columns are added on the right (red box) to rescale elevation values of input rasters by factor 10 (DTM-AV = column 'G'; Base level of HDS = column 'H'; Base level of TDS = column 'I'; Top Bedrock = column 'J'). The corresponding Excel formula (red circle) also sets "NoData" values (empty cells) to -9999. The metric distance along the stream course is given by column 'B' (MEAS). Column 'C' (distance) instead contains the shortest distance of the sampling point to the stream course (~ zero).

Data processing: "Profile construction"

Based on the "Stream profile table" in Fig. A6-34, the stream longitudinal profiles can be displayed with a few more processing steps. This is also done in ArcGIS, in order to benefit from useful axis scaling and symbology features. Tab. A6-13 lists the detailed processing steps, with subsequent figures containing corresponding illustrations.

This involved the creation of various shapefiles in ArcGIS that do not represent "real" geographic datasets and have therefore not been included in Appendix 5.B. However, the shapefiles can be found via filepath: .../Data/Profile_Construction_Stream_Profiles/ of the NAB 17-42 directory.

Tab. A6-13: Construction of stream longitudinal profiles.

Nr.	Processing step	Input dataset(s)	ArcGIS
1.	Creating point shapefiles, representing elevation values of extracted surfaces along stream long. profiles	Stream profile table	ArcCatalog > Create Feature Class > From XY Table... (Details in Figs. A6-35 and A6-36).
2.	Assigning label of the represented surface in the attribute table	Temporary shapefiles (step 1)	Attribute Table > Add Field... + Field Calculator (Details in Fig. A6-37)
3.	Creating one permanent shapefile, that contains the data points of all surfaces and streams	Temporary shapefiles (step 2)	Data Management Tools > General > Merge
4.	Clearing up the final point shapefile by deleting points plotted at elevation level of -9999 (~ "NoData")	"Stream_LP_JO_10x_All_Surfaces_Data_Points.shp"	Editor > Start Editing "Select Features" tools Attribute Table > "Delete selected" (Details in Fig. A6-38)
5.	Grouping the points according to the stream longitudinal profile and surface they belong to	"Stream_LP_JO_10x_All_Surfaces_Data_Points.shp"	Attribute Table > Add Field... + Field Calculator (Details in Fig. A6-39)
6.	Converting (grouped) profile points to profile lines "Stream_LP_JO_10x_All_Surfaces_Lines.shp"	"Stream_LP_JO_10x_All_Surfaces_Data_Points.shp"	Data Management Tools > Features > Point to Line (Details in Figs. A6-40 to A6-42)

The final editing of the resulting profiles is done in Adobe Illustrator (results in Appendix 3)⁶.

⁶ Unfortunately, converting points to lines according to Fig. A6-40 can result in linearly interpolated segments in the absence of data points (surface "Top bedrock", where Quaternary deposits < 5 m). These artificial connections have been removed manually in Adobe Illustrator.

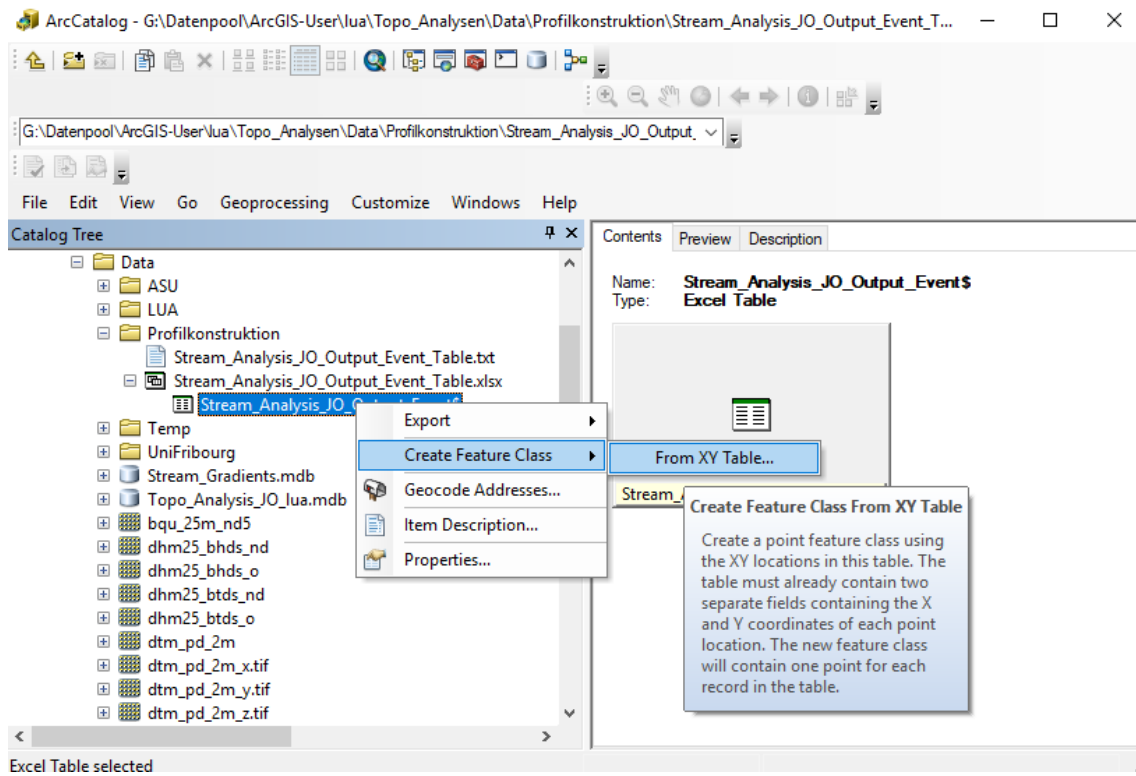


Fig. A6-35: Creating point shapefiles from the "Stream profile table" (Fig. A6-34), for representation of data points in (two-dimensional) stream longitudinal profiles.

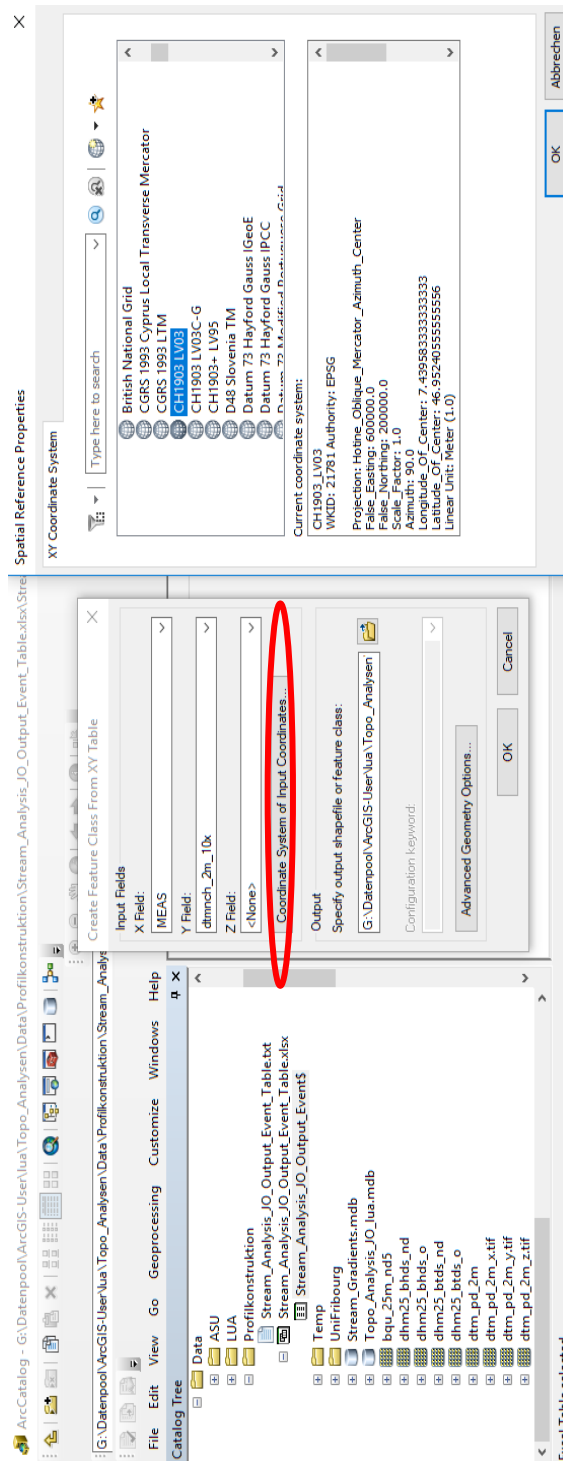


Fig. A6-36: Creating a shapefile of data points, representing elevation values of present topography along stream longitudinal profiles (continued from Fig. A6-35).

The input field 'MEAS' contains the distance of the sampling point along a stream longitudinal profile (see Fig. A6-33). The field dtmnh_2m_10x contains the elevation of present topography (DTM-AV) at the corresponding location, scaled by factor 10. The definition of the spatial reference system (Coordinate System of Input Coordinates) is required to ensure correct axis scaling. The procedure is repeated analogously for the data point representation of base level HDS, base level TDS and top bedrock.

FID	Shape	RID	MEAS	Distance	ORIG	FID	Id	dtmch_2m	dhm25_bhds	bqu_25m_nd	dtmch_2m_10x	dhm25_bhds_nd_10x	bqu_25m_nd_10x	Surface
0	Point	1	1	0	21	0	0	325.809988	523.974365	299.995239	5239.743652	4320.665283	2999.952393	DTM-AV
1	Point	1	1.12798	0.000021	21	0	0	325.799988	523.974365	299.995239	5239.743652	4320.665283	2999.952393	DTM-AV
2	Point	1	1.13.1279	0.000041	21	0	0	325.829987	523.974365	299.995239	5239.743652	4320.665283	2999.952393	DTM-AV
3	Point	1	1.23.1279	-0.00003	21	0	0	325.970001	524.126221	301.353943	5241.262207	4320.274353	3013.539429	DTM-AV
4	Point	1	1.23.1279	0.00001	21	0	0	326.140014	524.126221	301.353943	5241.262207	4316.887202	3013.539429	DTM-AV

Fig. A6-37: Attribute table of the temporary point shapefile created in Fig. A6-36 (representing elevation values of present topography along stream longitudinal profiles).

An additional field (type text) called "Surface" must be added to the attribute table. The label of the surface represented by the shapefile (here DTM-AV) is assigned with the 'Field calculator'. The procedure is repeated analogously for the shapefiles representing base level HDS, base level TDS and top bedrock.

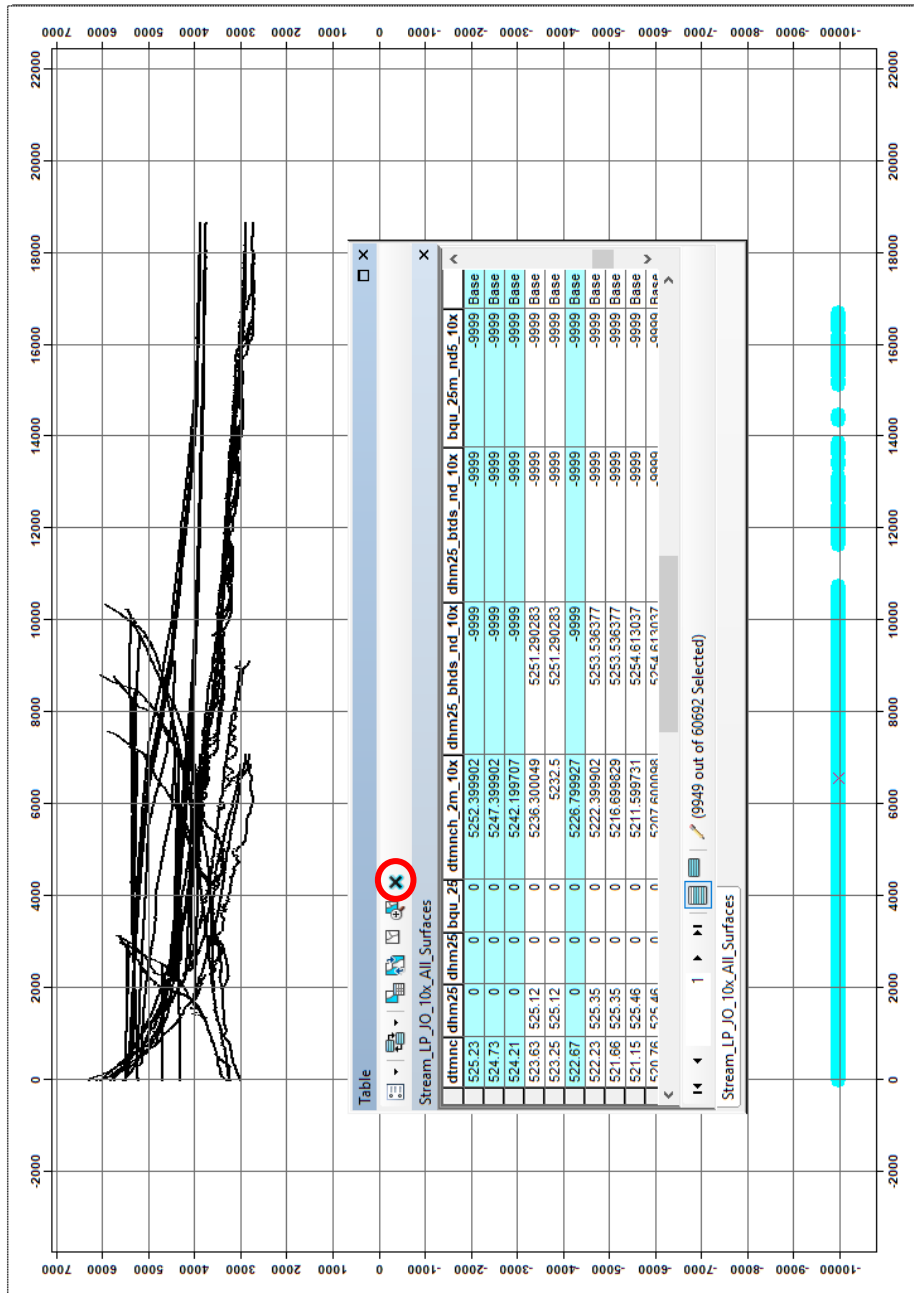


Fig. A6-38: Clearing up the final point shapefile by deleting data points plotting at elevation level -9999 ("NoData").

This is done by standard ArcGIS editing: "Select Features" tools + "Delete selected" (red circle) in attribute table.

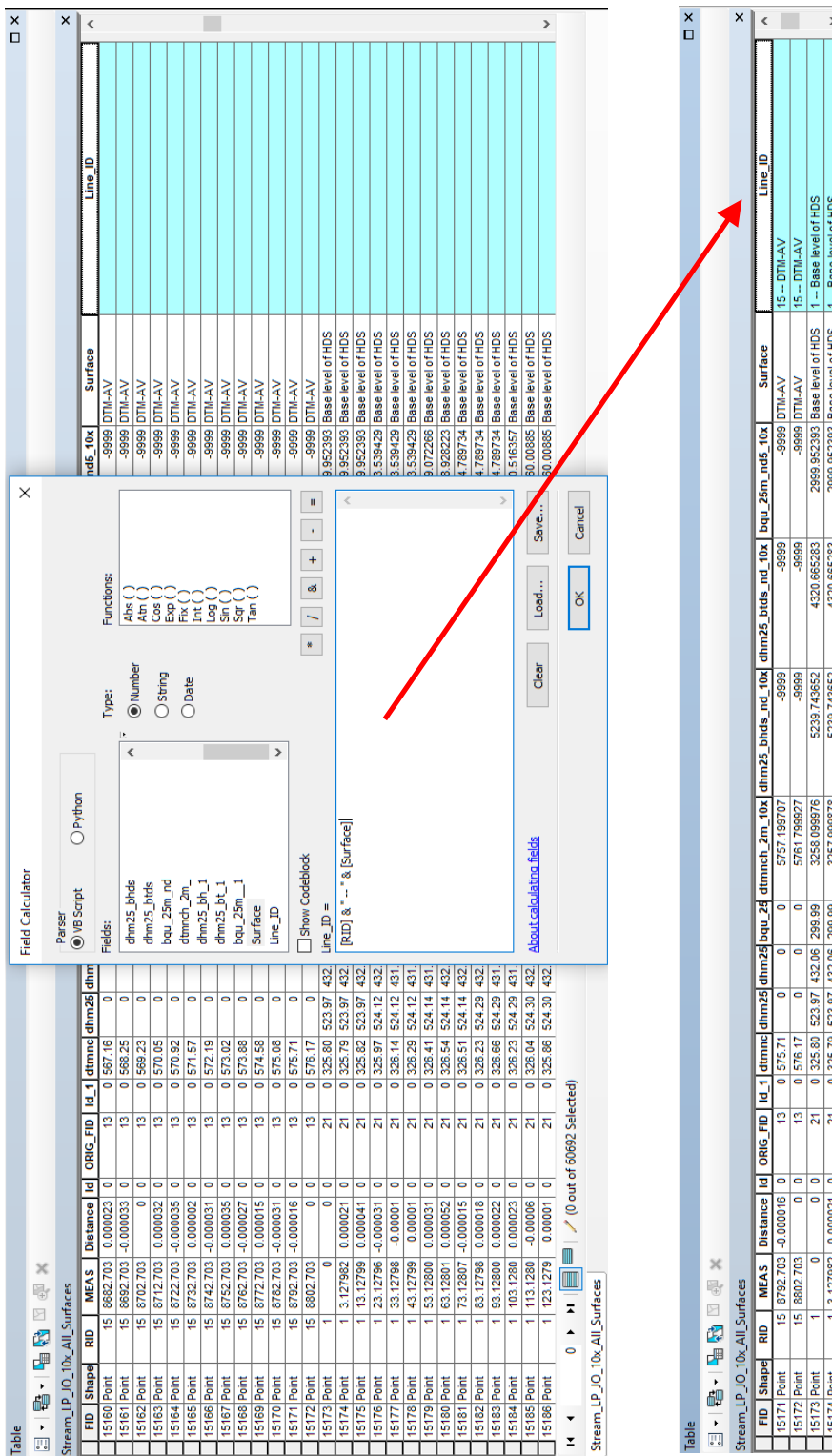


Fig. A6-39: Attribute table of the final point shapefile, representing elevation values of all surfaces along stream longitudinal profiles.

An additional field (type text) called "Line_ID" must be added to the attribute table. With the expression in the 'Field Calculator' data points are grouped by a label ("Line_ID"), which indicates the represented surface and the number of the stream longitudinal profile it belongs to (see resulting records at the bottom).

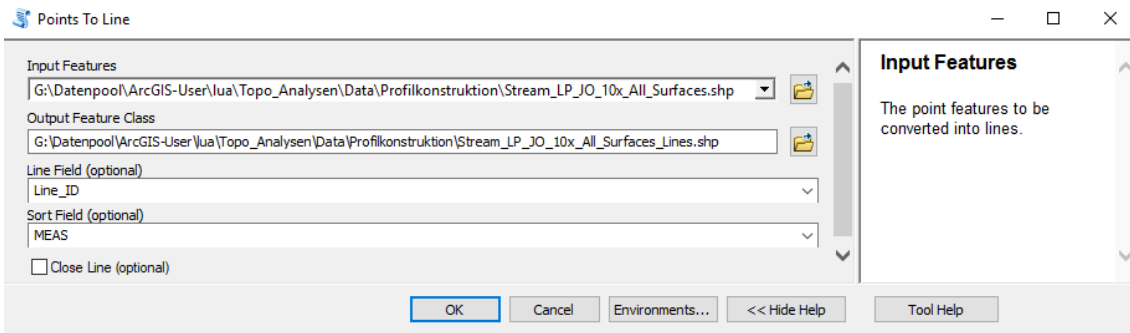


Fig. A6-40: Converting (grouped) profile points to profile lines.

The "Line_ID" controls which points are aggregated to one line (e.g. all points of base level HDS belonging to stream profile 5). The sort field 'MEAS', representing the distance along the stream longitudinal profile, ensures that vertices of the resulting polylines are connected in the right order.

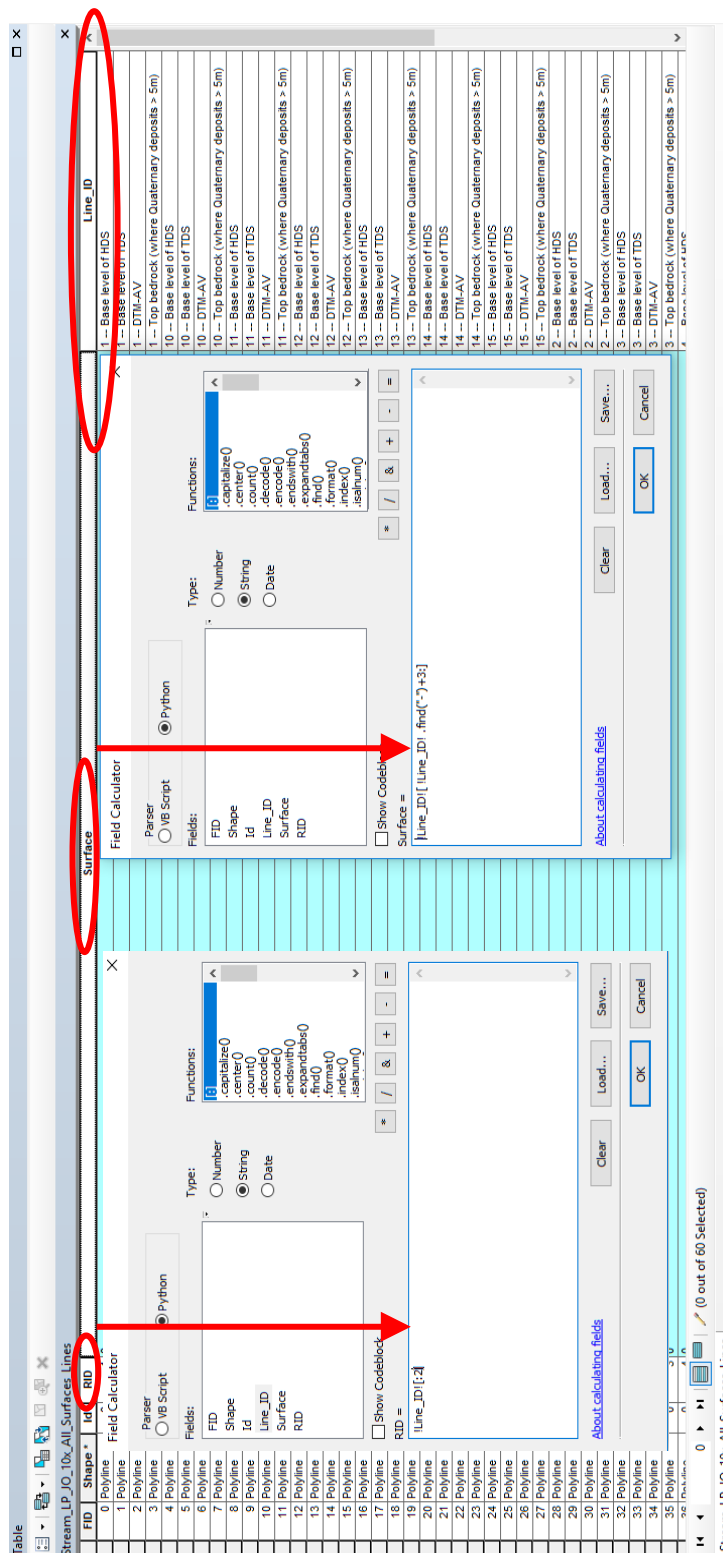


Fig. A6-41: Attribute table of the final line shapefile, representing elevation values of all surfaces along stream longitudinal profiles.

After converting the points to lines, only the field "Line_ID" (red circle) is preserved, which contains the aggregated information about both the (represented) stream longitudinal profile number and the surface. By the 'Add Field' and the 'Field Calculator' function, these attributes are split again into two separate fields ("RID": type long; "Surface": type string).

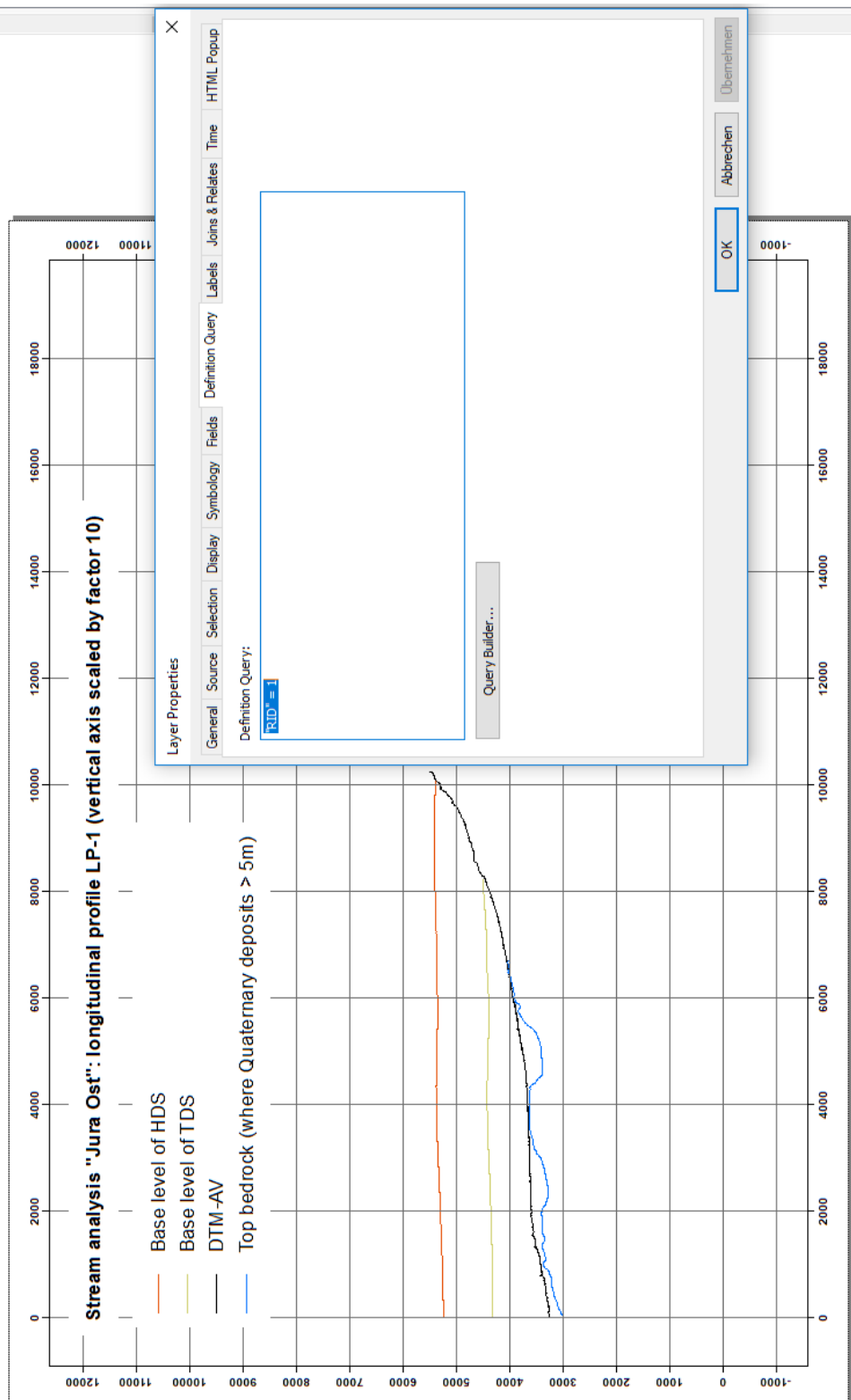


Fig. A6-42: Plotting stream longitudinal profiles (lines) in ArcGIS.

The attribute "RID" stores the number of the stream longitudinal profile (LP) and can therefore be used in the "Definition Query" to select which LP to display. The attribute "Surface" is used as the value field in the symbology setting, to visually differentiate the different surfaces.

Appendix 6**6.D Extracting topographic / geological profiles****Introduction (summarised from section 3.6):**

Regional profiles across the study area were extracted in north-south and east-west direction. The sampling lines of the topographic profiles have been defined manually, accounting for interesting locations. Sampling points have been generated along the profile sampling lines at horizontal distances of 10 m.

Apart from the present topography, the resulting profiles display the following information:

- Base level of HDS
- Base level of TDS
- Top bedrock (where Quaternary deposits > 5 m)
- Lithostratigraphic units of bedrock surface and projection at depth.
- Landslides (schematic illustration)
- Additional content (place names etc.)

Subsections of the regional topographic / geological profiles were also used for interpretation and illustration of landslide process types in the study area (section 4.2).

Data processing: "Extraction of elevation values"

The detailed working steps of extracting elevation values along the regional topographic / geological profiles in ArcGIS are listed in Tab. A6-14.

Tab. A6-14: Projection of sampling points (Topographic profiles (sampling points 10 m)) on profile lines (Topographic profiles (routes)).

Nr.	Processing step	Input dataset(s)	ArcGIS
1.	Preprocessing input raster datasets for extraction of lithostratigraphic boundaries at depth	Subsurface model NTB 14-02	Spatial Analyst Tools > Map Algebra > Raster Calculator (Details in Fig. A6-43)
2.	Manually defining sampling lines		Editing Tool > Create Features
3.	Creating sampling points along sampling lines (at regular distances of 10 m)	Topographic profiles (sampling lines)	Data Management Tools > Sampling > Generate Points Along Lines (analogous to Fig. A6-30)
4.	Extracting elevation values at sampling point locations	Topographic profiles (sampling points 10 m) DTM-AV Base level of HDS Base level of TDS Top bedrock Basis Tertiary Basis Malm (Wildeg-Formation) Top Opalinus Clay Top Lias	Spatial Analyst Tools > Extraction > Extract Multi Values to Points (Details in Fig. A6-44)
5.	Convert sampling lines to route elements (for linear referencing)	Topographic profiles (sampling lines)	Linear Referencing Tools > Create Routes (analogous to Fig. A6-32)
6.	Locating points along routes (measures distance of sampling points along the regional profiles)	Topographic profiles (sampling points 10 m) Topographic profiles (routes)	Linear Referencing Tools > Locate Features Along Routes (analogous to Fig. A6-33)
(*) preprocessed according to Tab. A6-10 (HDS, TDS) and step 1 of Tab. A6-12 (Top bedrock) resp. (**) preprocessed according to Fig. A6-43 (step 1 of this table)			

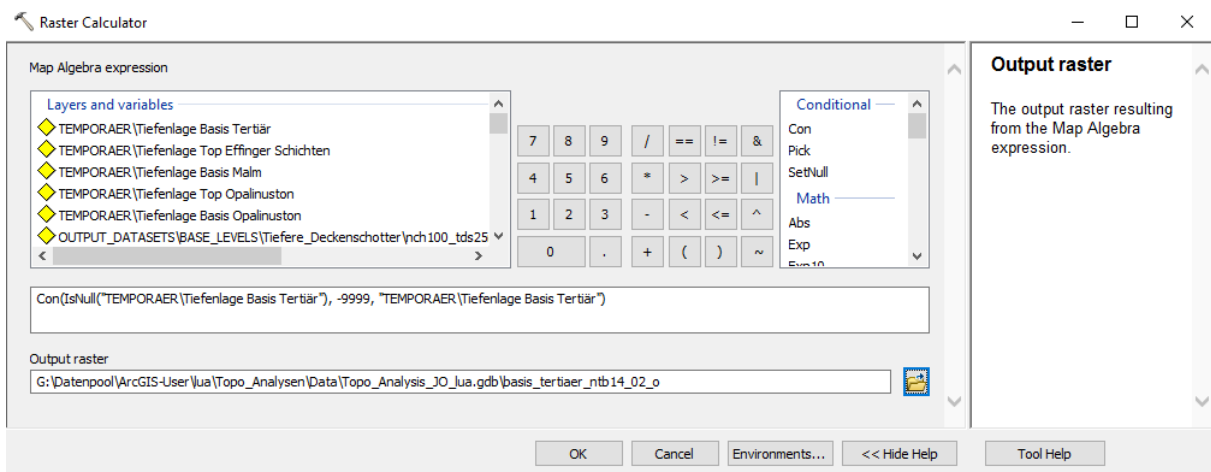


Fig. A6-43: Using Raster Calculator to preprocess input raster datasets for extraction of litho-stratigraphic boundaries at depth (from "Subsurface model NTB 14-02").

"NoData" values in the raster dataset (here "Tiefenlage Basis Tertiär", corresponding to file-name "BTe_union_20140930", Appendix 5.A) are thus replaced by -9999. This is required for the tool "Extract multi values to points" (Fig. A6-44) to be executed successfully. Analogously, the procedure is repeated for "Tiefenlage Basis Malm", "Tiefenlage Top Opalinuston" and "Tiefenlage Basis Opalinuston".

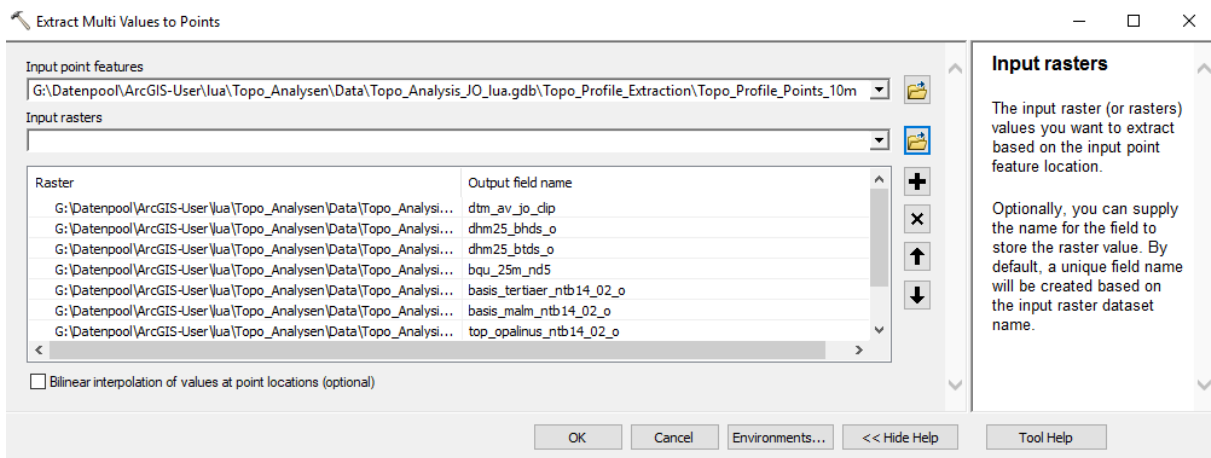


Fig. A6-44: Extracting elevation values at sampling point locations.

The selected input rasters correspond to: 1) DTM-AV (here "dtm_av_jo_clip"); 2) Base level of HDS; 3) Base level of TDS; 4) Top bedrock; 5) Basis Tertiary; 6) Basis Malm (Wildeg-Formation); 7) Top Opalinus Clay; 8) Top Lias. Preprocessing as referenced in Tab. A6-14, step 4.

The output of the processing steps in Tab. A6-14 is a txt-file containing elevation values and distance of sampling points along the regional topographic / geological profiles. The table has been exported and processed in Excel as "Topographic profile table"⁷.

In addition to Tab. A6-14, also the "lithostratigraphic boundaries" at surface (as displayed in Appendix 1.C) have been intersected with the sampling lines of the regional profiles (Tab. A6-15). This is used as additional reference for the final illustration of lithostratigraphic units in Appendix 4.

Tab. A6-15: Intersection points of topographic profiles (sampling lines) and lithostratigraphic boundaries at surface.

Nr.	Processing step	Input dataset(s)	ArcGIS
1.	Create intersection points	Lithostratigraphic boundaries Topographic profiles (sampling lines)	Analysis Tools > Overlay > Intersect
2.	Extracting elevation values (present topography) at intersection points	Intersection points of topographic profiles and lithostratigraphic boundaries at surface DTM-AV	Spatial Analyst Tools > Extraction > Extract Multi Values to Points (analogous to Fig. 44)
3.	Locating points along routes (measures distance of sampling points along the regional profiles)	Intersection points of topographic profiles and lithostratigraphic boundaries at surface Topographic profiles (routes)	Linear Referencing Tools > Locate Features Along Routes (analogous to Fig. 33)

The output of the processing steps in Tab. A6-15 is a txt-file containing elevation values, names of lithostratigraphic boundaries and distance of sampling points along the regional topographic / geological profiles. The table has been exported and processed in Excel as "Topographic profile table (intersection points of topographic profiles and lithostratigraphic boundaries at surface)"⁸.

Analogous to Fig. A6-34 (stream profiles), elevation values are scaled in the Excel tables by factor 10, to accentuate variations of local relief in the resulting illustrations (Appendix 4).

Data processing: "Profile construction"

Based on the resulting Excel tables above, the regional topographic / geological profiles have been displayed in analogy to the procedure described for the stream longitudinal profiles (Tab. A6-13, and Fig. A6-35 etc.). This involved the creation of various shapefiles in ArcGIS that do not represent "real" geographic datasets and have therefore not been included in Appendix 5.B. However, the shapefiles can be found via filepath: .../Data/Profile_Construction_Topo_Profiles/ in the NAB 17-42 directory.

⁷ Filepath within directory NAB 17-42: .../Data/Profile_Construction_Topo_Profiles/Topo_Profiles_JO_Output_Event_Table.xlsx

⁸ Filepath within directory NAB 17-42: ...Data/Profile_Construction_Topo_Profiles/Topo_Profiles_Litho_Surface_JO_Output_Event_Table.xlsx

Appendix 6

Since the lithostratigraphic boundaries at depth were not included in the first draft, the extracted surfaces are found in two separate shapefiles ("Topo_Profiles_JO_10x_All_Surfaces_Data_Points.shp" and "Topo_Profiles_JO_10x_Litho_Layer_Points.shp").

Also, the lithostratigraphic boundaries at depth ("Topo_Profiles_JO_10x_Litho_Layer_Points.shp") were not further converted into a polyline shapefile. Instead, the lines were drawn manually (and simplified) in Adobe Illustrator, based on the data points and the projected "intersection points of topographic profiles and lithostratigraphic boundaries at surface" ("Topo_Profiles_JO_10x_Litho_Intersection_Points.shp").

Apart from those point and polyline shapefiles with vertical axis scaled by factor 10, some shapefiles were also created without rescaling. These were used to create the geological cross sections (interpretation of landslide process types) in section 4.2 of the main report:

- "Topo_Profiles_JO_DTM_AV_Lines.shp"
- "Topo_Profiles_JO_Top_Bedrock_Data_Points.shp"
- "Topo_Profiles_JO_Litho_Intersection_Points.shp"